

The effects of laser-assisted zona pellucida manipulations on embryo competency and the mechanisms underlying embryo hatching in a mouse model

Yaqiong Liu

Nuffield Department of Women's and Reproductive Health
St Cross College
University of Oxford

Supervisor: Kevin Coward
Co-Supervisor: Ingrid Granne

A thesis submitted for the degree of

Doctor of Philosophy

Trinity 2021

Acknowledgements

I am greatly indebted to my principal supervisor, Dr Kevin Coward, for supervising me with his instructive criticism, valuable advice, and general support in my research project throughout my DPhil study. His optimism, enthusiasm, as well as confidence in research and life always encourage me to believe in myself and pursue the goals in front. In addition, I would love to express my sincere gratitude to Kevin for his selfless assistance and bottomless support in my scholarship and funding application. Without his help, I wouldn't have finished my study in Oxford without any financial pressure and worries. Finally, I am appreciated for his precious advice and critical review of this thesis, especially in this hardship of global pandemic that affected everyone's life and works. I also owe my deepest gratitude to my laboratory manager, Mrs Celine Jones. As my day-to-day supervisor, I love to thank her for mentoring my experiment, caring about my daily life as well as my mental health. Celine never failed to cheer me up when I feel upset, and she always encourages me to boost my capacity in the laboratory and shows me a positive way to think when I faced difficulties.

I am also profoundly grateful to my second supervisor, Professor Ingrid Granne, for her support during my study in Oxford. She gave me helpful feedback and advice when I need help, and she encourages me to consider problems from clinical aspects. In addition, I would love to express my gratitude to Professor John Aplin from the University of Manchester and Mrs Jenny Spencer for sharing their invaluable knowledge on the embryo implantation model and clinical application of laser-assisted techniques.

I wish to acknowledge the help provided by Dr Angela Lee and Helen Lockstone from the Wellcome Trust Human Genomics Centre for their assistance with the RNA

sequencing project. I would love to acknowledge Professor Chris Graham, Dr Jennifer Southcombe, Mrs Laura Rose, Mrs Janet Carver, Mrs Susie Barber from the Nuffield Department of Women's and Reproductive Health, Mrs Alison Bradford, and Mrs Laura Thomas from the Department of Biomedical Services, Dr Dhruti Babariya and Dr Katharina Spath from Juno Genetics for supporting and helping me to carry out my experiment.

I would love to acknowledge the HFEA (Human Fertility and Embryology Authority), ACE (Association of Clinical Embryologists), and SRF (Society for Reproduction and Fertility) for helping me circulating the survey and all the anonymous participants involved in this study. Furthermore, this research would not have been possible without the generous financial support from the Rosetree Trust and the Henry and Lester Trust. In addition, I am also grateful to the Chinese Scholarship Council and my parents to support my DPhil study financially.

Last but the most, I would love to take this opportunity to express my profound gratitude to my beloved parents, my elder sister, and my partner's parents back home for their endless love and bottomless support. I would love to thank my dearest friends, Mengni, Yiwen, Zhichao, Steven, Xin, Teresa, and Shiyan, who always support me and makes my life in Oxford more colourful and memorable. Finally, I owe a great debt of gratitude to my partner, Kevin Bin Liu, who inspired me to apply to Oxford in the first place. Thank you for always being my best companion, faithful friend, and inspiring teacher over the years. It is hard to imagine my DPhil journal without your encouragement and support.

Table of Contents

LIST OF ABBREVIATIONS ..... **I**

LIST OF FIGURES ..... **III**

LIST OF TABLES ..... **VII**

ABSTRACT **1**

CHAPTER 1 GENERAL INTRODUCTION **2**

1.1 Establishment of embryo implantation **3**

1.1.1 Preimplantation embryo development 3

1.1.2 Embryo zona pellucida and hatching 6

1.1.3 Embryo implantation 9

1.1.3.1 Differences in implantation between species 11

1.2 Infertility and assisted reproductive technology (ART) **14**

1.2.1 Aetiology of infertility 14

1.2.2 Assisted reproduction technology 15

1.2.3 Implantation failure and treatment 16

1.3 The development of laser technology in ART **19**

1.4 Laser applications in the embryo micromanipulation **22**

1.4.1 Laser-assisted embryo biopsy 22

1.4.1.1 Laser-assisted polar body biopsy (PBB) 23

1.4.1.2 Laser-assisted blastomere biopsy 24

1.4.1.3 Laser-assisted trophectoderm biopsy 26

1.4.2 Laser-assisted hatching (LAH) 29

1.4.2.1 The efficiency of laser-assisted hatching 30

1.4.3 Laser-assisted cryopreservation 33

1.4.3.1 Blastocoele collapse for vitrification 34

1.4.3.2 Laser-assisted removal of degenerated (lysed) blastomeres 35

1.4.4 Laser-assisted intra-cytoplasmic sperm injection (ICSI) 37

1.5 Controversy relating to the efficacy of laser-assisted embryo manipulations 39

1.5.1 Safety concerns for the embryo 39
1.5.2 Safety concerns for the offspring 43

1.6 The preimplantation mouse embryo as a model system 44

1.6.1 Advantages of the preimplantation mouse embryo as model 44
1.6.2 Differences between human and mouse preimplantation embryos 46

1.7 The aims of this thesis 49

CHAPTER 2 METHODS AND MATERIALS 51

2.1 Online survey 52

2.1.1 Questionnaire design 52
2.1.2 Survey distribution 52

2.2 Mouse embryo collection and culture 53

2.2.1 Fresh embryo collection 53
2.2.1.1 Maintenance of animals 53
2.2.1.2 Superovulation and mating 54
2.2.1.3 Embryo retrieval 54
2.2.2 Frozen embryo collection 55
2.2.2.1 Frozen embryo straws 55
2.2.2.2 Thawing embryos 56
2.2.3 Embryo culture 57
2.2.4 Inclusion criteria for embryos 57

2.3 Laser-assisted ZP manipulation procedure 58

2.4 The assessment of mouse embryo morphology 60

2.4.1 Developmental assessment 60
2.4.2 Morphological assessment of embryo hatching 61

2.5 Human cell culture 62

2.5.1 Ishikawa cell line maintenance 62
2.5.2 Ishikawa cell passage 62

2.6 The *in vitro* implantation model 63

2.6.1 Two-dimensional (2D) co-culture system ····· 63
2.6.1.1 Coverslip coating ····· 63
2.6.1.2 Ishikawa cell seeding and culture ····· 63
2.6.1.3 Embryo transfer ····· 64
2.6.2 Attachment assay ····· 65
2.7 Immunofluorescent staining ····· 66
2.7.1 Slide coating ····· 66
2.7.2 Immunostaining ····· 66
2.8 Cell apoptosis detection ····· 68
2.8.1 DNA fragmentation assessment ····· 68
2.8.2 The detection of Caspase-3/7 activity ····· 70
2.9 RNA extraction and cDNA synthesis for embryos and cells ····· 71
2.9.1 Mouse embryo cDNA synthesis ····· 71
2.9.2 Preamplification of mouse embryo cDNA ····· 71
2.9.3 Ishikawa cell RNA extraction ····· 73
2.9.4 Ishikawa cell cDNA synthesis ····· 74
2.10 Quantitative Reverse Transcriptase-PCR ····· 75
2.10.1 TaqMan method for detecting gene expression in embryos ····· 75
2.10.2 SYBR Green method for detecting gene expression in cells ····· 75
2.10.3 Calculation of gene expression levels ····· 77
2.11 Statistical analysis ····· 77
CHAPTER 3 CHARACTERISING THE DISPARITIES IN PRACTICES AND ATTITUDES REGARDING ASSISTED-HATCHING ····· 79
3.1 Introduction ····· 80
3.2 Results ····· 83
3.2.1 Demographics ····· 83
3.2.2 The application of AH ····· 85
3.2.3 The practice of AH ····· 86
3.2.3.1 The characteristics of AHpBP practice ····· 86
3.2.3.2 The characteristics of AHpET practice ····· 89

3.2.4 Attitudes regarding AH ····· 92

3.3 Discussion ····· 96

3.4 Limitations ····· 103

3.5 Concluding remarks ····· 103

3.6 Key findings ····· 104

CHAPTER 4 INVESTIGATING THE EFFECT OF LASER-ASSISTED ZP MANIPULATIONS ON THE PREIMPLANTATION MOUSE EMBRYO ····· 105

4.1 Introduction ····· 106

4.2 Results ····· 110

4.2.1 Evaluation of preimplantation mouse embryo development following laser ZP manipulations ····· 110

4.2.2 An investigation of mouse embryo hatching patterns following laser ZP manipulations ····· 112

4.2.2.1 Morphological assessment of hatching pattern at E4.5 ····· 112

4.2.2.2 Time-lapse imaging and analysis of embryo hatching patterns ····· 113

4.2.3 The assessment of cell number in preimplantation mouse embryos undergoing different laser ZP manipulations ····· 115

4.2.3.1 OCT4 and CDX2 staining of embryos undergoing different laser ZP manipulations ····· 115

4.2.3.2 A comparison of blastocyst cell numbers across different laser ZP manipulations ····· 117

4.2.4 The assessment of cell apoptosis mouse embryos undergoing different laser ZP manipulations ····· 119

4.2.4.1 The detection of DNA fragmentation in embryos undergoing different laser ZP manipulations ····· 119

4.2.4.2 An investigation of caspase-3/-7 activation in embryos undergoing different laser ZP manipulations ····· 121

4.2.5 The assessment of heat shock stress in embryos undergoing different laser ZP manipulations ····· 123

4.2.6 The expression of key genes in embryos undergoing different laser ZP manipulations ····· 126

4.3 Discussion ····· 129

4.3.1 Laser ZP manipulations did not affect embryo development ····· 130

4.3.2 Embryo hatching pattern alterations following laser ZP manipulations ····· 131
4.3.3 Hatching embryos treated with ZP drilling exhibited a reduced number of embryonic cells ····· 133
4.3.4 Laser ZP manipulations did not induce cell apoptosis ····· 134
4.3.5 The expression of HSP70 in blastocyst following different LAH treatments ····· 135
4.3.6 Laser ZP treatment did not alter the expression of key genes ····· 136

4.4 Limitations ····· 137

4.5 Concluding remarks ····· 137

4.6 Key findings ····· 138

CHAPTER 5 INVESTIGATING THE EFFECT OF LASER-ASSISTED ZONA PELLUCIDA MANIPULATIONS ON EMBRYO ATTACHMENT ····· 139

5.1 Introduction ····· 140

5.2 Results ····· 143

5.2.1 Verification of Ishikawa cells as a model of the endometrial epithelium ···· 143
5.2.2 Establishment of the *in vitro* implantation model ····· 144
5.2.3 Vitrification of mouse embryo attachment to Ishikawa cells ····· 147
5.2.4 Assessing the stability of embryo attachment ····· 149
5.2.5 The *in vitro* implantation model from E4.5 to E7.5 ····· 151
5.2.5.1 Embryo hatching and attachment in the *in vitro* implantation model ··· 151
5.2.5.2 The effects of different laser ZP manipulations on *in vitro* embryo hatching and attachment ····· 152
5.2.5.3 The effects of different laser ZP drilling-induced perforation size on *in vitro* embryo hatching and attachment ····· 154
5.2.6 The *in vitro* implantation model from E5.5 to E8.5 ····· 156
5.2.6.1 Embryo hatching and attachment in the *in vitro* implantation model from E5.5 to E8.5 ····· 156
5.2.6.2 A comparison of embryo hatching and attachment between E5.5 ET and E4.5 ET implantation model ····· 157
5.2.6.3 The effects of different laser ZP manipulations on *in vitro* embryo hatching and attachment of blastulation delayed embryos ····· 159

5.3 Discussion ····· 161

5.3.1 General summary of main findings ····· 161

5.3.2 The establishment and confirmation of *in vitro* embryo implantation ····· 161
5.3.3 The effect of laser ZP manipulation on *in vitro* embryo attachment ····· 163
5.3.4 Laser ZP manipulations and embryos with delayed blastulation ····· 166

5.4 Limitations ····· 167

5.5 Concluding remarks ····· 168

5.6 Key findings ····· 168

CHAPTER 6 REVEALING THE MECHANISMS UNDERLYING MOUSE EMBRYO HATCHING AND THE IMPACT OF LASER ZP DRILLING ON EMBRYO GENE EXPRESSION BY RNA SEQUENCING ····· 169

6.1 Introduction ····· 170

6.2 Method and materials ····· 176

6.2.1 Sample preparation ····· 176
6.2.2 Library preparation and RNA sequencing ····· 176
6.2.3 RNA-Seq data processing and quality control ····· 177
6.2.4 Differentially expressed genes (DEGs) analysis ····· 177
6.2.5 Functional enrichment analysis ····· 178
6.2.6 Construction and analysis of the protein-protein network ····· 179

6.3 Results ····· 182

6.3.1 Embryo sample collection ····· 182
6.3.2 cDNA library preparation and quality control ····· 183
6.3.3 RNA sequencing data quality control ····· 185
6.3.4 A comparison of hatching blastocysts and pre-hatching blastocysts from the control group ····· 189
6.3.4.1 Differential gene expression analysis ····· 189
6.3.4.2 GO (gene ontology) term enrichment analysis of DEGs ····· 192
6.3.4.3 Pathway analysis ····· 196
6.3.4.4 Upstream regulators analysis using IPA ····· 200
6.3.4.5 The expression of genes that are specific to embryo linage ····· 203
6.3.4.6 Protein-protein interaction (PPI) analysis of DEGs ····· 204
6.3.5 A comparison of laser-drilled hatching blastocysts and control hatching blastocysts ····· 207
6.3.5.1 Differential gene expression analysis ····· 207
6.3.5.2 GO term analysis ····· 210

6.3.5.3 Pathway enrichment analysis ····· 211
6.3.6 Validation of RNA sequencing results by quantitative real-time PCR ····· 214
6.3.6.1 Validation of housekeeping genes ····· 214
6.3.6.2 qRT-PCR validation of selected DEGs ····· 216
6.4 Discussion ····· 220
6.4.1 Genes and pathways related to the mouse blastocyst hatching process *in vitro* ····· 221
6.4.2 Potential upstream regulators during mouse blastocyst hatching ····· 225
6.4.3 Transcriptomic alterations in mouse blastocysts following laser-assisted ZP drilling ····· 227
6.5 Concluding remarks ····· 230
6.6 Key findings ····· 231
CHAPTER 7 GENERAL DISCUSSION AND FUTURE WORK ····· 232
7.1 General summary of main findings ····· 233
7.1.1 The disparity of assisted hatching (AH) practice ····· 233
7.1.2 The safety of laser-assisted ZP manipulations on preimplantation embryos ····· 235
7.1.3 The effect of laser-assisted ZP manipulations on the competency of embryo implantation ····· 237
7.1.4 Potential genes and mechanisms involved in blastocyst hatching ····· 239
7.2 Limitations of this thesis ····· 240
7.3 Future directions ····· 241
7.3.1 Further investigation of the embryo metabolism following laser-assisted ZP drilling ····· 241
7.3.2 Investigating the embryo implantation following laser-assisted ZP manipulation using *in vivo* model ····· 241
7.3.3 The future clinical studies ····· 242
7.3.4 Investigating the mechanism underlying embryo hatching ····· 243
7.4 General conclusion ····· 244
REFERENCES ····· 245

SUPPLEMENTARY APPENDICES **274**

Supplementary appendix 1 275
Supplementary appendix 2 279
Supplementary appendix 3 281
Supplementary appendix 4 282
Supplementary appendix 5 283
Supplementary appendix 6 284
Supplementary appendix 7 288
Supplementary appendix 8 289
Supplementary appendix 9 290
Supplementary appendix 10 292
Supplementary appendix 11 297
Supplementary appendix 12 299
Supplementary appendix 13 300

RESEARCH OUTPUT **301**

International peer-reviewed papers 301
Presentation at international and university conferences 301
Prizes and awards 302

List of abbreviations

The following is an explanation of commonly used abbreviations used throughout the text. Others, less commonly used abbreviations are explained within the text where appropriate.

ACE ····· Association of Clinical Embryologists
Actb ····· Actin beta gene
AGT ····· Angiotensinogen
AH ····· Assisted hatching
Aqp3 ····· Aquaporin 3 gene
ART ····· Assisted reproductive technology
ASRM ····· American Society for Reproductive Medicine
ATP ····· Adenosine triphosphate
Atp5b ····· ATP synthase F1 subunit Beta gene
Bax ····· BCL2 associated X gene
Bcl2l2 ····· BCL2 like 2 gene
cDNA ····· Complementary deoxyribonucleic acid
CDX2 ····· Caudal type homeobox 2
Cox8a ····· Cytochrome c oxidase subunit 8A gene
Ctsh ····· Cathepsin H gene
DAPI ····· 4′,6-diamidino-2-phenylindole
DEGs ····· Differentially expressed genes
DNA ····· Deoxyribonucleic acid
Dnmat3a ····· DNA methyltransferase 3A gene
Dnmt3l ····· DNA Methyltransferase 3 Like gene
ESHRE ····· European Society of Human Reproduction and Embryology
ET ····· Embryo transfer
FBS ····· Foetal bovine serum
FGF2 ····· Fibroblast growth factor 2
Gapdh ····· Glyceraldehyde-3-phosphate dehydrogenase gene
GO terms ····· Gene Ontology terms
Gpx7 ····· Glutathione peroxidase 7 precursor gene

HFEA ····· Human Fertilisation and Embryology Authority

HSP70 ····· Heat shock stress 70

ICM ····· Inner cell mass

ICSI ····· Intracytoplasmic sperm injection

IPA ····· Ingenuity Pathway Analysis

IVF ····· *In vitro* fertilisation

KEGG ····· Kyoto Encyclopedia of Genes and Genomes

Krt18 ····· Keratin 18 gene

KSOM ····· Potassium simplex optimization medium

LAH ····· Laser-assisted hatching

Lgals1 ····· Lectin, galactoside-binding, soluble, 1 gene

Lmna ····· Lamin A/C gene

Mvd ····· Mevalonate diphosphate decarboxylase gene

Mvk ····· Mevalonate kinase gene

Myl6 ····· Myosin light polypeptide 6 gene

NANOG ····· Nanog homeobox

Ndufa7 ····· NADH dehydrogenase 1 alpha subcomplex subunit 7 gene

OCT4 ····· Octamer-binding transcription factor 4

PBS ····· Phosphate buffered saline

PGT ····· Preimplantation genetic testing

Pou5f1 ····· POU class 5 homeobox 1 gene

PPI ····· Protein and protein interactions

PreAmp ····· Preamplification

RhoA ····· Ras homolog family member A

RNA ····· Ribonucleic acid

Rnd3 ····· Rho family GTPase 3 gene

RT-qPCR ····· Reverse transcription quantitative polymerase chain reaction

Sod1 ····· Superoxide dismutase 1 gene

SRF ····· Society for Reproduction and Fertility

TdT ····· Terminal deoxynucleotidyl transferase

TE ····· Trophectoderm

TEPs ····· Trophectodermal projections

TUENL ····· Terminal deoxynucleotidyl transferase dUTP nick end labelling

ZP ····· Zona pellucida

List of Figures

Figure 1-1. A schematic of mouse preimplantation embryo development.....4

Figure 1-2. Important transcription factors for mouse embryo lineage segregation.....6

Figure 1-3. The mouse embryo development and the zona pellucida 8

Figure 1-4. A schematic diagram of embryo implantation stages in humans...11

Figure 1-5. Implantation strategies in different species.....13

Figure 1-6. Schematic diagrams showing a 1480 nm diode laser device for ART applications 21

Figure 1-7. Laser-assisted polar biopsy 24

Figure 1-8. Laser-assisted blastomere biopsy 25

Figure 1-9. Laser-assisted trophectoderm biopsy.....27

Figure 1-10. The procedures commonly used for embryo LAH.....32

Figure 1-11. Laser-assisted blastocoele collapse.....35

Figure 1-12. Laser-assisted hatching and lysed cell removal 36

Figure 1-13. Resistance pattern of oolemma breakage during ICSI.....37

Figure 1-14. Laser-assisted ICSI.....38

Figure 1-15. The timing of the preimplantation development events in mouse (A) and human embryos (B).....47

Figure 2-1. A schematic showing the location of different stages of embryos in a mouse reproductive tract. 55

Figure 2-2. A schematic showing the procedures used to thaw frozen embryos. 56

Figure 2-3. A schematic showing the set-up for embryo culture dishes.....57

Figure 2-4. Morphological criteria for the inclusion of embryos 58

Figure 2-5. The laser-assisted ZP manipulation method used on mouse embryos during this research.....59

Figure 2-6. Morphological assessment of embryo development 60

Figure 2-7. Different hatching patterns 61

Figure 2-8. A schematic of the establishment of 2-dimension co-culture system 64

Figure 3-1. The geographical distribution of survey responders 83

Figure 3-2. The application rate of AH (assisted-hatching)..... 86

Figure 3-3. Opinions relating to AH among AH users 94

Figure 4-1. Representative images of the embryo hatching process using time-lapse imaging 114

Figure 4-2. Representative images of CDX2 and OCT4 staining of E4.5 blastocysts undergoing different laser ZP manipulations 116

Figure 4-3. A comparison of embryo cell number across different laser ZP manipulations groups 118

Figure 4-4. DNA fragmentation in E4.5 blastocysts undergoing different laser ZP manipulations 121

Figure 4-5. Caspase-3/-7 activation in E4.5 blastocysts undergoing different laser ZP manipulations 123

Figure 4-6. HSP70 expression in E4.5 blastocysts undergoing different laser ZP manipulation 126

Figure 4-7. A comparison of the expression of embryogenesis-related genes in E4.5 blastocysts undergoing different laser ZP manipulations..... 127

Figure 4-8. A comparison of the expression of apoptosis-related genes in E4.5 blastocysts undergoing different laser ZP manipulations 128

Figure 4-9. A comparison of *Dnmt3a* expression in E4.5 blastocysts undergoing different laser ZP manipulations..... 129

Figure 5-1. The expression of epithelial and mesenchymal cellular markers in Ishikawa cells 144

Figure 5-2. A schematic of the embryo-Ishikawa cells co-culture system 145

Figure 5-3. The *in vitro* mouse embryo implantation model 146

Figure 5-4. Representative images of Integrin αvβ3 and CDX2 staining in Ishikawa cells and the co-culture system 148

Figure 5-5. Representative images of osteopontin (OPN) and OCT4 staining in Ishikawa cells and the co-culture system 149

Figure 5-6. Representative images of scored embryo attachment using a four-point scale 150

Figure 5-7. The mouse embryo hatching and attachment in the *in vitro* implantation model from E4.5 to E7.5 151

Figure 5-8. The mouse embryo hatching and attachment in the *in vitro* implantation model from E5.5 to E8.5 156

Figure 5-9. A comparison of embryo hatching completion and attachment between E5.5 and E4.5 transferred embryos 158

Figure 6-1. A hypothetical schematic for mechanisms underlying embryo hatching 170

Figure 6-2. The workflow of RNA-sequencing (RNA-seq) and data analysis .. 174

Figure 6-3. A flow-chat showing RNA-seq experiment processing 181

Figure 6-4. Representative images of blastocyst samples for RNA-seq 182

Figure 6-5. Quality control assessment of resulted cDNA library 184

Figure 6-6. Advance quality control results of RNA-seq data from all samples (A) and samples excluding the outliners (B) 188

Figure 6-7. Differentially expressed genes (DEGs) between the hatching and pre-hatching blastocysts in the control group 190

Figure 6-8. The Gene Ontology (GO) analysis of differentially expressed genes (DEGs) between hatching and pre-hatching blastocysts in the control group 195

Figure 6-9. The canonical pathway analysis of differentially expressed genes (DEGs) between hatching and pre-hatching blastocysts in the control group 197

Figure 6-10. The Reactome pathways analysis of differentially expressed genes (DEGs) between hatching and pre-hatching blastocysts in the control group 199

Figure 6-11. Heatmaps of potential terms and pathways and related genes that are involved in the hatching process 200

Figure 6-12. Upstream regulator analysis of differentially expressed genes (DEGs) between hatching and pre-hatching blastocysts in the control group 202

Figure 6-13. The mouse embryo lineage-specific genes and differentially expressed genes between hatching and pre-hatching blastocysts 203

Figure 6-14. The MCODE (Molecular Complex Detection) predicted subnetwork of differentially expressed genes between hatching and pre-hatching blastocysts 206

Figure 6-15. Differentially expressed genes (DEGs) between laser-drilled hatching and control hatching blastocysts 208

Figure 6-16. Gene Ontology (GO) terms analysis of differentially expressed genes (DEGs) between laser-drilled hatching and control hatching blastocysts 211

Figure 6-17. Pathway enrichment analysis of differentially expressed genes (DEGs) between laser-drilled hatching and control hatching blastocysts 213

Figure 6-18. Validation of housekeeping genes in the comparison of hatching and pre-hatching blastocysts 215

Figure 6-19. Validation of housekeeping genes in the comparison of laser-drilled hatching and control hatching blastocysts 216

Figure 6-20. Validation of DEGs between hatching and pre-hatching blastocysts using qRT-PCR 218

Figure 6-21. Validation of DEGs between laser-drilled hatching and control hatching blastocysts using qRT-PCR 219

List of Tables

Table 1-1 The common causes of infertility.....15

Table 1-2 Assumed aetiologies for implantation failure and management 17

Table 2-1 The standard criteria for attachment stability measurement 65

Table 2-2. Antibody information 67

Table 2-3 The TaqMan assays used for the TaqMan preamplification and qPCR 72

Table 2-4 Primers used for the SYBER green qPCR experiment 76

Table 4-1 A comparison of embryo development across different laser ZP manipulation groups.....111

Table 4-2 A comparison of embryo hatching patterns across different laser ZP manipulation groups.....112

Table 5-1 A comparison of *in vitro* hatching and attachment across different laser-assisted ZP manipulations groups from E4.5 to E7.5.....153

Table 5-2 A comparison of the *in vitro* hatching and attachment across different ZP opening size groups.....155

Table 5-3 A comparison of *in vitro* embryo hatching and attachment across different laser ZP manipulation groups from E5.5 to E8.5 160

Table 6-1 Software and parameters for processing RNA seq data 180

Table 6-2 Sample preparation for RNA-seq 182

Table 6-3 The top 10 upregulated and downregulated DEGs between hatching and pre-hatching blastocysts in the control group 191

Table 6-4 The top-ranked upregulated and downregulated DEGs between laser-drilled hatching and control hatching blastocyst 209

Abstract

Mammalian embryo hatching from the zona pellucida (ZP) is a prerequisite to undergo subsequent implantation, but little is known about the involved molecules and regulatory mechanisms underlying the hatching process. Hatching failure can lead to implantation failure. Clinical laboratories have developed the non-contact infra-red diode laser to manipulate ZP for various purpose, such as assist embryo hatching and facilitate embryo biopsy procedure. Previous studies attempted to investigate the safety and efficacy of laser-assisted ZP manipulations; however, there is a significant paucity of safety evidence at the molecular level and the efficacy remains controversial. This thesis aimed to investigate the effect of laser-assisted ZP manipulations on embryo competency and transcriptome, and to uncover the regulatory mechanisms underlying the hatching process. In chapter 3, I analysed 181 questionnaires to characterise the clinical application pattern of ZP manipulation and found that laser-assisted ZP manipulation is extensively used in clinics, especially prior to embryo biopsy (89.5%). However, a huge disparity existed with regards to the current clinical practice, and no standardisation is evident at present. In chapter 4, mouse embryos were used to investigate the safety of the three most commonly used laser-assisted ZP manipulations, including ZP drilling (n=349), ZP partial drilling (n=319), and ZP thinning (n=297). No overt deleterious effects were identified with regards to the blastocyst development, cell apoptosis, heat shock stress (HSP70), and the expression of key developmental genes. However, the results demonstrated that laser-assisted ZP drilling significantly advance the hatching rate (81.1% (210) *vs* 40.1% (111), $P<0.0001$) and altered the pattern of embryo hatching at E4.5 ($P<0.0001$). In chapter 5, I further applied an Ishikawa cell *in vitro* implantation model to test the embryo attachment capability. The results demonstrated that laser-assisted drilling significantly increase the embryo entrapment rate (41.3% (19) *vs* 13.9% (28), $P<0.0001$) in a manner that may relate to the size of opening in ZP created by drilling. However, a potential benefit of laser-assisted drilling may occur for blastulation delayed embryos, shown by an improved attachment rate (100% (11) *vs* 50% (8), $P=0.006$). In chapter 6, I used the RNA-sequencing to compare the transcriptome of hatching (n=8) and pre-hatching mouse blastocysts (n=6), and 275 differentially expressed genes (DEGs) were identified (adjusted $P<0.05$). Furthermore, for the first time, the downstream analysis revealed that the *in vitro* blastocysts hatching is an ATP-dependent process; the significant activation of protein biosynthesis and organisation of cytoskeleton were also observed according to the transcriptomic alteration. In addition, the potential signaling pathway (such as RhoA signaling, Z-score=2.64, $P<0.05$) and upstream regulators (e.g., AGT, FGF2, and PRL) involved in the embryo hatching process were also revealed by the ingenuity pathway analysis. Finally, I further explored the effect of laser-assisted ZP drilling on embryo transcriptome using RNA-sequencing and found 48 DEGs (adjusted $P<0.05$). The downstream pathway analysis suggested the potential effect of laser-assisted drilling on embryo metabolic activity. In summary, this thesis provided safety evidence regarding the laser-assisted ZP manipulations, thus emphasising the importance of optimisation and refinement of clinical applications. Furthermore, this research also provides molecular profiling of hatching embryos, offering a useful asset for further exploring the mechanism underlying the embryo hatching process.



Chapter 1

General Introduction

1.1 Establishment of embryo implantation

The implantation of blastocysts into the maternal uterus is a crucial step in mammalian reproduction, the two critical components for successful implantation are the competent embryo and the receptive endometrium; together, these undertake intimate bilateral communication (Quenby et al., 2013, Aplin et al., 2017). In mammals, the beginning of a new life is seeded at fertilisation and followed by embryo development.

1.1.1 Preimplantation embryo development

The development of the preimplantation embryo encompasses the period from fertilisation to implantation (**Figure 1-1**). Since the development of mouse embryo has been studied extensively, I used the mouse embryos as a model to introduce preimplantation development. Fertilisation occurs in the fallopian tube (oviduct) and a one-cell zygote is formed by the fusion of a haploid sperm with a haploid oocyte on embryonic day 1 (E1.0). A zygote then undergoes several rounds of mitotic cell division by cleavage, producing increasing numbers of progressively smaller embryonic cells, known as blastomeres, without changes to the overall embryo size (Wang and Dey, 2006). A unique feature of the development at these stages is the presence of maternally stored RNAs and proteins. The initiation of transcription from the newly formed zygotic genome, known as zygotic genome activation (ZGA), is a remarkable transition during embryo development (Cockburn et al., 2010). The early cleavage divisions produce an 8-cell embryo that subsequently undergoes an increase in intercellular adhesion; this is known as embryo compaction. Embryo compaction is the first critical morphological event that transforms the embryo from a loose cluster of spherical cells into a tightly packed mass. After compaction, the mouse embryos

undergo two further rounds of cleavage, growing from 8-cell to 32-cells (Wang and Dey, 2006) .

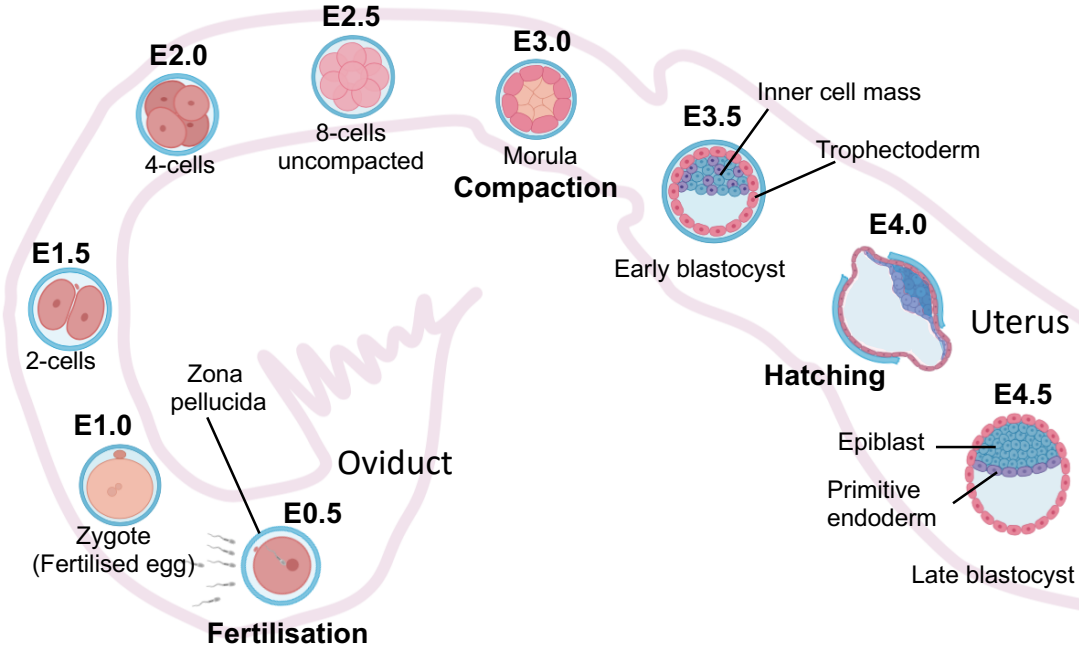


Figure 1-1. A schematic of mouse preimplantation embryo development

Following fertilisation in the oviduct, the mouse embryo undergoes several rounds of mitotic cell division and forms a compacted ball of cells called the morula. At the late morula stage, the embryo enters the uterine lumen and develops into a blastocyst containing a cavity with two distinct cell populations: the trophectoderm (TE), and inner cell mass (ICM). Before implantation, the blastocysts need to escape from the zona pellucida (ZP) and differentiates to produce additional cell types: the epiblast and primitive endoderm. Once the embryo has gained competency, the trophectoderm attaches to the endometrium to initiate implantation process. The image was created by the author with BioRender.com and adapted from (Wang and Dey, 2006).

As a result of cellular asymmetries, two distinct cell precursors are established: the blastomeres remaining outside are destined to form the trophectoderm (TE) linage, while the blastomeres inside the embryos are destined to form the inner cell mass (ICM) (Cockburn et al., 2010, Sozen et al., 2014). Starting from the 32-cell stage, the outside precursors begin pumping environmental fluids to form the fluid-filled cavity, known as the blastocoele (Waston and Barcroft, 2001). Blastocyst formation involves the activity of Na+/K+ ATPases, seals formed by tight junctions, and the water transporter aquaporin (Waston and Barcroft, 2001). The presence of a blastocoele is

essential for the development of the ICM and represents the first lineage segregation (Sozen et al., 2014).

TE and ICM linage segregation is controlled by a small group of transcription factors (**Figure 1-2**). Specifically, *Cdx2* (Caudal Type Homeobox 2) is required for TE development to enable epithelial specification; while the *Oct*-3/4 (pluripotency markers octamer-3/4), *Nanog* (Nanog Homeobox), and *Sox2* (SRY box-containing gene 2), are involved in establishing the ICM fate to promote pluripotency and resist differentiation (Sozen et al., 2014). *Cdx2* and *Oct-3/4* are ubiquitously co-expressed to maintain cells in an undifferentiated state; it is the interactions between these factors that promote the TE and ICM formation. In mouse embryos, the downregulation of *Oct-3/4* and the upregulation of *Cdx2,* following the fourth cleavage, trigger the differentiation of cells towards the TE. In contrast, the downregulation of *Cdx2* and the upregulation of *Oct-3/4,* trigger ICM differentiation. This reciprocal repression between lineage-specific transcription factors is the crucial event for establishing and maintaining TE/ICM segregation (Niwa et al., 2005, Strumpf et al., 2005). Mouse embryos take about 3.5 days to develop from the zygote to the blastocyst stage (Cockburn et al., 2010).

After blastocoele formation, two important events happen in the next 24 hours: the second lineage segregation of the ICM to the epiblast (EPI) and primitive endoderm (PE), and hatching from the zona pellucida (ZP). The PE is situated as a monolayer on the surface of the ICM, while the EPI is situated deep inside the ICM. A number of linage-specific transcription factors determine the second segregation: *Gata4*, *Gata6*, and *Sox17* lead to differentiation towards the PE fate; while *Nanog*, *Oct-3/4*, and *Sox2* are essential for EPI establishment by helping to promote pluripotency and escape differentiation (Sozen et al., 2014). Similar to the first segregation, reciprocal

repression between the linage-specific transcription factors *Nanog* and *Gata6*, is present for the second segregation (Yamanaka et al., 2010) (**Figure 1-2**). Once the embryo hatches out, the TE attaches to the endometrium of the uterus and initiates implantation, which occurs around E5.0.

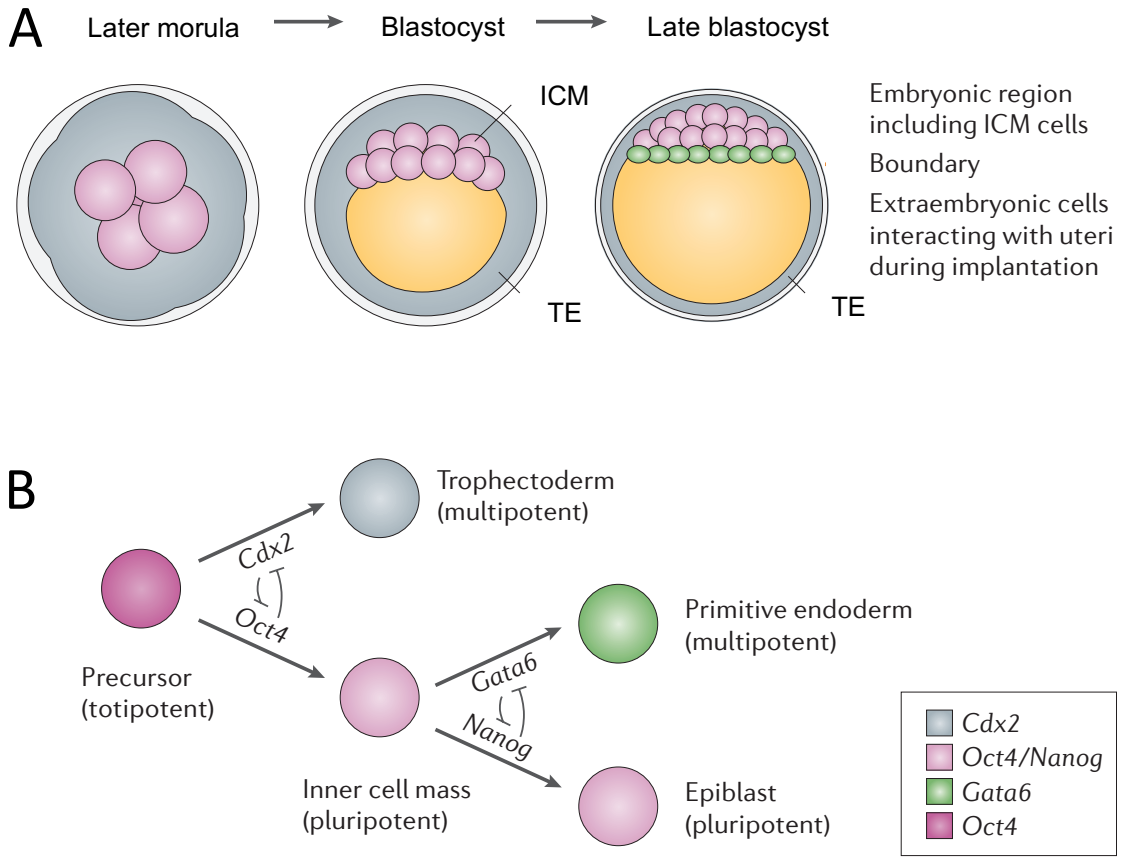


Figure 1-2. Important transcription factors for mouse embryo lineage segregation

This image represents the gene-expression pattern during blastocyst formation. *Oct4* (dark pink) is expressed throughout the embryo before the late morula stage. The expression of *Nanog* (light pink) is specifically induced in the inside cells of the late morula, while *Cdx2* (gray) is expressed in the outer layer of cells in the late morula. *Cdx2* is important for TE formation, and *Oct4* is crucial for ICM formation. At the late blastocyst stage, antagonism between *Nanog* and *Gata6* (green) segregates the epiblast and primitive endoderm within the ICM. *Gata6* is expressed in the primitive endoderm, where *Oct4* and *Nanog* are repressed. Images were adapted from (Wang and Dey, 2006).

1.1.2 Embryo zona pellucida and hatching

The mammalian embryo remains enclosed in a glycoproteinaceous coat, known as the zona pellucida (ZP), during preimplantation development. The ZP plays important

roles in the process of fertilisation and preimplantation development. The well-recognized functions of the ZP are the recognition of oocytes by the sperm and polyspermy blocking, the retention of blastomeres together during the cleavage period, and protecting embryo during the transport in the oviduct (Wassarman, 2008).

The mouse ZP is composed of 3 glycoproteins, designated as ZP1, ZP2, and ZP3; the human ZP is composed of ZP1, ZP2, ZP3, and ZP4 (Wassarman, 2008). In addition, the ZP is composed of bi-layered filaments: the filaments have a predominantly radial arrangement in the inner layer; whereas the filaments exhibit a laminal arrangement in the outer layer (Keefe et al., 1997). The thickness of the ZP varies from less than 2 μm to more than 25 μm for eggs and embryos from different mammals (Wassarman, 2008, Shafei et al., 2017). The diameter of fully mature mouse oocyte and early embryos is around 95 μm, and the oocyte ZP thickness is 6-7 μm. The diameter of human oocyte is 110-120 μm, and the ZP thickness is around 15-20 μm (Bleil et al., 1980, Wassarman, 1988, Khalili et al., 2013).

However, embryos must hatch from the ZP to gain competency to implant into the receptive endometrium (Shafei et al., 2017). *In vivo*, a human blastocyst hatches on day 6 or 7 after fertilisation, whereas the mouse embryos loses the ZP on late E4.0 or early E5.0 (McLaren, 1970, Sathananthan et al., 2003). Recent studies of embryo hatching process are mostly based on the observation of *in vitro* cultured human or mammalian embryos, especially using time-lapse imaging. The general scheme of embryo hatching is as follows: the blastocyst diameter increases as the embryo develops. Then, spontaneous ZP thinning occurs naturally, and the ZP becomes stretched and thinner (**Figure 1-3**). The human ZP thickness could reduce to 5 μm (Kirkegaard et al., 2012), and the mouse ZP thickness can reduce to 2.5-3 μm

(Leonavicius et al., 2018). Afterwards, the ZP breaks with the formation of a slot-like opening or by a direct of rupture. Human embryo hatching initiates 106-118 hours after fertilisation (Serdarogullari et al., 2014); mouse embryo hatching occurs approximately 88 to 116 hours after hCG (human chorionic gonadotropin) injection (Schimmel et al., 2014). Once the ZP has broken, the embryo performs active movements to escape through the gap. During this period, some of the blastocysts begin to undergo contractions, which is a series of successive steps involving collapse and bloating (Niimura, 2003). **Figure 1-3** shows mouse embryos ZP in different embryo stages and represents the typical hatching process.

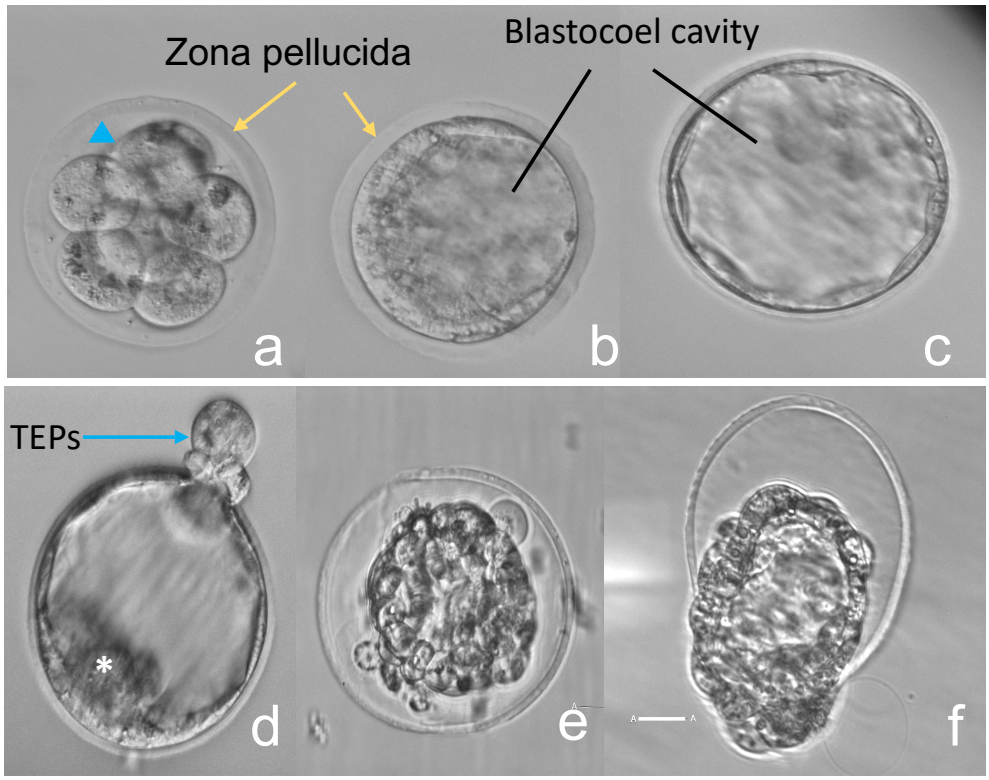


Figure 1-3. The mouse embryo development and the zona pellucida

(a) An 8-cell stage mouse embryo surrounded by the zona pellucida (ZP). The blue triangle indicates the perivitelline space (PVS). (b) An early blastocyst with the cavity formed, but the embryo volume and ZP thickness remain the same as cleavage stage embryo. (c) An expanded blastocyst, with increased total volume and a thinner ZP. (d) An embryo commencing the hatching process, with TEPs (trophectodermal projections) breaking the ZP. The asterisk indicates inner cell mass (ICM). (e) An embryo contracting, with a thinned and breached ZP. (f) An embryo undergoing the hatching process.

The hatching process is believed to be regulated by multiple factors, including the internal pressurization of the blastocyst cavity, dynamic cellular components known as trophectodermal projections (TEPs), and a variety of autocrine and paracrine molecules such as protease and growth factors (Shafei et al., 2017, Leonavicius et al., 2018). In addition, the *in vitro* hatching pattern and period is known to be influenced by the fertilisation method and the culture environment (e.g., oxygen concentration and the supplementation of growth factors and amnio acids) (Paria et al., 1990, Houghton et al., 2002, Zhan et al., 2018). Further details about the potential hatching mechanism are discussed in **Chapter 6**.

1.1.3 Embryo implantation

The physiological and molecular processes involved in implantation are intimate but highly organised. Apart from the implantation-competent blastocyst, uterine receptivity is also a significant factor to accommodate the competent embryos (Egashira et al., 2013). The uterus receptivity allows an appropriate endometrial preparation with stromal proliferation and epithelial differentiation stimulated by ovarian steroids before the phase of embryo-uterine interactions (Dey et al., 2004). In this process, the progesterone-dependent morphological changes in the endometrial stroma can be observed. Then, the small spike of ovarian oestrogen is followed by an acquisition of the endometrial status, and then the endometrium provides the embryo with adhesion activity. Therefore, the uterus enters into receptive phase (Weimar et al., 2013). However, the receptive phase of the uterus is transient, and unless the blastocyst adhesion occurs, the endometrium will enter into the refractory phase (Egashira et al., 2013). As a result, the endometrium is receptive to implantation in the restricted period, referred to as the 'window of implantation' (Egashira et al., 2013). In mice, the ‘window

of implantation' is estimated from day 4 to day 5.5 post-ovulation (Egashira et al., 2013); in humans, it is from approximately day 20 to day 24 of the menstrual cycle (Achache et al., 2006);.

An embryo will encounter the endometrium about 5 days after fertilisation (equivalently 4 days in mouse). Once hatched out, embryos gain implantation competency and start implanting into the endometrium (Chen et al., 2005, Yoshinaga, 2013). Embryo implantation is known as a three-step process: (1) the blastocyst becomes closely apposed to the endometrial luminal epithelium (apposition); (2) the trophoblast cells attach to the luminal epithelial surface (adhesion); and finally (3) the invasive trophoblast cells cross the endometrial epithelial basement membrane and invade into the underlying stromal cell compartment (invasion) (Weimar et al., 2013) (**Figure 1-4**).

Once positioned on the endometrium, the embryo begins to interact physically with the uterine epithelium for more stable adhesion; the association of the TE and epithelium is sufficiently intimate to resist the dislocation of blastocyst by flushing the uterine lumen. By this time, the trophoblast cells at the implantation site have formed masses of cytotrophoblasts and syncytiotrophoblasts. During the invasion phase, syncytiotrophoblasts penetrate through the endometrial epithelium and then the underlying basement membrane to invade the endometrial stroma. Eventually, the trophoblast cells destroy the wall of the maternal spiral arteries, converting them into the flaccid sinusoidal sacs lined with endovascular trophoblast, so that the maternal spiral arteries can maintain high blood flow between the foetus and the mother (**Figure1-4**) (Dey et al., 2004, Weimar et al., 2013, Davidson et al., 2016).

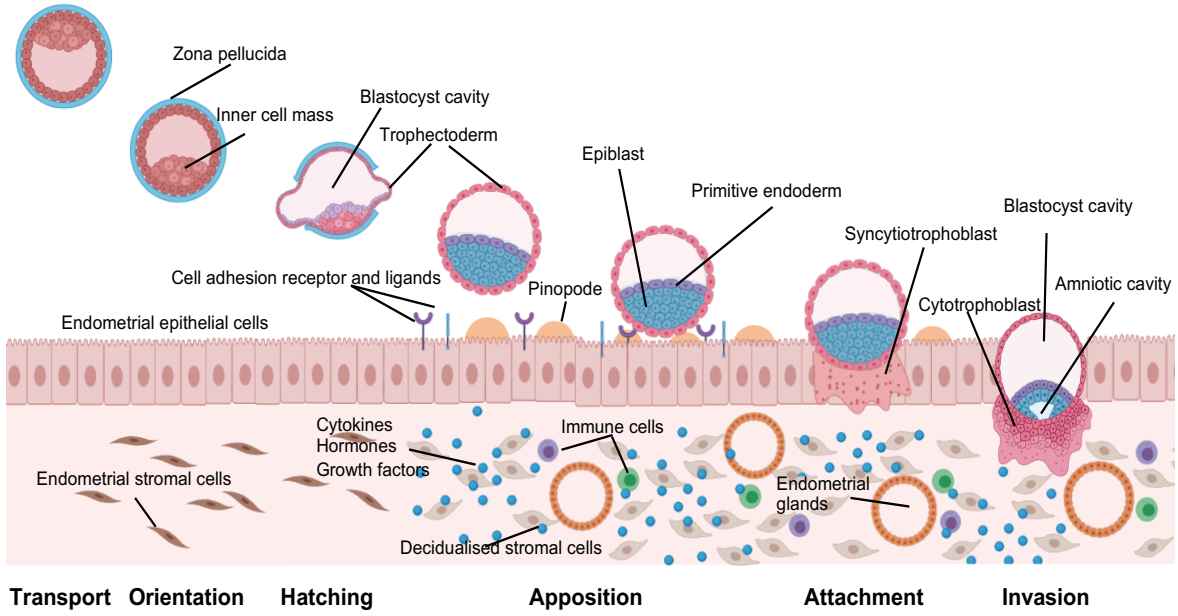


Figure 1-4. A schematic diagram of embryo implantation stages in humans

An illustration of an embryo arriving at the uterine cavity and the subsequent implantation process. The inner cell mass shows orientation towards the endometrial lining and the embryo hatches from the ZP. The embryo, in close contact with the endometrium (apposition), starts to attach to the endometrial epithelium via polar trophectoderm (attachment). Finally, the trophoblast cells proliferate and differentiate into the inner cytotrophoblast and outer syncytiotrophoblast. The syncytiotrophoblast invades into the decidualised endometrium.

1.1.3.1 Differences in implantation between species

Despite the common steps of implantation and eventual placentation, the mechanism underlying how these stages are accomplished is species dependent. Based on ultrastructural studies, there are different modes of implantation: trophectoderm-derived trophoblast cells can breach the uterine luminal epithelium (LE) (displacement), coalesce (fuse) with it, or trespass (intrusive) between the uterine epithelial cells to invade into the underlying stroma (Dey et al., 2004, Wang and Dey, 2006).

The blastocyst of mice, rats, and hamsters are small and show only modest expansion. In these species, the implantation chambers are formed by invagination of the luminal epithelium, which surround the trophoblast. In addition, the attachment of the blastocyst to the epithelium imparts the local epithelial apoptosis at the site of attachment, thus facilitating the penetration of trophoblast cells through the LE layer into the stroma (Dey et al., 2004, Wang and Dey, 2006) (**Figure 1-5 A**).

For guinea pigs, the blastocysts become embedded in the wall of the uterus; this is known as the interstitial mode of implantation. The blastocyst develops an implantation cone composed of the syncytiotrophoblast at the opposite pole from the ICM. This implantation cone makes focal protrusions through the ZP and intrudes between epithelial cells, eventually embedding the embryo into stroma (Wang and Dey, 2006, Carter, 2007) (**Figure 1-5 B**).

In the human and primates embryo, the syncytiotrophoblast is formed near the ICM, which then invades into the stroma by intruding between the epithelial cells and by penetrating the basal lamina (Wang and Dey, 2006, Nimbkar-Joshi et al., 2009) (**Figure 1-5 C**). The last model of implantation is seem in rabbits, clusters of trophoblast cells adhere to the apices of the LE and fuse with the apical ends of the epithelial cells to form the symplasma, before penetration into the stroma (Wang and Dey, 2006, Nicholls et al., 2011) (**Figure 1-5 D**).

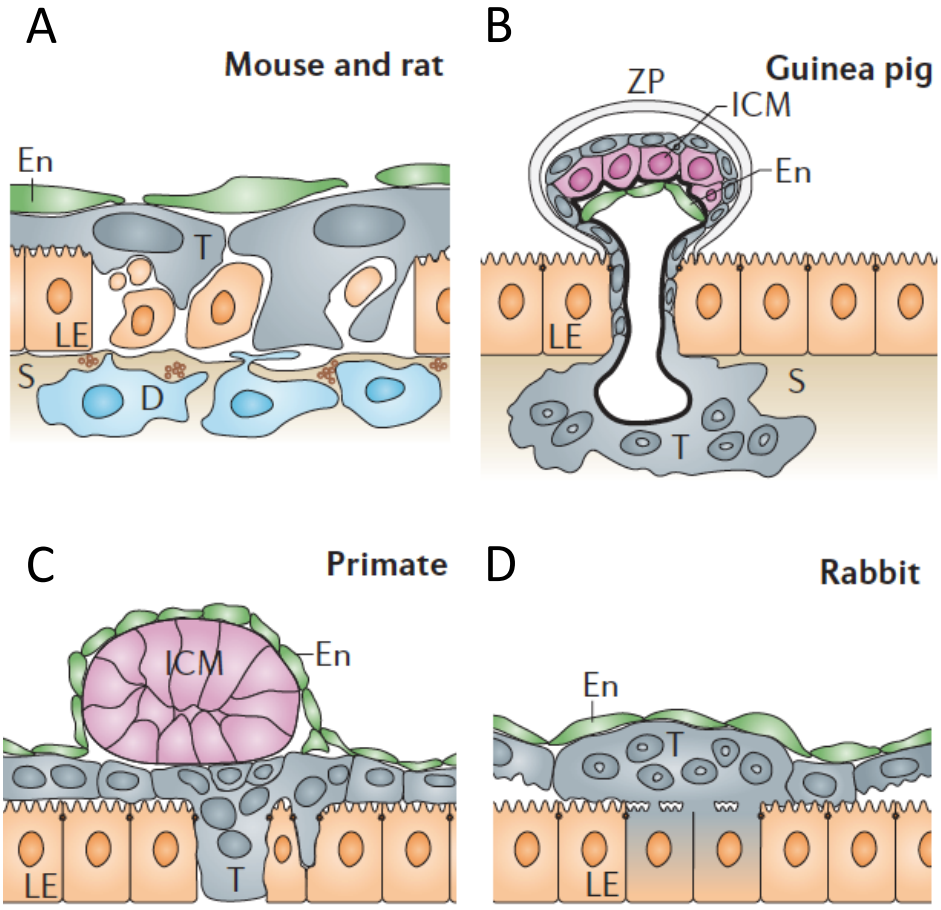


Figure 1-5. Implantation strategies in different species

A schematic illustrating different modes of implantation. (A) In mouse and rat, the blastocyst penetrates the luminal epithelium layer by imparting local apoptosis in the epithelial cells at the site of attachment. (B) In the guinea pig, the syncytial trophoblast (opposite to the ICM) makes a focal protrusion through the ZP and penetrates between the epithelial cells. (C) In primates, the syncytial trophoblast (near the ICM) intrudes between the uterine epithelial cells and penetrates the basal lamina. (D) In the rabbit, the cluster of trophoblast cells fuse with the epithelial cells. En: Embryo endoderm; T: syncytial trophoblast; LE: luminal epithelium layer; S: uterine stroma; D: decidual cells; ICM: inner cell mass. ZP: zona pellucida. Images were adapted and modified from (Wang and Dey, 2006).

1.2 Infertility and assisted reproductive technology (ART)

Infertility has become a common health issue, with 9-18% of the general population of reproductive age experiencing difficulty to conceive (Aghajanova et al., 2017). Clinical infertility is diagnosed as the failure of conception after at least 12 months of unprotected intercourse (American Society for Reproductive Medicine and Society for Assisted Reproductive Technology [ASRM], 2013). Normally, after 12 months, 85% of couples attempting conception will have been successful. However, human reproduction is considered highly inefficient. Even among fertile couples, the probability of achieving a pregnancy in one menstrual cycle is only approximately 20-30% (Zinaman et al., 1996).

1.2.1 Aetiology of infertility

Approximately 20-30% of infertility cases are caused by physiological problems in men, 20-35% in women, and 25-40% of cases are because of problems in both partners. However, in 10-20% cases, no cause is found (Tharakan et al., 2018). According to clinical assessments and diagnostic investigations, fertility problems can be summarised into four different categories: ovulation disorders, tubal infertility, uterine/cervical infertility, and male infertility. Furthermore, unexplained, or idiopathic infertility can be caused by many factors, such as fertilisation failure, unusual gamete factors, implantation failure, and imbalanced maternal immunity. However, these factors are difficult to be evaluated or cannot be evaluated in an appropriate manner. Types of infertility and the common related causes are listed in **Table 1-1** (Irvine, 1998, Smith et al., 2003, Ray et al., 2012, Fields et al., 2013).

Table 1-1 The common causes of infertility

Adapted and modified from (Smith et al., 2003, Ray et al., 2012, Fields et al., 2013)

Type of infertility	Common causes
Ovulation disorders	Ageing: a decline in ovarian reserve Disorder of gonadotrophin regulation: Hyperprolactinemia, Kallmann syndrome, and weight loss. Gonadotropin deficiency: pituitary tumour Disorder of gonadotrophin action: polycystic ovary syndrome (PCOS) Premature ovarian failure: genetic and autoimmune factors.
Tubal abnormalities	Pelvic inflammatory disease, previous ectopic pregnancy, previous tubal surgery.
Uterine/cervical causes	Congenital uterine anomaly, endometriosis, fibroids, polyps, and infection issues.
Male infertility	Sperm disorders (oligozoospermia, azoospermia), varicoceles, obstruction, ejaculatory or sexual dysfunction, or immunological infertility.
Unexplained infertility	Maternal immunity disorders, fertilisation failure, defective embryo, tubal transport problems, implantation failure.

1.2.2 Assisted reproduction technology

ART has expanded significantly over the past 40 years since the first *in vitro* fertilisation (IVF) baby was born in 1978. Many underlying causes of infertility have been overcome by IVF and embryo transfer (ET) techniques, and it is now estimated

that more than 9 million babies have been born worldwide using ART (European society of human reproduction and embryology [ESHRE], 2016). During conventional ART cycle, ovarian stimulation is firstly carried out to achieve the growth of multiple follicles and the collection of multiple eggs. Then, the oocytes are fertilised by sperm *in vitro* and then cultured to develop embryos, which are then monitored and transferred to the uterus 3-6 days after fertilisation (Farquhar et al., 2018). In addition, revolutionary techniques, such as intracytoplasmic sperm injection (ICSI), gamete and embryo cryopreservation, and preimplantation genetic testing (PGT), have been widely applied to improve the success rate of infertility treatment and health of offspring.

Nevertheless, the implantation rate and live birth rate following ART remains disappointingly low. According to the United State (US) national summary from the National Centre for Chronic Disease Prevention and Health Promotion (CDC), the pregnancy rate is 52.9% per transfer in <35 years old women, whereas implantation rate and live birth rate drops to 41.8% and 45% per transfer, respectively. In addition, the success rates decrease as female age increases (CDC, 2016). In some cycles, embryos do not implant successfully, even after the transfer of morphologically good-quality embryos. Embryo implantation failure, and especially recurrent implantation failure (RIF), has become a significant challenge in ART (Bashiri et al., 2018).

1.2.3 Implantation failure and treatment

During natural pregnancy, it is estimated that the incidence of pregnancy loss after natural implantation is 25%-40% (Zinaman et al., 1996). However, the incidence of implantation failure after ART accounts for 75% of the pregnancy loss; these cases are not clinically recognized as pregnancies (Norwitz et al., 2001). In clinical practice,

implantation failure can only be diagnosed in the setting of IVF/ICSI-ET cycles, given that natural implantation failure may occur unnoticed (Comins-Boo et al., 2016). Although implantation failure represents the major limiting factor in ART, the aetiology of this problem remains elusive. The causes of implantation failure can be generally classified as maternal and embryological factors. Maternal factors include alternations in endometrial receptivity, an unfavourable immune system, and the blood hypercoagulability state. On the other hand, chromosomal abnormalities, oocyte defects, ZP hardening, and suboptimal embryo development represent the embryonic reasons underlying implantation failure (Margalioth et al., 2006, Comins-Boo et al., 2016, Bashiri et al., 2018). **Table 1-2** shows the potential causes of implantation failure and related treatments.

Table 1-2 Assumed aetiologies for implantation failure and management

Data adapted and modified from (Simon et al., 2012, Bashiri et al., 2018)

Factors	Causes	Management
Defective embryonic development	Genetic abnormalities	Karyotyping, PGT-A
	Zona abnormality (thickening, hardening)	Assisted hatching
	Suboptimal culture and embryo transfer (ET) conditions	Improving embryo culture and ET technique
Decreased endometrial receptivity	Uterine cavity abnormalities	Hysteroscopy
	Thin endometrium	Treatment of thin endometrium
	Endometriosis	Treatment of endometriosis
	Hydrosalpinx	Salpingectomy
	Altered expression of receptive endometrial molecules	Endometrial scratching

Table 1-2 (continued)

	Immunological factors: Antiphospholipid syndrome, Thyroid autoimmunity, Celiac disease, Pro-inflammatory disbalance, and NK cell expansion.	Immunotherapy (intravenous immunoglobulin, steroids, and aspirin)
Other factors	Thrombophilia	Anticoagulant therapy
	Infection	Antibiotics
	Suboptimal ovarian stimulation	Personal stimulation protocols
Risk factors	Maternal age Smoking BMI	Lifestyle intervention

Chromosomal abnormality, especially aneuploidy, is well established as the major cause for repeated implantation failure. Moreover, the increased incidence of chromosomal translocation, mosaicism, inversions and deletions has been demonstrated in women with higher-order implantation failure (Das et al., 2012). To reduce implantation failure induced by chromosomal abnormality, clinics are increasingly applying parental karyotype testing and preimplantation genetic screening. Using preimplantation genetic testing for aneuploidy (PGT-A) and selecting chromosomally normal embryos for transfer lead to a significant increase in the implantation rates of patients suffering from recurrent implantation failure (Margalioth et al., 2006, Das et al., 2012, Bashiri et al., 2018).

The ZP abnormality is considered to be another potential factor that contributes to implantation failure in that the embryo fails to escape from the ZP, thus resulting in impaired implantation (Das and Holzer, 2012). It was reported that the thickness and density of the human embryo ZP are both quantitatively correlated with embryo quality and pregnancy rate; embryos presenting with a thick ZP (>15 μm) may have a reduced

ability to hatch (Germond et al., 2000). Furthermore, the hardness and thickness of the ZP has been shown to be correlated with patients age, basal FSH (follicle-stimulating hormone) level, and oestradiol level (Germond et al., 2000, Jing et al., 2015). A secondary hardening of the ZP is suspected to occur during *in vitro* culture and manipulations, which may be related with the prolonged exposure to the artificial culture medium, cryopreservation procedures, or temperature changes (Petersen et al., 2006, Davidson et al., 2019). Consequently, a procedure known as assisted hatching (AH) is offered to promote embryo hatching, thus improving the success rate of implantation, especially in patients with recurrent implantation failure or when using frozen/thawed embryos (Margalioth et al., 2006, Das and Holzer, 2012, Davidson et al., 2019).

1.3 The development of laser technology in ART

The use of laser techniques to manipulate gametes and embryos began in the late 1980s and early 1990s. The first solid-state laser applied in this field was used to trap sperms, which is a neodymium: yttrium-aluminium garnet (Nd:YAG) laser operating at a wavelength of 1064 nm (Tadir et al., 1989, 1990). After that, Tadir et al. (1991) coupled an Nd:YAG laser with a potassium titanylphosphate crystal to double the working wavelength to 532 nm; and the laser was applied tangentially to the sphere of the oocyte in order to drill the ZP of oocytes (Tadir et al., 1991). Over the next few years, multiple groups explored the ability of different lasers to manipulate preimplantation embryos.

Early laser techniques were found effective for drilling the ZP in animal models; however, these lasers had limited value for clinical application because of the

increased the risk of cytotoxic and mutagenic effects, caused by the DNA-damaging range of UV light (Kochevar, 1989). In 1992, the erbium-yttrium-aluminium-garnet (Er:YAG) laser was introduced, which operated in the near infra-red range (at a wavelength of 2900nm, outside of the DNA-damage range) and therefore avoided potential genetic damage to embryos (Feichtinger et al., 1992). However, this laser required direct contact between the laser fibre and the gametes/ embryos, thus raising further concerns related to contamination (Obruca et al., 1994).

The following years saw the emergence of non-contact lasers working in the infra-red or near infra-red range (800-1500nm), further away from the DNA absorption peak of 260nm. The first laser to have a significant impact upon the advancement of ART was the indium-gallium-arsenic-phosphorous (InGaAsP) semiconductor diode laser, operating at 1480nm (infra-red) (Rink et al., 1994). Rink et al. were the first to use this InGaAsP laser to drill mouse oocytes without the need for direct contact or micromanipulation to stabilize the oocytes (1994). In contrast, the 2100nm holmium:yttrium-scandian-gallium-garnet (Ho:YSGG) laser could be applied when embryos moved to quartz slides, thus limiting the clinical application (Ebner et al., 2005).

Since the first live birth using 1480 nm laser was reported in 1995 (Germond et al., 1995b), this laser has become a valuable tool for ART, and is still commonly used today (Davidson et al., 2019). To ensure the consistent, reliable and reproducible results during ART manipulations, the laser must be integrated into the equipment required for routine laboratory procedures in an efficient and non-hazardous manner (Germond et al., 2000). Modern infrared (IR) diode lasers are constructed such that the 1480nm laser beam was coupled with a visible aiming pilot red-light laser beam

(630-650 nm); these collinear beams were directed through an inverted microscope objective of 40X or 20X magnification. These objectives are then fitted onto inverted microscopes with bright field, phase contrast, and Hoffman modulation optics, which are used routinely in ART (**Figure 1-6**) (Germond et al., 2000).

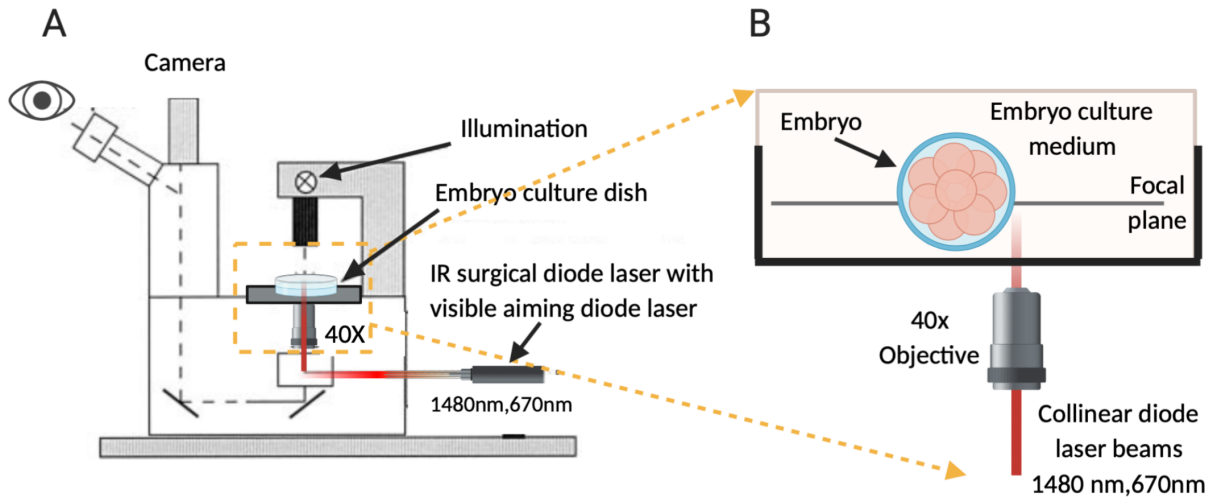


Figure 1-6. Schematic diagrams showing a 1480 nm diode laser device for ART applications

(A) The diode laser system includes an inverted microscope, camera, and computer (not shown) to provide an optical system for laser-assisted applications. A visible aiming pilot red-light laser beam (630-650 nm) is coupled with the 1480 nm laser. The collinear laser beams are then injected into the inverted microscope and then directed along the microscope's optical axis. (B) The two beams are focused on the object plane by a 40X microscope objective. Figures were adapted and modified from (Germond et al., 2000).

The unique absorption characteristics of 1480nm laser beam in water and culture media allowed for non-contact application in standard culture dishes, thus enabling routine application without special equipment or additional steps (Montag et al., 2009). This system presents an ideal tool for microsurgical procedures, as energy is easily focussed on to the targeted area, thus producing a controlled and precise hole that remains consistent between operators (Germond et al., 2000).

1.4 Laser applications in the embryo micromanipulation

1.4.1 Laser-assisted embryo biopsy

The genetic testing and diagnosis of embryos is becoming increasingly applied to test for chromosomal abnormality and hereditary disorders, respectively. In particular, in clinics PGT-A has been developed as a common clinical tool for improving implantation and reducing the risk of miscarriage (Das and Holzer, 2012). Embryonic cells must first be biopsied from a viable preimplantation stage embryo in order to perform such tests. There are three types of biopsy technique performed to obtain genetic material for testing: (1) polar body biopsy, which involves the genetic screening of material from the unfertilized maternal oocyte; (2) blastomere biopsy, where a single cell is extracted from a cleavage stage embryo, and (3) trophectoderm (TE) biopsy, where a cluster of trophectoderm cells from a blastocyst-stage embryo are collected.

Before the laser technique was adapted into an embryo biopsy procedure, acid Tyrode's solution was first used to create a hole in the ZP for biopsy purpose. In addition, a mechanical method was developed as an alternative; this used sharp glass pipettes to breach the ZP (Tarín et al., 1993). However, both acid and mechanical techniques are highly variable and lead to inconsistent hole sizes. In current clinical practice, laser is the preferred method of choice since it simplifies the process, shortens the biopsy time, and reduces damage to the oocyte or embryo, while resulting in more intact blastomere cells and equivalent pregnancy outcomes (Joris et al., 2003, Chatzimeletiou et al., 2005, Geber et al., 2011, Aoyama et al., 2020). According to the ESHRE PGT Consortium data collection XVI-XVIII (2020); by 2015, the use of Acidic

Tyrode's solution for zona breaching was almost entirely replaced by laser-assisted zona drilling, the latter practice covering 98% of all PGT cycles.

1.4.1.1 Laser-assisted polar body biopsy (PBB)

Polar bodies are by-products of the mitotic division of the oocyte and not required for fertilisation and embryo development. In comparison with blastomere biopsy and TE biopsy, PBB avoids false-positive errors due to the appearance of mosaicism; however, it only provides maternal genetic information, which accounts for 90% of human aneuploidies (Schenk et al., 2018).

Laser-assisted polar body biopsy was first explored in 1997 by Montag and colleagues. They found that a laser diode beam (to drill a 14- to 18-μm opening in the ZP) combined with the use of blunt-ended micropipettes greatly reduced the risk of damage to the zygote or polar body, by avoiding the deformation of embryos (Montag et al., 1998). The authors suggested that the laser-assisted microdissection of the ZP makes PBB more accurate and effective (Montag et al., 1998). In addition, it was demonstrated that laser-assisted PBB had no deleterious effects on *in-vitro* matured oocytes, in terms of oocyte lysis, oocyte activation, or chromosome breakage in embryos (Hammoud et al., 2010). **Figure 1-7** shows a typical laser-assisted polar body biopsy.

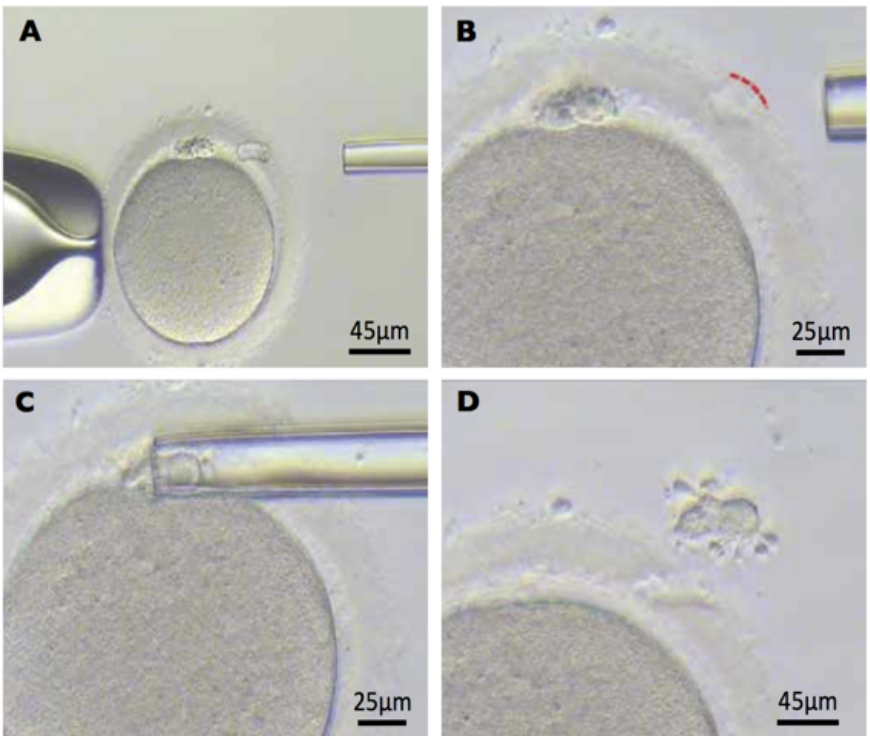


Figure 1-7. Laser-assisted polar biopsy

A laser was used to drill a gap in the ZP of oocyte (A and B) (the red dashed line shows the gap), and the polar body is then harvested for genetic analysis using a blunt micropipette (C and D). Images were adapted from (Davidson et al., 2019).

1.4.1.2 Laser-assisted blastomere biopsy

Blastomere biopsy for PGD has become a well-accepted method; this is because of its diagnostic ability for both maternal and paternal contributions, especially for severe monogenic disorders. Blastomere biopsy was still the most commonly used method of all biopsy procedures (70%, 65% and 58%) performed in Europe between 2013 and 2015 (ESHRE, 2020). Since the first application of laser-assisted blastomere biopsy were reported (Boada et al., 1998), laser pulses have been extensively used in this clinical procedure (Joris et al., 2003). During blastomere biopsy, a diode laser is used to create a 20 to 50 µm in the ZP adjacent to the blastomere to be removed. The desired blastomere is then gently aspirated with a biopsy pipette while avoiding contact or disruption of the remaining cells of the embryo (**Figure 1-8)**. Compared to

acid Tyrode method, using a laser to open the ZP for blastomere biopsy was found to be an easier procedure, resulting in significantly more intact blastomeres (Joris et al., 2003). In addition, it was reported that laser-assisted blastomere biopsy does not impair embryonic development, blastocyst expansion, or the number of cells in the ICM and TE (Jones et al., 2006).

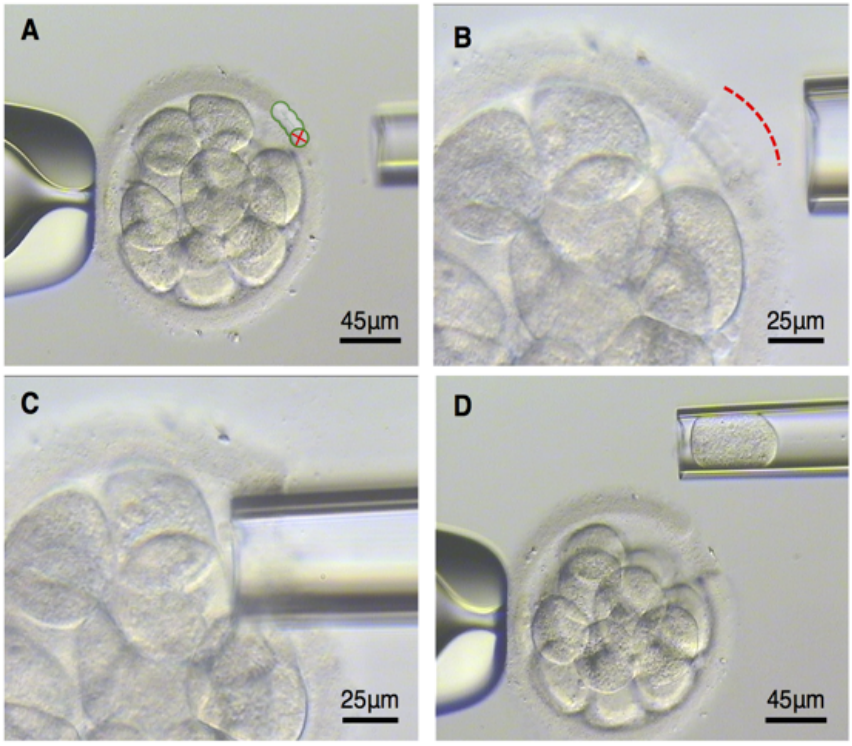


Figure 1-8. Laser-assisted blastomere biopsy

A cleavage-stage embryo is positioned by a holding pipette and treated with a laser pulse to create an opening in the ZP (A and B) (the dashed line indicates laser-drilled opening). A glass micropipette is inserted into ZP and to extract a blastomere, which is the close to the periphery of the embryo (C), followed by blastomere extraction (D). Images were adapted from (Davidson et al., 2019)

Nevertheless, blastomere biopsy is an invasive procedure that involves breaching the ZP and disrupting of cell adhesion. The negative results of blastomere biopsy were shown in the time-lapse studies with delayed embryo compaction, embryo blastulation, and embryo hatching (Bar-El et al., 2016). In addition, blastomere biopsy was shown to impair human embryo implantation (Scott et al., 2013a). Furthermore, the potential

risk of impaired pre- and postnatal development following blastomere biopsy was demonstrated in a mouse model (Sampino et al., 2014). These studies have encouraged clinicians and scientists to investigate the potential long-term risk of this technique. Further studies of the effect of blastomere biopsy on the long term health of offspring is clearly necessary (Zacchini et al., 2017).

1.4.1.3 Laser-assisted trophectoderm biopsy

Trophectoderm (TE) biopsy is performed between days 5 to 7 post-fertilisation. The advantage of blastocyst biopsy is that multiple TE cells can be collected for genetic analysis, thus allowing for more reliable results. Furthermore, TE biopsy is non-invasive to the inner cell mass (ICM), so that it won't affect the foetal development. Although the majority of biopsies are still performed at the cleavage stage, the use of TE biopsy expanded and accounted for 36% of all PGT-A cycles in 2015, with comprehensive diagnostics increasing to 58% (Coonen et al., 2020). Compared to blastomere biopsy, TE biopsy has no measurable impact on embryonic developmental competence, in terms of implantation and live-birth rates (Scott et al., 2013b). TE biopsy even resulted in significantly higher implantation rate in one previous study (Kokkali et al., 2007).

Historically, ZP breaching and TE cell collection were performed by mechanical methods. However, according to good practice recommendations from the ESHRE, the use of non-contact lasers is highly recommended for blastocyst biopsy, first to make a hole in the ZP, and second to excise the TE cells (2020). The laser procedure is much faster, requires less experience and skill, and imposes less mechanical stress on the blastocyst (Montag et al., 2009). Several procedures for TE biopsy are used in clinical practice: (1) pre-hatching may be performed on day 3-4 post fertilisation to

allow hatching and TE herniation formed, with the removal of TE cells on day 5-7 (**Figure 1-9**); (2) pre-hatching may be performed early on the day of blastocyst formation, followed by a period of culture to allow hatching before the removal of TE cells; (3) simultaneous ZP opening and TE cell excision on the day of full blastocyst expansion (ESHRE, 2020). However, an optimal protocol for TE biopsy has yet to be approved. The vital TE biopsy procedures have been discussed the in Naoki's review, including whether to perform pre-hatching or not, the optimal time for ZP drilling, the size of pre-hatching opening, or the time required to perform the biopsy. The authors claimed that each technique of TE biopsy has benefits and disadvantages (Aoyama et al., 2020).

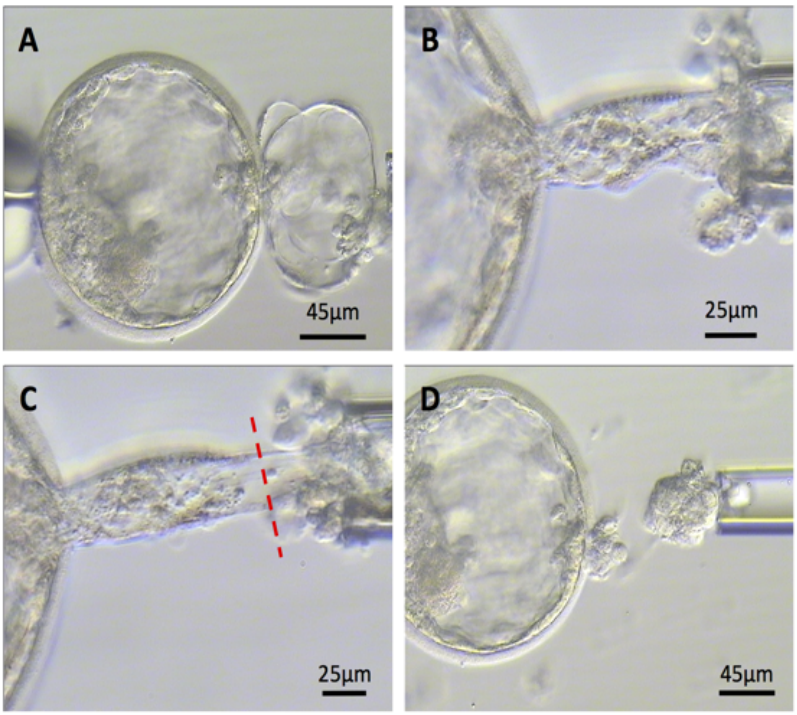


Figure 1-9. Laser-assisted trophectoderm biopsy

In this method, prehatching is conducted on day 3, allowing part of the trophectoderm to begin to hatch out from the ZP through the small opening drilled by the laser (A). An aspiration pipette is then used to hold the herniated cells and create tension between the hatched cells and the rest of embryo (B). The laser pulses are applied at the cell junction to separate the trophectoderm cells from the embryo (the red dashed line indicates the continuous laser pulses) (C). Finally, a micropipette is used to collect the trophectoderm cells (D). Images were adapted from (Davidson et al., 2019).

Apart from drilling ZP, laser pulses can be applied in the TE biopsy procedures: in the 'pulling' method of TE biopsy, blastocysts are held firmly with the holding pipette, and the biopsy needle is used to pull TE cells away from the blastocyst (**Figure 1-9**). At the same time, laser pulses are applied at the cell junction to separate the trophectoderm cells from the embryo (Aoyama et al., 2020). An abstract presented at the 2019 ESHRE conference claimed that the this method results in a higher percentage of intact biopsied cells (Marina et al., 2019).

Nevertheless, there is a controversy about whether laser-assisted biopsy will introduce mosaic or chaotic changes to the biopsied cells (Aoyama et al., 2020). One study used H1 human embryonic stem cell models to quantify laser impact, and showed that laser in the range of common usage for TE biopsy had no impact on mosaic anomalies (Kelk et al., 2017). In contrast, a clinical retrospective study showed that mosaicism apparently increased when more than 7 laser pulses were applied, although this was based on the small sample size; no significant implication of laser parameters on the incidence of mosaicism was found (Scarica et al., 2018). Furthermore, Herrero et al. claimed that when compared with the 'flicking' method, the 'pulling' method of TE biopsy needs more laser shots and may increase the risk of mosaicism (Herrero et al., 2019). Thus, it was assumed that the number of laser shots given during TE biopsy may both influence the induction of mosaicism. However, sample quality and biopsy technique may also affect the results (Aoyama et al., 2020). However, the research regarding the effects of trophectoderm biopsy on the further development of offspring, epidemiological changes, and other changes at the molecular level, remains sparse (Zacchini et al., 2017).

1.4.2 Laser-assisted hatching (LAH)

Assisted hatching (AH) is a form of assisted reproductive technology in which an opening or weakness is made in the ZP to help the embryo escape from the ZP, thereby facilitating embryo implantation (Cohen et al., 1990). Although the exact mechanism underlying implantation improvement by AH remains unclear, there are several commonly recognized hypotheses: (1) AH provides a route for the transfer of nutrients from the culture medium, thus enhancing embryo development (Hershlag et al., 2005); (2) AH may promote the initiation of implantation since embryos can make contact with the endometrium through the ZP opening earlier than embryos with an intact ZP (Malter et al., 1989); (3) the artificial opening created by AH may serve as a channel for the exchange of metabolites and growth factors between the embryo and endometrium prior to hatching, which subsequently facilitates implantation (Hammadeh et al., 2011).

Previously, the primary technique for AH used by clinics was the mechanical method or the chemical method with acid Tyrode's solution (Hammadeh et al., 2011). With the development of non-contact infrared diode laser, the ease of use, efficiency, and reproducibility rendered the laser technique a more favourable option for AH (Hammadeh et al., 2011). Compared with acid Tyrode's solution, LAH was found related with a significantly higher implantation rate, clinical pregnancy rate, and live birth (Hsieh et al., 2002). In contrast, some studies found no benefit of using LAH on clinical outcomes, when compared with other AH methods (Balaban et al., 2002, Lanzendorf et al., 2007). Nonetheless, as ART laboratories strive for consistency and less variability between technicians to optimize pregnancy outcomes, LAH has become a preferred method.

1.4.2.1 The efficiency of laser-assisted hatching

The assisted hatching technique became increasingly common in fertility centres in the USA (from 25,724 in 2000 to 35,518 cycles in 2010); However, there was no significant association between assisted hatching application and the improvement of pregnancy outcomes (Kissin et al., 2014). Nevertheless, this study lacked specific details regarding the types of assisted hatching utilised, which may have varied over time or from one clinic to another. The introduction of laser technology created an option for standardised and reproducible method of assisted hatching for the first time; this is paramount when analysing results from multi-centre trials and comparing results from different studies.

However, the clinical relevance of LAH remains controversial and requires further investigations. In 2012, Carney et al.(2012) analysed 36 randomised controlled trials (RCT) studies and found that AH slightly improved the clinical pregnancy rate (odds ratio (OR)=1.13, 95% confidence interval (CI) 1.01 to 1.27), especially in women who had had a previous failed attempted at IVF (OR=1.42, 95% CI 1.11 to 1.81); but no improvement was detected in the live birth rate. When analysed the effect of LAH on pregnancy outcomes from 15 RCTs, no significant difference was found in clinical pregnancy rates (OR=1.04, 95% CI 0.9 to 1.19), live birth rates (OR=1.01, 95%CI 0.81 to 1.26), and miscarriage rates (OR=0.98, 95%CI 0.59 to 1.63) between the LAH group and control group (Carney et al., 2012). Nevertheless, an updated meta-analysis, based on 36 RCTs, showed a significant increase in the clinical pregnancy (OR=1.16, 95% CI 1.0-1.36) in AH groups. Especially, when stratified by hatching method, significant results were observed in chemical (OR=1.26) and mechanical methods

(OR=1.68); however, no improvement was found in laser method (OR=1.03) (Li et al., 2016).

Considering the potential embryonic damage and zona hardening caused during freezing/vitrifying or thawing/warming, an increasing number of studies focused on the effect of LAH on vitrified-warmed/ frozen-thawed embryo transfer cycle. In 2013, an RCT study categorised patient groups based on age and frozen-thawed embryos and found a significant improvement in clinical pregnancy rates following LAH in patients who were 35 years or older (70.0% *vs* 25.0%), and in frozen-thawed embryos transfer cycles (62.5% *vs* 29.5%) (Elhussieny et al., 2013). In addition, the quarter laser-assisted zona thinning was also found to improve the clinical outcomes of vitrified-warmed blastocysts, especially for day 6 blastocysts that developed from low-grade cleavage-stage embryos (Wan et al., 2014). Zhou et al (2014) investigated the pregnancy outcomes in 480 cryopreserved embryo transfer cycles where LAH was carried out on day-3 cleavage-stage embryos and found a higher implantation rate, clinical pregnancy rate, and live birth rate (Zhou et al., 2014). Conversely, a prospective RCT study found that quarter laser-assisted zona thinning did not improve the implantation rate in cryopreserved embryo transfer cycles, compared with control groups (Debrock et al., 2011). Intriguingly, a meta-analysis that included 12 RCTs demonstrated that LAH was related with a higher clinical pregnancy rate, implantation rate, and multiple pregnancy rate, for cryopreserved-thawed embryos; however, LAH was unlikely to improve the live birth rate (Zeng et al., 2017). Recently, another research group showed that when compared with laser-assisted thinning, laser-assisted ZP breaching could increase the implantation and live birth rates in single frozen-thawed blastocyst transfer cycles (Liu et al., 2020).

The contradictory efficacy of LAH may be correlated with the variety of LAH procedures used in clinics. The variety of protocols and manipulations introduced over the years ranges from zona breaching, in which a gap of varying size is introduced, to zona thinning, in which ZP ablation is conducted in various invasion and extension (**Figure 1-10)** (Alteri et al., 2018). Apart from the method, embryo stages and the clinical scenarios are various in clinic practice, which could be responsible for the contradictory results (Alteri et al., 2018, Davidson et al., 2019). Further details about the clinical practice will be discussed in **Chapter 3**.

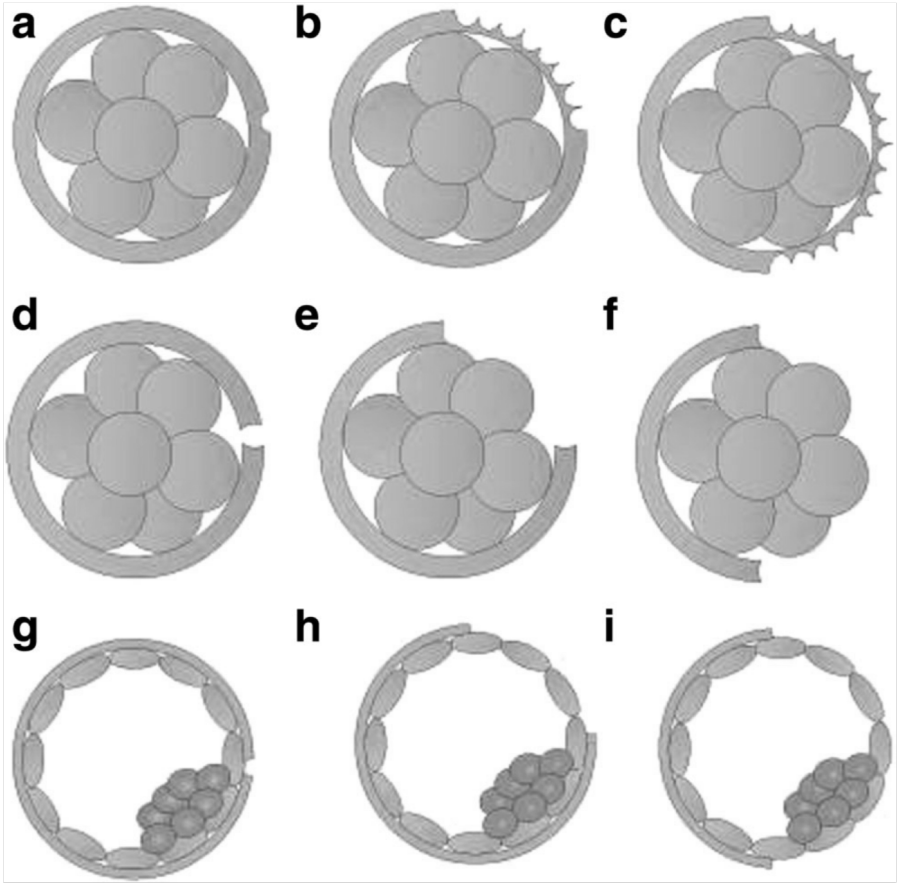


Figure 1-10. The procedures commonly used for embryo LAH

The embryo is thinned with a single hole without reaching the inner membrane (a) or the thinning area extend to a quarter (b) or half (c) of the embryo ZP circumference. In addition, the embryo ZP is breached with a single hole (d), or a quarter (e), or a half (f) of ZP circumference. Furthermore, the LAH is also applied on blastocyst to drill a single hole (g), a quarter (h), or a half (i) of ZP drilled. Figure was adapted from (Alteri et al., 2018).

Overall, the precise efficiency of different LAH procedures is still unclear. Due to the insufficient evidence for AH, the ASRM committee recommended that AH should not be recommended routinely for all patients undergoing IVF (ASRM, 2014). In addition, the UK's national Institute for Health and Care Excellence (NICE) guideline stated that AH is not recommended as it has not been shown to improve pregnancy rates (NICE, 2017).

1.4.3 Laser-assisted cryopreservation

With the evolution of techniques in ART, embryo cryopreservation and frozen/thawed embryo transfer have become as a routine practice to reduce the risk of ovarian hyperstimulation syndrome, to overcome the negative effect of the elevated progesterone levels of fresh cycles on pregnancy outcomes, and to avoid the morbidity of multiple gestation. According to the HFEA 2020 report, the number of fresh embryo transfer cycles decreased by 11% between 2013 and 2018, while the number of the frozen embryo transfers almost doubled, accounting for 38% of all IVF cycle (2020). In the meantime, the elective 'freeze all' cycles, where all fresh embryos are frozen after IVF to be used in subsequent cycles, have become more common in clinical practice. It has been reported that there has been a significantly increasing trend of 'freeze all' cycles in the US from 2003 (15.6%) to 2013 (40.7%) (Christianson et al., 2020). Thus, it is necessary to refine the procedure of embryo vitrification to reduce the potential damage on the embryo.

1.4.3.1 Blastocoele collapse for vitrification

During embryo vitrification, by applying a high concentration of cryoprotectants and rapid cooling rates (embryos are plunged directly into sterile liquid nitrogen), water can remove from the blastocoele rapidly and the cells and the surrounding solution directly solidify to a glass-like (vitreous) state, thus eliminating both intracellular and extracellular ice crystal formation (Liebermann et al., 2002). Vitrification is a simple, fast and inexpensive technique, which has become a fundamental tool in fertility treatment in recent years (Rienzi et al., 2017).

Nevertheless, this high concentration of cryoprotectant is also the main concern since it might lead to osmotic shock, thus affecting embryo survival (Quinn et al., 1986). To reduce the amount of blastocoele fluid and the time exposed in the protectant solution, blastocysts can be collapsed before dehydration (Vanderzwalmen et al., 2002). The artificial blastocyst collapse can be achieved by performing a short laser pulse between the TE cells (Mukaida et al., 2006) (**Figure 1-11**). Several studies have shown that when compared to non-collapsed blastocysts, human blastocysts vitrified after collapse show fewer damaged cells, significantly better blastocyst hatching and improved pregnancy outcomes (Hur et al., 2011, Cao et al., 2014). Furthermore, laser-assisted collapse has been proven to be an effective method with a shorter re-expansion time, a significantly higher blastocyst hatching rate, higher rates of expansion, lower levels of DNA damage, longer average gestational duration, and a lower premature birth rate when compared to the mechanical method (Desai et al., 2008, Cao et al., 2014).

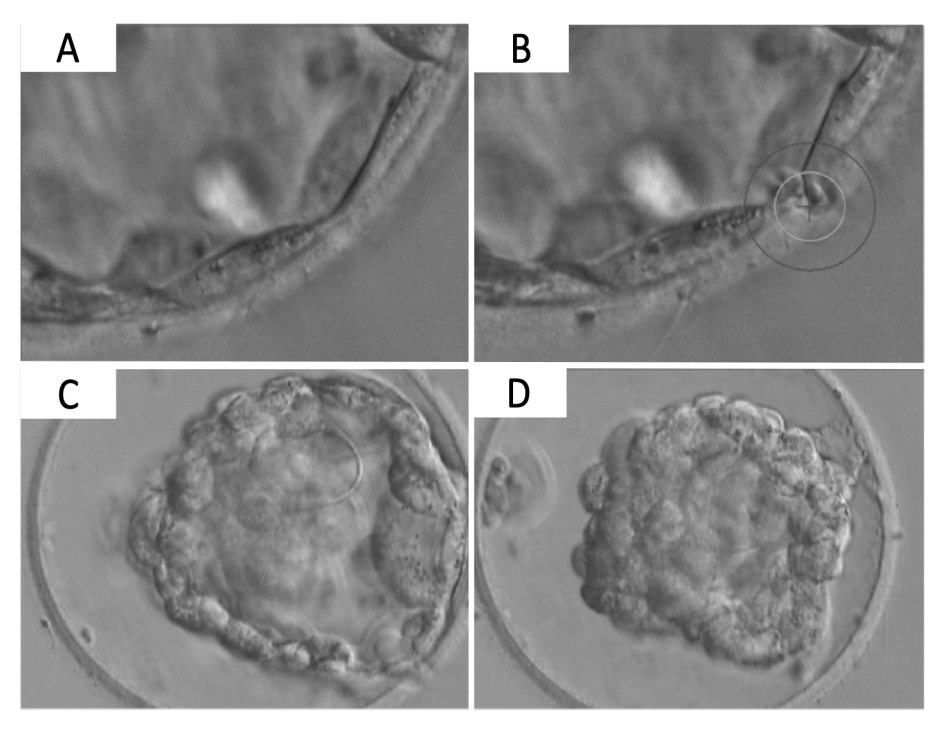


Figure 1-11. Laser-assisted blastocoele collapse

A laser pulse is fired at the targeting point- the joint between 2 trophectoderm cells (A and B). The collapsing process started from pushing the embryo to the side where the laser pulse targeted (C). The embryo then collapsed on itself as the fluid left the cavity (D). Images were adapted and modified from (FUJIFILM Irvine scientific, 2020).

Nevertheless, it is important to note that the necessity to apply blastocoele collapse to vitrified/warmed blastocysts may be a cryoprotectant-induced phenomenon. Using the glycerol containing, DMSO-free, vitrification solutions (Stachecki et al., 2008) or applying HA (sodium hyaluronate), an extracellular adhesion molecule (Stachecki et al., 2014) were found to achieve the high blastocysts survival and pregnancy rates without pre-collapse of blastocysts.

1.4.3.2 Laser-assisted removal of degenerated (lysed) blastomeres

The developmental potential of partially damaged (less than 25% cells lysed) cryopreserved human day 3 embryos was found comparable to fully-intact embryos (Zheng et al., 2008). However, such embryos have lower implantation rates and

pregnancy rates than fully-intact embryos (Guerif et al., 2002, El-Toukhy et al., 2003); this may be may be due to the release of toxic metabolites from necrotic blastomeres as well as the ZP hardening caused by cryopreservation procedures (De Vos et al., 2000, Rienzi et al., 2002). Thus, a combination of laser-assisted hatching with the removal of lysed blastomeres was proposed to improve the implantation potential in this case, where a small hole created by a laser in the ZP facilitates the aspiration of necrotic blastomeres from the embryo (**Figure 1-12**) (Rienzi et al., 2002).

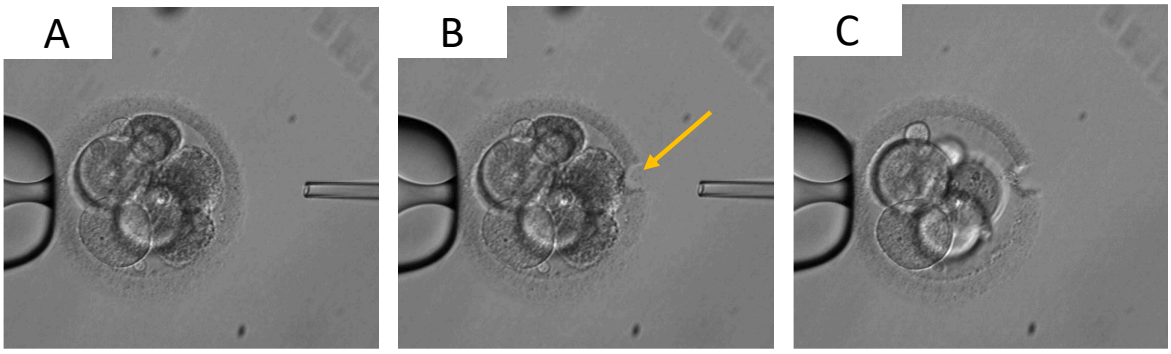


Figure 1-12. Laser-assisted hatching and lysed cell removal

(A) The embryo is held by a holding pipette, and the lysed blastomere can be observed; (B) A laser pulse is used to create an opening (yellow arrow) in ZP; (C) The lysed blastomeres are then removed by using a pipette to aspirate the lysed cells. Images were adapted and modified from (Nagy et al., 2005).

This procedure has been shown to significantly increase the developmental potential of partially-damaged frozen-thawed embryos, which were equivalent to those of fully survived embryos (Rienzi et al., 2005). Indeed, clinical pregnancy rates and implantation rates are more than double when compared to keeping the necrotic blastomeres (Rienzi et al., 2002, Liu et al., 2005, Nagy et al., 2005).Therefore, it was strongly advised against discarding embryos of poor-quality when they are the only option for transfer. This is because although with lower implantation potential, once embryos successfully implanted, the poor-quality embryos have the same potential for

live birth as the embryos of fair- and good-quality. In addition, the laser-assisted removal of lysed blastomeres, by improving the implantation potential, might facilitate the live birth of transferred poor-quality day 3 embryos (Kirillova et al., 2020). However, before applying as a clinical routine, more clinical data are now needed to confirm the benefit of this uncommon technique, we should also evaluate the health of offspring produced after transferring such embryos.

1.4.4 Laser-assisted intra-cytoplasmic sperm injection (ICSI)

Conventional ICSI requires the mechanical piercing of the ZP and ooplasmic membrane with an injection pipette (Palermo et al., 1992); this can result in unusual and extensive deformation of the oocytes (the oocyte has to be strongly compressed); especially when the oolemma or the ZP is very resistant to the penetration of the ICSI injection needle (**Figure 1-13**). This deformation can subsequently compromise the quality of oocyte and the survival of embryos (Abdelmassih et al., 2002, Danfour et al., 2010). In addition, it was reported that ICSI is associated with a 5-10% risk of oocyte degeneration (ESHRE, 2017).

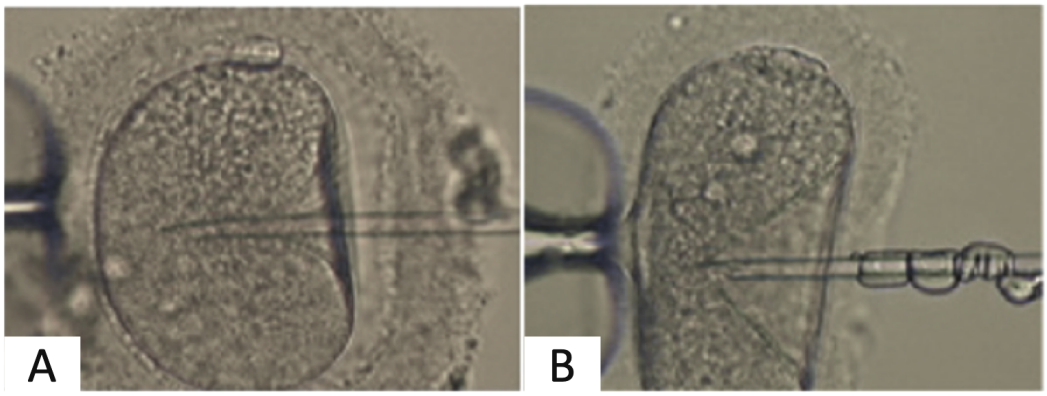


Figure 1-13. Resistance pattern of oolemma breakage during ICSI

(A) Mild resistance from the oolemma (Curved shape); (B) Serious resistance from the oolemma (funnel shape). Images were adapted and modified from (Danfour et al., 2010).

In laser-assisted ICSI (LA-ICSI), a precise hole (5-7 μm) is drilled in the ZP, leaving the innermost layer of the zona intact, thus allowing easier access of the needle through the barrier with minimal membrane deformation (**Figure 1-14**). Previous studies supported that LA-ICSI results in less trauma following penetration of the injection needle, thereby resulting in the reduced the oocyte and embryo degeneration, improved the fertilization, embryonic development and blastocyst hatching rate (Abdelmassih et al., 2002, Rienzi et al., 2004, Verza et al., 2013). In addition, the better clinical pregnancy outcomes were also achieved following the LA-ICSI in patients with a fragile oolemma, difficult zona pellucida penetration, repeated IVF failure, or even in unselected infertility population (irrespective of the oocyte quality and previous history) when compared with conventional ICSI (Rienzi et al., 2004, Choi et al., 2011).

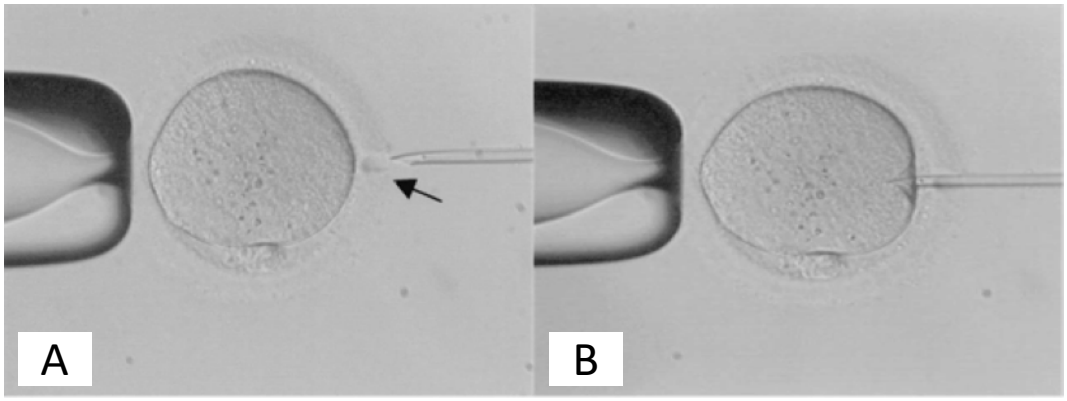


Figure 1-14. Laser-assisted ICSI

(A) A hole in ZP (black arrow) is created in a metaphase II oocytes by a laser pulse. (B) The micropipette is then introduced for intracytoplasmic sperm injection. Images were adapted and modified from (Rienzi et al., 2004).

However, LA-ICSI has not been widely adopted in clinics, as there are debates regarding the overall benefit of the procedure. Richter et al. claimed that there were no advantages of LA-ICSI over conventional ICSI in terms of oocyte survival, embryo quality, or clinical outcomes (Richter et al., 2006a). In addition, a recent RCT study

suggested that although LA-ICSI improves oocyte survival, it has no beneficial effect on embryo development and utilisation in unselected patients when compared to conventional ICSI (Fawzy et al., 2020). In addition, some embryologists believe that it is the resistance and stretching ability of the oolemma around the cells, rather than the ZP itself, that is related to oocyte degeneration following conventional ICSI. Therefore, researchers believe that such damage could be reduced by simply using good techniques and good quality injection needles (Danfour et al., 2010).

1.5 Controversy relating to the efficacy of laser-assisted embryo manipulations

When the use of lasers was widely introduced in ART, there were understandable safety concerns, mainly due to its application at such a delicate stage of human development, which would potentially pose a significant impact on pregnancy and prenatal outcomes.

1.5.1 Safety concerns for the embryo

Since pre-implantation embryos are fragile and valuable, the procedure used for laser-assisted ZP manipulation must be well controlled and reliable. The wavelength, the duration of the pulse, the laser spot size, and the light energy delivered, are all factors that need to be considered. In contrast to ultraviolet wavelengths, the near-infrared laser, especially a laser operating at a wavelength of 1480 nm, minimizes potential mutagenetic effects and shows unique absorption characteristic in water and culture media (Montag et al., 2009). However, apart from the wavelength, laser power (range from 20 to 400mW) and pulse duration (range from 1 ms to 100 ms) are the crucial

factors that determine performance, the delivery of energy, and hence its effects on embryos. If the laser power is increased, the diameter of the hole created, and the delivered energy, would also increase. Similarly, a longer duration of laser pulse would result in more heat, and the generation of larger hole sizes (Taylor et al., 2010).

The estimated temperature of ZP ablation is between 140-160°C for bovine oocytes and 130-150°C for mouse embryos. Therefore, laser beams, with a peak central temperature reaching 200°C in the water, could rapidly dissolve the ZP. However, there are high thermal gradients in the medium following laser pulsed ZP ablation; it is reported that the temperature of the medium surrounding the embryo can increase to 60-80°C (Douglas-Hamilton et al., 2001). The risk of thermal damage is a cause for significant concern since this could potentially heat and damage the surrounding cells of embryo.

In initial studies, 1480 nm diode lasers, with a range of laser pulse durations (3-100ms) and power (22-70 mW), were used to drill openings from 4.5 to 20 μm in diameter in the ZP of mouse oocytes and zygotes. The size of the laser spot was 2–8 μm, and laser energy was 0.28–4.7mJ. These studies failed to detect any laser-induced structural alterations of the neighbouring cytoplasm under scanning and transmission electron microscopy following laser treatment (Germond et al., 1995a, Rink et al., 1996a, Rink et al., 1996b). However, Chatzimeletiou *et al* (2001) reported the immediate effect of laser drilling on blastomere viability, and they emphasized the importance of the distance between the laser pulse and adjacent blastomere, in order to avoid immediate damage to embryos. They found that the minimum safe working distance was 8 μm for 2-cell mouse embryos when three to five laser pulses (5 ms) were applied. Also, these authors believed that it is not possible to drill the ZP at the

8-cell mouse stage when the blastomeres are generally <8 μm away from the ZP (Chatzimeletiou et al., 2001). However, this damage may be related to inappropriate laser parameter settings. Another study recommended a maximum of a 5 ms pulse duration to minimise the potential thermal damage on embryo when using a 200mW laser beam (Douglas-Hamilton et al., 2001). In addition, when laser treatment was carried out with 400mW laser beam and a 350 μm pulse length, no blastomere fragmentation adjacent to the point of the laser pulse was founded (Uppangala et al., 2016).

Laser power is normally dependent on manufacturers and specific models but is constant for each specific laser beam. A reduced power requires a much longer pulse length to have the same effect as a laser beam with high levels of power and a shorter pulse length. Previous study demonstrated that a laser with a higher power and a shorter pulse length will produce smaller temperature gradients than a laser with lower power but longer pulse lengths (Taylor et al., 2010). Therefore, the newer lasers now utilised a higher power (such as 300mw and 400mW) as opposed to the older lasers that utilised less power. By using a 400mW laser beam, a study compared three different laser pulse lengths (0.604 mS, 0.708 mS and 1.010 mS, which corresponded to hole size of 10.5 μm, 13.5 μm, and 16.5 μm respectively) on human embryos. This study demonstrated that a larger laser pulse length (1.010 mS) can be safe since it did not lyse blastomeres nor impact the quality of day 5 embryos (Taylor et al., 2010).

Although many previous studies did not demonstrate the significant impact of laser treatments on preimplantation embryo development (Wong et al., 2003, Yano et al., 2006), recent studies started to understand the changes of embryo development patterns using time-lapse monitoring technology. A morphokinetic study showed that

LAH drilling, rather than LAH thinning, could advance the hatching process 14 hours of mouse embryos earlier than controls; however, LAH thinning does not facilitate hatching but disrupted the *in vitro* hatching process (60.7% did not complete the hatching process) (Schimmel et al., 2014). In contrast, a recent study indicated that LAH thinning could promote the onset of hatching earlier at day 4 and increase the fully hatched rate of vitrified-warmed mouse embryos, with a larger proportion of 'U'-shape hatching by day 5 (Huang et al., 2019).

Apart from embryo development, studies have indicated that laser-assisted ZP manipulations may affect embryonic biology and might cause impact on embryo at the molecular level. Many studies have investigated the effect of laser-assisted ZP manipulations on blastocyst cell numbers; however, results are contradictory. Some studies found the decline in the blastocyst embryonic cell number after laser ZP manipulations (Chailert et al., 2013, Honguntikar et al., 2015); meanwhile, one study demonstrated the increased embryonic cell number in the laser-treated embryos (Park et al., 2014). Furthermore, researchers paid attention to the impact of laser on embryo cell apoptosis: Honguntikar et al. (2015) demonstrated that laser drilling (400mW, 350 μs) at either the 2-cells or 6-8 cells stages increase levels of DNA fragmentation at the blastocyst stage. However, a more recent study failed to detect any induced apoptosis in the laser-treated embryos by evaluating the expression level of apoptosis-related genes (Huang et al., 2019).

In addition, the thermal damage induced by laser manipulation was investigated by Hartshorn et al, by measuring the expression level of heat shock protein (Hsp70i). The results demonstrated that laser drilling did not stimulate Hsp70i expression, even in the blastomeres which were close to the laser beam; thus suggesting that the laser

pulses used during LAH do not cause heat stress to embryos (Hartshorn et al., 2005). Furthermore, another study investigated epigenetic changes following laser ZP manipulation in the mouse embryo model, showing that laser drilling of embryos at the 2-cell stage impair the expression of two *de novo* methyltransferases (*Dnmt3a* and *Dnmt3b*) in blastocyst (Honguntikar et al., 2017). In terms of embryo metabolism, Uppangala et al by analysing the component of the embryo culture media, found that laser manipulation would not cause any immediate metabolic or functional abnormalities in embryos for at least 24 hours following laser treatment (Uppangala et al., 2016).

1.5.2 Safety concerns for the offspring

Only a few follow-up studies have been published with regards to the health of children born following LAH. Thus far, 23 malformations and two anomalies following LAH have been reported. Of these malformations, nine were major, such as umbilical deformity, spina bifida and congenital heart disease, and 14 were minor, such as atrial septal defect, torticollis, and congenital naevus. However, there is no increasing trend when compared to pregnancies achieved without assisted hatching (Kanyo et al., 2003, Primi et al., 2004, Hagemann et al., 2010, Zhou et al., 2014).

Nevertheless, three meta-analysis studies showed that multiple pregnancy rates were significantly increased when assisted hatching or LAH was conducted (Carney et al., 2012, Li et al., 2016, Zeng et al., 2017). Although the majority of ART-related multiple pregnancies are dizygotic, some trials have reported monozygotic (MZ) twinning (Hurst et al., 1998, Schieve et al., 2000, Hagemann et al., 2010). A recent study revealed that AH represents a potential risk factor for zygotic splitting in the retrospective investigation of 937,848 single embryo transfer cycles in Japan

(Yamashita et al., 2019). In contrast, other studies failed to identify the AH as a risk factor for MC twinning, when analysing the data from 6 RCTs (Carney et al., 2012) as well as the summary of eight years clinical data (Knopman et al., 2014). Overall, there is insufficient data at present to allow us to describe the impact of AH upon offspring in a definitive manner.

Thus far, research involving both animal models and human subjects have provided some clues of how laser application may impact embryos at the molecular level. However, there is insufficient evidence to demonstrate the negative impact of using laser manipulation on embryos. Furthermore, more robust evidence of pregnancy outcomes and the health of offspring are now needed to support the long-term safety of laser techniques in ART.

1.6 The preimplantation mouse embryo as a model system

Due to the scarcity, ethical and logistical challenges of research with the human embryo, it is necessary to use animal models for developing new technologies. The mouse is the most frequently used animal model in embryo-related studies and has played a critical role in understanding embryo biology, and the refinement of ART techniques (Summers et al., 2003, Edwards, 2005, Taft, 2008). Mouse embryos have been proposed as a 'pharmacotoxicological tool' with which to determine the suitability of the methods, techniques, and materials used for human IVF (Ménézo et al., 2002).

1.6.1 Advantages of the preimplantation mouse embryo as model

The small size, short generation interval, high fecundity, and ease of handling, make mouse embryos a relatively low cost, readily available and attractive model for

research. In contrast, embryos from other species are difficult or expensive to obtain (Taft, 2008). In addition, humans and mice are similar with regards to the embryo development process. The critical processes of embryo fertilisation, cleavage, compaction, blastocyst formation, and cell segregation are evident in both the human and mouse. Therefore, mouse embryos are the most widely used model for screening culture media and techniques used in clinical IVF, by assaying embryos development at multiple time points and quantitating vital parameters, such as blastocyst cell numbers (Gardner et al., 2005).

Furthermore, the sizes of mouse oocyte and embryos make them very useful as practice models for various research studies. The mean diameter of mouse embryos is about half that of human embryos, thus making the volume of the human embryo approximately 8-fold larger than mouse embryos (Quinn et al., 1998, Taft, 2008). Most embryo micromanipulations, including cryopreservation, ICSI, ZP manipulations, blastomere biopsy, and TE biopsy, were all performed on mouse embryo models before been applied on human embryos (Kimura et al., 1995, Parikh et al., 2018). The well-established mouse model is informative, and the outcomes of embryo manipulations can be readily studied via the *in vitro* culture of preimplantation embryos.

Compared to other models, the mouse has a unique advantage: the mice in the same inbred strains are nearly genetically identical; this can reduce phenotypic variability. Thus, using inbred strain makes it possible to use the minimum number of animals to complete an experiment (Festing, 2004). Furthermore, 99% of mouse genes have human homologs, and the order of genes is conserved between mice and human. Mutations in mouse genes, and their human homologs, often have similar sequences

(Waterston et al., 2002). Therefore, mouse embryos have been used extensively as a model system for studying gene regulation during embryogenesis.

1.6.2 Differences between human and mouse preimplantation embryos

All models have certain limitations. Differences in physiology among species make it inappropriate to extrapolate directly from mouse to human. First of all, the size of mouse oocyte and embryos are small than human's oocyte and embryos; the diameter of human oocyte is 150-180 μm, while diameter of mice oocyte is 70-100 μm (Ménézo et al., 2002). In addition, the human ZP is much thicker than the mice ZP; the average thickness of cleave stage embryo is around 16 μm for the human ZP, and is 11 μm for the mouse ZP (Balakier et al., 2012). Although human preimplantation embryos development closely resembles that of mouse embryos, the human embryo goes through developing stages later than the mouse embryo. Firstly, the ZGA (zygotic gene activation) occurs later in the human embryo than in the mouse, at the 4- to 8-cell stage (Braude et al., 1988). Furthermore, compaction often occurs at 16-cell stage (around day 3.5) in human embryos, which is later than that in mouse embryos (at the 8-cell stage (E2.5)) (Cockburn et al., 2010). In addition, the blastocyst formation happens at E3.5 in the mouse embryo, while in the human embryo, it appears to take place at approximately day 4.5 (Cockburn et al., 2010). As for lineage development, there is a retardation of linage segregation in human preimplantation development when compared to mouse embryos. Oct4 restriction to the ICM in human embryo (at day 6) occurs two days later than in the mouse embryo; the Cdx2 expression is first detectable in the TE layer following cavitation (day 5) in human embryos, while the expression of *Cdx2* is detectable prior to cavitation in the mouse embryo (Sozen et al.,

2014). Furthermore, the human embryo blastocyst undergoes the second segregation to form the PE (primitive endoderm) and EPI (pluripotent epiblast) from day 6 and completes this phase at approximately day 7. In the mouse embryo, the second segregation begins at E3.5 and the three embryonic lineages can be distinguished clearly at E4.5 (Sozen et al., 2014) (**Figure 1-15**).

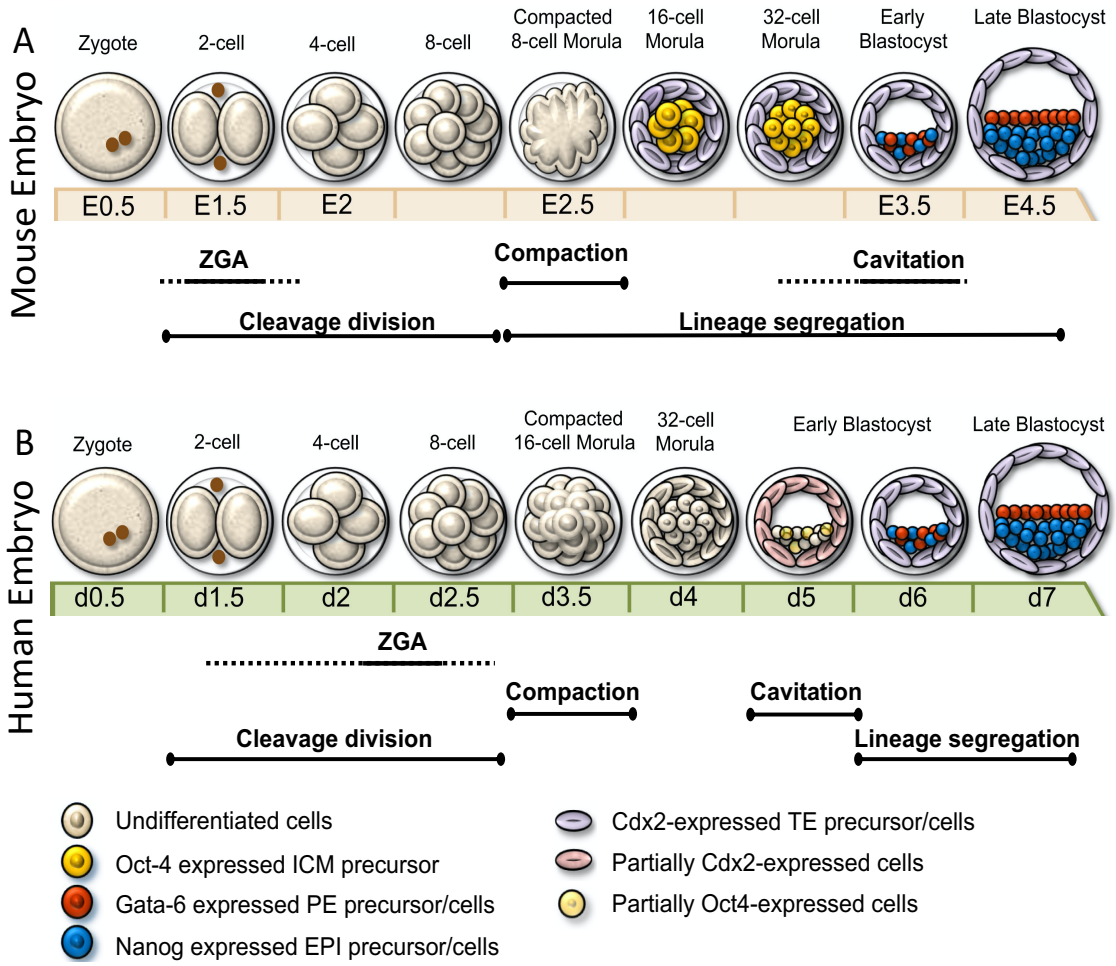


Figure 1-15. The timing of the preimplantation development events in mouse (A) and human embryos (B)

A schematic of the preimplantation embryonic developmental timeline for both mouse (A) and human (B) embryo, from the zygotic to the late blastocyst stage. Figure was adapted and modified from (Sozen et al., 2014).

Furthermore, the susceptibility to chromosomal aberrations varies considerably between the human and mouse (Carbone et al., 2015). In humans, it has been

demonstrated that 50-80% of embryos at the cleavage stage have one or more blastomeres that are aneuploid (Vanneste et al., 2009). Despite the higher probability of arrest at the cleavage stage, the aneuploid embryo can still form a blastocyst that is almost morphologically indistinguishable from euploid embryos (Baltaci et al., 2006). In addition, chromosomal abnormalities have been reported in the majority of cases of spontaneous miscarriage in human (Benkhalifa et al., 2005); and 90% of chromosomal abnormalities are of maternal origin, caused by female age-related chromosomal errors (Cohen, 2002, Chiang et al., 2012). In contrast, in the mouse, only 0.05-1% of oocytes are typically aneuploid; and aneuploid rates are approximately 1% in mouse embryos, depending on the strain (Lightfoot et al., 2006). Unlike human embryos, which continue to divide and undergo cellular fragmentation in response to aneuploidy, aneuploid mouse embryos will lyse rather than divide, and won't survive for implantation (Chavez et al., 2012).

In addition, there are differences in embryo metabolism between mouse and human embryo. For example, the human embryo does not utilize glucose; however, the embryos of some mouse strains can metabolize glucose (El Mouatassim et al., 1999, Taft, 2008). Furthermore, in contrast to human embryos, mouse embryos do not require amino acids to develop to the blastocyst stage (Lane et al., 1997). In addition, mouse embryos are less sensitive to and recover more easily form pH changes than human embryos (Ménézo et al., 2002).

Overall, the mouse embryo is a valuable and robust model for developing and refining ART techniques that need to be subsequently tested on human embryos. However, it is important not to overlook the differences between these two species.

1.7 The aims of this thesis

The primary aim of this thesis was to evaluate the safety and efficiency of laser-assisted embryo ZP manipulations. In addition, this thesis aimed to investigate the mechanism responsible for embryo hatching, which may, allow for the discovery of potential therapeutic targets for human IVF. The particular objectives and approaches have been summarized and organized by chapters as shown below:

(1) I hypothesised that inconsistencies in the way in which ZP manipulations are carried out, especially for assisted hatching, represent the main reason for the evident contradictories in its clinical efficacy. To characterise the variation of clinical practice, and to identify potential opportunities for standardisation, in **Chapter 3**, I designed an online survey to investigate the utilisation, methods and the attitudes of clinical embryologists and clinicians towards assisted hatching from different countries and clinics.

(2) I hypothesized that various laser-assisted ZP manipulations may have different impacts on embryo development and quality. **In Chapter 4,** in order to evaluate the effect of commonly used laser-assisted ZP manipulations on preimplantation embryos, I performed laser-assisted ZP drilling, partial drilling, and ZP thinning, on mouse embryos, and investigated their relative impacts on embryos from different aspects, including embryo development, hatching pattern, embryonic cell number, embryonic cell differentiation, cell apoptosis, as well as heat shock stress.

(3) The efficacy of assisted hatching on embryo implantation was hypothesised to be affected by different laser-assisted ZP manipulations. Therefore, to investigate the efficiency of these treatments on embryo implantation capability, I used the Ishikawa

cell based *in vitro* implantation model, to assess mouse embryo competency, especially with regards to hatching completion and embryo attachment, following laser-assisted ZP manipulations.

(4) To investigate the potential mechanisms underlining embryo hatching, I used RNA sequencing and downstream pathway analysis to identify the potential molecules and pathways involved in the hatching process in **Chapter 6**. In addition, the transcriptional impacts of laser-assisted ZP drilling on the embryo was explored by comparing the transcriptome between laser treated and untreated mouse embryos.



Chapter 2

Methods and Materials

2.1 Online survey

2.1.1 Questionnaire design

Based on an extensive literature search and expert opinions, I developed a 32-item questionnaire, named “The Application of Assisted Hatching in IVF Centres”. The questions focused on (1) clinical demographics: the location and name of the centre, the treatments provided, and whether the centre was privately or publicly funded; (2) the strategies used for assisted-hatching prior to embryo biopsy (AHpBP) or assisted-hatching prior to embryo transfer (AHpET), including the clinical indications, frozen/thaw or fresh embryo status, embryo stage, embryo culture and embryo-transfer strategy, as well as detailed information regarding the AH technique, protocol (ZP drilling or ZP thinning), and the ZP opening size and extension of thinning; (3) attitudes and opinions about AH: the advantages of AH to their work routine, the safety of AH, the effect on embryo development, the improvement of implantation, and the improvement of live birth. For each question, multiple-choice answers were provided, from which one or more answers could be chosen. A text box was provided after each question for the respondent if they would like to add any comments. In addition, 5-point scale questions, with answers from ‘very unlikely’ to ‘very likely’, were designed to measure attitudes towards AH. A detailed questionnaire is provided in the **Appendix 1**.

2.1.2 Survey distribution

This anonymous questionnaire was conducted through an online survey platform (SurveyMonkey Inc., San Mateo, California, USA, www.surveymonkey.com). To increase the number of respondents, the questionnaire was translated into Chinese

and conducted through a Chinese survey platform (Wenjuanxing, Shanghai, China, www.wjx.cn). The survey link was sent to the medical societies, especially those related to embryologists and fertility clinicians, including the HFEA (Human Fertility and Embryology Authority), ACE (Association of Clinical Embryologists), and SRF (Society for Reproduction and Fertility). Then, the societies circulated the survey link through their society newsletters. Then, the survey was completed by unnamed members within the society. To ensure the survey was anonymous and voluntary, no personal information was collected, and responders could terminate the survey under any circumstance. As such, the ethical permission was not required. The online survey collector was open between October 2019 and March 2020.

2.2 Mouse embryo collection and culture

2.2.1 Fresh embryo collection

2.2.1.1 Maintenance of animals

Mice were raised in the Biomedical Services (BMS) Unit at the University of Oxford and treated according to the principles of laboratory animal care. Superovulation and mouse maintenance/care were approved by the Ethics Committee of Department of Physiology, Anatomy and Genetics, University of Oxford (Licence number:30/3301). C57BL/6JOlaHsd female mice (3-4 weeks-of-age) were used for all experiments. All mice were kept under standard conditions of 12 hours light and 12 hours dark at 20-22°C, 40-60% humidity, and with access to food and water *ad libitum*.

2.2.1.2 Superovulation and mating

Fresh embryos were obtained under protocol BMS//JRSOP 285. Female mice were injected with 0.1 ml (5 IU) of Pregnant Mara's Serum Gonadotrophin (PMS, Follogon, Intervet) and 0.1 ml (5 IU) of Human Chorionic Gonadotropin (hCG, Chorulon) sequentially, with a 45 to 48 hours interval. Eight hours post hCG injection, female mice were allowed breed, and examined for the vaginal plug in the following morning. E1.0 was defined as the day when a vaginal plug was first observed and was considered as an indicator of successful mating.

2.2.1.3 Embryo retrieval

On the morning of E2.0, female mice with vaginal plugs were sacrificed by cervical dislocation. The reproductive tracts, including the ovaries, were harvested into a 1.5 ml microcentrifuge tube prefilled with M2 medium (Millipore, Abingdon, UK). The reproductive tracts were immediately transferred from the BMS to the Institute of Reproductive Science (IRS) laboratory, and embryo retrieval was commenced within an hour. For the retrieval of mouse embryos, the reproductive tracts were transferred to a 35 mm IVF Petri Dish (Thermo Fisher, UK) containing 250 µL of M2 medium at room temperature. Eight-cell embryos were obtained by shredding the oviducts and uterine horns with fine and curved forceps in the M2 medium; these procedures were conducted under the dissecting microscope (SMZ1500, Nikon, UK). An illustration of the embryo stages and location within the mouse reproductive tract is summarised in **Figure 2-1.** Finally, the resultant embryos were then picked-up using a Flexipet (EZ-Grip) and a 145 µm transfer pipette (EZ-Tip) (Cooper Surgical, Falmouth, UK), and transferred to a drop of fresh M2 medium to rinse off the debris. Finally, the embryos

were rinsed through several drops of M2 medium before being transferred into a fresh 35 mm IVF Petri Dish with embryo culture medium.

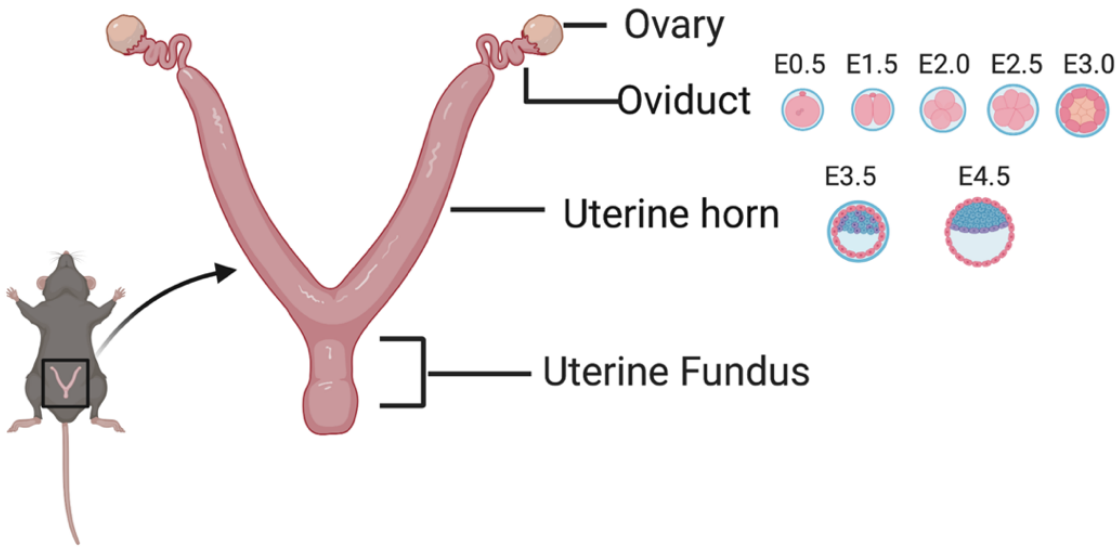


Figure 2-1. A schematic showing the location of different stages of embryos in a mouse reproductive tract.

Mouse embryos, from the fertilised oocyte (E0 zygotic stage) to the compacted morula (E 3.0 stage), were located mainly in the oviduct. As embryos grow to the blastocyst stage, they transfer from the oviduct towards the uterus. Thus, the embryos from the early blastocyst stage to the hatched blastocyst stage can be found in the uterine horn.

2.2.2 Frozen embryo collection

2.2.2.1 Frozen embryo straws

Cryopreserved 8-cell stage mouse embryos (B6C3F1 × B6D2F1) were purchased from Embryotech Laboratories (Wilmington, MA, USA) and used for transcriptional profiling. Each straw contained 20 embryos, which were randomly collected from embryo-pools harvested from 8 to 12 mice. The batch number of the straw was marked according to the origin of the embryos it contained. An illustration of an embryo straw is shown in **Figure 2-2 A**.

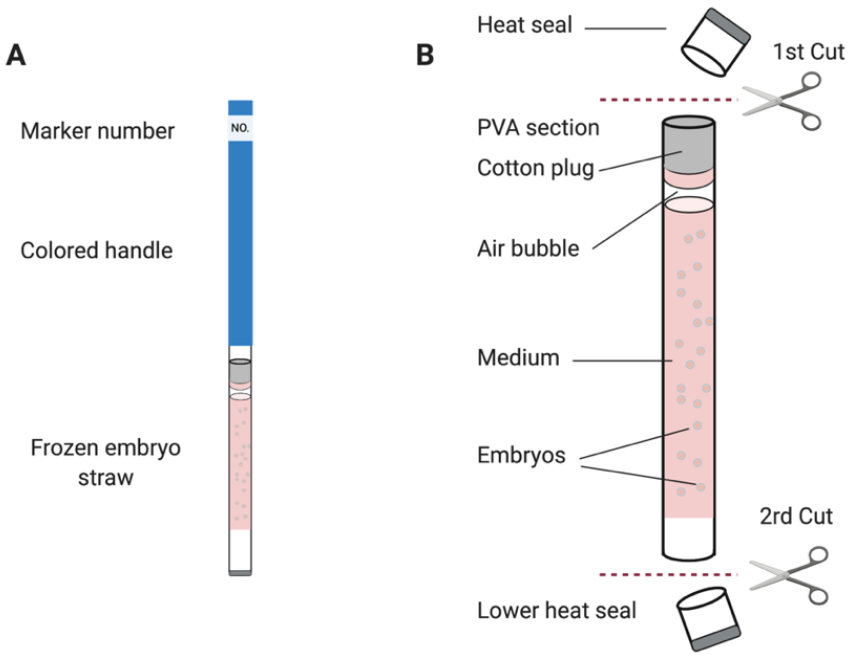


Figure 2-2. A schematic showing the procedures used to thaw frozen embryos.

(A) A diagram of a frozen mouse embryo straw; (B) Brief illustration of the procedure used to thaw mouse embryos held in a straw.

2.2.2.2 Thawing embryos

Embryos were thawed in accordance with the instructions provided by the supplier. Specifically, once out of the liquid nitrogen tank, a straw was removed from the cane immediately and equilibrated to room temperature (RT) briefly for 2 minutes before incubation in the water bath at 37°C for 1 minute. After the straw was wiped dry, and its coloured handle was removed, the straw was cut to bisect the cotton plug at the PVA section, and then a second cut was made between the lower heat seal and the column of media. Prior to thawing, three drops of M2 media were prepared in an IVF petri dish. The contents of the straw were expelled into one drop of M2 by pushing the cotton plug down using a provided stylet. The embryos were sequentially rinsed twice in the other two drops of M2 media, and then transferred into embryo culture media (**Figure 2-2 B**).

2.2.3 Embryo culture

Embryos were cultured individually in one drop of potassium-supplemented simplex optimised medium with the addition of ½ Amino Acids (KSOM-AA) (EmbryoMax KSOM Mouse Embryo Media, Millipore, Abingdon, UK) (20 µL) and further covered with mineral oil (FertiPro NV, Beernen, Belgium). A maximum of 8 embryos were cultured in a 35 mm IVF Petri Dish, as demonstrated below (**Figure 2-3**). Embryos were incubated at 37°C with 5% CO_2 for 1-2 hours (for fresh embryos) or 10 minutes (for frozen/thawed embryos) prior to LAH treatment. All embryo manipulation was performed using a Flexipet (EZ-Grip) and a transfer pipette (EZ-Tip) (Cooper Surgical, Falmouth, UK).

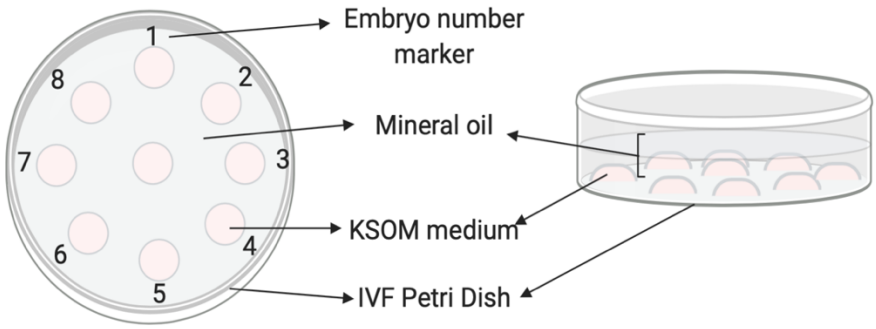


Figure 2-3. A schematic showing the set-up for embryo culture dishes

The culture dishes were numbered from 1 to 8, marking individual mouse embryos. The pink circles represented drops of KSOM medium with a layer of mineral oil on the top. The drop of medium in the middle of the dish is for washing embryo before transfer to the culture drop.

2.2.4 Inclusion criteria for embryos

Prior to LAH treatment, embryos were assessed for their morphology and included for experiments if they were (1) cleavage stage embryos containing more than six cells or at the compacted morula stage, and (2) contained blastomeres of equivalent size (**Figure 2-4: A-C**). In contrast, embryos containing cytoplasmic fragments, unevenly

sized blastomeres, or showing developmental arrest (**Figure 2-4: D-F**) were excluded from studies (Van Soom et al., 2003).

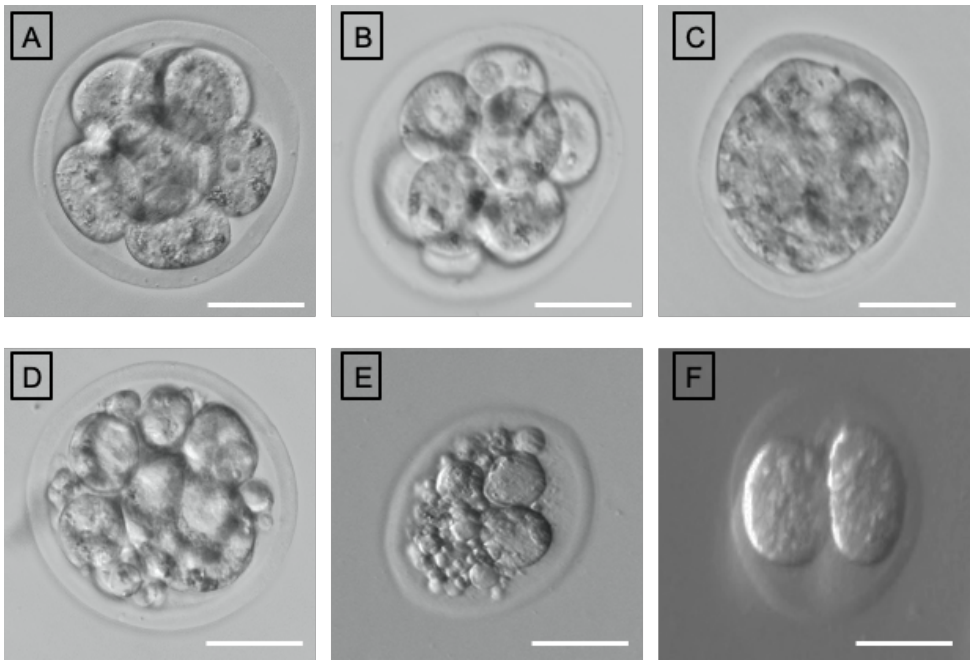


Figure 2-4. Morphological criteria for the inclusion of embryos

Representative examples of embryos included in this study: (A-B) cleavage embryo with more than six blastomeres; (C) Compacted morula stage embryo. (D-F) The criteria for exclusion: Embryo with obviously uneven size of blastomeres; Embryo with obvious cytoplasmic fragments; embryo with development blocked. (Scale bar=40 μM)

2.3 Laser-assisted ZP manipulation procedure

The Saturn 5 Laser System (Cooper Surgical Fertility Companies, Denmark) was used for laser-assisted ZP manipulation related experiments, with the following parameter settings: wavelength (1.48 μm), power (400 mW), and laser diameter (7.5 μm). The three laser-assisted ZP manipulations were used in this study, to reflect clinical practice: (1) laser ZP drilling, in which both the outer and inner side of the ZP were drilled to create an opening (drilling from the inner to the outer side of the ZP), and the diameter of the ZP opening is 7.5 μm; (2) laser ZP partial drilling, in which the inner

side of the ZP remained intact while the thickness of the ZP was thinned by more than 50% at a particular area (e.g. **Figure 2-5 C**); and (3) laser ZP thinning, in which a quarter of the ZP circumference received partial laser ablation (**Figure 2-5 D**). Embryos in the control group were also placed onto the pre-warmed stage of the micromanipulator for morphological assessment but were not subject to the laser drilling procedure. Embryos collected freshly from the mouse reproductive tract, or thawed embryos from straws, were randomised into either the control group or one of the treatment groups. Following LAH treatment, embryos were transferred back to the incubator and cultured at 37°C, 5% CO_2 for 48 hours to develop from E2.5 8-cell embryos to E4.5 blastocysts (*in vitro* culture started from 12 pm on day 1 to 12 pm on day 3).

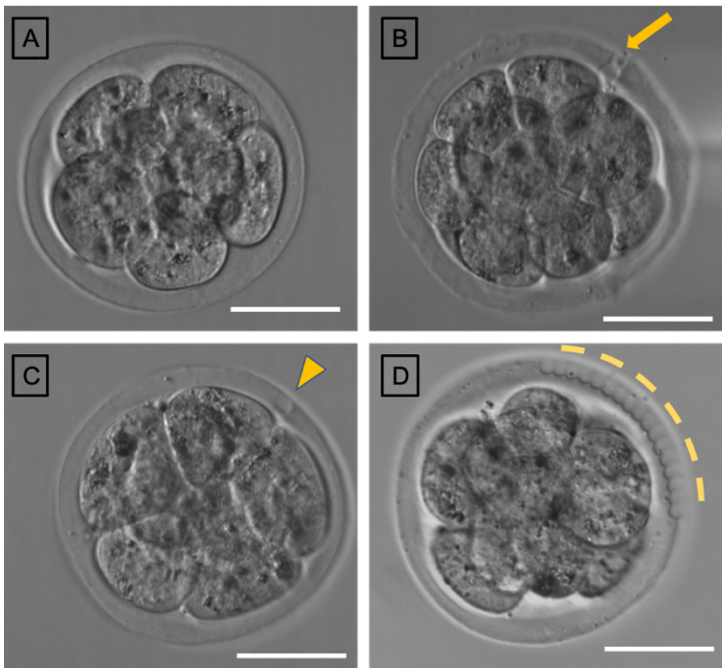


Figure 2-5. The laser-assisted ZP manipulation method used on mouse embryos during this research

(A) Frozen-thawed compact 8-cell embryo; (B) Laser ZP drilling: a single hole (yellow arrow) completely drilled through the zona pellucida; (C) Laser ZP partial drilling: a single hole (yellow triangle) created without reaching the inner membrane; (D) Laser ZP thinning: around a quarter of the ZP circumference, partially drilled (yellow dashed line). (Scale bar=40 μM)

2.4 The assessment of mouse embryo morphology

2.4.1 Developmental assessment

After 48 hours of *in vitro* culture, the E4.5 embryos were observed on a pre-warmed microscope stage (12 pm on day 3). Based on their morphology at the E4.5 stage, embryos were designated as either (1) blastocyst-stage embryos, including early blastocysts (beginning of the blastocoele cavity-forming stage), blastocysts (complete formation of the blastocoele cavity but without an expansion in total embryo size), expanded blastocysts (expansion in total embryo size), and hatching embryos, or (2) fragmented embryos and arrested embryos, including cleavage embryos and morulae (**Figure 2-6**). The number of developed blastocysts, hatching blastocysts, and arrested/fragmented embryos, were quantified.

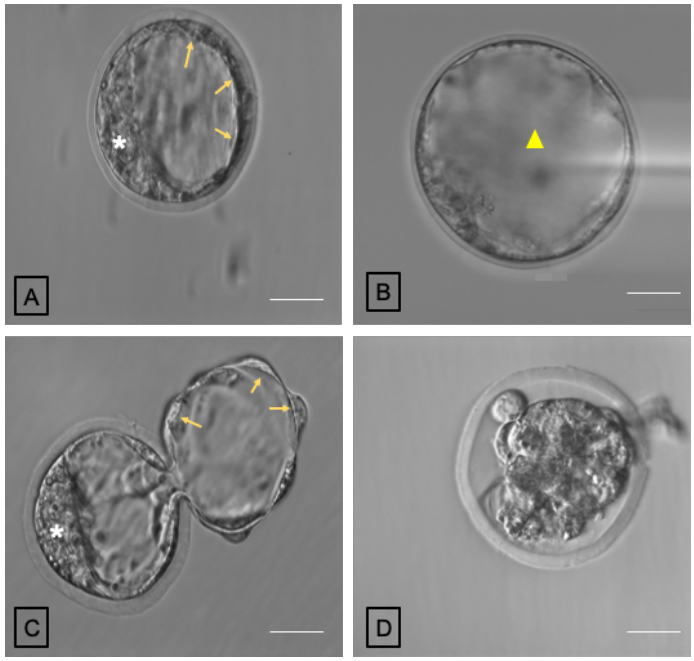


Figure 2-6. Morphological assessment of embryo development

(A) Blastocyst featured with ICM (white star) and TE (yellow arrow); (B) Expanded blastocyst with large size cavity (yellow triangle) and thinner ZP; (C) Hatching blastocyst; (D) Dead embryos: no blastocoele formation but with fragment. (Scale bar= 25 μm)

2.4.2 Morphological assessment of embryo hatching

Hatching blastocysts were further evaluated and sorted according to hatching patterns (Yan et al., 2015, Onodera et al., 2017). Specifically, the blastocyst was defined as "starting to hatch" if the hatching region was less than 1/5 of the total size of the embryo (**Figure 2-7 A**). An '8'-shape hatching blastocyst was characterised by two blastocoels divided by the ZP, with an ZP opening of ≤ 25 μm at the time of observation (**Figure 2-7 B**). Conversely, when the ZP opening exceeded 25 μm, the blastocysts were regarded as displaying the 'U'-shape hatching pattern (**Figure 2-7 C**). Blastocysts with multiple hatching points (≥2) were referred to as multiple-point hatching blastocysts (**Figure 2-7 D**). The number of starting hatching blastocysts, '8'-shape hatching blastocysts, 'U'-shape hatching blastocysts, and multiple point blastocysts were quantified.

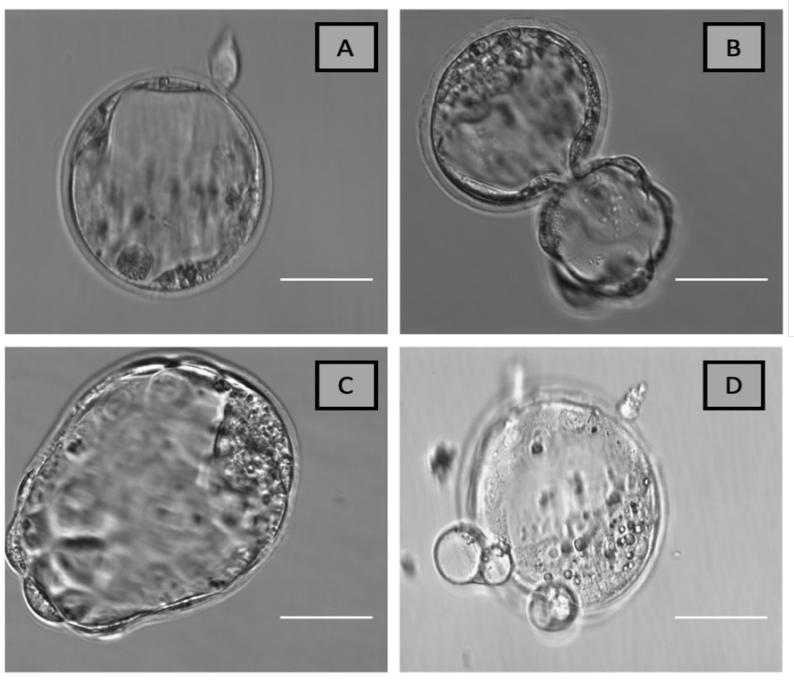


Figure 2-7. Different hatching patterns

Four different hatching patterns were observed at E4.5, including (A) starting to hatch, (B) '8'-shape hatching, (C) 'U'-shape hatching, and (D) multi-point hatching (Scale bar= 50 μm).

2.5 Human cell culture

2.5.1 Ishikawa cell line maintenance

Ishikawa cells, a human endometrial adenocarcinoma cell line of epithelial origin, was purchased from the European Collection of Authenticated Cell Culture (ECACC 99040201). Cells were maintained in conditional medium (1:1 Dulbecco's modified Eagle's medium: Ham's F12 (DMEM:F12) (Sigma-Aldrich, UK)) supplemented with 10% foetal bovine serum (FBS) (Sigma-Aldrich, UK), 100 µg/ml streptomycin (Sigma-Aldrich, UK), 100 IU/ml penicillin (Sigma-Aldrich, UK), and 20 µg/ml gentamicin (Sigma-Aldrich, UK). Cells were cultured at 37°C and 5% CO_2, and the medium was replenished every other day for maintenance.

2.5.2 Ishikawa cell passage

Cells were grown in 75 cm^2 culture flasks (Thermo Fisher, UK) and passaged when they reached 90% confluency. For passaging, 5 ml of 0.05% trypsin with EDTA (Ethylenediaminetetraacetic acid) was added to a 75 cm^2 flask and incubated at 37°C for 5 minutes for cell dissociation. Following trypsinisation, detached cells were neutralised with 5 ml of conditioned media containing FBS and subsequently collected into a 50 ml Falcon tube. The cell suspension was then centrifuged at 1000 rpm (5430 R, Eppendorf, UK) for 10 minutes. After centrifugation, the supernatant was discarded, and cell pellets were resuspended in 1 ml of conditioned media containing FBS. Cells were then counted using a haemocytometer (**Appendix 2** for a detailed quantification protocol), and the appropriate number of cells were then seeded in 75 cm^2 flasks for maintenance or into 24-well plates for further experiments. The Ishikawa cells were

used between passage 8 to 10 for experiments. The details of freezing and thawing of Ishikawa cells were described in **Appendix 2**.

2.6 The *in vitro* implantation model

2.6.1 Two-dimensional (2D) co-culture system

2.6.1.1 Coverslip coating

Before diluting the Matrigel, all the tips, plates and pipettes were pre-chilled overnight. The next day, Phenol red-free Matrigel (Corning, Flintshire, UK) was thawed and diluted 1 in 8 with ice-cold phenol-red free DMEM: F12 (Sigma, UK) on ice. Then, 13 mm coverslips were placed into 24-well culture plates and covered with 300 µL of diluted Matrigel and incubate at 37°C for at least 30 minutes. Before seeding cells, the diluted Matrigel solution was removed, and the coated wells were washed twice with pre-warmed PBS.

2.6.1.2 Ishikawa cell seeding and culture

To form the endometrial epithelial layer of the implantation model, 3×10^5 Ishikawa cells were seeded on coated 13 mm coverslips in 24-well plates and cultured with conditioned media (contained 10% charcoal-treated FBS) overnight in existing culture conditions. The following morning, the media on the confluent Ishikawa cells was replaced with co-culture media (phenol-red free DMEM: F12 medium, supplemented with 0.1% charcoal-treated FBS (Sigma-Aldrich, UK), 100 µg/ml streptomycin, 100IU/ml penicillin, and 20 µg/ml gentamicin) and cultured for an additional 24 hours.

2.6.1.3 Embryo transfer

Between one and five E4.5 blastocysts or E5.5 blastocysts (blastulation delayed embryos) were collected from KSOM and transferred onto the Ishikawa cell monolayer using a Flexipet (EZ-Grip) and a 200 µm transfer pipette (EZ-Tip) (Cooper Surgical, Falmouth, UK) under a dissecting microscope (Nikon, UK). The number of transferred embryos per well was dependent on the number of live embryos available. Once the embryos settled on the Ishikawa cell layer, the 24-well plates were transferred to an incubator and cultured under existing culture conditions for 72 hours. **Figure 2-8** shows schematic of the establishment of 2-D embryo-Ishikawa cell co-culture system.

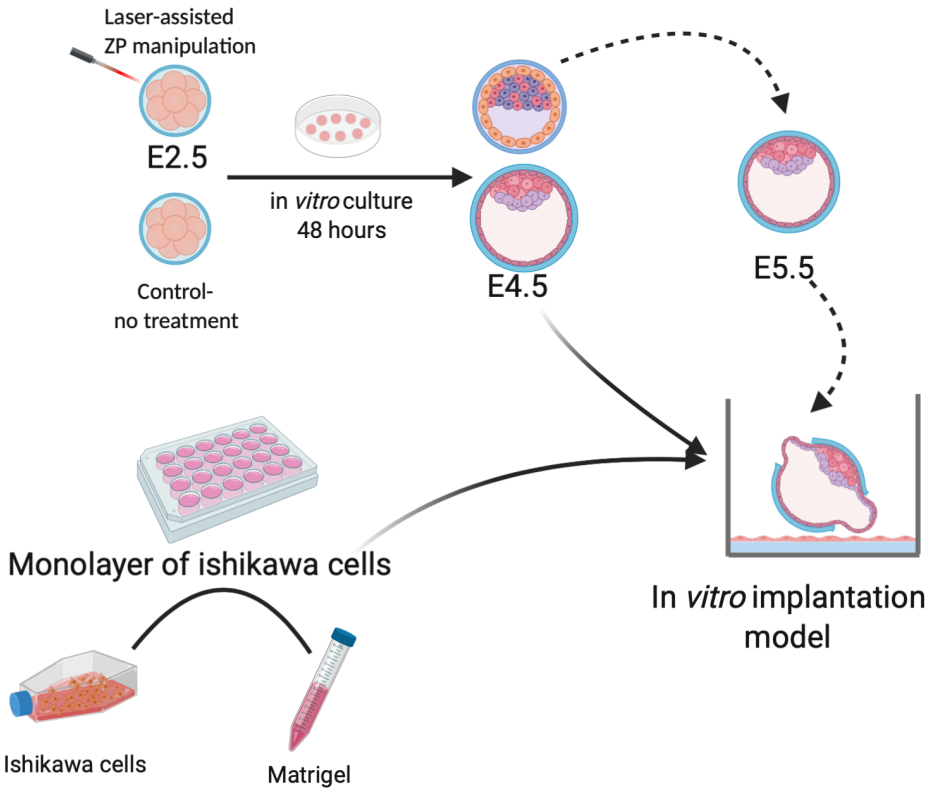


Figure 2-8. A schematic of the establishment of 2-dimension co-culture system

E2.5 Embryos were treated with different laser ZP manipulations, followed by *in vitro* culturing 48 hours. While Ishikawa cells were grown on Matrigel-coated coverslips before embryo transfer. Once the embryos grew to blastocyst stage (expanded or hatching blastocysts at E4.5 or E5.5), they were transferred onto the Ishikawa cell layer in the 24-well plates and started the co-culture.

Embryos were assessed every 24 hours on a warmed microscope stage. Embryo survival and hatching status, including fully hatched or hatching, and unhatched, was recorded. The embryos were counted as 'trapped embryos' if they remained in hatching status at 72 hours after co-culture.

2.6.2 Attachment assay

To evaluate the attachment capability of embryos to the Ishikawa monolayer, an attachment assay was conducted. Specifically, the 24-well plates were shaken horizontally three times before placing onto a microscope. Then, the attachment stability was assessed using a four-point scale of blastocyst behaviour upon agitation of the co-culture system, by gently pressing the microscope table 2-3 times in accordance with a previous study (**Table 2-1**) (Ruane et al., 2017). The attachment stability score was recorded every 24 hours, and 3 times in total. Stably attached embryos were only counted when they were fully hatched and attached to Ishikawa cells with a 4-point score.

Table 2-1 The standard criteria for attachment stability measurement

Score	Stability stage	Agitation
1	Not attached	Movement upon agitation
2	Weakly attached	High oscillation upon agitation
3	Intermediately attached	Low oscillation upon agitation
4	Stably attached	No oscillation upon agitation

2.7 Immunofluorescent staining

2.7.1 Slide coating

An adhesion slides (VWR, UK) were coated with 0.01% (v/v) poly-D-lysin (Thermo Fisher, UK) for 30 minutes at room temperature.

2.7.2 Immunostaining

Prior to fixation, E4.5 blastocysts were washed with 0.01% (V/V) Poly (vinyl alcohol) (PVA) - PBS buffer 3 times by transferring the blastocyst into three consecutive drops of 0.01% PVA-PBS buffer. Ishikawa cells were washed with 500 µL PBS three times on a shaker machine (5 minutes/wash). Following the washing step, blastocysts or cells were fixed with 4% Paraformaldehyde (PFA) for 20 minutes (Embryos were transferred into a drop of 50 µL 4% PFA on an adhesion slid. For cells, 200 µL of 4% PFA was added into the 24-well plates). After fixation, the embryos or cells were washed three times with PBS for (as described earlier). Then, permeabilization was performed using 0.05% Triton X-100 (Sigma-Aldrich, UK), and incubated for 10 minutes (For embryos, a drop of 30 µL 0.1% Triton X-100 was added onto embryos; for cells, 200 µL of 0.05% Triton X-100 was added into the 24-well plates). For embryos, blocking was performed by incubating the embryos in 50 µL of Mouse on Mouse (M.O.M) blocking buffer (Vector Laboratories, UK), which was prepared by adding 4 drops of M.O.M original buffer into 2.5 ml PBS. For cells, blocking was conducted by adding 0.5 - 5% bovine serum albumin (BSA) (Sigma-Aldrich, UK) into the 24-well plates and incubating for 1 hour at room temperature (RT).

After blocking, embryos or cells were then incubated with one or two primary antibodies overnight at 4°C (listed in **Table 2-2**). The following morning, embryos or cells were washed three times with PBS prior to incubation with a Fluorescein isothiocyanate (FITC)-conjugated goat anti-mouse secondary antibody, and/or a FITC-conjugated donkey anti-rabbit secondary antibody (both from Invitrogen, Thermo Fisher, UK) for 1 hour at RT. Cells or embryos were then briefly washed three times with PBS before mounting with mounting medium containing DAPI (Vector Laboratories, UK). Images were taken on the confocal microscope platform (Leica Sp5 microsystem) and the fluorescence microscope (Nikon, UK). Finally, Image J software (Version 2.0.0-rc-69/1.52p) was used to quantify the number of cells and the intensity of target protein (mean grey value (arbitrary unit)).

Table 2-2. Antibody information

Target protein	Blocking buffer	Primary antibody	Dilution	Second antibody	Dilution
CDX2	M.O.M blocking buffer	CDX2 (NBP2-58280) Novus Biological, UK	1:200	Donkey anti-Rabbit IgG Alexa Fluor 594	1:1000
OCT4	M.O.M blocking buffer	OCT-3/4 (sc-5279) Santa Cruz, UK	1:500	Goat anti-Mouse IgG Alexa Fluor 488	1:1000
Heat shock protein 70 (HSP70)	M.O.M blocking buffer	HSP70 (MA3A-006) Invitrogen, UK	1:150	Goat anti-Mouse IgG Alexa Fluor 488	1:500

(Table2-2 continued)

Target protein	Blocking buffer	Primary antibody	Dilution	Second antibody	Dilution
Cytokeratin-18	0.5% (v/v) BSA-PBS buffer	Cytokeratin-18 (sc-6259) Santa Cruz, UK	1:300	Goat anti-Mouse IgG Alexa Fluor 488	1:1000
Vimentin	0.5% (v/v) BSA-PBS buffer	Vimentin (sc-6260) Santa Cruz, UK	1:100	Goat anti-Mouse IgG Alexa Fluor 488	1:1000
Integrin avβ3	0.5% (v/v) BSA-PBS buffer	Integrin avß3 (sc-7312) Santa Cruz, UK	1:100	Goat anti-Mouse IgG Alexa Fluor 488	1:1000
OPN	5% (v/v) BSA-PBS buffer	OPN (ab8448) Abcam, UK	1:3000	Donkey anti-Rabbit IgG Alexa Fluor 594	1:3000

For Heat Shock Protein 70 (HSP70) staining, heat shock (HS) treated embryos were used as a positive control. HS was induced before the embryo fixation, by placing the blastocyst at 43°C for 30 minutes (Hartshorn et al., 2007) , followed by a recovery period at 37°C for 30 minutes to produce HSP70. An antibody staining was then performed as described above.

2.8 Cell apoptosis detection

2.8.1 DNA fragmentation assessment

The extent of DNA fragmentation was determined in E4.5 blastocysts with a TdT-mediated dUTP nick-end labelling (TUNEL) kit (Promega, UK), by catalytically

incorporating fluorescein-12-dUTP at the 3'-OH DNA ends using recombinant Terminal Deoxynucleotidyl Transferase (rTdT). rTdT forms a polymetric tail using the principle of the TUNEL assay, which enables fluorescein-12-dUTP-labeled DNA to be visualised directly by fluorescence microscopy.

After fixation and permeabilization as described above, the embryos were rinsed three times in fresh PBS to remove residue Triton X-100. Embryos were then equilibrated in a 50 µL drop of Equilibration Buffer at RT for 10 minutes. After removing the Equilibration Buffer, a 50 µL drop of rTdT incubation buffer (mixing 45µL of Equilibration buffer with 5 µl Nucleotide Mix and 1 µL rTdT Enzyme) was added onto the embryos and incubated at 37°C for 60 minutes inside a humidified chamber. The chamber was covered with a lid to avoid light. During this time, the 20× SSC buffer was diluted 1 in 10 with deionized water. To terminate the reaction, the rTdT buffer was discarded and replaced with 100 µL of diluted SSC onto the embryos and incubated for 15 minutes at RT. The embryos were washed 3 times with PBS to remove the unincorporated fluorescein-12-dUTP and mounted with mounting medium containing DAPI (Vector Laboratories, UK) before being covered with a coverslip. The TUNEL-positive signal (green fluorescence) indicated DNA fragmentation, while DAPI staining(blue) showed the cell nuclei. The apoptotic index (%) for each embryo was calculated as follows: the number of the TUNEL-positive cells / the number of the DAPI-positive cells.

DNase I treatment of the fixed cells leads to fragmentation of the chromosomal DNA and exposure of multiple 3'-OH DNA ends for labelling; this results in the majority of the treated cells emitting green fluorescence. Thus, to create a positive control for the TUNEL assay, embryos were treated with DNase I (50 IU/ml) for 10 minutes at RT

after fixation and permeabilization. After washing off the DNase I buffer, the procedure was the same as described above. To create a negative control, the embryos were treated with DNase I, but without labelled rTdT reagents.

2.8.2 The detection of Caspase-3/7 activity

Caspase-3/-7 activity was detected in embryos using a fluorescent inhibitor of caspase (FLICA) kit (Image-iT™ LIVE Green Caspase-3 and -7 Detection Kit, Invitrogen, UK). The FLICA reagent is thought to interact with the enzymatic reactive centre of an activated caspase via the recognition sequence (aspartic acid-glutamic acid-valine-aspatric acid (DEVD)), and a carboxyfluorescein group (FAM) is attached as a reporter. The FLICA reagent is cell-permeant and non-cytotoxic, so that the unbound FLICA molecules can diffuse out of the cell and be washed away. The remaining green-fluorescent signal is a direct measure of the amount of active caspase present at the time the inhibitor was added. Before conducting the experiment, 1× Wash Buffer was prepared by adding 1 part of 10× apoptosis Wash Buffer to 9 parts of deionized H_2O. To prepare 150× FLCIA reagent stock solution, 50 µL of DMSO was added to the vial of lyophilized FLICA reagent. Finally, the 30× FLICA reagent working solution was prepared by diluting 1 part of 150× stock solution 5 times with 4 parts PBS (pH 7.4). Regarding the biological positive control, E4.5 embryos were transferred to pre-warmed KSOM with 1 µM staurosporine (kindly provided by Mr Z. Ai, University of Oxford), and incubated for 2 hours at 37°C before labelling. Once washed with KSOM, the embryos were transferred into a 50 µL drop of 1× FLICA (diluted with KSOM), and cultured for 1 hour under existing culture conditions, protected from light. Next, the embryos were washed twice with KSOM. Embryos were then transferred into a 50 µL drop of 1 µM Hoechst 33342 stain medium and incubated for 10 minutes at 37°C. The

fixative solution was prepared by diluting 1 part of 10× apoptosis fixative solution to 9 parts of 1× Wash buffer. After washing twice, the embryos were transferred into a drop of 10 µL diluted fixative solution and then gently covered with coverslips. The mean grey value (arbitrary unit) of activated caspase-3/-7 was generated by Image J software and used to quantify the activation of caspase-3/-7.

2.9 RNA extraction and cDNA synthesis for embryos and cells

2.9.1 Mouse embryo cDNA synthesis

Embryo cDNA was directly synthesised from 3 whole blastocysts using the cell-to-cDNA kit (Invitrogen, UK). In brief, blastocysts were collected from culture medium and washed three times in 0.01% PVA-PBS buffer. Three blastocysts were then combined and lysed in 10 µL of cell Lysis buffer by incubation at 75°C for 10 minutes in a thermal cycler. Next, 0.3 µL of DNAse I was added to the cell lysate followed by a brief vortex mic before incubation at 37°C for 15 minutes to degrade genomic DNA. The reaction was inactivated by heating the sample to 75°C for 15 minutes. The dNTP mix (4 µL) and oligo first-strand primer (2 µL) were added into the sample mixture and incubated at 70°C for three minutes. Finally, 2 µL Reverse transcription buffer, 1 µL reverse transcriptase, and 1 µL RNase inhibitor, were added into the sample mixture and incubated at 42°C for 45 minutes to initiate the reverse transcription. The reaction was terminated at 95°C for 10 minutes and kept at -20°C before further use.

2.9.2 Preamplification of mouse embryo cDNA

Pre-amplification of target cDNA was conducted using the TaqMan PreAmp Master Mix Kit (Applied Biosystems, UK). The TaqMan Assay Pool was first prepared by

diluting the 20× TaqMan Gene Expression Assays (consisted of target specific primers and one probe) 100-fold with nuclease-free water (0.2×). The preamplification reaction was prepared by mixing 20 µL TaqMan PreAmp Master Mix (2×) (Applied Biosystems, UK), 10 µL Pooled assay mix (0.2×), and 10 µL embryo cDNA. Preamplification reactions were initiated with a 10-minute pre-incubation at 95°C, followed by 14 amplification cycles of 15 seconds denaturation at 95°C, and 4 minutes annealing/extending at 60°C. Finally, the reaction was terminated at 99°C for 10 minutes. The preamplification product was stored at -20°C for subsequent use.

Table 2-3 The TaqMan assays used for the TaqMan preamplification and qPCR

Gene name	TaqMan Assay ID	Dye
Dnmat3a	Mm00432881	FAM-MGB
Sod1	Mm01344233_g1	FAM-MGB
Gpx7	Mm00481133_m1	FAM-MGB
Gapdh	Mm99999915_g1	VIC-MGB
Pou5f1	Mm03053917_g1	FAM-MGB
Nanog	Mm02019550_s1	FAM-MGB
Cdx2	Mm01212280_m1	FAM-MGB
Bax	Mm00432051_m1	FAM-MGB
Bcl2l2	Mm00432054_m1	FAM-MGB
Actb	Mm02619580_g1	FAM-MGB
Rnd3	Mm00512162_m1	FAM-MGB
Myl6	Mm02342525_g1	FAM-MGB
Cox8a	Mm02342396_g1	FAM-MGB
Tmeff1	Mm05907935_s1	FAM-MGB

Table 2-3 (continued)		
Gene name	**TaqMan Assay ID**	**Dye**
Ctsh	Mm00514455_m1	FAM-MGB
Lgals1	Mm00839408_g1	FAM-MGB
Krt18	Mm01601704_g1	FAM-MGB
Aqp3	Mm01208559_m1	FAM-MGB
Atp5b	Mm01160389_g1	FAM-MGB
Ndufa7	Mm00458227_m1	FAM-MGB
Mvk	Mm00445773_m1	FAM-MGB
Mvd	Mm00507014_m1	FAM-MGB
Dnmt3l	Mm00457635_m1	FAM-MGB
Lmna	Mm00497783_m1	FAM-MGB

2.9.3 Ishikawa cell RNA extraction

For cell RNA analysis, the total cellular RNA was extracted using RNeasy Mini Kit buffers (Qiagen, West Sussex, UK) and Silica Membrane Mini Spin Columns (EconoSpin). In brief, cells in 24-well plates were harvested and lysed in wells by scraping with 150 µL/well buffer RLT containing 0.1% (v/v) β-mercaptoethanol. The cell lysate was transferred into labelled RNase/DNase-free tubes and mixed thoroughly with 150 µL of 70% (w/v) ethanol/tube. The entire 300 µL was then transferred into a mini-column (EconoSpin) and centrifuged at 8000g for 1 minute. The flow-through was discarded, and the columns washed with 350 µL/column of RW1 buffer followed by centrifugation at 8000 g for 1 minute. The flow-through was discarded, and 80 µL of DNAse mix, comprising 70 µL RDD buffer (Qiagen, UK) and

10 µL RNase-free DNase (Qiagen, UK) was carefully added into the central filter of each mini-column for genomic DNA elimination. The columns were incubated for 15 minutes at room temperature, washed again with 350 µL/column of RW1 buffer, and centrifuged at 8000 g for 1 minute. The flow-through was discarded, the columns washed twice with 500 µL/column of RPE buffer. This was followed by a centrifugation step at 8000 g for 1 minute and the waste was discarded. The columns were then centrifuged for an additional two minutes at 8000 g. The mini-columns were then transferred into newly labelled RNase/DNase-free tubes. RNA samples were eluted by adding 30 µL of RNase-free water into the central filter and incubating for two minutes at room temperature. The columns were centrifuged at 8000 g for 1 minute and the RNA concentration measured using a NanoDrop Lite Spectrophotometer (Thermo Fisher Scientific, UK). RNA samples were then stored at -20°C and used as required.

2.9.4 Ishikawa cell cDNA synthesis

Equal amounts of RNA (500-1000ng) were added into labelled MicroAmp® Reaction Tubes (Applied Biosystems) and diluted with DEPC-treated water (Invitrogen) to a final volume of 14.2 µL per tube. 5.8 µL/ sample RT master mix (comprised of 2 µL 10× RT buffer, 0.8 µL 100mM 25× dNTP, 2 µL 10× RT Random Primers, and 1 µL MultiScribeTM) Reverse Transcriptase from a High-Capacity Reverse Transcriptase kit (Applied Biosystems), was prepared and added to each RNA sample tube accordingly. Single-stranded cDNA synthesis was performed on a Veriti® 96-Well Thermal Cycler (Applied Biosystems). Samples were initially incubated at 25°C for 10 minutes, followed by reverse transcription at 37°C for 120 minutes. The reaction was

terminated at 85°C for 5 minutes and finally kept at 4°C before sample collection. cDNA samples were stored at -20°C and used as required.

2.10 Quantitative Reverse Transcriptase-PCR

2.10.1 TaqMan method for detecting gene expression in embryos

Quantitative PCR was carried out using the TaqMan Gene Expression System (Applied Biosystem, UK). 5 µL of TaqMan gene expression master mix, together with 1 µL of TaqMan probe [(0.5 µL of target probe + 0.5 µL of *Gapdh* probe) or (1 µL of one target/housekeeping gene probe)], and 4 µL of cDNA (diluted five times in RNase free), was premixed and added into a 96 well PCR plate (Applied Biosystems). Amplifications were performed on an Applied Biosystems QuantStudio 3 (Thermo Fisher, UK) using standard thermocycler parameters. Reactions were initiated with 10 minutes preincubation for enzyme activation at 95°C, followed by 45 amplification cycles of 15 seconds denaturation at 95°C, and 1-minute annealing and extension at 60°C. No template water controls were included.

2.10.2 SYBR Green method for detecting gene expression in cells

2 µL cDNA, together with 1.8 µL of associated premixed primer sets (final concentration in mix = 200nM), 5 µL 2× SYBR Green JumpStart Taq ReadyMix (Sigma-Aldrich), 0.2 µL ROX reference dye (Invitrogen), and 1 µL DEPC-treated water per well, were added into a MicroAmp® Optical 384-Well Reaction Plate (Applied Biosystems), with a final volume of 10 µL for each reaction. Amplifications were then performed on a QuantStudio 6 Flex Real-Time PCR System (Applied Biosystems). Reactions were initiated with 2 minutes pre-incubation at 95°C, followed by 50

amplification cycles of 30 seconds denaturation at 95°C, 30 seconds annealing at 55°C, and 30 seconds extension at 72°C. Melt curve analysis was performed to rule out non-specific amplification, and no template controls were included. Primers for human genes were designed using Primer-BLAST (http://www.ncbi.nlm.nih.gov/tools/primer-blast/), and primer efficiency was confirmed to be between 90-100% before use.

Table 2-4 Primers used for the SYBER green qPCR experiment

Protein	Gene	Forward (5'-3')	Reverse (5'-3')
Estrogen receptor 1	*ESR1*	TGGCCATTCATTTGCTTGCT	TTGGAATCCCTTTGGCTGTT
Progesterone receptor	*PGR*	GCGTGTCACTAAATTGCCGT	TGGGGAGCGCAAGAAAAAGT
Caherin-1	*CDH1*	TGGGCACAGATGGTGTGATT	TTCAGCGTGACTTTGGTGGA
Caherin-2	*CDH2*	TGCTGCAGAAAATCAAGTGC	TGGGGGCAAAATAAGGGTTT
Vimentin	*VIM*	AATCCAAGTTTGCTGACCTCTCT	AGCTTCAACGGCAAAGTTCT
Fibronectin-1	*FN1*	TGGGCAACTCTGTCAACGAA	AAGCCTAAGCACTGGCACAA
Cytokeratin-18	*FRT-18*	ACCATGCAAAGCCTGAACGA	AAGTGCTCCCGGATTTTGCT
Beta-2-Microglobuin	*B2M*	CTCGCGCTACTCTCTCTTTCT	CATTCTCTGCTGGATGACGTG

2.10.3 Calculation of gene expression levels

The relative expression levels of all target genes were calculated using the $2^{(-\Delta\Delta Ct)}$ method (Livak et al., 2001) by normalising to a housekeeping gene (B2M (cells)/ *Gapdh* (embryo)) ($2^{-(\text{CT target gene-CT housekeeping gene})}$), and the relative expression of target genes in the treatment group was presented as the fold change relative to the control group ($2^{-(\text{CT treatment-CT control})}$).

However, as regarding the RT-qPCR experiment for RNA-sequencing result confirmation, the housekeeping genes were validated. The mean Ct value of the validated housekeeping genes was used as the internal control for the relative expression. The detailed validation results were shown in **Chapter 6, Section 6.3.6**.

2.11 Statistical analysis

For the statistical analysis of the above experiment, quantitative data were analysed using Prism 8 software (GraphPad Software, CA, USA). Before comparison, the D'Agostino & Pearson test was conducted for data normality test. Normally distributed data are presented as mean ± SD (standard deviation); while the data that were not normally distributed are presented as medians (25% percentile, 75% percentile). Data between the 4 groups were compared using one-way ANOVA (Analysis of Variance) or Kruskal-Wallis non-parametric test with relevant post-hoc tests for multiple comparisons according to the data and comparison strategies, while data between 2 groups were compared using a T-test or Mann-Whitney nonparametric test. In addition, with respect to the 5-point scale questions in the questionnaire, the Mann-Whitney U test (also known as the Wilcoxon rank-sum test) was used to compare the Likert Scale

weights of two groups (Jamieson, 2004, Joshi et al., 2015). A probability (*P*) value of <0.05 was considered to be statistically significant. A detailed description of statistical analysis is shown in the figure legends.

As for qualitative data, χ2 (Chi-Square) test or χ2 Fisher's exact test were used to analyse the frequency distribution of categorical variables using the SPSS 22.0 software package (SPSS Inc., Chicago, IL). In addition, the pairwise z-test was used as post hoc tests for χ2 independence test to compare the proportion between two subgroups. A probability (*P*) value of <0.05 was considered to be statistically significant. A detailed description of statistical analysis is shown in the table or figure legends.



Chapter 3

Characterising the disparities in practices and attitudes regarding assisted-hatching

3.1 Introduction

Assisted-hatching (AH) has been proposed as a technique to create weaknesses or openings on the ZP by drilling or thinning, thus facilitating embryo hatching and increasing the chances of implantation. Cohen et al. reported the first application of AH in 1990 when mechanical force was used to partially dissect the ZP (PZD) of embryo (Cohen et al., 1990). Since then, several procedures have emerged; these show significant variability in terms of techniques, methods, embryo stages, the modes of application, and patient groups (Alteri et al., 2018).

To date, the most widely applied AH techniques include mechanical incision, chemical solutions, and laser-assisted hatching (LAH) (Alteri et al., 2018). Specifically, mechanical AH was the first AH technique used to create an opening in the ZP via the mechanical force generated by an injection/dissecting pipette (Stein et al., 1995). Later, chemical solutions (acidified Tyrode's solution or Pronase) were introduced as an alternative method for AH (Yano et al., 2007, Feng et al., 2009). However, both mechanical and chemical techniques require extensive skills to maintain unified, well-controlled, and standardised procedures as even a marginal difference may affect outcomes. Furthermore, sophisticated manipulations also involves extensive exposure of embryos outside of the incubator, with resultant variations of pH and temperature leading to potential detrimental effects on embryo development (Hammadeh et al., 2011). Nevertheless, the laser technique, especially the non-contact infrared diode laser, is more easily focused on the target areas, and can thus produce controlled, reproducible, and precise openings/ablations on the ZP (Davidson et al., 2019). Furthermore, laser-assisted ZP manipulation is easier to perform, with the duration, size of the laser pulse, and the location readily defined and visualised on

the laser platform. This advantage makes it possible to precisely manipulate the ZP of the morula or even expanded blastocyst (Alteri et al., 2018, Davidson et al., 2019).

Aside from the different techniques, various methods are also used in assisted hatching. ZP breaching/drilling was the first method used to create a gap (10-40 μm) in the ZP. Then, ZP thinning is proceeded by using chemical solution or laser beam to digest or ablate the ZP partially, creating different extension (in the measurement of 5-80 μm or 1/4 to 1/2 of ZP circumference) of ablation to the ZP (Danfour et al., 2010, Alteri et al., 2018). Additionally, the ZP removal is to expose an embryo to a chemical solution in order or digest the ZP completely. However, all of these methods have their drawbacks. For instance, ZP drilling/ breaching increases the risk of losing blastomeres through the opening and may predispose an embryo to uterine fluid enriched with high concentrations of nutrients and antibodies (Hiraoka et al., 2009). On the other hand, ZP thinning may increase embryo contraction-expansion cycles and an elongated duration of fully hatching (Schimmel et al., 2014). Additionally, potential damage resulting from the mechanical traumas, attachment to glass/plastic surfaces, or the loss of the ZP protection from infection were viewed as the possible drawbacks of ZP removal (Alteri et al., 2018).

Furthermore, AH can be performed at different embryo stages, followed by various embryo transfer strategies. For example, 2-cell embryos, morulae, as well as Day 5-6 blastocysts are the most commonly used embryo stages for AH related studies (Baruffi et al., 2000, Kutlu et al., 2010, Wan et al., 2014, Lu et al., 2015). Following AH, embryo transfer (ET) can be performed either immediately or delayed for several minutes to hours according to the protocols used in different clinics (Kanyo et al., 2003, Alteri et

al., 2018, Aoyama et al., 2020). In addition, some authors have reported the blastocyst transfer following Day-3 AH treatment (Graham et al., 2000, Kung et al., 2003).

Apart from the variability in technique and methods, AH has been applied in different clinical scenarios, including female patients with advanced age (Lanzendorf et al., 1998, Edirisinghe et al., 1999, Hsieh et al., 2002), with a history of recurrent IVF failure (Sagoskin et al., 2007, Hagemann et al., 2010, Wan et al., 2014), or patients with endometriosis (Çıray et al., 2005). Furthermore, frozen-thawed or vitrified-warmed embryos (Valojerdi et al., 2010, Liu et al., 2020) are reported frequently as study groups in previous research. Furthermore, AH is also being used to dissect the ZP prior to polar biopsy, blastomere biopsy, and trophectoderm biopsy to facilitate the subsequent biopsy procedures (Joris et al., 2003, Chatzimeletiou et al., 2005, Geber et al., 2011, Capalbo et al., 2016).

Nevertheless, after more than 25-years of application in clinics, there is still a lack of standardisation with regards to AH protocols. Also, much of the published data on the efficacy of AH are contradictory, inconclusive, or confounded by variables, due to the challenge of controlling techniques and methods in a reliable manner (Sallam et al., 2003, Kissin et al., 2014, McLaughlin et al., 2019). On the other hand, although guidelines and systematic reviews are available to suggest the overall usage of AH (Carney et al., 2012, ASRM, 2014, Li et al., 2016), and much effort has been made to study the association between various methods and the criteria of AH with pregnancy outcomes (Mantoudis et al., 2001, Balaban et al., 2002, Hsieh et al., 2002, Wong et al., 2003, Lanzendorf et al., 2007, Alteri et al., 2018), there has been little consensus regarding evidence-based guidelines to optimise the AH protocol. Most importantly, sparse data is available relating to the current practice patterns for AH in IVF centres.

The aim of this chapter was to investigate the specific manner in which AH is used in current IVF scenarios. Firstly, I tried to characterise the AH methods being used in clinical practice and identify potential opportunities for standardisation. Secondly, I evaluated opinions regarding the safety and efficacy of AH from embryologists and clinicians.

3.2 Results

3.2.1 Demographics

A total of 189 people participated the survey and 181 of them completed all the questions, and these respondents were from 17 countries/regions, including the UK (40.1%,73), China (47.8%,87), and other countries (12.1%, 22), including Argentina, Cambodia, Canada, Cyprus, Denmark, Egypt, Greece, India, Italy, Malaysia, New Zealand, Norway, Qatar, Spain, and the USA (**Figure 3-1**).

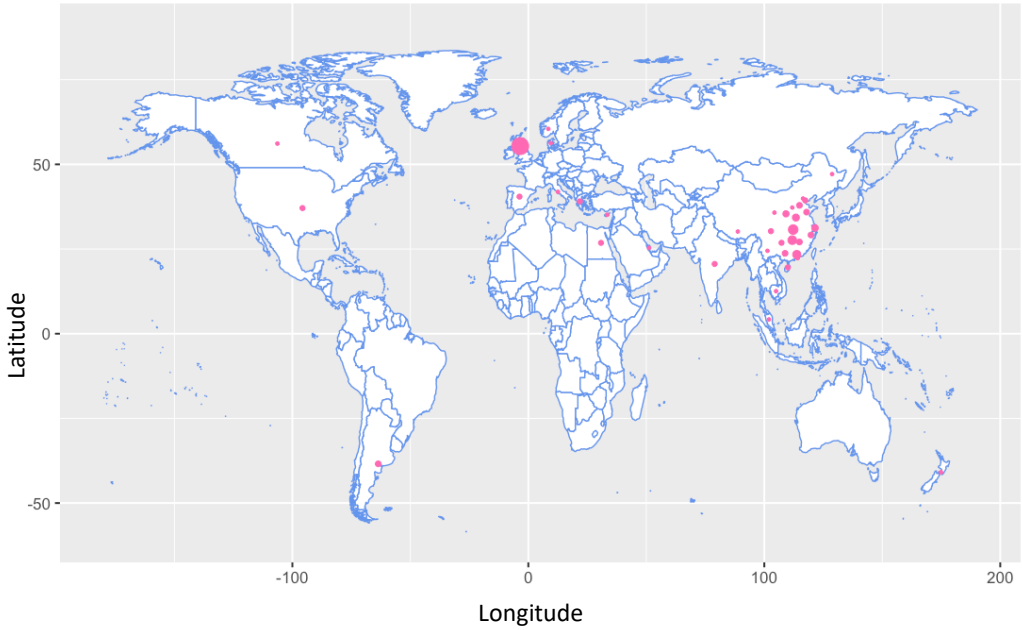


Figure 3-1. The geographical distribution of survey responders

The pink dots represent the survey responders, and the size of the dot represent the number of responders in one area. This figure was created in the R environment, using the *ggmap and ggplot* packages.

Among all respondents, 79.6% were embryologists, 15.5% were clinicians, and rest of them are in other related professions. Considering that clinicians may not be familiar with the technique details used in embryology laboratory, the 'I don't know' and skip options was provided in order to reduce the misinterpretation due to the uncertainty. 89.0% of responders works in the clinics providing advanced ART treatment, such as IVF and ICSI; of which 51.6 % reported performing embryo biopsy for PGT. Furthermore, 11.0% of responders works in the clinics only providing intrauterine insemination (IUI) treatment, and these responders only answered the question regarding their attitude and opinion towards AH, instead of the application details (**Table 3-1**).

Table 3-1 The demographics of responders

Demographics	n	%
Total response received	181	
Profession		
Embryologists	144	79.6
Clinicians	28	15.5
Nurse	5	2.7
Other *	4	2.2
Clinic location		
United Kingdom	73	40.3
Countries within the EU	8	4.4
Countries outside the EU	100	55.2

Table 3-1 (continued)

Demographics	n	%
Type of clinics		
Publicly funded clinics providing publicly funded cycles	32	17.7
Publicly funded clinics providing privately/publicly funded cycles	71	39.2
Private clinics providing privately and publicly funded cycles	61	33.7
Private clinics providing privately funded cycles	40	22.1
ART treatment provided by clinics		
Advanced ART treatment, e.g., IVF, ICSI, and PGT	161	89.0
Only basic fertility treatment, e.g., ovulation induction, IUI	20	11.0
PGT (embryo biopsy) available in your clinic?		
No	78	48.4
Yes	83	51.6

*: 2 Laboratory Directors and 2 trainee Embryologists
ART: assisted reproductive technology; IVF: *in vitro* fertilization; ICSI: intracytoplasmic sperm injection; PGT: preimplantation genetic testing; IUI: intrauterine insemination.

3.2.2 The application of AH

To separate the application of AH with regards to different purposes, AH can be classified as AH prior to embryo transfer (AHpET) and AH prior to embryo biopsy (AHpBP). The application rate of AHpET was 61.5% among all of the respondents practising advanced ART treatments, while the application rate of AHpBP was 89.2% among all biopsy users. Furthermore, 66.2% of AHpBP users would also perform AHpET (**Figure 3-2 A**). Intriguingly, the application of AHpET in the UK was significantly lower compared with that from other countries: AHpET (43.1% *vs* 76.4%,

P<0.0001), and AH prior to both ET and biopsy (52.8% *vs* 81.1%, *P*=0.006); while no difference was found in the application of AHpBP (86% *vs* 92.5%) (**Figure 3-2 B**).

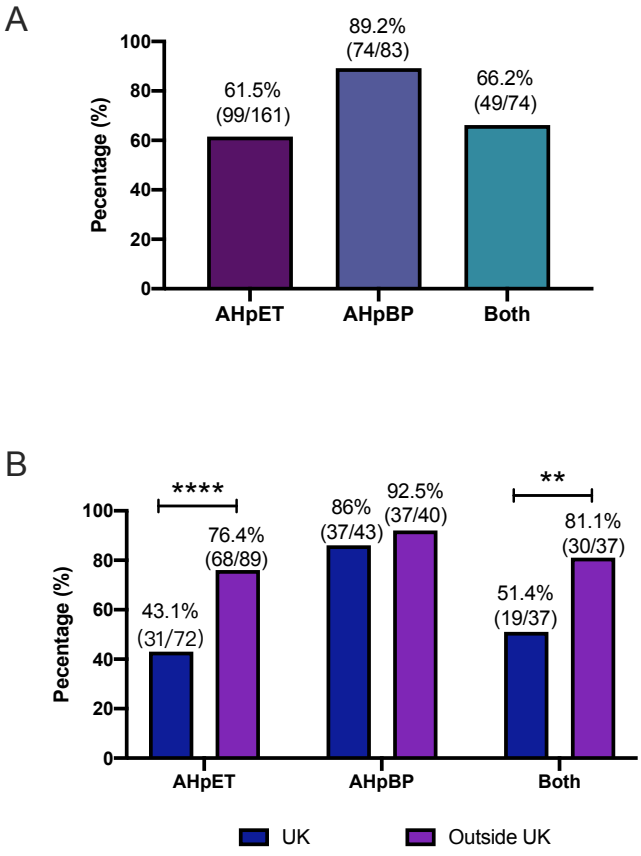


Figure 3-2. The application rate of AH (assisted-hatching)

(A) The application rates of AHpET (AH prior to embryo transfer), AHpBP (AH prior to biopsy), and both AHpET and AHpBP. (B) A comparison of application rates between areas outside of the UK and in the UK. The Chi-square ($\chi 2$) test was used to compare frequencies between the two groups (***P*<0.01; *****P*<0.0001).

3.2.3 The practice of AH

3.2.3.1 The characteristics of AHpBP practice

The clinical practice of AHpBP is summarised in **Table 3-2**. 73.5% (61/83) of the responders performed only TE biopsy in their clinics, while 22.9% (19/83) of responders conducted both Day 3 embryo and TE stage biopsy. Among all the biopsy

users, 89.2% (74/83) of them would perform AHpBP; however, the time points for performing AH varied. 55.4% of them performed AH before the day of biopsy, 24.3% on the day of biopsy, and 18.1% immediately before biopsy. In addition, as for the embryo stage for AHpBP: most of AHpBP were performed at blastocysts (44.7%), or Day 3 embryos (35.5%); interestingly, there were 18.4% of responders performed AHpBP on Day 4 embryos.

Specifically, for TE biopsy procedure, 90.0% (72/80) of responders would use AHpBP: 55.6% (40/72) of them performed on the day before biopsy, 25% (18/72) performed on the day, and even 19.4% (14/72) of them performed AHpBP immediately before biopsy at blastocyst stage. Furthermore, 47.2 % (34/72) of the AHpBP are conducted at blastocyst-stage, while 52.8% (38/72) of AHpBP for TE biopsy are performed at cleavage-stage. Precisely, 31.9% (23/72) are performed on Day 3 and 19.4% (14/72) on Day 4.

Regarding the practice details of AHpBP, laser-assisted AH was the predominant technique (97.4%), and ZP drilling was the primary method (90.6%), no matter it was performed at cleavage-stage AH (92.9% (39/42)) or at blastocyst stage AH (88.2% (30/34)). However, the details of AHpBP drilling were inconsistent: 71.1% of respondents created a small ZP opening (<15 μm), with 36.5% for opening size <10 μm and 34.6% for opening size: 10-15 μm. Whereas only 28.3% responders drilled ZP larger than15 μm. When applying the ZP drilling for TE biopsy at cleavage stage, 74.1% (20/27) of the responder drilled the ZP with small opening (<15 μm) (44.4% (12/27) with <10 μm and 29.6% (8/27) with 15-25 μm). Moreover, only 21.6% (16/74) responders performed ZP thinning for AHpBP, and 64.3% of respondents ablated less than 1/4 of the ZP circumference.

Table 3-2 The characteristics of AHpBP practice

Characteristics/ details	n	%
Embryo stage for biopsy		
Day 3 embryos	3	3.6
Blastocyst embryos	61	73.5
Both of Day 3 and blastocyst embryos	19	22.9
The time of AHpBP prior to biopsy		
Before the day of biopsy	41	55.4
On the day of biopsy	18	24.3
Immediately before biopsy	15	18.1
Embryo stage for AHpBP		
Cleavage stage (Day 2)	1	1.3
Cleavage stage (Day 3)	27	35.5
Morula stage (Day 4)	14	18.4
Blastocyst stage (Day 5-7)	34	44.7
Technique for AHpBP		
Laser-assisted method	72	97.4
Chemical method	1	1.3
Mechanical method	1	1.3
Method for AHpBP		
ZP drilling	58	78.4
ZP thinning	7	9.5
Both	9	12.2
The opening size of drilling	(14 responders replied “don’t know”)	
<10 μm	19	36.5
10-15 μm	18	34.6
15-25 μm	12	23.1
>25 μm	3	5.7

Table 3-2 (continued)

Characteristics/ details	n	%
The extension of ZP thinning	(2 responders replied “don’t know”)	
< Quarter of the circumference	9	64.3
Quarter of the circumference	1	7.1
Quarter to half the circumference	1	7.1
Half the circumference	0	0
> Half the circumference	3	21.4

3.2.3.2 The characteristics of AHpET practice

Table 3-3 presents tabulated data regarding the details of the practice of AHpET. For the clinical indication of AHpET treatment, ‘embryos with a thick ZP’, ‘patient with a poor prognosis’, and ‘frozen/thawed embryos’ were reported with the same importance, accounting for 34%, 31.4%, and 30.9% of respondents. In some cases, AHpET was performed on the patient’s request; this was mentioned by five respondents in the UK.

When asked about ‘whether AHpET is applied to fresh or frozen/thawed embryos’, more than half of respondents (58.5%) reported that AHpET would be used on both fresh and frozen/thawed embryos. In contrast, 37.2% would only apply AHpET on vitrified/warm and/or slow freeze/thaw embryos. The survey asked for comments about the reasoning behind performing AHpET on vitrified/warm or slow frozen/thawed embryos only; 71.4% (25/35) of the respondents claimed that the cryopreservation process would cause ZP abnormities, such as ZP hardening or ZP thickening, thus leading to difficulty during hatching. Moreover, 14.3% (5/35) of these responders believed that AHpET could provide better outcomes for the FET cycle.

In response to AHpET performance time, 44.4% of respondents applied AH on Day 3 stage embryos, and the same number of responders applied AH on Days 5-7 blastocyst stage embryos. From the data collected, although laser-assisted AH was the main technique used in the clinics approached (96.0%), there was 62.9 % of respondents would use ZP drilling, the 53.6% would use ZP thinning (**Table 3-3**).

Table 3-3 The characteristics of AHpET practice

Characteristics/ details	n	%
Indications for AHpET		
Embryos from patients with a poor prognosis	61	31.4
Embryos with a thick zona pellucida	66	34.0
Slow frozen/thaw or vitrified/warm embryos	60	30.9
Only when patient requests	5	2.6
All embryos	2	1.0
Fresh or frozen/thaw embryos		
Fresh embryos	4	4.3
Vitrified/warm embryo only	27	28.7
Slow freeze/ thaw embryo and vitrified/warm embryo	8	8.5
All embryos	55	58.5
Embryo stage for AHpET		
Cleavage stage (Day 2)	8	5.6
Cleavage stage (Day 3)	63	44.4
Morula stage (Day 4)	8	5.6
Blastocyst stage (Day 5-7)	63	44.4
Technique for AHpET		
Laser-assisted method	94	96.0
Chemical method	1	1.3
Mechanical method	2	2.7

Table 3-3 (continued)

Characteristics/ details	n	%
Method for AHpET		
ZP drilling	45	46.4
ZP thinning	36	37.1
Both	16	16.5
The opening size of drilling	(19 responder replied “don’t know”)	
<10 μm	16	37.2
10-15 μm	15	34.9
15-25 μm	6	13.9
>25 μm	6	13.9
The extension of ZP thinning	(7 responders replied “don’t know”)	
< Quarter of the circumference	15	33.3
Quarter of the circumference	17	37.8
Quarter to half the circumference	11	24.4
Half the circumference	1	2.2
> Half the circumference	1	2.2
Continuously culture embryo after AHpET	(1 responder replied “don’t know”)	
Yes, culture to blastocyst stage	9	9.6
No, embryo(s) will be transferred very soon (within few hours)	57	60.6
Both, depends on embryo development or biopsy needs	27	28.7

More variation was shown in the invasive degree of ZP manipulation for AHpET. For ZP drilling method, 72.1% of the responders created the small size opening (<15 μm), and 37.2% of them chose <10 μm. In contrast, only 13.9 % created a larger than 25 μm opening. To be specific, when applying AHpET at cleavage-stage, 77.4%% (24/31) of responder drilled ZP with small opening size (<15 μm), and only 19.4% (6/31) of responders drilled ZP with >15 μm opening size.

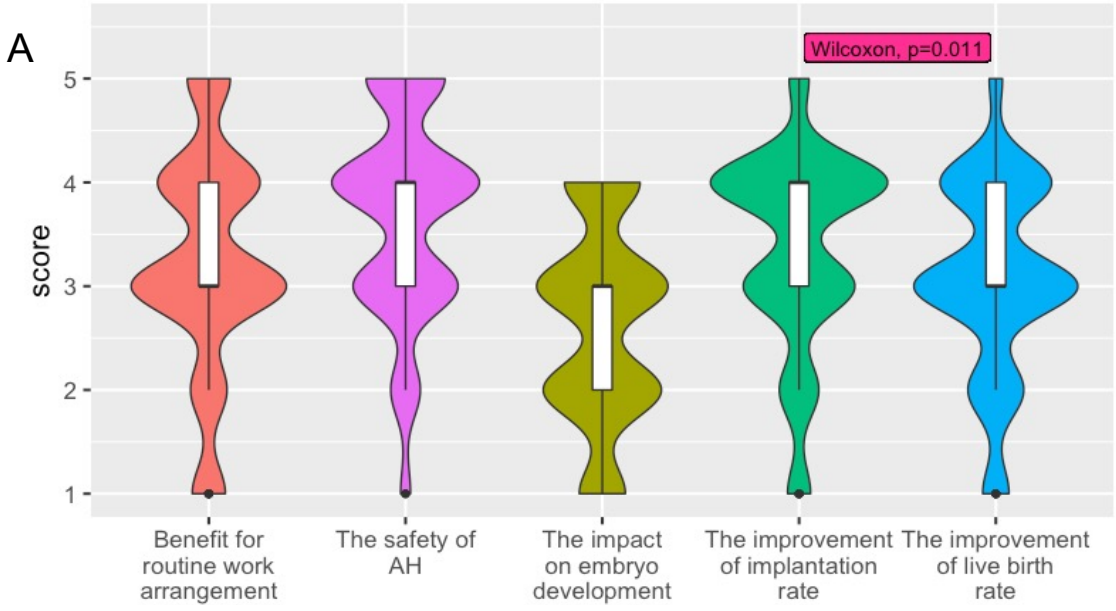
For extension of ZP thinning, 37.8% of them ablate 1/4 of the ZP circumference, approximately 33% ablate less than 1/4 of the ZP circumference. Specifically, the 69.2% of the cleavage-stage ZP thinning are aiming for less (28.2%) or equal (41.0%) to 1/4 of the ZP circumference ablation.

When asked whether they will continue to culture embryos after AH, most of the respondents stated that they would transfer the embryo within few hours without extending the embryo culture (60.6%), no matter whether AHpET was conducted at the pre-blastocyst stage (58% (40/68)) or the blastocyst stage (68% (17/25)). On the contrary, only 9.6% of AHpET users cultured the embryo to the blastocyst stage and 28.8% of respondents stated that it depends on embryo development or biopsy need.

3.2.4 Attitudes regarding AH

AH users were asked five questions about their opinion regarding AH; **Figure 3-3** represents the weight distributions of these Likert Scale questions. The weight score of the question 'how helpful do you think AH is to the routine work' was 3 (3, 4). Interestingly, the score weight was significantly higher among AH users from outside the UK when compared with those from the UK (3 (3, 4) *vs* 2 (2, 3.75), *P*=0.005). Regarding the safety of AH, more AH users stated that it was likely to be safe; however, the score was also significantly higher among respondents outside of the UK (4 (3, 5) *vs* 4 (3, 4), *P*=0.049). Furthermore, most of the AH users held a neutral opinion regarding the question 'Will AH have an impact on embryo development', with a score significantly lower in the responders from UK (2 (1.5, 3) *vs* 3 (2, 3.75), *P*=0.0005). In addition, this score was significantly higher in the non-AH user group (3 (3, 4)) in compared with AH users (*P*=0.026) (**Appendix 3 Fig S.2**).

None of these respondents reported any side effects among the children born following AH in their experience. However, three respondents had the concerns about the potential laser thermal effect on embryos. Regarding the efficacy of AH, questions referred to implantation rate and live birth rate. Intriguingly, the score for an improvement of implantation rate was significantly higher than the score regarding live birth rate (4 (3, 4) *vs* 3 (3,4), *P*=0.011). Notably, AH users from the outside of the UK believed that AH is more likely to improve the implantation rate (4 (3, 4) *vs* 3 (2, 4), *P*<0.0001).



B-1 The benefit for routine work arrangement

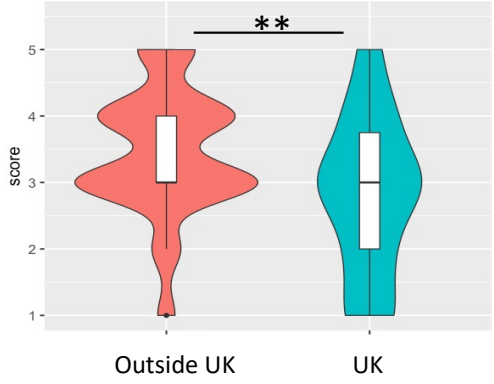


Figure 3-3 (Continued on next page, legend follows)

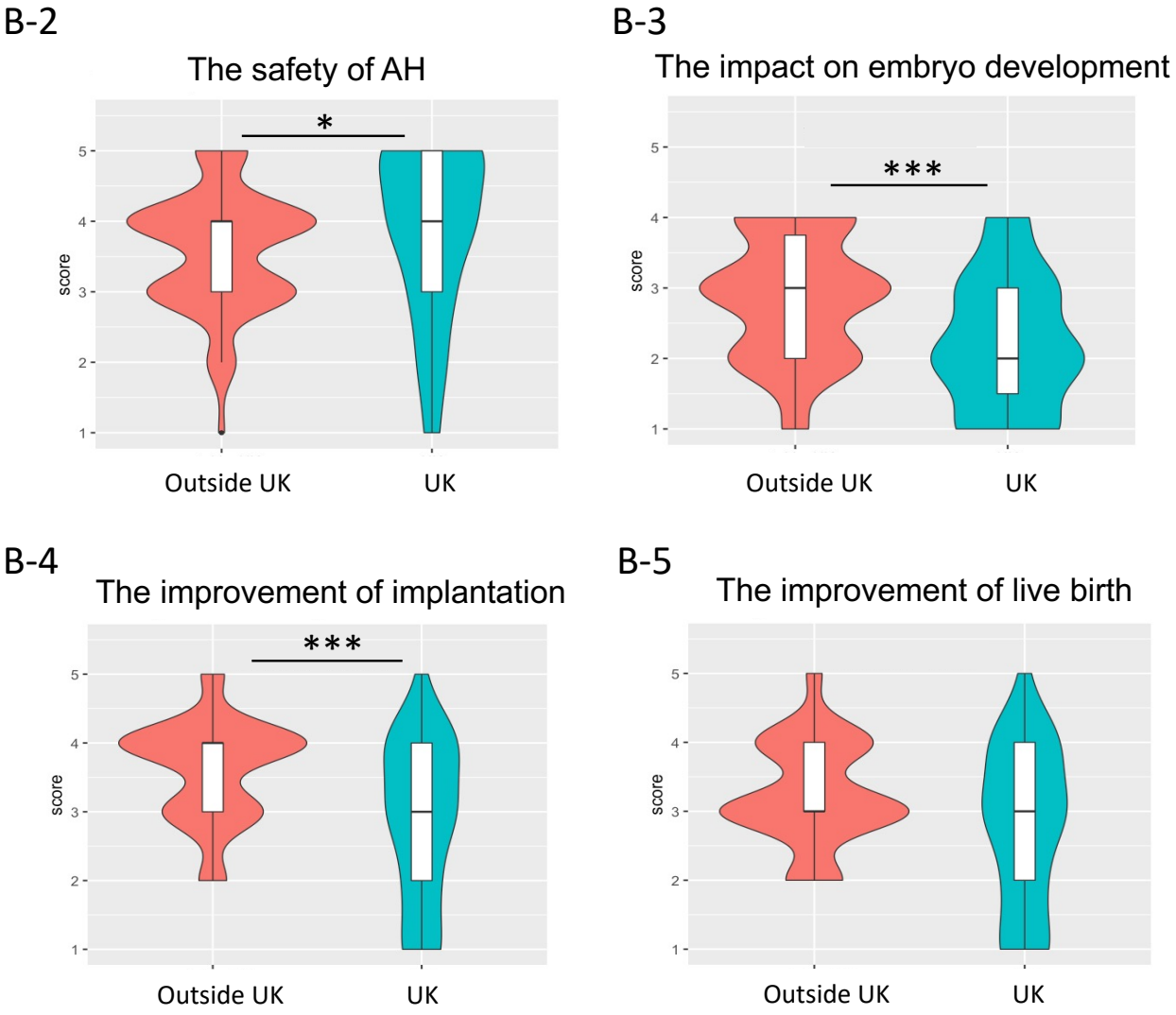


Figure 3-3. Opinions relating to AH among AH users

The violin plots show the Likert scale (1 to 5 point) resulting for the opinions relating to AH from all AH users (A); The comparison of scores between AH users in and outside of the UK: (B-1) the benefit for routine work arrangement, (B-2) the safety of AH, (B-3) the impact on embryo development, (B-4) the improvement of implantation, and (B-5) the improvement of live birth. Boxplots present the median and range of the first quantile to the third quantile. The Wilcoxon rank-sum test was used to compare scores between two groups. *P<0.05, **P<0.01, ***P<0.001

For those AHpBP users, when asked the reason of not applying AHpET (**Figure 3-4 A**), 76.0% of the responders claimed that there was no evidence for the efficacy of AHpET, 16.0% were cautious because of concerns over safety, and 8.0% (2/25) had no equipment or need for AHpET. Furthermore, two of the respondents pointed out

that they do not apply AHpET because it was considered as a red-traffic light at the time of the survey on the HFEA (Human Fertilisation & Embryology Authority) system. Furthermore, for those participants who do not perform AH in any scenarios (before ET or biopsy), although more people said it was because of a lack of equipment (28.6%), 54.8% claimed no evidence of efficacy, and 16.7% of them were unsure of safety (**Figure 3-4B**).

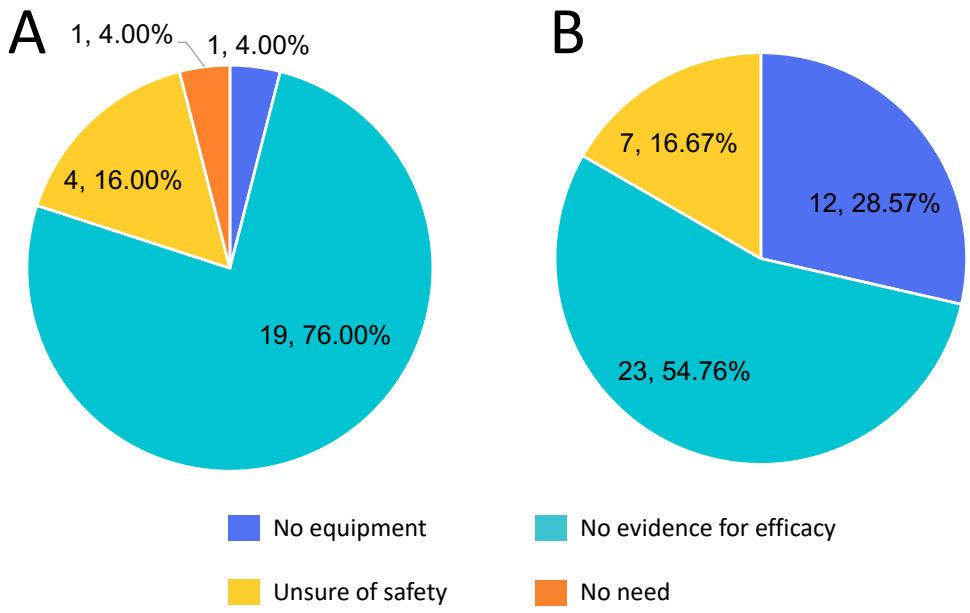


Figure 3-4. Reasons for not applying AHpET

These pie charts show the reasons given for not applying AHpET among AHpBP users (A) and among all non-AH users (B).

Regarding the charges for AH, 34.8% of respondents reported that they do not charge on additional fee for this application; however, 46.4% confirmed that all AH procedures incur a charge, 12.5% charged for improved outcomes only, and 6.3% (7/112) charge for AHpBP only. Compared with the AH users outside of the UK, the percentage of participants of clinics that do not charge was significantly higher in the UK (60.5 % (23/38) *vs* 21.6 % (16/74), P=0.000009) (**Figure 3-5**).

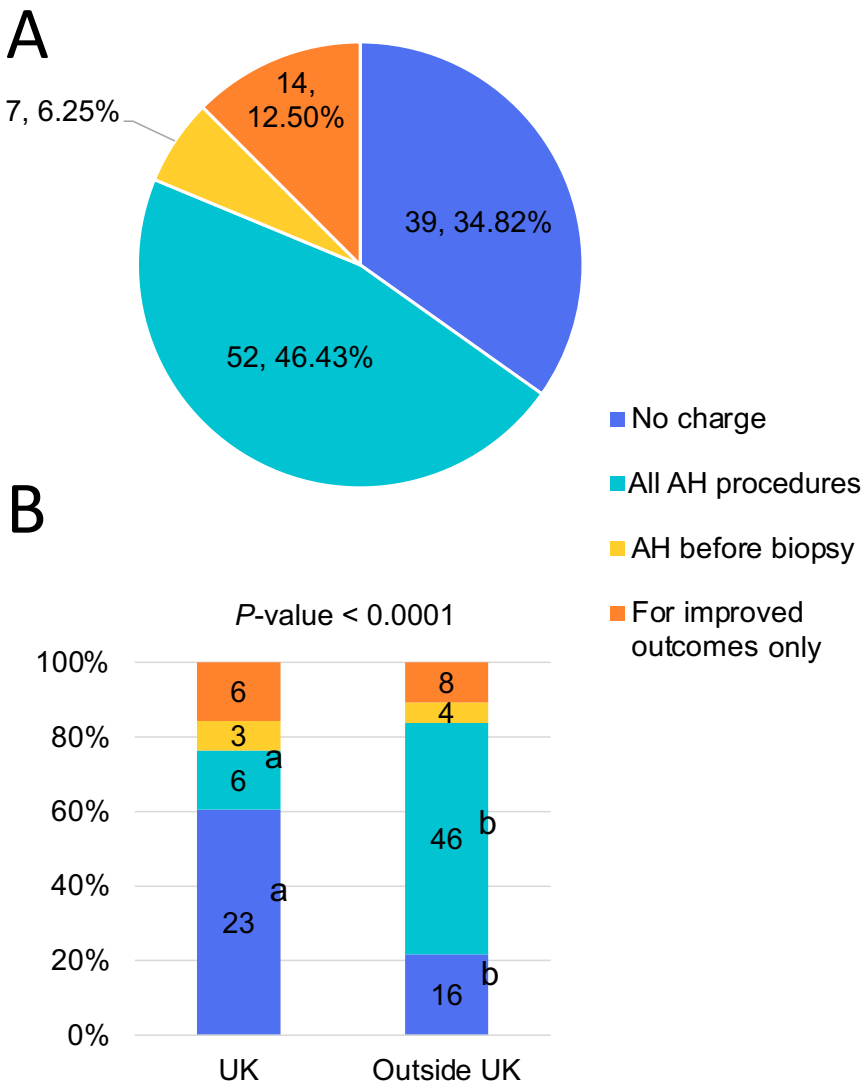


Figure 3-5. Charges associated with AH application

(A) Charge for AH in different clinical scenarios; (B) A comparison of the charges incurred by AH between UK responders and those outside of the UK. The Chi-Square test was used to compare the proportion between the two groups. Each subscript letter (a, b) denotes a subset of group categories whose proportions did not differ significantly from each other at the 0.05 level

3.3 Discussion

The contradictory efficacy of AH may be correlated with the variety of AH procedures used in clinical practice. Most worrying is the fact that there is no standardisation or guidelines that regulate the application of AH. Here in this chapter, I have described

the first survey to date representing the clinical practice of AH across different IVF centers. The most recent national summary report on AH showed that the utilization of AH in the US significantly increased more than 1.38-times from 2000 to 2010 (Kissin et al., 2014). This increase trend may rely on the ASRM guideline published in 2008, suggesting AH may be clinically useful in patients with poor prognosis (ASRM, 2008). Although no updated global registry is available to reflect the exact application rate of AH, according to the results in this chapter, it seems that AH is still being actively widely used in ART cycles. In addition, AH is more extensively used prior to biopsy than embryo transfer, especially that 90% of responders used AHpBP for TE biopsy.

Intriguingly, the usage of AH was significantly lower in UK according to the survey, only 43.1% of the responders in UK used AHpET in their clinics. However, in 2001, a multi-centre survey revealed that AH is performed widely (65%) in HFEA listed clinics (British Fertility Society Policy Practice Sub-Committee, 2001). This change is highly likely to be due to the NICE guideline updated in 2017, which state that AHpET is not recommended as it has not been shown to improve pregnancy rates(NICE, 2017).

It is commonly agreed that AHpET should only be applied to patients with specific clinical indicators rather than to a universal population. In this chapter, embryos from patient with poor-prognosis, a thick ZP, or frozen/thawed embryos, were identified as the main clinical indications for AHpET with the same importance. According to the ASRM 2008 guideline, poor prognosis patient was suggested as the clinical indicator (ASRM, 2008), and some researches had shown AH improved the pregnancy rate and implantation rate (Petersen et al., 2005, Elhussieny et al., 2013) However, in 2014, ASRM updated the guideline and suggested that it is premature to recommend AH in all patients with poor prognosis, because of the insufficient evidence (ASRM, 2014).

However, it is noteworthy that different clinics may use different sub-groups of poor prognosis patients as the AH indications, which may partially explain the inconsistency of AH efficacy in this patient group, and thus masking the efficacy of AH contradictory. For instance, a RCT meta-analysis conducted by Wellington et al (2011) found that AH could only improve the clinical pregnancy rate and live birth rate in women who had experienced previous repeated failure, rather than women of advanced age. On the other hand, it is understandable that patients with a poor prognosis may seek any possible medical intervention in order to achieve pregnancy. Thus, in reality, until we have robust and validated evidence, clinics will apply the AH in the ART cycles to fulfil patients' psychological needs after fully informing the risk and chances of success.

Apart from patients with a poor prognosis, the other important indications for AH were frozen/thawed embryos and embryos with a thick-ZP. Parts of the responders believed that the cryopreservation process could cause abnormalities in the ZP, such as hardening and thickening, thus leading to difficulty in hatching. Indeed, AH has been demonstrated to improve the pregnancy outcome of frozen/thawed embryos at different embryo stages (Martins et al., 2011, Wan et al., 2014, Zhou et al., 2014, Elnahas et al., 2018). However, a recent meta-analysis reviewed 12 RCT and discovered that when performed on cryopreserved-thawed embryos, AH was correlated with the higher clinical pregnancy rate and implantation rate, but had little effect on live birth rate (Zeng et al., 2017). Furthermore, a recent longitudinal study showed that AH could even reduce the live-birth rate in first FET (frozen/thawed embryo transfer) cycle, especially in patients aged 38 years or over (Knudtson et al., 2017). However, detailed characterisation of these AH approaches, embryo stages, and embryo quality, is still lacking. Therefore, a more comprehensive evaluation of the use of AH in frozen/thawed embryos and different patient groups is very important.

As revealed in this survey, laser pulse has become the predominant technique in clinical practice, regardless of AHpBP or AHpET. However, this survey also identified that an extensive disparity exists in the practice of AH. Traditionally, AHpET is most widely performed at the cleavage stage (Avella et al., 2019). Nevertheless, we found that AHpET is now also widely performed at blastocyst stage. The increasing trend to perform AHpET at the blastocyst stage is likely to be due to the high precision and control provided by laser beams, which makes it easier and capable of performing AH at the blastocyst stage. Although numerous studies have focused on the outcomes of AH, there were the only few studies considering AH at the blastocyst stage (Vanderzwalmen et al., 2003, Miyata et al., 2010, Ren et al., 2013, Wan et al., 2014), and no study to date has compared the effect of AHpET on the different embryo development stages. Therefore, studies focusing on the correlation between different AHpET timepoint and outcomes may be very informative for the evaluation of its efficacy.

Furthermore, so far, there is no consensus with regards to the timing of embryo transfer following AHpET in clinical practice. In this survey, most respondents said they would transfer embryos soon after AH rather than culturing them to the blastocyst stage, no matter AH was conducted at pre-blastocyst stage or blastocyst stage. Meanwhile, several lines of evidence have suggested that blastocyst transfer is the more desirable choice; since extending embryo culture allows the natural selection of embryos, thus increasing the implantation rate (Cutting et al., 2008, ASRM, 2017). Therefore, continuing culture embryo after AHpET may be helpful for the selection of embryos. However, the evaluation of AH on Day 3 embryos followed by blastocyst transfer is exceptionally sparse (Graham et al., 2000, Stones et al., 2004). In order to enhance the knowledge, the efficacy of AH on Day 3 followed by blastocyst transfer

was assessed using an *in vitro* implantation model; these data are described in **Chapter 5**.

Although trophectoderm (TE) biopsy has become the dominant biopsy method, the procedure used for AHpBP shows significant variation in clinical practice and no standard protocol was recommended by the current guideline. According to the best practice guideline by ESHRE consortium, ZP drilling can be performed on Day 3 or the morning of Day 5, followed by TE cell removal (Harton et al., 2011). In this survey, apart from Day 3 (32%) and blastocyst stage (47.2%), 19% of AHpBP for TE biopsy were performed on Day 4, which in slight disagreement with the current the recommendation. However, so far, there is a significant lack of research with regards to the effect of different timepoints for AHpBP on subsequent TE biopsy procedures and pregnancy outcomes. Only one recent study compared the Day 3 prehatching protocol (AH on Day 3 and biopsy at blastocyst stage) and sequential hatching and biopsy protocol (AH and biopsy at blastocyst stage); they found that the pregnancy outcomes were significantly better in the sequential hatching and blastocyst biopsy protocol (Rubino et al., 2020). In addition, previous studies demonstrated that the pre-hatching at cleavage stage for TE biopsy could potentially increase the risk of ICM incarceration and may require extra manipulation during biopsy (Aoyama et al., 2020, Rubino et al., 2020). Therefore, it is very important to comprehensively investigate the potential effect of different AH protocols on TE biopsy procedures and related pregnancy outcomes.

Another huge variation is found as regards the details of ZP manipulation. For instance, the survey discovered that ZP drilling was more commonly used in AHpBP (78.4%), while ZP drilling and ZP thinning were used in similar frequencies in AHpET (46.4%

vs 37.1%). As discussed in a systematic review, even only using the laser-mediated approach, it is unclear whether embryo benefits from ZP beaching (drilling) or thinning (Alteri et al., 2018). In order to optimise the AH method, I compared laser-assisted ZP drilling, ZP-partial drilling, and ZP-thinning methods, and investigated their effects on embryo quality and embryo implantation. These data are described in **Chapter 4** and **Chapter 5** of this thesis.

Although there is no universal protocol for ZP drilling or ZP thinning, it is important to notice that the invasive extension of ZP manipulation plays significant role on the AH outcomes. According to the result, the extension of ZP thinning was consistent, that most of the responders would ablate the ZP with less or equal to 1/4 of the ZP circumference. On the other hand, the majority of the responders would drill ZP with a small opening (<15 μm), regardless of AHpBP or AHpET. The mean thickness of human ZP is 16.18 μm according to previous study (Balakier et al., 2012), thus drilling the ZP opening small than the thickness of ZP is the main protocol in current practice. Although a significant relationship between the size of ZP opening and the *in vitro* hatching has been described in many animal studies (J Cohen and FeldbergCohen et al., 1991, Hiraoka et al., 2009, Chailert et al., 2013), sparse attention was paid to the correlation between the size of drilling and embryo hatching outcomes in clinic. This is because the embryos would only keep in short culture time to blastocyst, if not been transferred very soon following AH. Thus, in **Chapter 4** and **Chapter 5**, I used the 7.5 μm (equivalent to 15 μm in human embryo) as laser beam diameter for ZP drilling in mouse embryo model and thinned ZP with one area as well as 1/4 of the ZP circumference, to mimic the most common clinic practice of laser-assisted AH. Furthermore, to understand the effect of ZP opening size, I also compared the

hatching and attachment outcomes among different opening size in the ZP created by drilling, the results were shown in **Chapter 5**.

Despite the ongoing debate and lack of robust randomised controlled trials, most respondents believed that AH was likely to improve implantation rate. Interestingly, they also considered AH is less likely to help with live birth rate. This is consistent with the review and guideline that the evidence so far is insufficient to conclude the association of AH and live birth rate improvement (Carney et al., 2012, Kissin et al., 2014, ASRM, 2014). Furthermore, no side-effect of children born was reported according to this survey, which may be due to the limited number of respondents. However, there are some evidence demonstrating that the multiple pregnancy rate is significantly increased following AH treatment (Martins et al., 2011, Carney et al., 2012, Li et al., 2016), especially the potential risk factor for zygotic splitting (Yamashita et al., 2019). The long-term studies are required to investigate the effect of different AH on the health of offspring, which is important to evaluate the safety of AH on offspring. For the safety of this technique, most responders believed that AH is unlikely to affect embryo development, though concerns about the potential thermal damage caused by laser pulses on embryos still existed. To address this, I investigated the impacts of these commonly used laser-assisted ZP manipulations on embryo quality, especially at the molecular level; these data are described in **Chapter 4** and **Chapter 6**.

As indicated from this study, owing to considerable disparity in AH practice, the narrow patient inclusion criteria, and the complex nature of pregnancy, it is possible that the beneficial effects of AH may be masked in a well-defined patient population. Thus, the complete rejection of AH may seem rather unfair and premature. As suggested by Macklon *et al.* (2019), while waiting for the next large-scale and rigorous RCTs to test

the efficacy of AH, researchers and clinical communities could work together, using bioinformatics and data management techniques, to develop large prospective well-phenotyped cohorts to comprehensively characterise AH and guide their application in clinical practice.

3.4 Limitations

The study in this chapter was limited by the bias in that the respondents may not have been a representative sample of the IVF centres worldwide since the sample size is limited and most of the respondents were from the UK and China. In addition, given that the survey was voluntary, the respondents were not asked to answer every question prior to submission; Thus, there were slight differences in the numbers of responses from the question to question. Finally, to limit the length of the survey, some factors that may also affect the clinical efficiency were not included, such as the laser facility, power and irradiation time of the laser beam, the mean length of time embryos were left outside of the incubator, the site of drilling/thinning, and the depth of ZP ablation. Future studies to investigate the clinical practice of AH are needed, which can be conducted by using a larger scale, more comprehensive, and international survey system.

3.5 Concluding remarks

The data reported in this chapter confirmed that AH is still widely used, especially prior to embryo biopsy; and that AH is believed to be a safe technique and is likely to improve implantation according to the respondents. However, there is a huge disparity

in the clinical practice regards to the application time-points, the ZP manipulation protocols, and subsequent biopsy/transfer strategies. This evident inconsistency may explain the contradictory clinical efficacy, thus highlighting the need for protocol standardisation, in order to investigate the true value of AH.

3.6 Key findings

- AH is still commonly used in IVF centres, especially AHpBP
- The application rates of AH are lower in the UK than outside the UK
- Patients with poor-prognosis, cryopreserved/thawed embryo, and embryos with a thick ZP are the main clinical indications for AHpET
- Laser-assisted ZP manipulation is the dominant method for AH; however, a vast disparity still exists in the clinical practice with regards to the ZP manipulation procedure, embryo stage, and transfer strategy
- Most of the AH users surveyed herein believe this technique is likely to improve embryo implantation



Chapter 4

Investigating the effect of laser-assisted ZP manipulations on the preimplantation mouse embryo

4.1 Introduction

Over the last few decades, laser technology has been introduced as an alternative method for ZP manipulations. Lately, the non-contact infrared (IR) diode laser has been widely applied in IVF laboratories since it has significantly reduced the procedure time while increasing the consistency and reproducibility of traditional ART techniques (Davidson et al., 2019). As described in **Chapter 3**, although the IR laser has now become the predominant technique for both AHpET and AHpBP; optimal parameters and methods remain unclear.

Laser-assisted ZP manipulation involves the application of a high energy form of light that produces heat to dissolve or ablate the ZP (Taylor et al., 2010). This heat is dissipated and transferred through culture media, thus creating a temperature gradient in the culture media immediately surrounding an embryo (Douglas-Hamilton et al., 2001, Tadir et al., 2007). However, the temperature is an important factor in the embryo culture system; even slight variations of 0.5 °C can have significant impact on embryo development (Walters et al., 2020). Furthermore, as a critical structure, the ZP protects an embryo from external factors, including toxins, microorganisms, and antibodies (Primi et al., 2004, Hammadeh et al., 2011). Laser-assisted drilling, as an invasive technique, inevitably exposes an embryo to the external environment and may cause the loss of blastomeres and a reduction in embryonic autocrine secretion, thus creating potential risk to embryo development (O'neill, 1997, Alteri et al., 2018). Therefore, the energy delivered to an embryo during laser-assisted ZP drilling or ZP thinning, and the drilling technique itself, might affect the quality of an embryo.

As mentioned in **Chapter 1, Section 1.5.1,** several research studies have attempted to evaluate the laser-assisted ZP manipulation technique on human embryos or

embryos acquired from animal models. On a positive note, many of these studies failed to detect any adverse effects on embryo quality and preimplantation development potential, especially when applying a laser beam to manipulate the ZP at high power laser (400mW and 300mW) and appropriate durations of time (Montag et al., 1999, Douglas-Hamilton et al., 2001, Taylor et al., 2010, Uppangala et al., 2016). Nevertheless, recent studies demonstrated that laser treatment may exert significant impacts from other biological aspects.

As a vital indicator of developmental potential, embryonic cells are positively correlated with blastocyst quality (Matsuura et al., 2010). Worryingly, some studies have reported a reduction in the number of embryonic cells following different laser ZP manipulations (Chailert et al., 2013, Park et al., 2014, Honguntikar et al., 2015). Apart from the embryonic cell number, sequenced embryonic segregations are important events during embryo preimplantation development, where some transcription factors play key roles in cell linage regulation (introduced in **Chapter1, Section 1.1.1)**. For example, OCT-3/4 (encoded by gene *Pou5f1*) is specifically required for cells to acquire a pluripotent identity, which expression is restricted to the ICM (Nichols et al., 1998). While transcription factor CDX2 is required for proper TE specification, which is the TE marker (Niwa et al., 2005). Furthermore, NANOG is essential for the specification of epiblast during the second segregation (Osorno et al., 2011).

Aside from developmental potential, cellular apoptosis is another biological process that can serve as a useful indicator of an inadequate or suboptimal *in vitro* environment or the detrimental effects of embryo manipulation (Betts et al., 2001). In most cases, cell apoptosis is under genetic control, with the activation regulated by local

environmental changes (Penaloza et al., 2006). Two main pathways involved in cell apoptosis: cytochrome c liberation from mitochondrial (intrinsic pathway) and activation of death receptor (extrinsic pathway). The intrinsic pathway is mainly controlled by BCL-2 (B-cell lymphoma 2) family proteins; the family members can act as either pro-apoptotic (e.g., BAX and BAK) or anti-apoptotic (e.g., BCL-2 and BCL2L2) (Kiraz et al., 2016). Furthermore, reactive oxygen species (ROS) and the resulting oxidative stress also play a pivotal role in apoptosis; while cells have the intact antioxidative enzyme families, such as superoxide dismutase (SOD) and glutathione peroxidase (GPX), to reduce hydrogen peroxide and protect against oxidative stress (Kannan et al., 2000). It has been demonstrated that the embryo death and developmental arrest during the first week of *in vitro* development is often due to ROS (Betts et al., 2008). Cell apoptosis can be detected using different methods. The TUNEL reaction is the most frequently used method to detect apoptotic cells by labelling DNA fragmentation. A recent study, using TUNEL assay, found that laser-assisted ZP drilling at either 2-cell and 6 to 9-cell stage embryos significantly induce embryo DNA damage (Honguntikar et al., 2015). However, the specificity of the TUNEL assay is relatively low. Consequently, it is evident that future studies must use other methods to detect cellular apoptosis, including the expression levels of apoptosis- and stress-related genes and the activation of caspase-3 (Fernández-Gonzalez et al., 2004, Park et al., 2006, Huang et al., 2019).

Although laser-assisted ZP manipulations has been used in clinics for a long period of time, very few studies have specifically investigated the impact of this technique on embryos at the molecular level. As yet, none of these previous studies have detected any significant changes in the expression levels of genes related to heat shock stress (Hartshorn et al., 2005) or epigenetic mark (Honguntikar et al., 2017) following laser-

assisted drilling. The mammalian stress response is characterised by the rapid induction of HSP (heat shock protein) expression. It is presumed the HSP70 expression is a potentially quantitative indicator of environmental stress and toxicity in mouse and human cells and embryo (Luft et al., 1999). Embryonic cells express HSP70s either constitutively from the 2-cell stage or in response to the stress; HSP70-1/3 is heat-inducible in the 4-cell stage, 8-cell stage, and blastocyst (Edwards et al., 1995, Luft et al., 1999). Hartshorn et al. demonstrated that heat produced from laser pulses would not induce instant heat stress in cleavage-stage embryos, by detecting the mRNA expression of Hsp70-1/3 soon after the laser treatment (Hartshorn et al., 2005); however, it is unclear whether the laser ZP manipulations induce stress response during embryo development.

Epigenetic reprogramming in the preimplantation period is essential for appropriate development, and regulates the expression of early embryonic genes, cell cleavage, and cell determination (Jacob et al., 2005). A previous study found that the laser drilling at the 2-cell stage embryos, but not 6-8 cell and blastocyst stage embryos, could impaired the expression of *Dnmts* (DNA Methyltransferases) (*Dnmt3a* and *Dnmt3b*) (Honguntikar et al., 2017). However, no studied so far investigate the laser ZP thinning on the epigenetic changes in embryos.

Thus far, current evidence has drawn researchers' attention to the safety of the laser-assisted ZP manipulations. In addition, the wide disparities relating to the ZP manipulations between researchers and clinics make it more intricate to explain these findings. I hypothesised that the effects of different laser ZP manipulations on preimplantation embryos may vary. Thus, to address the paucity of literature regarding the effect of laser treatment on embryo at the molecular level, and to compare the

impact of different ZP manipulations; I applied three methods: laser-assisted ZP drilling, partial drilling, and ZP thinning to mimic the clinical practice of ZP manipulations. Furthermore, the assessments of safety on mouse embryos were characterised from a variety of biological and molecular aspects: embryo development, embryos hatching patterns, cell number, embryo segregation, cell apoptosis, as well as embryonic cell stress.

4.2 Results

4.2.1 Evaluation of preimplantation mouse embryo development following laser ZP manipulations

To understand the effect of different laser ZP manipulations on preimplantation embryos, mouse embryos were assessed at 4.5 after 48 hours *in vitro* culture following laser treatment at E2.5. As laser ZP manipulation was commonly used on both fresh and frozen/thawed embryos, in the first part of experiment, I tested the effect of these laser ZP manipulations on both fresh and frozen embryos.

As shown in **Table 4-1**, regardless of whether fresh or frozen/ thawed embryos were used, blastocyst formation and embryo arrested/fragmentation were similar across all four groups tested. However, the percentages of hatching blastocysts were significantly higher in the ZP-drilling groups when compared with the other three groups ($P<0.0001$). In addition, the percentages of hatching blastocysts were slightly higher in both ZP-partial drilling and ZP thinning groups when compared with control group; however, these differences did not reach significant significance. Since the effect of different laser-assisted ZP manipulations were similar between fresh and

frozen/thawed embryos, the following assessment in this study did not distinguish between fresh or frozen/thawed embryos.

Table 4-1 A comparison of embryo development across different laser ZP manipulation groups

Fresh embryos	**ZP-drilling**	**ZP-partial drilling**	**ZP-thinning**	**Control**	***P* * value**
Total number	n=349	n=319	n=297	n=360	
Resulting blastocysts	259 (74.2%)	240 (75.24%)	223 (75.08%)	277 (76.94%)	0.862
Hatching blastocysts	210 [a] (81.08%)	119 [b] (49.58%)	115 [b] (51.57%)	111 [b] (40.07%)	<0.0001
Arrested/Fragmented embryos	90 (25.8%)	79 (24.8%)	74 (24.9%)	83 (23.1%)	0.862
Frozen-thawed embryos	**ZP-drilling**	**ZP-partial drilling**	**ZP-thinning**	**Control**	***P* * value**
Total number	n=76	n=74	n=75	n=88	
Resulting blastocysts	61 (80.26%)	58 (78.38%)	63 (84.00%)	75 (85.23%)	0.65
Hatching blastocysts	56 [a] (91.8%)	34 [b] (58.62%)	30 [b] (47.62%)	29 [b] (38.67%)	<0.0001
Arrested/Fragmented embryos	15 (19.74%)	16 (21.62%)	12 (16.00%)	13 (14.77%)	0.65

***** $\chi 2$ test or $\chi 2$ Fisher's exact test with pairwise z-test was used to compare the proportions across four groups. Bonferroni method was used to adjust *P*-value in multiple comparison.

a, b: Each subscript letter denotes a subset of laser ZP manipulation groups whose proportion did not differ significantly from each other at the 0.05 level.

4.2.2 An investigation of mouse embryo hatching patterns following laser ZP manipulations

4.2.2.1 Morphological assessment of hatching pattern at E4.5

Morphological assessment of E4.5 hatching blastocysts post-ZP manipulations revealed a wide disparity with regards to the hatching patterns among different methods (*P*<0.0001). As shown in **Table 4-2**, 75% of the blastocysts in the ZP drilling group had adopted an '8-shape' morphology, significantly higher than other groups (*P*<0.05). In contrast, the proportion of 'U-shape' hatching embryos was higher in LA-ZP thinning group (25.8%), especially when compared to the ZP-drilling group (*P*<0.05). In addition, the proportion of multiple-point hatching embryos was lowest in the ZP-drilling group and was significantly different when compared to the ZP-partial drilling group and control group (*P*<0.05).

Table 4-2 A comparison of embryo hatching patterns across different laser ZP manipulation groups

	ZP-drilling (n=140)	ZP-partial drilling (n=79)	ZP-thinning (n=66)	Control (n=77)	*P* * value
Starting	19 (13.6%) [a]	34 (43%) [b]	29 (43.9%) [b]	41 (53.2%) [b]	<0.0001
8-shape	105 (75%) [a]	26 (32.9%) [b]	15 (22.7%) [b]	15 (19.5%) [b]	
U-shape	13 (9.3%) [a]	10 (12.7%) [a,b]	17 (25.8%) [b]	11 (14.3%) [a,b]	
Multiple point	3 (2.1%) [a]	9 (11.4%) [b]	5 (7.6%) [a,b]	10 (13%) [b]	

* χ2 test or χ2 Fisher's exact test with pairwise z-test was used to compare the proportions across four groups. Bonferroni method was used to adjust *P*-value in multiple comparison.

a, b: Each subscript letter denotes a subset of laser ZP manipulation groups whose proportion did not differ significantly from each other at the 0.05 level.

4.2.2.2 Time-lapse imaging and analysis of embryo hatching patterns

To understand how the typical hatching patterns observed at E4.5 is related with the hatching result in untreated *in vitro* developed embryos, the live image microscope system (Zeiss, UK) was used to record time-lapse images of the morphokinetics of untreated embryos every 10 minutes for 72 hours. In order to record the whole hatching process, embryo culture was started in the imaging system from E3.5 to E6.5.

As shown in **Figure 4-1**, 12 embryos (include one 2-cell stage embryos) were recorded in this experiment, starting from the morula stage (a) to blastocyst formation (b to d), embryo expansion, and finally hatched out from the ZP. In total, 5 embryos successfully hatched out by the end of culture (marked with letters in yellow and green) and 2 embryos failed to fully hatch out (letters in red); while 4 out of 12 embryos were fragmented/dead (shown by blue asterisks). Interestingly, although the '8-shape' hatching embryo started hatching earlier (without contraction prior to hatching) (at E4.5-E5.0), both embryos failed to hatch out until E6.5 (embryos marked with A and B in red). In contrast, despite several incidence of contraction and re-expansion occurred prior to hatching in the 'U-shape' hatching embryos (starting contraction at E4.5), these three embryos successfully hatched out at around E5.5 to E6.5 (embryos marked with C, D and E in yellow).

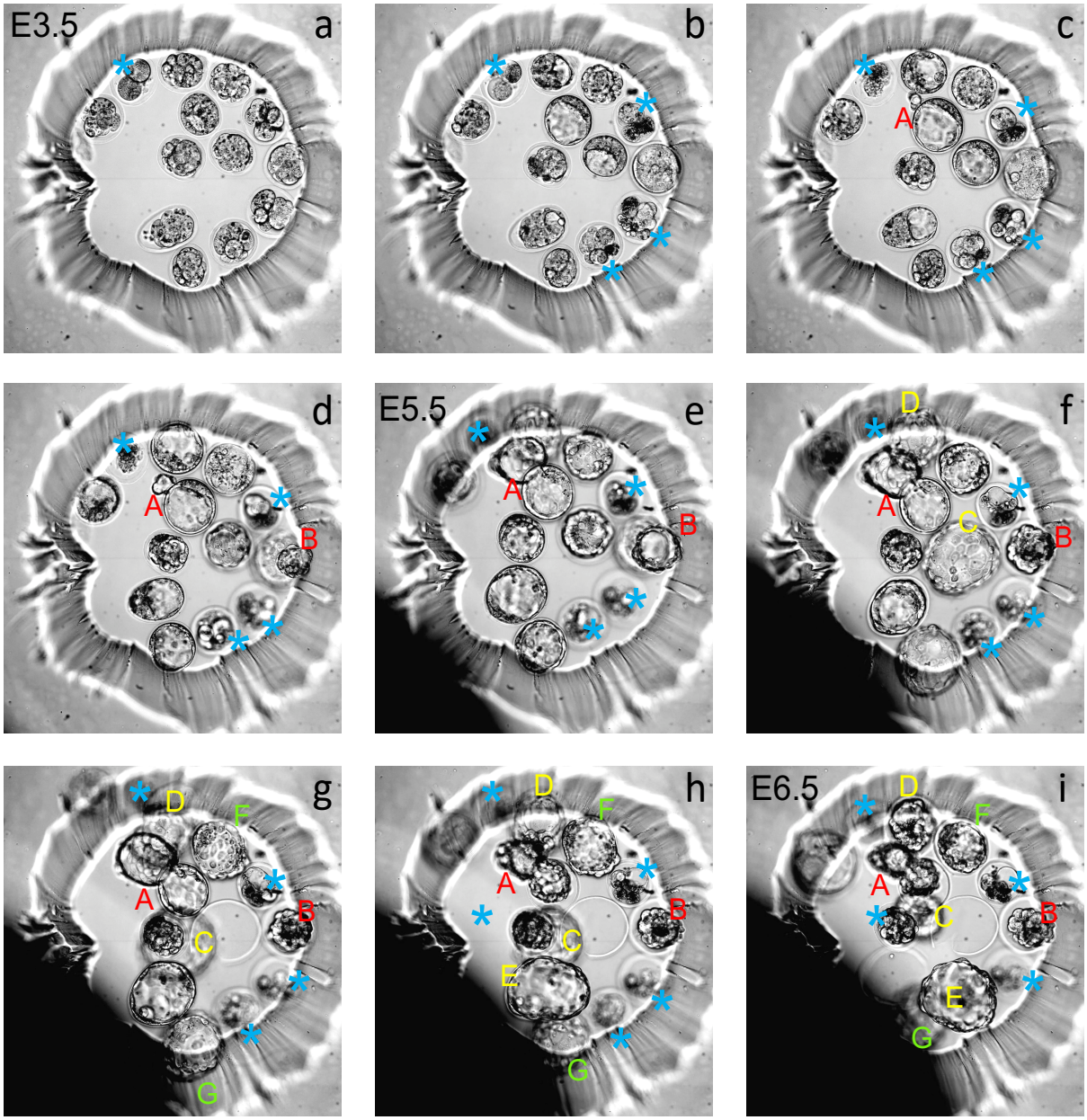


Figure 4-1. Representative images of the embryo hatching process using time-lapse imaging

Representative images including morula stage mouse embryos (E3.5) (a), blastocyst stage (b-e) (e represents E5.5), hatching embryo stage (c-i) (i represents E6.5). The blue asterisks indicate dead/fragmented embryos; red 'A' and 'B' represent '8-shape' hatching embryos; yellow 'C', 'D', and 'E' indicate 'U-shape' hatching embryos; and the green 'F' and 'G' indicate hatched embryos (but I was unable to observe the hatching pattern).

4.2.3 The assessment of cell number in preimplantation mouse embryos undergoing different laser ZP manipulations

Embryo cell number is an important indicator for developmental potential and is positively correlated with blastocyst quality. To investigate the effects of laser ZP manipulation on blastocyst cell composition and count, I stained embryos with OCT4 and CDX2 as biomarkers for the ICM and TE; additionally, all nuclei were stained with DAPI. The validation of OCT4 and CDX2 antibodies were shown in the **Supplementary appendix 4**, **Figure S.3**.

4.2.3.1 OCT4 and CDX2 staining of embryos undergoing different laser ZP manipulations

Three-dimensional images of CDX2 and OCT4 double-stained blastocysts were visualised in the four groups using confocal microscopy (**Figure 4-2**). OCT4 expressed in almost all the cells; but according to the merged images, cells with strong OCT4 signals were ICM (while-arrows), while strong CDX2-positive signals indicated TE cells. In addition, cells in mitosis phase were only stained with DAPI, but not CDX2 or OCT4. The intensity of OCT4 and CDX2 staining was similar among blastocysts among four groups. Thus, the cell numbers of TE, ICM, and mitosis phase cells were counted after double staining and in the merged images, respectively.

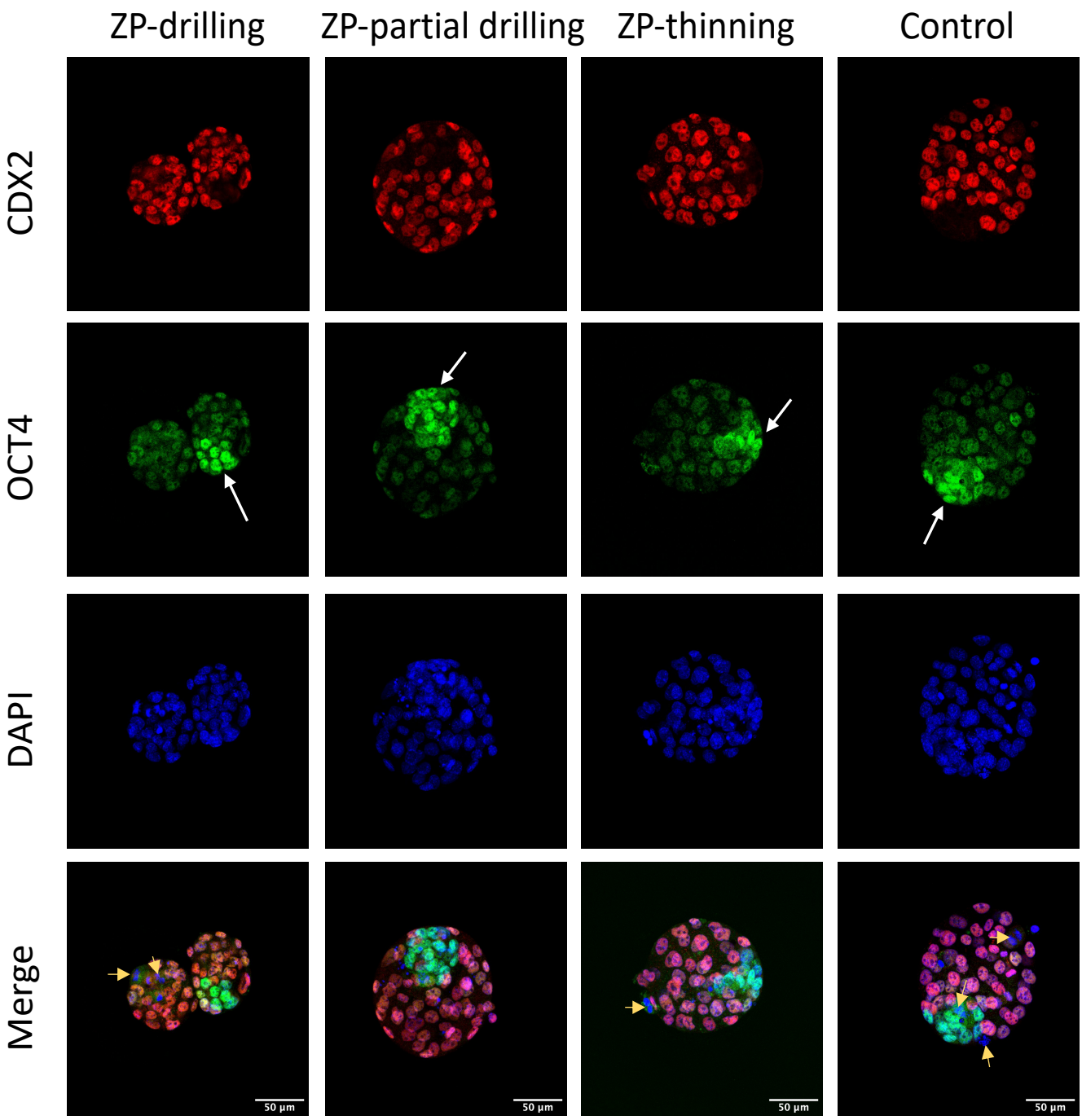


Figure 4-2. Representative images of CDX2 and OCT4 staining of E4.5 blastocysts undergoing different laser ZP manipulations

CDX2 (red), OCT4 (green), and DAPI (blue) were visualized by confocal microscopy. The CDX2 was present in the nuclei of TE cells; and the high intensity of OCT4 was present in the nuclei of ICM cells (while arrows). Yellow arrows indicate cells in mitosis phase. The z-stacked images are shown. Scale bar=50 µm (630× magnification).

4.2.3.2 A comparison of blastocyst cell numbers across different laser ZP manipulations

As shown in **Figure 4-3 A**, there were no significant differences in the TE, ICM, M-phase cell numbers, and the total cell number of blastocysts across the four groups (all $P>0.05$). However, the total cell number and TE cell number were marginally lower in the ZP-drilling group than other groups ($P>0.05$).

Interestingly, when I compared the cell number of hatching embryos (**Figure 4-3 B**), there was a significant difference in total cell number across the four groups; the total cell number in the ZP-drilling group was significantly lower than that of the control group (51.83 ± 12.9 *vs* 66.71 ± 18.6, $P=0.026$); while no statistical difference was found between other groups. A similar pattern was found for TE cell number; however, the difference between the ZP-drilling and control groups (35.5 ± 12.9 *vs* 46.28 ± 16.83, $P=0.068$) did not reach statistically significance. In addition, no difference was shown in the ICM cell numbers across the four groups (**Figure 4-3**). Furthermore, the ratio of TE/ICM was also comparable across these groups, without significant differences (**Appendix 5**).

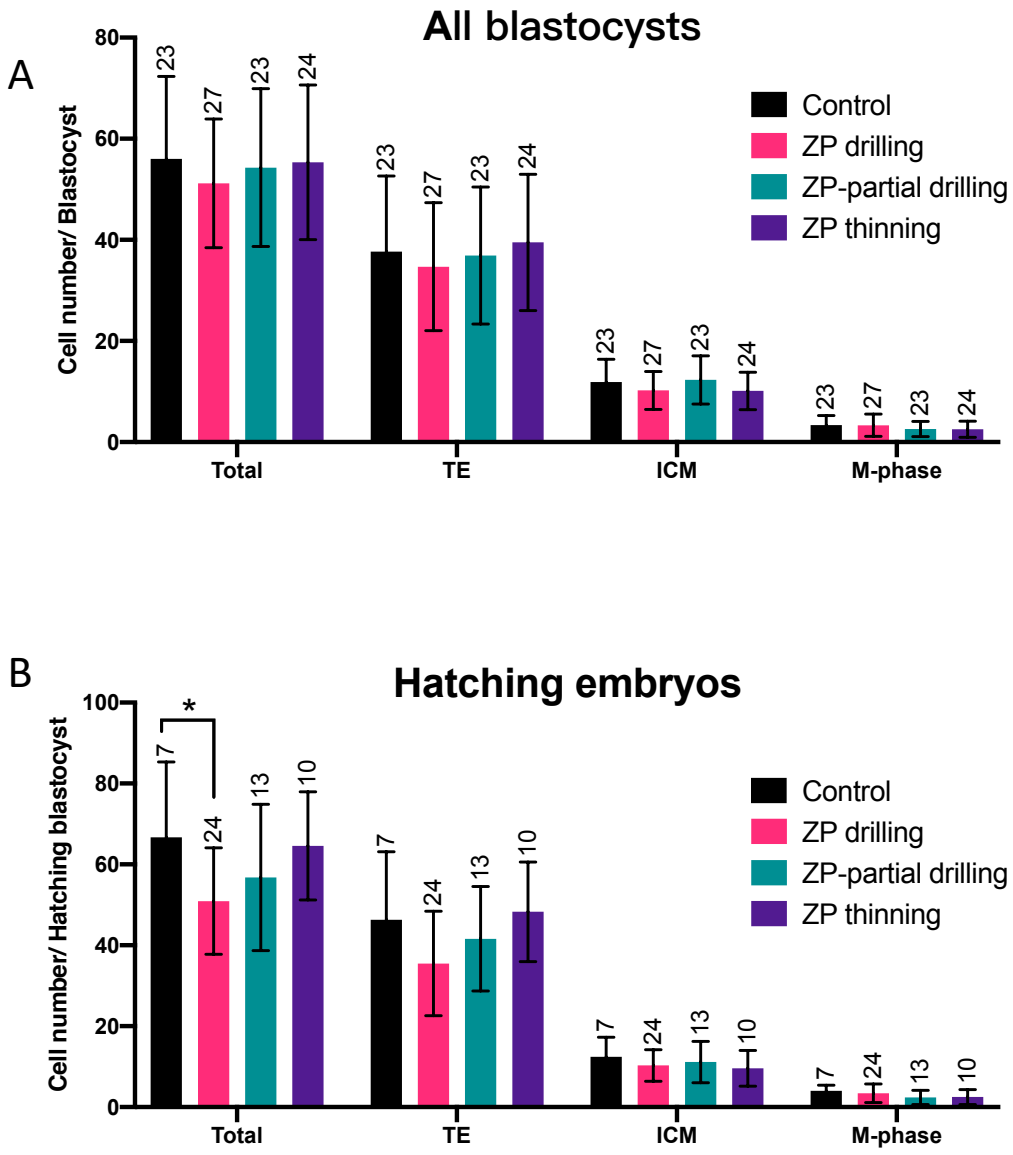


Figure 4-3. A comparison of embryo cell number across different laser ZP manipulations groups

The cell number of TE, ICM, mitosis phase cell, and the total cell number of all blastocysts (A) or the hatching blastocysts (B) were compared across the four groups. Data are presented as mean ± SD. Statistical analysis was carried out using one-way ANOVA with Dunnett's multiple comparisons test to identify differences between each treatment group and the control group. *: The adjusted *P*<0.05. The number of embryos tested was shown above each bar.

4.2.4 The assessment of cell apoptosis mouse embryos undergoing different laser ZP manipulations

Programmed cell death, or apoptosis, is an essential feature of many normal processes and pathological conditions and can serve as a useful indicator of an inadequate *in vitro* environment or the detrimental effects of embryo manipulation. In this part of the study, I detected cell apoptosis by investigating DNA fragmentation and caspase-3/7 activity to assess the potentially harmful effect of different laser ZP manipulation on embryos.

4.2.4.1 The detection of DNA fragmentation in embryos undergoing different laser ZP manipulations

The degradation of DNA into oligo nucleosomal fragments is one of the features of apoptosis and can be detected by the TUNEL assay. In **Figure 4-4 A**, the positive control group (embryos treated with DNase) presented with a positive green signal in all nuclei; in contrast, the negative control group (DNase treated but without TdT reagent) showed no positive signal. Interestingly, in the experimental groups, positive signals were also found in all embryos in the ZP manipulations groups, even in control embryos (**Figure 4-4 B**).

Furthermore, the apoptosis indexes were similar across the ZP drilling, ZP-partial drilling, and control groups (4.25 (1.93, 8.08), 3.85 (0.49, 7.96), and 4.64 (1.32, 5.59), respectively). Interestingly, the apoptosis index in ZP thinning group was slightly lower (2.42 (1.22, 3,78)) than other groups, although there was no significance difference.

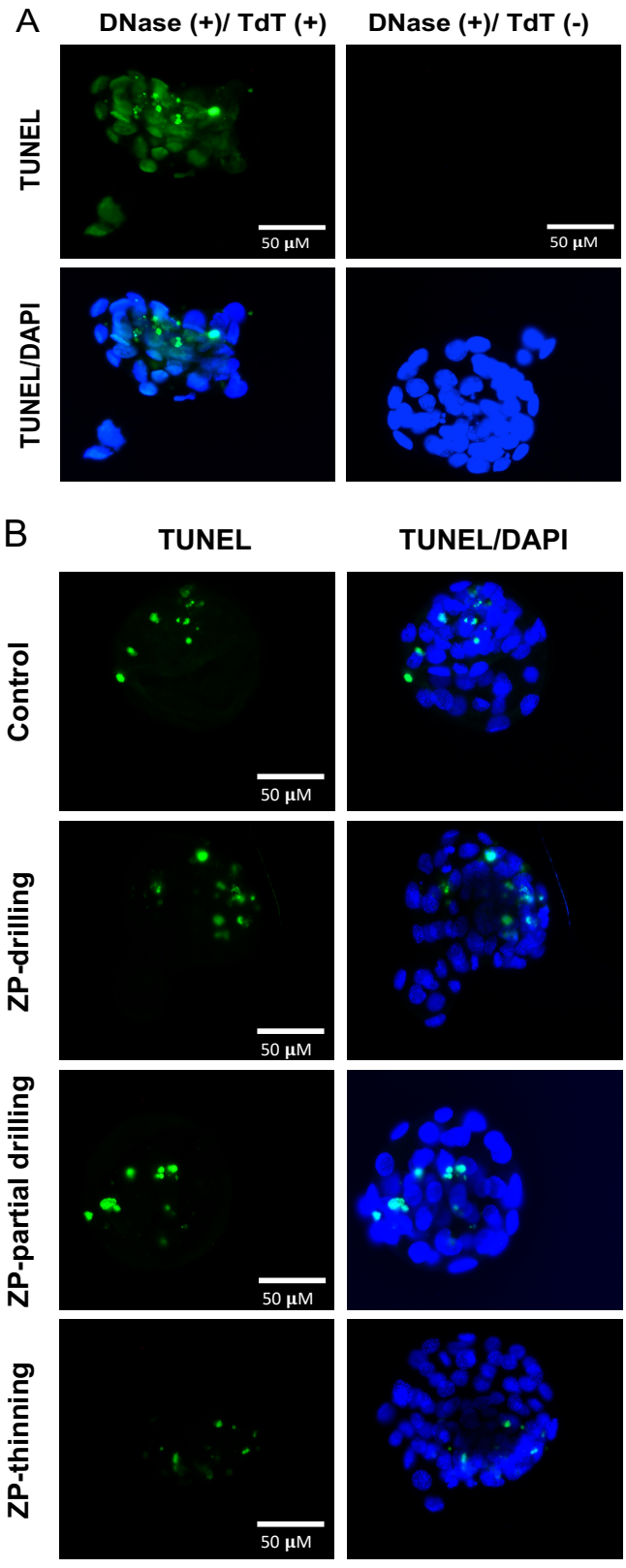


Figure 4-4 (Continued on next page, legend follows)

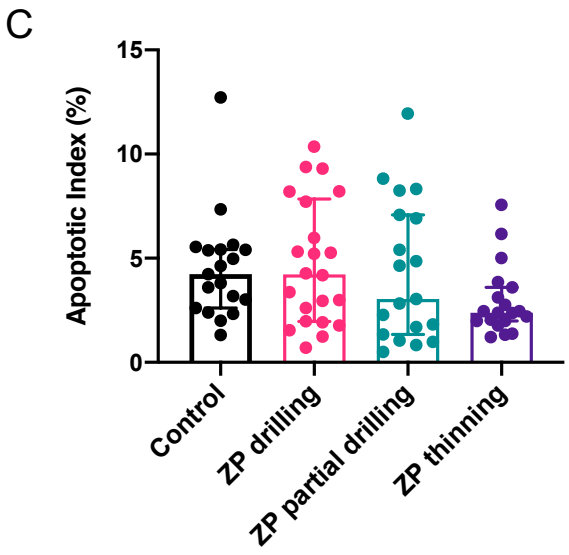


Figure 4-4. DNA fragmentation in E4.5 blastocysts undergoing different laser ZP manipulations

Fluorescein-12-dUTP labelled DNA fragments (green) and DAPI stained nuclei (blue) were visualised by microscopy (×400 magnification). (A): For positive controls, embryos were treated with both DNAse and TdT reagent; while, for negative controls, the embryos were treated with DNase, but no TdT reagent. (B): Representative images of DNA fragmentation detection in embryos undergoing different ZP manipulations (Scale bar=50 μm). (C): Apoptosis rates are presented as the median with interquartile range (box and error bar). Statistical analysis was carried out using Kruskal-Wallis test with Dunnett's post hoc comparisons test to show differences between each treatment group and control group.

4.2.4.2 An investigation of caspase-3/7 activation in embryos undergoing different laser ZP manipulations

The activation of caspase-3/7 is another distinctive feature of the mid stages of apoptosis. Caspase activation participates in a series of reactions in response to pro-apoptosis signals and results in cleavages of the protein substrate and the subsequent disassembly of the cell. In this study, fluorescent inhibitor of caspase (FLICA) methodology was used to detect activated caspase-3/-7. In **Figure 4-5 A**, an obvious and bright positive signal for activated caspase-3/-7 was evident in the biological positive control (Staurospotine-treated embryos). However, the caspse-3/-7 activation signals were very weak in embryos from the experimental groups (**Figure 4-5 B**).

In addition, no statistical differences were detected in the mean gray value of cleaved caspase-3/-7 across the four groups [ZP drilling (34.1 ± 18.8), ZP partial drilling (29.1 ± 11.6), and ZP thinning (33.9 ± 18.8), and control group (40.9 ± 19.6)].

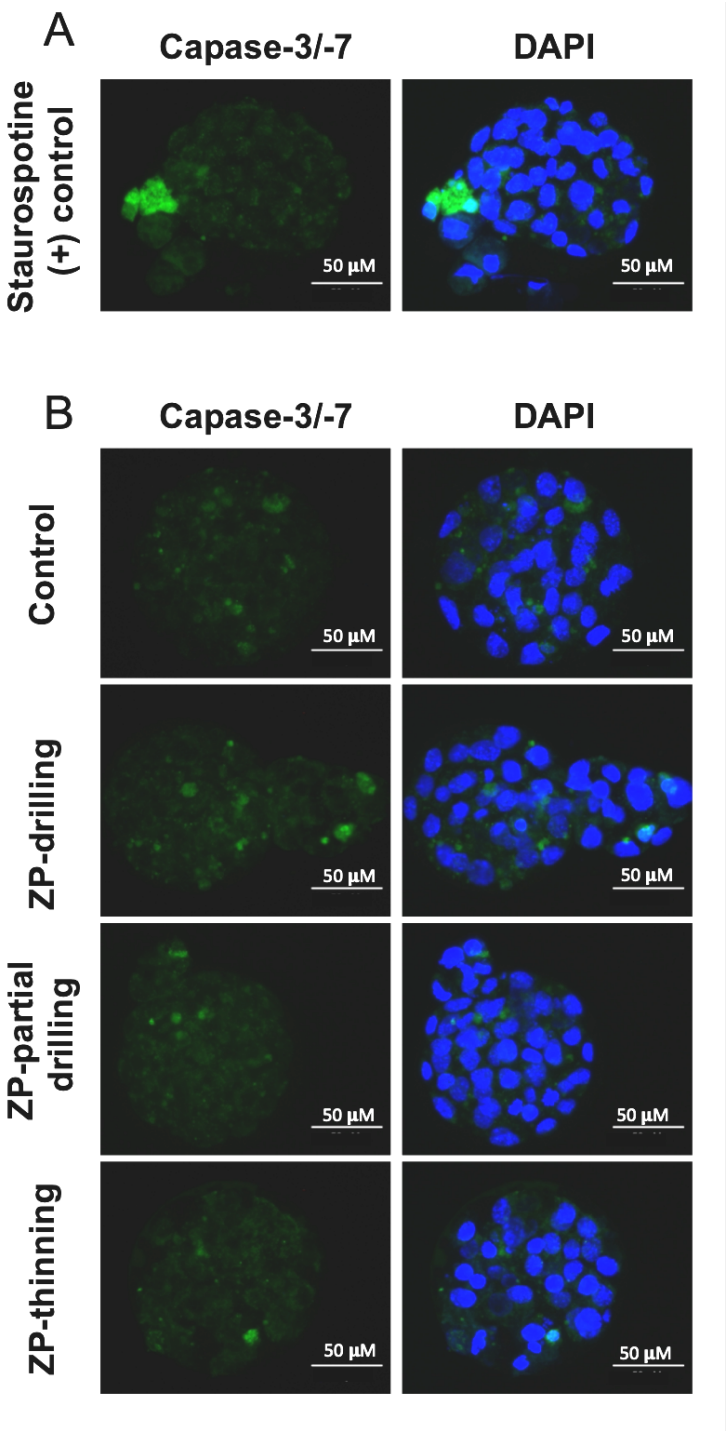


Figure 4-5 (Continued on next page, legend follows)

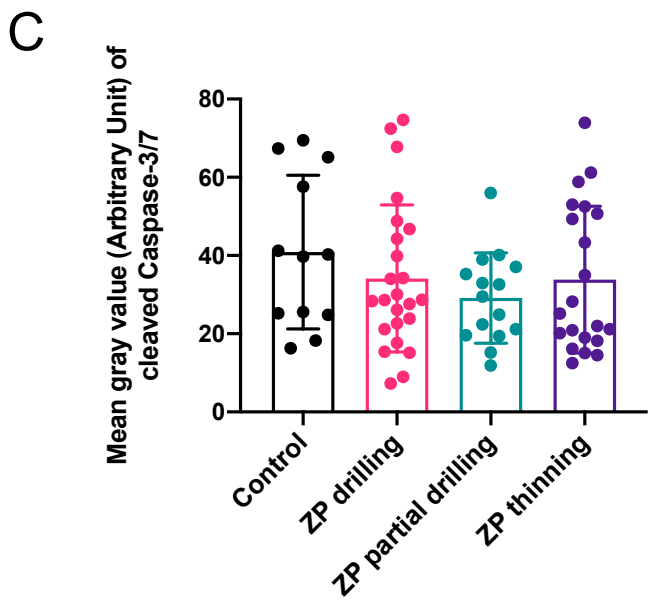


Figure 4-5. Caspase-3/-7 activation in E4.5 blastocysts undergoing different laser ZP manipulations

Cleaved casase-3/-7 (green) and nucleus (stained with Hoechst 3342) (blue) were visualised (×400 magnification). (A): For positive control: embryos were treated with 1μM of Staurospotine for 2 hours, showing intensive signals. (B): Representative images of caspse-3/-7 activation detection in embryos undergoing different laser ZP (Scale bar=50 μm). (C): The mean gray values of cleaved caspase-3/-7 are presented as mean ± SD. Statistical analysis was carried out using one-way ANOVA with Dunnett's post hoc comparisons test to show differences between each treatment group and the control group.

4.2.5 The assessment of heat shock stress in embryos undergoing different laser ZP manipulations

The cellular response to stress, including exposure to environmental, pathological, or physiological stimuli, is characterized by the rapid induction of proteins in the heat shock family, especially the hsp70 protein family (Huang et al., 2001). In this study, I detected the expression of HSP70 in blastocysts at the protein level to understand whether laser ZP manipulations at cleavage induce a stress response during embryos development.

Before conducting the experiment, the HSP70 antibody validation was performed with an antibody titration and the blocking buffer optimization (**Appendix 6**). In subsequent experiment, I diluted the primary antibody to 1:50 and the secondary antibody to 1:500; besides, the M.O.M (Mouse on mouse) blocking buffer was used.

For the positive control of HSP 70 staining, the mouse blastocysts were treated with HS (heat shock), which was induced by incubating the embryos at 43°C for 30 minutes and followed by a recovery period at 37°C for 30 minutes. As shown in **Figure 4-6 A**, the brightest signal for HSP70 protein was presented in HS-treated embryos, especially in cells that hatched out of the ZP. In addition, HSP70 was also expressed in embryos from all four experimental groups, but brighter signals were found in cells that had hatched out (**Figure 4-6 A**). However, there was a significant difference in the mean gray value of HSP70 among the four groups as demonstrated by one-way ANOVA (P<0.0001); ZP thinning group showed a significantly deceased level of HSP70 when compared with the control group (15.86 ± 3.70 *vs* 26.26 ± 6.46, P=0.006). However, no difference was detected when comparing ZP drilling (31.54 ± 7.51) and ZP-partial drilling (20.19 ± 5,64) with the control group (**Figure 4-6 B**).

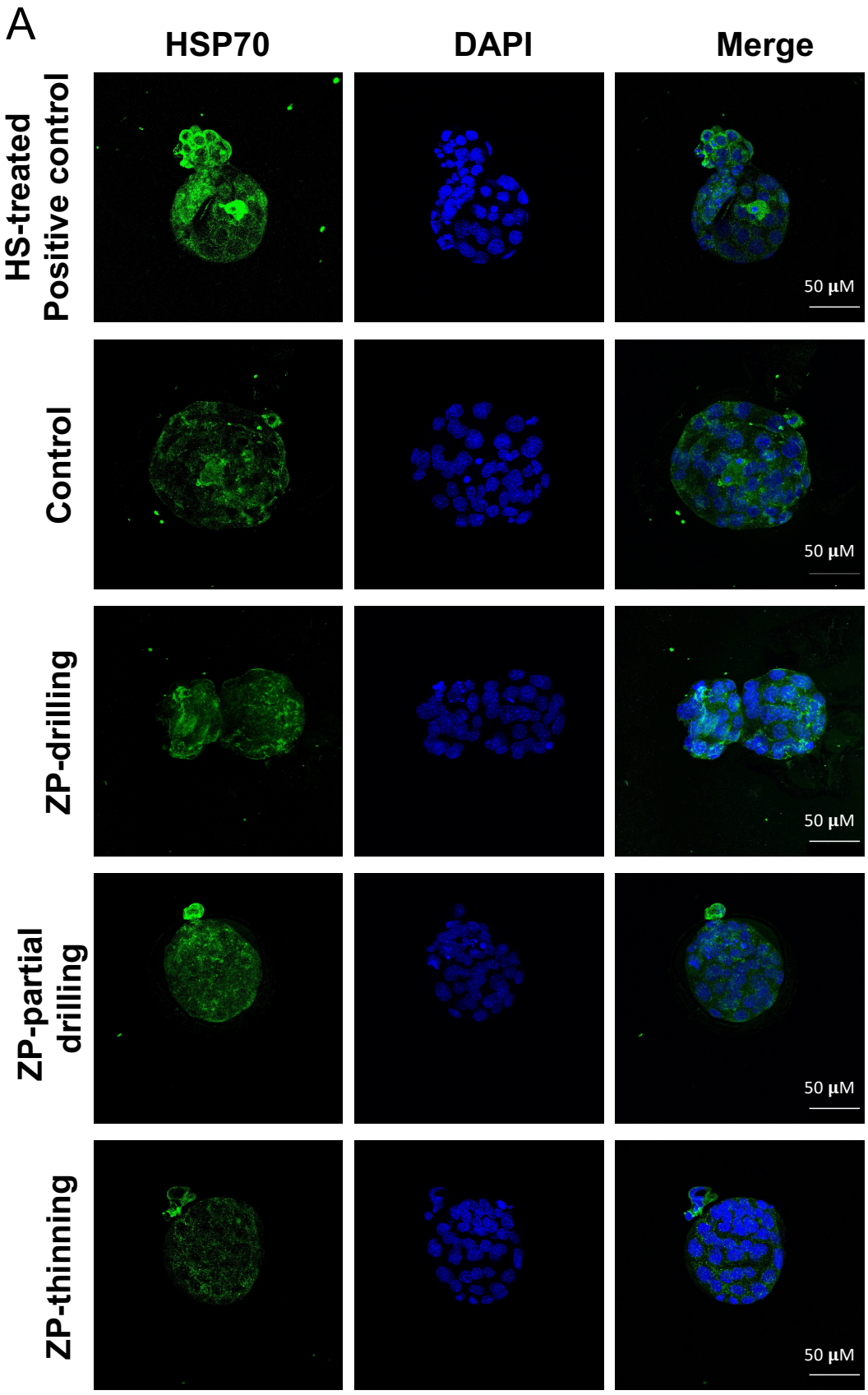


Figure 4-6 (Continued on next page, legend follows)

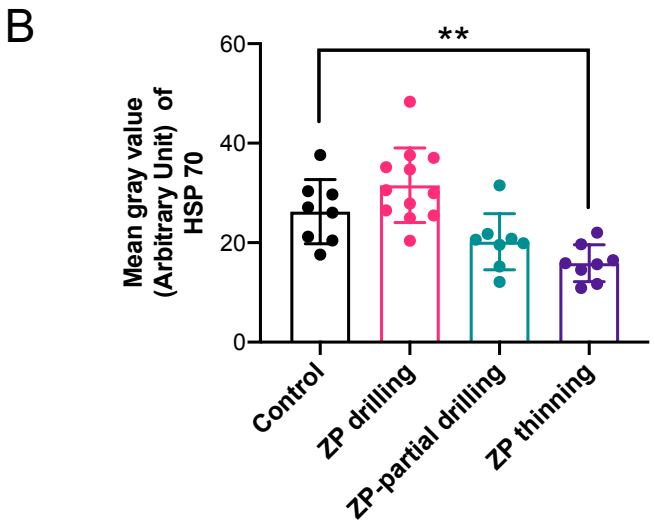


Figure 4-6. HSP70 expression in E4.5 blastocysts undergoing different laser ZP manipulation

(A): HSP70 (green) and nuclei staining DAPI (blue) were visualized by confocal microscope (× 630 magnification), including a positive control (HS-treated embryos) and embryos undergoing different laser ZP manipulation. For the positive control, embryos were incubated at 42°C for 10 minutes and then at 37°C for 30 minutes before fixation (Scale bar=50 μM). (B): The expression of HSP70 was quantified by measuring the mean gray value using Image J. Data presented as mean ±SD. Statistical analysis was carried out using one-way ANOVA with Dunnett's post hoc comparisons test to show differences between each treatment group and the control group. **:P<0.01

4.2.6 The expression of key genes in embryos undergoing different laser ZP manipulations

Having shown that laser ZP manipulations do not significantly impact embryo at biological level, I then questioned whether they would cause deleterious effect from the transcription levels. I chose a panel of 8 genes related to different aspects of physiology, including embryogenesis (*Pou5f1*, *Nanog,* and *Cdx2*), apoptosis (*Bax* and *Bcl2l2*), oxidative stress (*Sod1* and *Gpx7*) and DNA methylation *(Dnmt3a*). I used RT-qPCR to detect the expression levels.

The cDNA generated from a single embryo was very limited, thus, preamplification of target genes was conducted to harvest a detectable amount of cDNA. The validation

of embryo number, cDNA synthesis process, preamplification, and cDNA dilution, were then conducted before proceeding with the experiment (**Appendix 7**). In the final embryo RT-qPCR experiments, in order to harvest enough cDNA, the frozen/thawed embryos were used. In addition, three blastocysts were collected directly for cDNA synthesis; 15 cycles of preamplification and a 1 in 5 dilution of pre-amp cDNA was adopted for the qPCR experiment.

To test the effect of ZP manipulation on embryo segregation, I chose three key genes: *Pou5f1, Nanog*, and *Cdx2*. As shown in **Figure 4-7**, although the expression of *Pou5f1* slightly fluctuated, there was no significant difference in these three genes across four groups, as demonstrated by one-way ANOVA (all $P>0.05$).

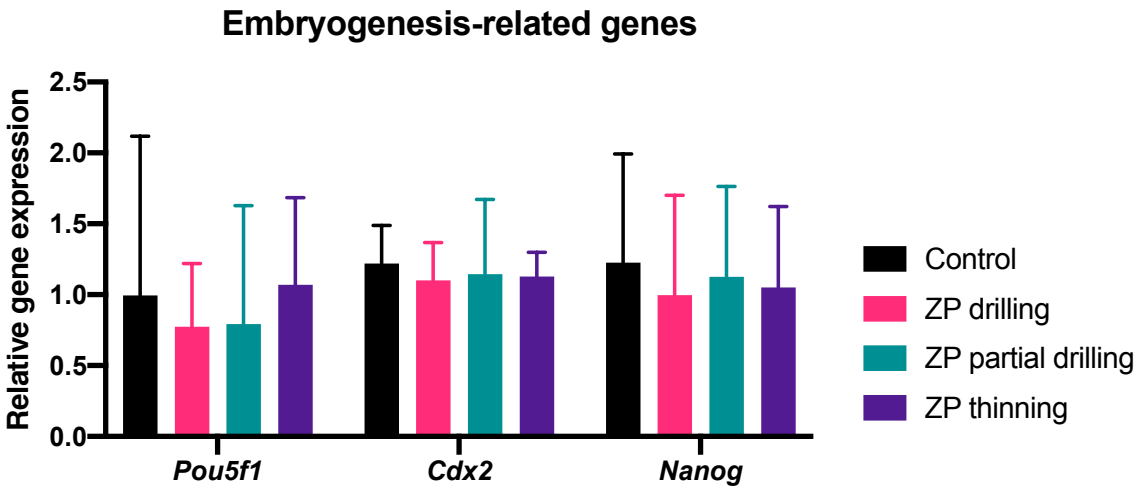


Figure 4-7. A comparison of the expression of embryogenesis-related genes in E4.5 blastocysts undergoing different laser ZP manipulations

The mRNA expression of *Pou5f1, Nanog,* and *Cdx2* was detected using real-time PCR. The amount of mRNA was quantified by measuring the Ct value. The relative expression of each transcript was normalized to *Gapdh* (ΔCt), and the ΔCt value of different groups were normalized to the mean value of control group ($\Delta\Delta$Ct). Data are presented as mean ± SD. Statistical analysis was carried out using one-way ANOVA with Dunnett's multiple comparison test to show difference between ZP manipulations groups and the control group (n=5 biological repeats).

Apart from DNA fragmentation and caspase-3 activation that were detected, the gene expression level of anti-apoptotic protein (*Bcl2l2*), pro-apoptotic protein (*Bax*), as well as antioxidative enzyme families (*Sod1* and *Gpx7*), were tested to understand whether laser ZP manipulations will cause the alteration in apoptosis intrinsic pathway or oxidative stress in embryos. Consistent with the previous results of DNA fragmentation and caspase-3 activation, no significant difference was found in the expression of *Bax*, *Bcl2l2, Sod1, and Gpx7* among the four groups, although the expression levels fluctuated (**Figure 4-8**).

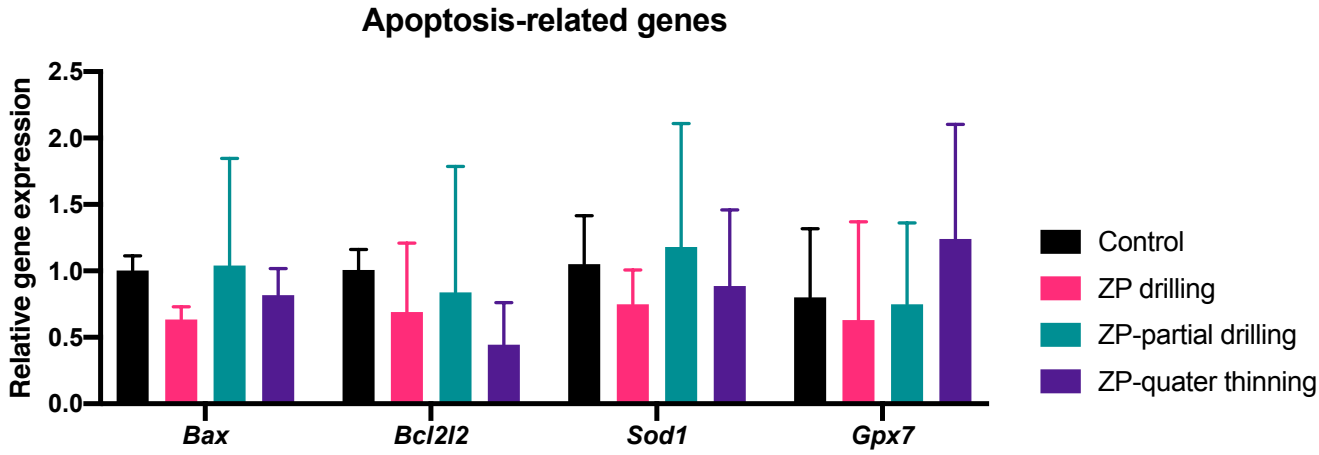


Figure 4-8. A comparison of the expression of apoptosis-related genes in E4.5 blastocysts undergoing different laser ZP manipulations

The mRNA expression of *Bax, Bcl2l2, Sod1, and Gpx7* was detected using real-time PCR. The amount of mRNA was quantified by measuring the Ct value. The relative expression of each transcript was normalized to *Gapdh* (ΔCt), and the ΔCt value of different groups were normalized to the mean value of control group (ΔΔCt). Data are presented as mean ± SD. Statistical analysis was carried out using one-way ANOVA with Dunnett's multiple comparison test to show difference between ZP manipulations groups and the control group (n=5 biological repeats).

Finally, to investigate epigenetic changes in the preimplantation embryo, I tested the expression level of *Dnmt3a*, which is thought to function in *de novo* methylation and important for embryonic development. However, there was no significant change in embryos treated with the 3 laser ZP manipulations in the expression of *Dnmt3a* levels.

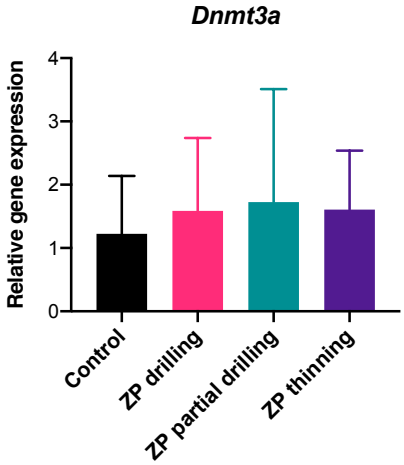


Figure 4-9. A comparison of *Dnmt3a* expression in E4.5 blastocysts undergoing different laser ZP manipulations

The mRNA expression of *Dnmt3a* was detected using real-time PCR. The amount of mRNA was quantified by measuring the Ct value. The relative expression of each transcript was normalized to *Gapdh* (ΔCt), and the ΔCt value of different groups were normalized to the mean value of control group (ΔΔCt). Data are presented as mean ± SD. Statistical analysis was carried out using one-way ANOVA with Dunnett's multiple comparison test to show difference between ZP manipulations groups and the control group (n=5 biological repeats).

4.3 Discussion

Despite the fact that laser-assisted ZP manipulation has been widely used in clinics for over 20 years, its clinical efficacy and safety still remains controversial. As described in the chapter 3, although most embryologists and clinicians believe assisted hatching is a safe technique, concerns about the potential thermal damage caused by laser beams still exist. In this chapter, I have characterised the safety of

three commonly used laser ZP manipulations upon preimplantation mouse embryos from different aspects.

In clinical practice, most of ZP manipulation is commonly performed on Day3 and Day5, while some cases are conducted on Day4. However, in my experiments, no ZP manipulations were conducted at the blastocyst stage. It is because the embryo development varies highly after the morula stage, and mouse preimplantation embryo development is faster than human (Madissoon et al., 2014); thus, making it even more difficult to keep mouse embryos at the same stage for ZP manipulations. In order to standardize the embryo condition, I only treated mouse embryos at E2.5 in this study to mimic one of the most common ZP manipulation (Day 3) in clinics.

4.3.1 Laser ZP manipulations did not affect embryo development

Since the ZP works as a protective shell during embryo development, manipulation of the ZP may affect embryo viability. Herein, to investigate the effect of different laser ZP manipulations on embryo viability, the experimental embryos were cultured for 48 hours until E4.5 (equivalent to Day 5-6 human embryos). Similar to previous studies (Montag et al., 2000a, Chailert et al., 2013, Park et al., 2014, Schimmel et al., 2014), all three laser ZP manipulations showed no determined effects on blastocyst formation at E4.5, regardless of whether they were fresh embryos or frozen/thawed embryos.

Intriguingly, I found that ZP drilling substantially advanced hatching at E4.5, in both fresh and frozen/thawed embryos. Similar findings were also reported in other studies involving both mouse (Montag et al., 2000b, Chailert et al., 2013, Park et al., 2014, Schimmel et al., 2014) and human embryos (Yano et al., 2006). In addition, previous studies demonstrated that only ZP opening reduce the time for embryos to initial

breaching while zona-thinning did not (Yano et al., 2006, Park et al., 2014, Schimmel et al., 2014). Consistent with these findings, in this present study, I observed the similar hatching rates at E4.5 in the ZP thinning, partial drilling, and control groups. Taken together, these findings indicate that laser-assisted ZP drilling, by advancing the hatching of embryos, might be a more efficient method for subsequent TE biopsy procedures, than ZP thinning and partial drilling for AHpBP.

4.3.2 Embryo hatching pattern alterations following laser ZP manipulations

In this chapter, I found that laser-assisted drilling altered the pattern of embryo hatching, and a greater number of embryos adapted the '8'-shape hatching morphology. This distinct '8'-shape hatching behaviour was first reported in 1989 in the zona drilled human and mouse embryos (Malter et al., 1989); and this phenomenon in which embryos hatch slowly through a small opening in the ZP is referred to as "herniation" (Blake et al., 2001). The TE herniation of blastocysts induced by pre-hatching facilitates separation of the TE during blastocyst biopsy and helps embryologists to arrange their work routine; thus, laser-assisted drilling on day 3 embryos is widely used as a strategy for blastocyst biopsy in clinics (Capalbo et al., 2016). One explanation of the "herniation" might be that the hatching process was restrained by the small opening created by drilling. A previous study showed that in the small zona dissection group, a high percentage of embryos underwent '8'-shape hatching; while in the lager zona dissection group, no '8'-shape hatching was found. However, no details about the size of zona dissection was provided in this ESHRE abstract (Lyu et al., 2015). I initially planned to increase the size of the opening to explore whether this may affect hatching morphology. However, the preliminary data

showed that when increasing the opening size to 15 μm in diameter (equivalent to around 30 μm in human embryos), 2/14 embryos lost blastomeres immediately, while 6/14 embryos degenerated (data not shown). This finding may be related with the improper manipulation; but it also proposed that a large opening in the ZP may pose a higher risk of losing blastomeres through the hole as laser ZP manipulation is performed prior to compaction. Thus, considering of the time and sample consuming, the large opening size (15 μm) created by laser drilling was excluded from my study. More importantly, by using time-lapse imaging, I observed that among those untreated embryos, two '8'-shape hatching embryos breached ZP earlier; but they failed to fully hatch out at E6.5. These results proposed a possibility that laser ZP drilling may impact the embryo hatching completion. Thus, in **Chapter 5**, I used the *in vitro* implantation model to investigate whether these laser ZP manipulation, especially the ZP drilling, would affect the hatching completion.

On the other hand, the high frequency of the '8-shape' hatching following laser ZP drilling clearly demonstrates that this technique represents a potential risk factor for cleavage of the ICM. A previous mouse study showed that '8-shape' hatching affects ICM herniation and increases ICM splitting risk (Yan et al., 2015). In addition, three clinical case reports showed that the transfer '8-shaped' hatching and double ICM-like masses blastocysts resulted in two monozygotic twin pregnancies (MZT) and monochorionic triamniotic triplet pregnancy (Van Langendonckt et al., 2000, Behr et al., 2003, Sutherland et al., 2018). Thus, the high frequency of '8-shape' hatching of ZP drilled embryos observed in this study may explained the findings in a previous retrospective study, which demonstrated that assisted hatching represents a potential risk factor for zygotic splitting (Ikemoto et al., 2018). In contrast, a retrospectively study, by investigating 992 single blastocyst transfer cases, demonstrated that ICM

incarceration in ‘8’-shaped hatching blastocyst did not increase the incidence of MZT pregnancy in the PGT/PGS patients (Gu et al., 2018). Since the incidence of MZT is very rate in clinics, large-scale follow-up studies are now needed to reveal the specific risk of perinatal complications following laser-assisted drilling.

Interestingly, the current study identified a slightly higher frequency of ‘U’-shape hatching following laser ZP thinning; and the untreated embryos adopting in ‘U’-shape hatching pattern hatched out successfully as recorded by time-lapse microscopy. Previous studies have shown that more than 80% of *in vivo* developed embryos underwent this ‘U’-shape hatching pattern, with ICM splitting occurring in only in 1.9% of these embryos (Lyu et al., 2015, Yan et al., 2015). The higher percentage of ‘U’-shape hatching pattern in the ZP thinning group suggests that the change of integrity of the ZP, by laser thinning, could mimic a natural hatching process and hence may assist embryo hatching. In **Chapter 5**, I’ve further investigated the effect of laser ZP thinning on hatching completion and embryo attachment capability.

4.3.3 Hatching embryos treated with ZP drilling exhibited a reduced number of embryonic cells

In this study, I found that the laser-assisted manipulations would not impact the blastocysts cell number. However, I observed that the total cell number of hatching embryos was significantly lower in the ZP drilling group; this observation concurred with previous findings (Montag et al., 2000a, Chailert et al., 2013). One possible explanation for this is that ZP drilling allows embryos to start hatching without reaching a certain embryonic cell number. Meanwhile, a sufficient number of embryonic cells, to overcome the ZP resistance, are necessary for embryos to hatch out from an intact ZP (untreated, partial ZP drilling, and ZP thinning). This theory is in line with a previous

finding that the embryo hatching *in vitro* is dependent on a sufficient number cells, while hatching *in vivo* is accomplished by uterine or trophectodermal factors that are absent *in vitro* (Montag et al., 2000a). Although the number of TE cells of blastocysts was slightly lower in the laser drilling group, no differences in ICM cells, TE/ICM ratio, and the expression of embryo segregation-relate genes (*Pou5f1, Cdx2*, and *Nanog*) were observed across four groups; thus, indicating that laser ZP manipulations may not affect the embryo segregation.

4.3.4 Laser ZP manipulations did not induce cell apoptosis

Cell apoptosis plays an important role in development and maintenance of tissue hemostasias; it is an essential feature of many pathological conditions. The fragmentation of nuclei and DNA featured cells undergoing apoptosis, which can be seen in the morula and blastocyst (Hardy, 1999, Penaloza et al., 2006). Induced DNA damage was previously reported in embryos undergoing laser-assisted hatching treatment (Honguntikar et al., 2015). The discrepancies could be associated with a variety of factors related to laser manipulation, such as the duration of laser pulses or the time interval between two consecutive laser pulses. In addition, the methods used to evaluate cell apoptosis also differ. In a previous study, only the DNA fragmentation (calculated as the number of TUNEL-positive cells/total cell number) was used (Honguntikar et al., 2015). However, in this present study, apart from DNA fragmentation, I also observed that no overt induced caspase-3 activation or any alteration in the expression of apoptosis-related genes (*Bax, Bcl2l2*, *Sod1*, and *Gpx7*). Taken together, results here suggested that laser-assisted ZP manipulations would not induce cell apoptosis if conducted properly.

4.3.5 The expression of HSP70 in blastocyst following different LAH treatments

The potential for thermal damage is one of the major concerns when using laser pulses on embryos since preimplantation embryos are particularly sensitive to thermal changes (Douglas-Hamilton et al., 2001, Hartshorn et al., 2007). The cellular response to stress, such as thermal injury is characterized by the rapid induction of HSP70 expression (Beere et al., 2001). A previous study demonstrated that laser drilling did not induce a rapid upregulation of *Hsp70i* mRNA expression, even in cells that were closest to the laser beam (Beere et al., 2001). In that study, the expression of *Hsp70i* was detected 2 hours after the laser treatment, in order to permit hsp70i RNA accumulation and investigate the possible heat shock effect generated by laser beam itself. However, in the present study, I investigated the expression of HSP70 at the blastocyst stage; therefore, the level of hsp70 expression at this stage would act as an indicator for the cell stress caused by laser-drilling treatment rather than the laser beam itself. Similarly, we did not see an increase in the protein expression of HSP70 in the laser-assisted ZP drilling group or ZP-partial drilling group, thus suggesting that laser-assisted drilling does not induce cellular stress in preimplantation embryos.

Intriguingly, embryos in LA-ZP thinning showed a significant suppression of HSP70 in blastocysts, which suggested that this technique might decrease the embryonic cell stress. Under *in vitro* culture circumstances, the expansion and compression of the blastocyst would generate physical pressure to confront the stiffness of the ZP, thus allowing the embryo to hatch (Leonavicius et al., 2018). I proposed that the physical pressure exerted by the blastocyst may result in a certain degree of stress; and the expression of HSP70 during hatching may be interpreted as a protective reaction since

HSP70 would provide resistance to stress-induced apoptosis (Mosser et al., 1997). On the other hand, laser ZP thinning, by decreasing the thickness of the ZP and changing the integrity of ZP, might decrease the blastocyst pressure; thus, suppressing the HSP70 expression. This theory may, at least in part, explain the lower level of HSP70 expression in the LA-ZP thinning group. However, the role of HSP70 during hatching is unclear and further studies are needed.

4.3.6 Laser ZP treatment did not alter the expression of key genes

Only few studies to date have investigated the transcriptional changes of embryos following ZP manipulation. A recent study investigated the epigenetic alterations in embryos following LAH treatment and showed the downregulation of *Dnmt3a* and *Dnmt3b* when treated embryos at the 2-cell stage. However, these changes disappeared when LAH was performed at the 6-8 cell and blastocyst stage (Honguntikar et al., 2017). In the present study, we did not observe significant alteration of *Dnmt3a* expression in E4.5 stage embryos in response to laser ZP manipulation. Nor did I see a change of the embryo segregation markers *Pou5f1, Cdx2,* and *Nanog.* Similar to the cell apoptosis assays, the expression of apoptosis-related genes (*Bax, Bcl2l2, Gpx7* and *Sod1*) was also not altered by laser ZP manipulations. These data provide a line of evidence that laser-assisted ZP manipulations may not cause detrimental effects to embryos if performed at the cleavage stage; however, it is too early to claim that laser-assisted ZP manipulation would not cause any alteration in embryo transcriptome. To investigate the potential transcriptomic changes, in **Chapter 6,** I used the RNA-sequencing analysis to compare the transcriptome between laser ZP drilling embryo and untreated embryo.

4.4 Limitations

In this part of the study, both fresh and frozen/thaw mouse embryos were used to investigate the impact of these Laser-assisted ZP manipulations. Ideally, these embryos should be from the same bred strain of mice. However, to reduce the potential damage caused by improper cryopreservation procedure and waste of samples for practice; the frozen embryos were directly purchased from the company. Thus, the fresh and frozen embryos were from two different stains. Furthermore, in this study, I only detected the heat shock response of embryos from the expression of HSP70 at protein level; and it is unknown of the alternation at the mRNA level. Therefore, further studies are needed to investigate the mRNA expression of *Hsp70s* genes.

4.5 Concluding remarks

Collectively, the data reported in this chapter demonstrate that laser-assisted ZP manipulation does not impact embryo preimplantation development or cause detrimental effects with regard to the embryonic cell number, cell apoptosis, embryo segregation, and cell stress. Furthermore, laser ZP drilling was found to advance embryo hatching and change the hatching pattern, which makes it an effective AHpBP method for subsequent TE biopsy. In addition, ZP thinning might reduce blastocyst pressure, manifesting in the reduced levels of HSP70 expression. However, how these ZP manipulations may affect embryo attachment and whether they induce transcriptional alteration will be further explored in the **Chapter 5** and **6**.

4.6 Key findings

- Laser-assisted ZP drilling, partial drilling, and ZP thinning did not impair *in vitro* preimplantation embryo survival and development

- Laser-assisted ZP drilling, partial drilling, and ZP thinning did not induce cell apoptosis nor affect embryo segregation

- Laser-assisted ZP drilling facilitated the initiation of embryo hatching with lower total embryo cell numbers in hatching blastocysts. Most of the hatching embryos adopted ‘8’-shape hatching morphology

- Laser-assisted LA-ZP thinning reduced cell stress in the blastocyst as evidenced by a lower level of HSP70 expression



Chapter 5

Investigating the effect of laser-assisted zona pellucida manipulations on embryo attachment

5.1 Introduction

The precise efficacy of laser-assisted ZP manipulation on clinical outcomes remains contradictory. Some studies support an improved implantation rate, while others show unchanged or even reduced pregnancy and live birth rate when ZP manipulation was applied for assisted hatching (Li et al., 2016, Zeng et al., 2017, Alteri et al., 2018), and for pre-hatching prior to embryo biopsy (Zhao et al., 2019, Rubino et al., 2020). Therefore, it is imperative to understand how these laser ZP manipulations might affect the embryo competency for implantation.

The variety of laser ZP manipulations used and the differences in patient groups make it complicated to explain the clinical results (Alteri et al., 2018), since embryo implantation is known to be affected by both embryo competency and the uterus receptivity. In preparation for embryos to implant, the uterus endometrium undergoes temporal changes driven by ovarian steroid hormones (Weimar et al., 2013). Meanwhile, embryos encounter the endometrium approximately five days after fertilization (an equivalent to Day 4 in the mouse). Once reaching the blastocyst stage and hatching out from the ZP, embryos acquire the implantation competency (Hamatani et al., 2004, Yoshinaga, 2013).

Studying human embryo implantation is practically and ethically challenging. In addition, the early stages of embryo implantation (apposition and adhesion) in both humans and mice are of short duration (Bergh et al., 1992, Aplin, 2000), making it difficult to both observe and perform experimental studies. Thus, although *in vitro* studies cannot completely mimic the intrauterine environment, they can serve as a suitable surrogate for studying early implantation by modelling some of the potential interactions and providing a framework within which molecular parameters may be

manipulated (Weimar et al., 2013). Furthermore, it is difficult to evaluate the efficacy of laser ZP manipulations on embryo hatching completion *in vivo* since the uterine factors, e.g., zona lysin, may also affect the *in vivo* hatching process (McLaren, 1970, Illera et al., 2000). In contrast, the *in vitro* implantation model is less confounding as it purely focuses on embryo implantation competency, without being affected by other maternal factors such as uterine fluid components which could enhance blastocyst development and endometrium receptivity (Salamonsen et al., 2013). Taken together, this suggests that it is more appropriate to assess blastocyst competency following ZP manipulation using the *in vitro* model (Ueno et al., 2016).

Endometrial epithelial cells are essential for the establishment of *in vitro* implantation; however, obtaining sufficient epithelial cells from endometrial tissue is difficult, if not impossible (Hannan et al., 2010). Alternatively, the endometrial epithelial cell line is more accessible, easily handled, and hence is more ideal for providing consistent samples and reproducible results (Hannan et al., 2010, Weimar et al., 2013). Ishikawa cells, a well-differentiated endometrial adenocarcinoma cell line derived from a 39-year-old Japanese woman, is widely used for studying implantation (Hannan et al., 2010). This is because that many structural proteins found in the normal endometrial epithelium, such as Integrins (ITGAV, ITGB3, ect.), KRT-18 (Keratin 18), MUC-1 (Mucin 1) and OPN (Osteopontin/ Secreted Phosphoprotein 1) (Park et al., 2000, Mo et al., 2006, Singh et al., 2009), along with functional steroid receptors such as oestrogen, progesterone, and androgen receptors (Lessey et al., 1996) were also expressed in the Ishikawa cell. On the other hand, co-culturing mouse blastocysts with Ishikawa cells has been well documented as an appropriate model for studying embryo-endometrium interaction during the early stages of implantation (Kang et al., 2014, Green et al., 2015, Ruane et al., 2017). H singh *et al* (2010) first developed a

model in which mouse embryos attached to human Ishikawa cells, and demonstrated that the mouse embryo implants interstitially after a transient interaction with the epithelium (Singh et al., 2010). Later on, Integrin αVβ3-OPN interactions was found playing a role in the attachment of mouse and human embryos using the Ishikawa cell implantation model (Kang et al., 2014). In addition, this implantation model reflects the changes in blastocyst adhesion competency and the differentiation of trophoblasts during implantation; thus, facilitating the assessment of attachment and the subsequent developmental potential of the blastocyst (Ruane et al., 2017). Therefore, the mouse embryo and Ishikawa cell co-culture system was considered as a useful model for evaluating the efficacy of ZP manipulation on the competency of embryo implantation.

Based on the inconsistency of clinical data, I hypothesized that various laser ZP manipulations may exert different effects on embryo implantation competency. In this chapter, by using the Ishikawa cell *in vitro* implantation model, I investigated the completion of embryo hatching *in vitro,* as well as the kinetics of blastocyst attachment following different laser-assisted ZP manipulations. In addition, I tested the effect of different-sized perforations in the ZP created by laser drilling. Finally, the efficacy of ZP manipulation on developmentally delayed embryos was assessed using blastulation delayed embryos.

5.2 Results

5.2.1 Verification of Ishikawa cells as a model of the endometrial epithelium

Epithelial cells are generally characterized by the expression of markers such as E-cadherin (also known as Cadherin 1) and Keratin 18. In contrast, the mesenchymal phenotype is identified as the expression of vimentin, N-cadherin (also known as Cadherin 2), and fibronectin (Lim et al., 2012, Owusu-Akyaw et al., 2019). **Figure 5-1** shows that Ishikawa cells expressed high mRNA levels of *CDH1* (E-cadherin) and *KRT18* (Keratin 18), and Keratin 18 was strongly expressed in the cytoplasm of Ishikawa cells. In contrast, the expression levels of the mesenchymal markers *CDH2* (N-cadherin), *VIM* (vimentin) and *FN1* (fibronectin) were too low to be detected in Ishikawa cells. In addition, the intensity of Vimentin staining was very low.

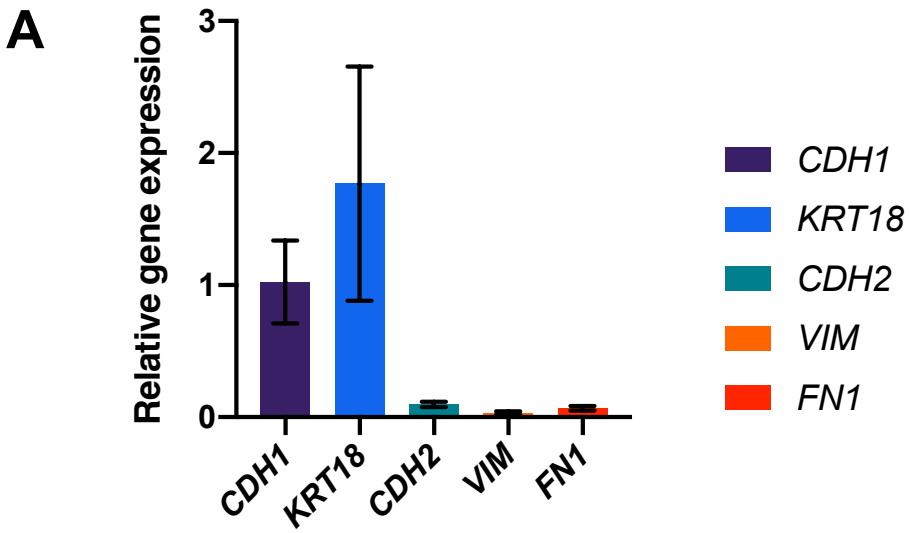


Figure 5-1 (Continued on next page, legend follows)

B

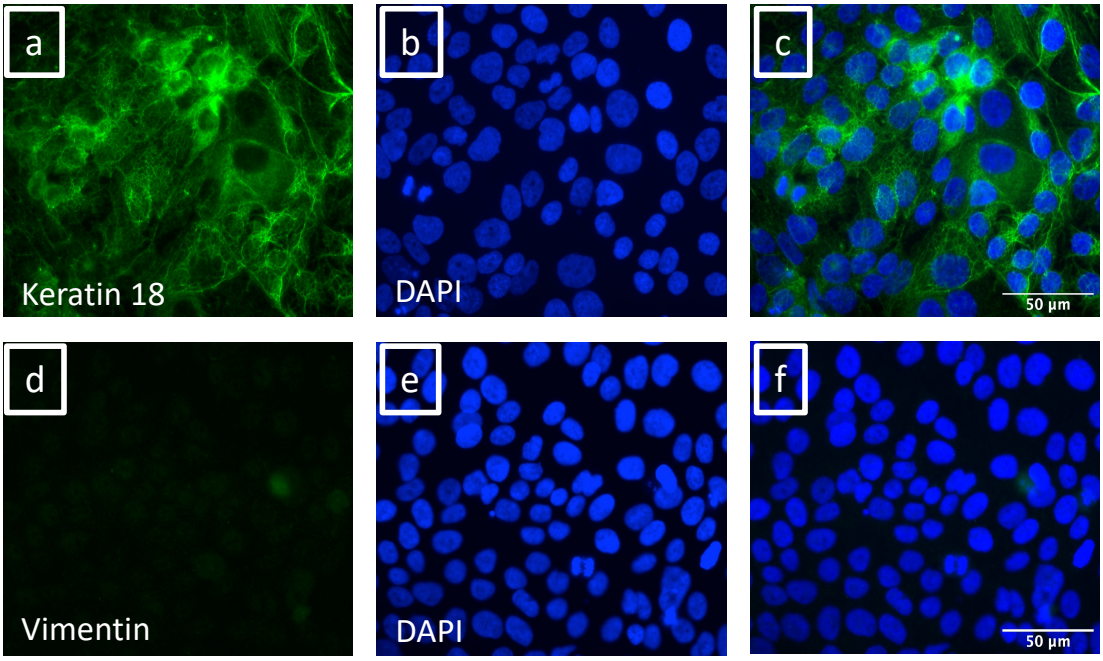


Figure 5-1. The expression of epithelial and mesenchymal cellular markers in Ishikawa cells

(A) The mRNA expression of *CDH1*, *KRT18*, *CDH2*, *VIM* and *FN1* was detected using real-time qPCR. The amount of mRNA was quantified by measuring C_t values. Relative expression of each transcript was normalized to *B2M* (ΔC_t). Data presented as mean ± SD (n=5 biological replicates). (B) Ishikawa cells grown on Matrigel-coated coverslips were immune-stained for Keratin 18 (a) and Vimentin (d). Nuclei were counter-stained using DAPI (b and e). Merged images are shown in (c) and (f). Scale bars = 50 µm (400x magnification).

5.2.2 Establishment of the *in vitro* implantation model

The Ishikawa cell *in vitro* model of embryo-epithelial interactions was successfully established. Embryo hatching states and attachment was observed every 24 hours following the transfer of E4.5 or E5.5 mouse embryos; the total period of the co-culture of embryos and Ishikawa cells were 72 hours. **Figure 5-2** shows a schematic of the embryo-Ishikawa cell co-culture system.

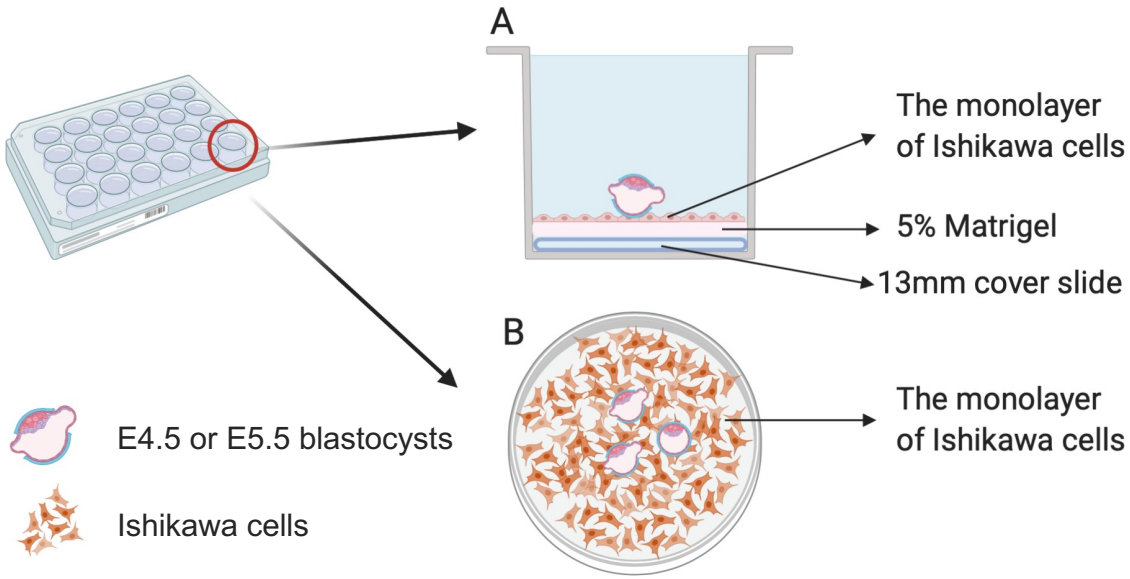


Figure 5-2. A schematic of the embryo-Ishikawa cells co-culture system

(A) A side-view of the co-culture system showing an E4.5 embryo and a monolayer of Ishikawa cells; (B) A view of embryos and Ishikawa cells under a dissecting microscope.

At the first observation time point, embryos were clearly visible, and most of the embryos were undergoing the hatching process; very few embryos had hatched out or attached to the Ishikawa cells. However, this attachment was easily lost when tapping the microscope stage (**Figure 5-3 A, B**). At 48 hours of co-culture, there was an increased number of hatched embryos as well as attached embryos. The outgrowth of trophectoderm (TE) cells was observed in this *in vitro* model (**Figure 5-3 C, D**). Finally, at 72 hours post-transfer, more embryos hatched out; most of these were attached to the Ishikawa cells. In addition, some outgrowth of TE cells breached the Ishikawa cells layers and invaded into the Matrigel, and the disruption of underlying Ishikawa cells was observed surrounding the location of embryo implantation (**Figure 5-3 E, F**).

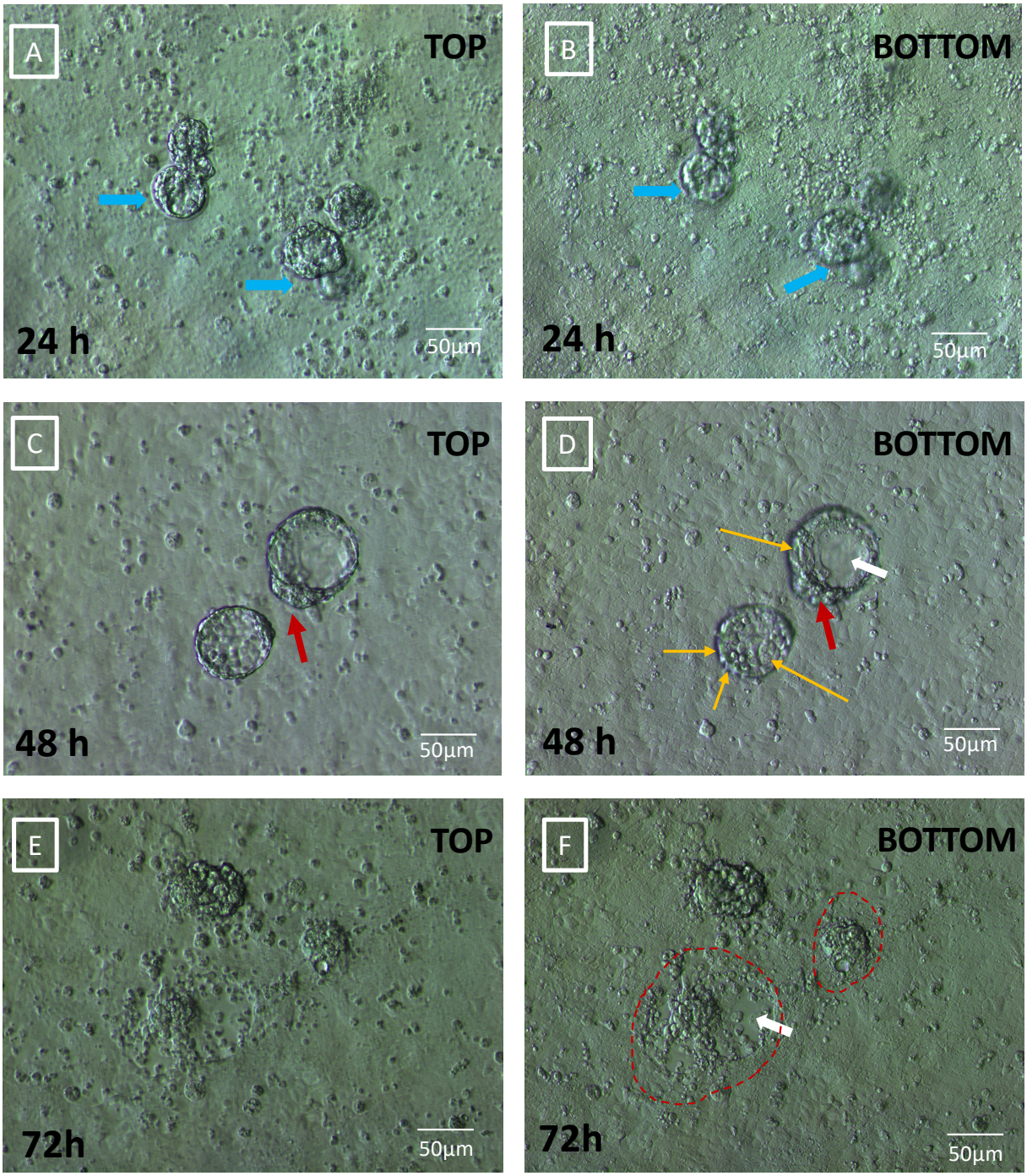


Figure 5-3. The *in vitro* mouse embryo implantation model

Exemplary phase-contrast images of co-cultured mouse embryos and Ishikawa cells at 24h (A and B), 48h (C and D) and 72h (E and F) post embryo transfer. Blue arrows indicate mouse embryos undergoing hatching. For the embryos attached to Ishikawa cells, red markers indicate the inner cell mass, thin yellow arrows mark the outgrowth of TE (trophectoderm) cells, and white arrows show the disruption of Ishikawa cells. The outgrowing embryos which breached the Ishikawa cell layer and invaded into Matrigel are indicated with red circles.

5.2.3 Vitrification of mouse embryo attachment to Ishikawa cells

According to previous studies, Integrin αvβ3 and its ligand osteopontin (OPN) (also known as secreted Phosphoprotein 1 (SSP1)), are expressed in endometrial cells during implantation (Kang et al., 2014, Ruane et al., 2017). Thus, I stained the embryos and Ishikawa cells in the co-culture system with antibodies against Integrin αvβ3 and OPN to confirm embryo implantation. As shown in **Figure 5-4 A**, Integrin αvβ3 was weakly expressed in Ishikawa cells in the absence of embryos, predominantly at cell borders in areas where there was cell-to-cell contact. Nevertheless, in the co-culture system, the intensity of integrin αvβ3 staining was locally increased at the site of embryo attachment, especially in the cell adjacent to the mouse embryo (**Figure 5-4 B and C**).

OPN was weakly expressed in the cytoplasm of the cells, exhibiting a mosaic expression pattern (**Figure 5-5 A**). In the enlarged image (**Figure 5-5 B**), some vesicle-like staining was captured. Similar to Integrin αvβ3, the mouse blastocyst attachment locally increased the intensity of OPN in the co-culture system (**Figure 5-5 C**). In addition, for the invaded embryos, OPN was strongly expressed in the cytoplasm of the outgrowing TE cells, which connected the embryos with surrounded Ishikawa cells (**Figure 5-5 D**). Taken together, these immunostaining results demonstrate that mouse embryos attached to Ishikawa cells at the molecular level.

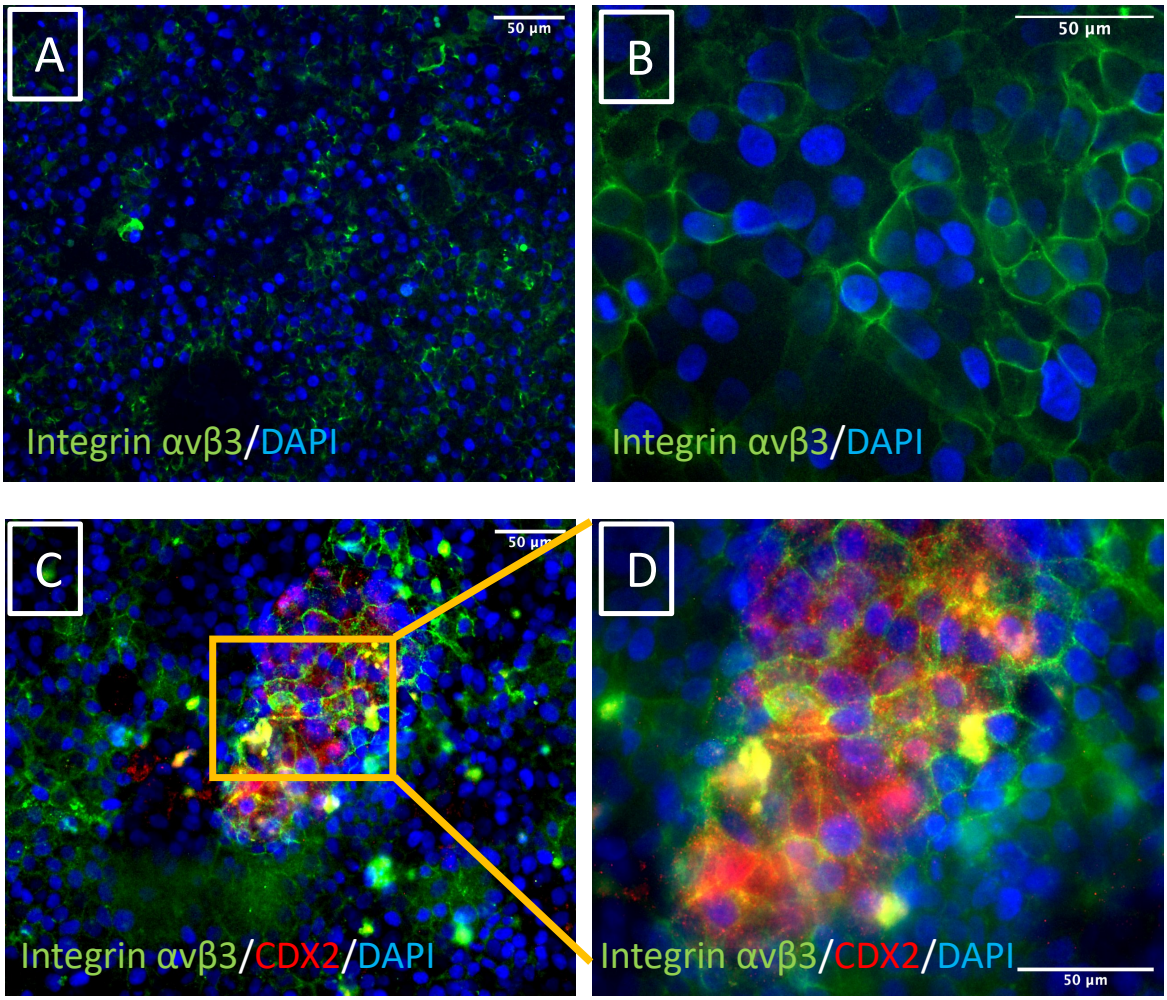


Figure 5-4. Representative images of Integrin αvβ3 and CDX2 staining in Ishikawa cells and the co-culture system

The expression of Integrin αvβ3 (green), and CDX2 (red) were detected in Ishikawa cells (A and B), as well as in the mouse embryo and Ishikawa cell co-culture system (C and D). Images were captured at 200× magnification (A, C) and 400× magnification (B, D). The region highlighted by the yellow square in image (C) was captured at an optical magnification of 40X and enlarged digitally (D). Scale bars = 50 μm.

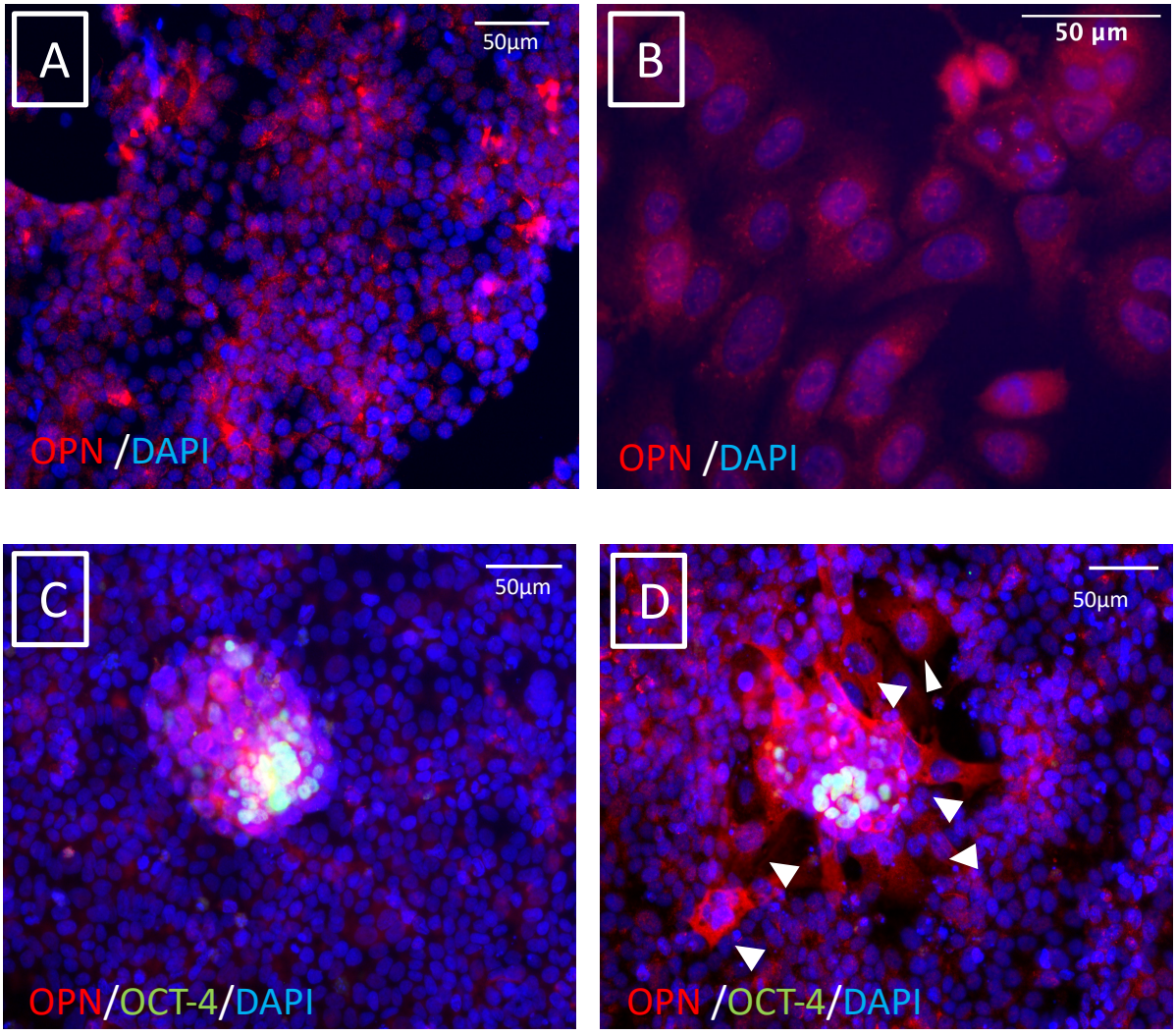


Figure 5-5. Representative images of osteopontin (OPN) and OCT4 staining in Ishikawa cells and the co-culture system

The expression of OPN (red), OCT4 (green), and DAPI (blue) was detected in Ishikawa cells (A and B), and in the mouse embryo and Ishikawa cell co-culture system (C and D). Images were captured at 200× magnification (A, C, and D) and 400× magnification (B). White triangles indicate the outgrowth of TE cells. Scale bars= 50 µm.

5.2.4 Assessing the stability of embryo attachment

An established four-point scale of blastocyst attachment behaviour upon agitation was used to quantify the stability of embryo attachment. For 1-point attachment, the embryos were unattached, and the apparent translocation of embryos could be

observed upon agitation. Weakly attached (2-point) embryos oscillated around an attachment point upon agitation. Embryos showing intermediate attachment (3-point) oscillated slightly upon agitation. In contrast, no oscillation was observed when the embryos stably were attached to Ishikawa cells (4-point). In **Figure 5-6**, I provide some images captured from the video recordings to represent the typical extent of embryo oscillation.

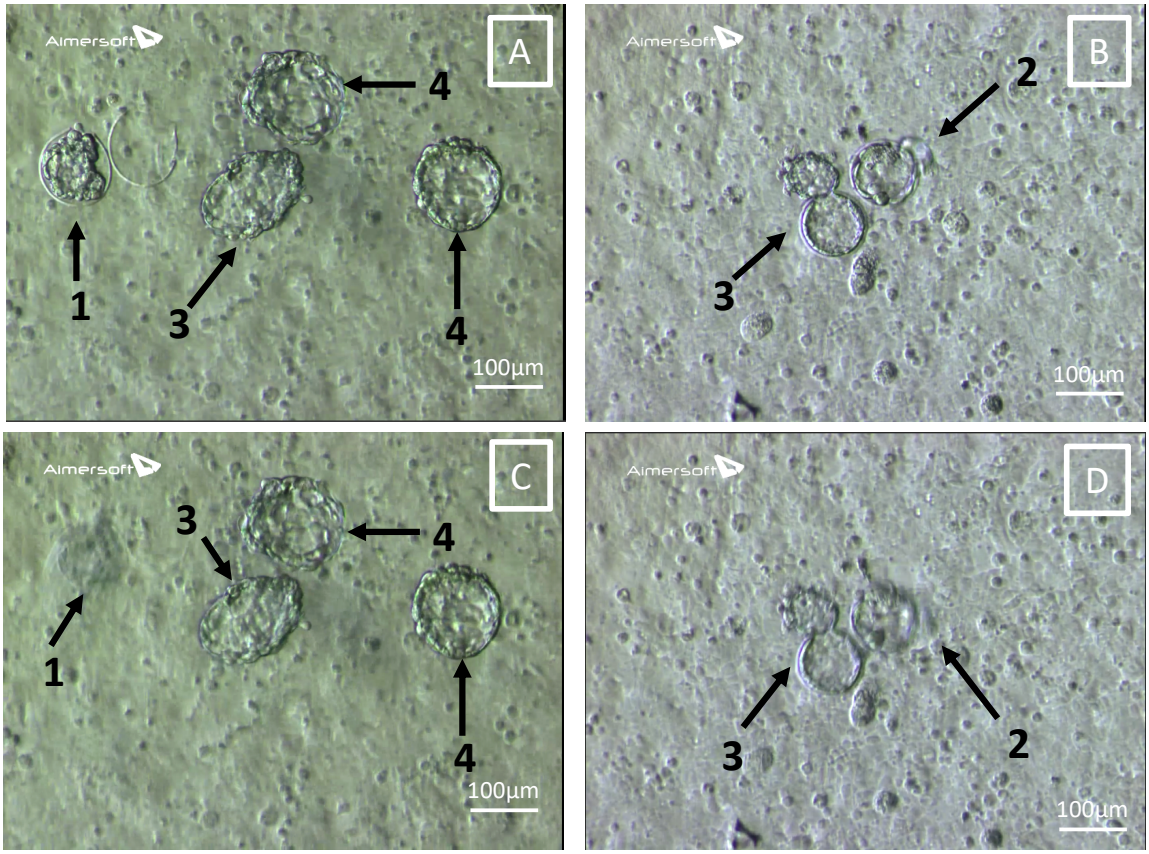


Figure 5-6. Representative images of scored embryo attachment using a four-point scale

Images were captured from video recordings of the embryo attachment assay. Blastocysts are indicated by the arrows and the attachment stability scores. The images were taken prior to (A and B) and after (C and D) agitation. The videos were recorded at 100× magnification. Scale bars =100 µm

5.2.5 The *in vitro* implantation model from E4.5 to E7.5

5.2.5.1 Embryo hatching and attachment in the *in vitro* implantation model

To mimic the clinical procedure of blastocyst transfer, I transferred E4.5 mouse blastocyst (equivalent to Day 5-6 human embryo) into the Ishikawa cells of the *in vitro* implantation model. Overall, 175 E4.5 mouse blastocysts were transferred. As shown in **Figure 5-7**, the number of hatched embryos and stably attached embryos increased significantly as the time of co-culture increased. At 24 hours of co-culture, only 14.9% (26/175) of the transferred embryos fully hatched out, while a few embryos weakly attached to the Ishikawa cells. Another 24 hours later, the proportion of fully hatched embryos markedly increased to 56% (98/175), and 43.4% (76/175) of embryos stably attached. At the end of the observation time (72 hours), 69.1% (121/175) of transferred embryos successfully hatched out; and 81.1% (142/175) of embryos stably attached.

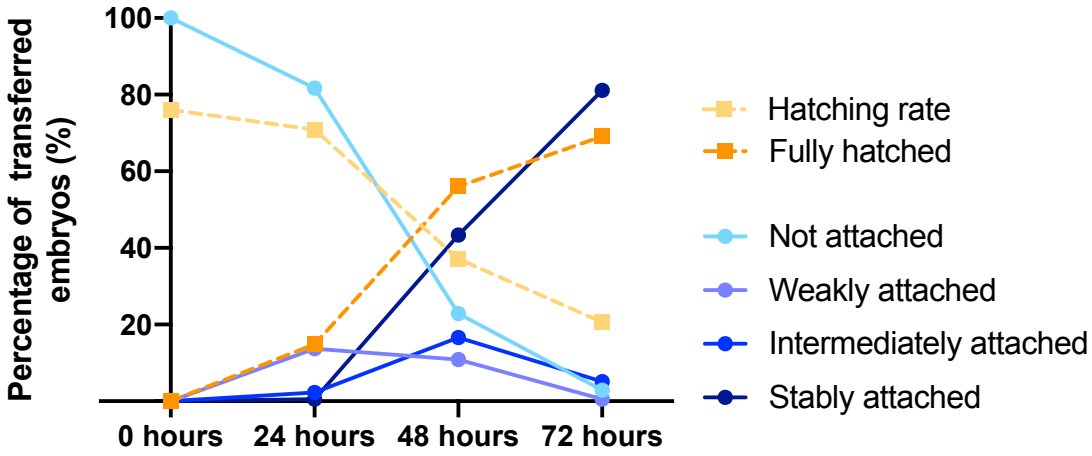


Figure 5-7. The mouse embryo hatching and attachment in the *in vitro* implantation model from E4.5 to E7.5

Embryos hatching statues (dashed line) and attachment stability (full line) were observed at 24h, 48h, and 72h of co-culture. The percentages of hatching (yellow) and hatched (orange) embryos, and the proportions of embryos with different degrees of attachment at different time-points were present.

The results suggested the fully hatched embryo can be observed after 24 hours, while the stable attached embryos started to show after 48 hours. Thus, I compared the fully hatched rates and the stably attached rate from 24 hours and 48 hours of co-culture, respectively.

5.2.5.2 The effects of different laser ZP manipulations on *in vitro* embryo hatching and attachment

E4.5 embryos subjected to laser ZP drilling (n=46), partial drilling (n=28), ZP thinning (n=26), and control embryos (n=36) were transferred into the co-culture system. As indicated in **Table 5-1**, the proportion of fully hatched embryos in ZP thinning group [23.1% (6/26)] was more than doubled than other three groups at 24 hours, although the difference did not reach the statistical significance. Intriguingly, at the 48 hours of co-culture, there was a significant difference across four groups, that the proportion of fully hatched embryos in the ZP drilling group was lower than other three groups, especially when compared with the control group (39.1% (18/46) *vs* 72.2% (26/36), $P<0.007$). In addition, at 72h of co-culture, the proportion of fully hatched embryo was still lower in the ZP-drilling group [52.2% (24/46)], while the proportions in the other three groups were similar. In contrast, more embryos in the ZP drilling group were trapped at 72h of co-culture (41.3% (19/46)), which was significantly higher than the other three groups ($P<0.0001$). Among the transferred embryos subjected to laser ZP drilling, 58.7% (27/46) were 8-shaped hatching blastocysts; 70.4% (19/27) of these 8-shaped embryos ended up with entrapment.

To assess embryo attachment capability, I compared the attachment stability scores of all transferred embryos; however, no difference was found across four groups at three different times (**Appendix 8. Fig S.5-A**). I then compared the percentages of

attached embryos among all transferred embryos; there was no statistically significant difference among the four groups at 48h and 72h of co-culture (both *P*>0.05).

Since only fully hatched embryos could implant into the endometrium, I also compared the proportion of attached embryos among the fully hatched embryos. It was indicated that there was a statistical difference across four groups (*P*=0.023). All the hatched embryos in the ZP drilling (24/24) and ZP thinning groups (19/19) had attached to Ishikawa cells, while 10.7% (3/28) and 17.4% (4/23) of hatched embryos in the control group and the partial drilling group did not stably attach at the end of observation.

Table 5-1 A comparison of *in vitro* hatching and attachment across different laser-assisted ZP manipulations groups from E4.5 to E7.5

		ZP-drilling (n=46)	ZP-partial drilling (n=28)	ZP-thinning (n=26)	Control (n=36)	*P* * value
Fully hatched	24h	5 (10.9%)	3 (10.7%)	6 (23.1%)	3 (8.3%)	NS
	48h	18 (39.1%) [a]	19 (67.9%) [a,b]	18 (69.2%) [a,b]	26 (72.2%) [b]	0.007
	72h	24 (52.2%)	23 (82.1%)	19 (73.1%)	28 (77.8%)	0.021
Trapped	72h	19 (41.3%) [a]	0 [b]	3 (11.5 %) [a,b]	5 (13.9%) [b]	<0.0001
Stable attachment	48h	23 (50%)	11 (39.3%)	12 (46.2%)	17 (47.2%)	NS
	72h	36 (78.3%)	19 (67.9%)	22 (84.6%)	30 (83.3%)	NS
Fully hatched and attached	72h	24 (100%)	19 (82.6%)	19 (100%)	25 (89.3%)	0.023

* χ2 test or χ2 Fisher's exact test with pairwise z-test was used to compare the proportions across four groups. Bonferroni method was used to adjust *P*-value in multiple comparison.

a, b: Each subscript letter denotes a subset of laser ZP manipulation groups whose proportion did not differ significantly from each other at the 0.05 level.

5.2.5.3 The effects of different laser ZP drilling-induced perforation size on *in vitro* embryo hatching and attachment

As the results above shown that ZP drilling could impact the embryo hatching completion, I tried to drill holes in the ZP with different laser diameters, including 5 μm (n=15), 7.5 μm (n=24), and 10 μm (n=15), to investigate the effect of the size of ZP opening. These embryos were compared with 16 embryos from the control group. The data here were generated from 2 independent experiments. As shown in **Table 5-2**, the percentage of fully hatched embryos in the control group was higher than other three drilling groups at 48 hours of co-culture (P=0.014), especially when compared with the 5 μm opening groups (87.5% (14/16) and 33.3% (5/15), P<0.05). However, at 72 hours of co-culture, the difference was not significant, although the percentage was still lower in the three drilling groups. In contrast, the proportion of trapped embryos was substantially higher in the 5 μm group [33.3% (5/15)].

Regarding embryo attachment, no significant difference was found among the four groups in terms of the proportion of stably attached embryos at 48 hours and 72 hours (both P>0.05). In addition, similar to the previous result, almost all fully hatched embryos stably attached to Ishikawa cells (**Table 5-2**).

The proportion of fully hatched embryos in the control group and the 7.5 μm opening group in this experiment was slightly higher (not significantly) than in the previous experiment; this was mainly due to the small sample.

Table 5-2 A comparison of the *in vitro* hatching and attachment across different ZP opening size groups

		5 μm (n=15)	7.5 μm (n=24)	10 μm (n=15)	Control (n=16)	*P* * value
Fully hatched	24h	4 (26.7%)	6 (25%)	5 (33.3%)	1 (6.3%)	NS
	48h	5 (33.3%) [a]	12 (50.0%) [a,b]	10 (66.7%) [a,b]	14 (87.5%) [b]	0.014
	72h	9 (60.0%)	18 (75.0%)	12 (80.0%)	15 (93.8%)	NS
Trapped	72h	5 (33.3%)	4 (16.7%)	2 (13.3%)	1 (6.3%)	NS
Stable attachment	48h	4 (26.7%)	9 (37.5%)	6 (40.0%)	8 (56.3%)	NS
	72h	13 (86.7%)	22 (91.7%)	13 (86.7%)	15 (93.8%)	NS
Fully hatched and attached	72h	9 (100%)	17 (94.4%)	12 (100%)	14 (93.3%)	NS

* χ2 test or χ2 Fisher's exact test with pairwise z-test was used to compare the proportions across four groups. Bonferroni method was used to adjust *P*-value in multiple comparison.

a, b: Each subscript letter denotes a subset of ZP opening size groups whose proportion did not differ significantly from each other at the 0.05 level.

5.2.6 The *in vitro* implantation model from E5.5 to E8.5

5.2.6.1 Embryo hatching and attachment in the *in vitro* implantation model from E5.5 to E8.5

To investigate the hatching and attachment in embryos with delayed blastulation, I extended the *in vitro* culture of early blastocysts or unexpanded E4.5 blastocyst from E4.5 to E5.5; and collected the expanded or hatching E5.5 for transfer. Overall, 53 resulting E5.5 blastocysts were transferred into the *in vitro* implantation model, and 41.5% of them were hatching embryos. At the first 24 hours, 45% (24/53) of embryos fully hatched out, but extending the co-culture period to 48 hours [64.2% (34/53)] and 72 hours [64.7% (33/51)] did not significantly increase the percentages of fully hatched embryos (P>0.05). In contrast, the stably attached embryos increased significantly from 11.3% at 24 hours to 45.3% (24/53) at 48 hours. At 72 hours of co-culture, there were 64.2% (34/53) of embryos stably attached (**Figure 5-8**).

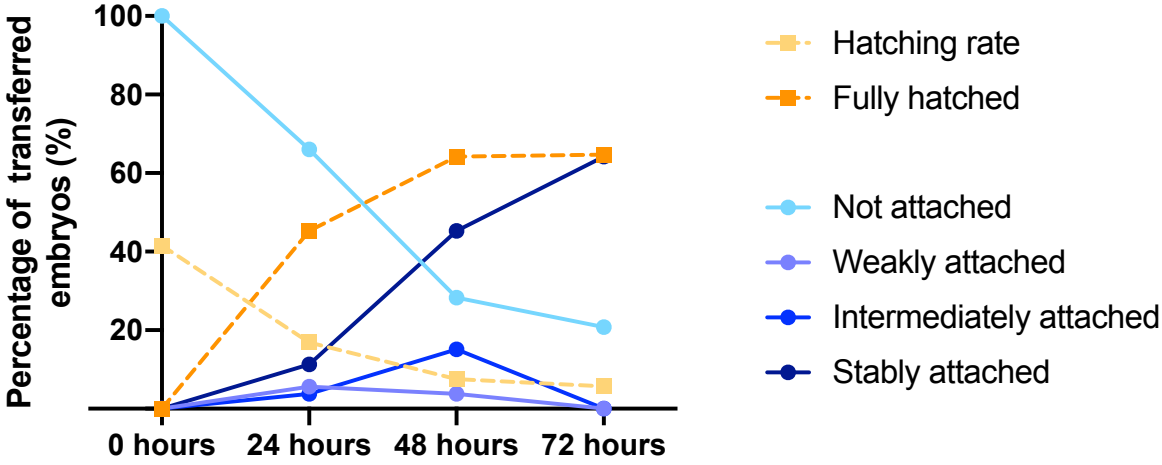


Figure 5-8. The mouse embryo hatching and attachment in the *in vitro* implantation model from E5.5 to E8.5

Embryos hatching statues (dashed line) and attachment stability (full line) were observed at 24h, 48h, and 72h of co-culture. The percentages of hatching (yellow) and hatched (orange) embryos, and the proportions of embryos with different degrees of attachment at different time-points were present.

5.2.6.2 A comparison of embryo hatching and attachment between E5.5 ET and E4.5 ET implantation model

When comparing E5.5 and E4.5 blastocysts transferring implantation model, the percentage of fully hatched embryos was significantly higher in E5.5 ET embryos at 24 hours post ET ($P<0.0001$). However, no difference of fully hatched embryos was shown at 72 hours. When counting the untreated embryos, a higher percentage fully embryos was shown in the E5.5 ET embryos at 24 hours ($P<0.05$); however, the percentages of fully hatched at 48 hours (56.3% vs 72.2%) and 72 hours (56.3% *vs* 77.8%) were substantially lower in the E5.5 embryos when compared with E4.5 ET embryos.

In addition, the percentage of stably attached embryos at 72 hours of co-culture were significantly lower among E5.5 ET embryos when compared with E4.5 embryos (64.2% *vs* 81.1%, $P<0.01$). The similar finding was shown in untreated embryos; a significant reduction in embryo attachment was also found in the E5.5 untreated embryo at 72h of co-culture (50% *vs* 83.3%, $P<0.05$) (**Figure 5-9**).

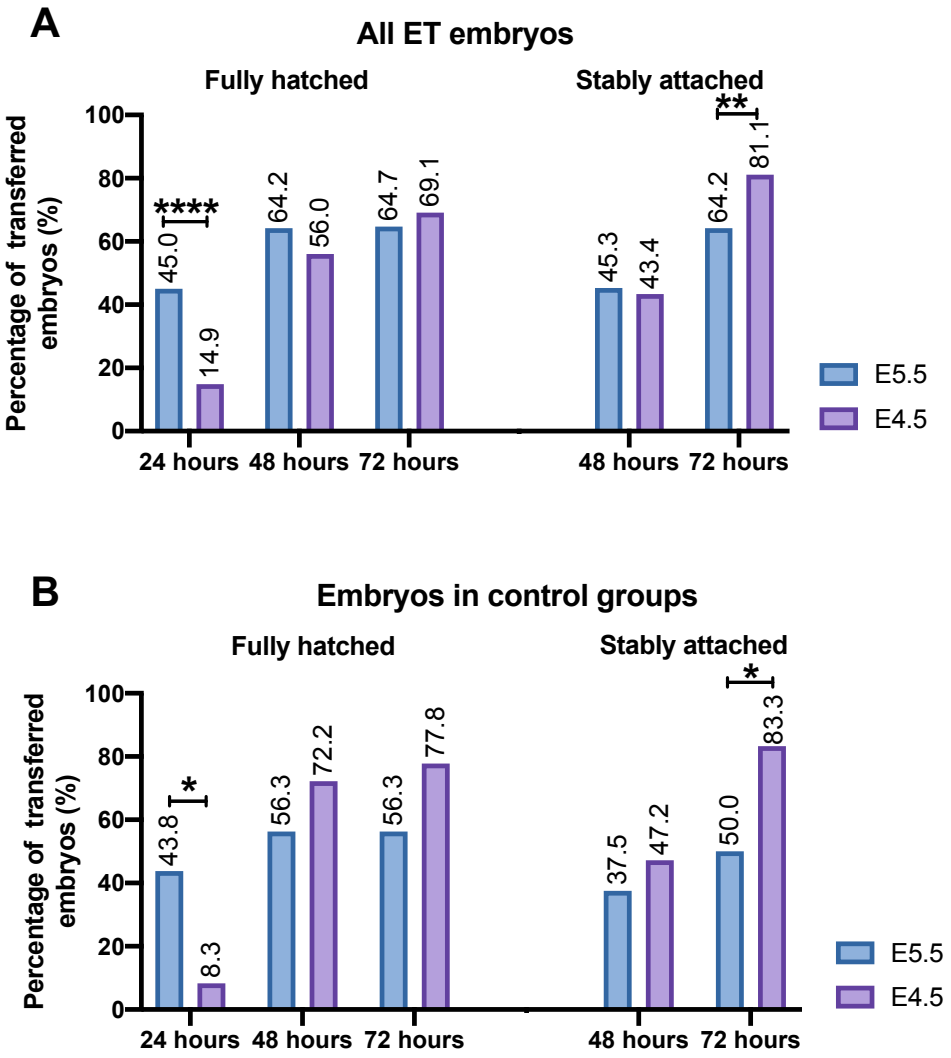


Figure 5-9. A comparison of embryo hatching completion and attachment between E5.5 and E4.5 transferred embryos

The percentages of fully hatching and stably attached embryos were compared between the E5.5 ET and E4.5 ET implantation model in all ET embryos (A) and the untreated embryos in the control group (B) at 24h, 48h, and 72h of co-culture. Statistical analysis was carried out using the Chi-Squared or Fisher's exact test (****P<0.0001; **P<0.01, *P<0.05).

5.2.6.3 The effects of different laser ZP manipulations on *in vitro* embryo hatching and attachment of blastulation delayed embryos

E5.5 blastocysts from laser ZP drilling (n=11), partial drilling (n=16), ZP thinning (n=10), and control groups (n=16) were transferred into the co-culture system. As shown in **Table 5-4**, at 24 hours of co-culture, the percentage of fully hatched embryos was slightly higher in the ZP drilling group [63.6% (7/11)] compared to other three groups. In addition, more embryos hatched out in the ZP drilling [81.8% (9/11)] and ZP thinning groups [80% (8/10)] at 48 hours and 72 hours, compared with control groups [56.3% (9/16)]. Extending the co-culture duration to 72 hours did not increase the number of hatched embryos in each group. Due to the limited sample size, these differences did not reach statistical significance (P>0.05).

In terms of embryo attachment, there was a statistically significant difference among the four groups during the first 24 hours of co-culture (P=0.045), with more embryos stably attached in the ZP drilling group (36.4% (4/11)). In addition, at 72 hours of co-culture, the proportion of attached embryos was significantly higher in the laser ZP drilling group when compared with control groups (100% (11/11) *vs* 50% (8/16), P=0.004). Furthermore, the stability scores were also substantially higher in laser ZP drilling and thinning groups (**Appendix 5 Fig S.3-B**). When counting the number of fully hatched embryos at 72 hours of co-culture, no difference was found across four groups; all hatched embryos in treatment stably attached to the Ishikawa cells, but 11.1% of the hatched embryos in the control group failed to stably attach (**Table 5-4**).

Table 5-3 A comparison of *in vitro* embryo hatching and attachment across different laser ZP manipulation groups from E5.5 to E8.5

		ZP-drilling (n=11)	ZP-partial drilling (n=16)	ZP-thinning (n=10)	Control (n=16)	*P* * value
Fully hatched	24h	7 (63.6%)	5 (31.3%)	5 (50%)	7 (43.8%)	NS
	48h	9 (81.1%)	8 (50%)	8 (80%)	9 (56.3%)	NS
	72h	9 (81.8%)	9 (56.3%)	8 (80%)	9 (56.3%)	NS
Trapped	72h	1 (9.1%)	1 (6.3%)	0	1 (6.3%)	NS
Stable attachment	24h	4 (36.4%)	1 (6.3%)	0	1 (6.3%)	0.045
	48h	6 (54.5%)	6 (37.5%)	6 (60%)	6 (37.5%)	NS
	72h	11 (100%) **a**	9 (56.3%) **a,b**	8 (80%) **a,b**	8 (50%) **b**	0.006
Fully hatched and attached	72h	9 (100%)	9 (100%)	8 (100%)	8 (88.9%)	NS

***** χ2 test or χ2 Fisher's exact test with pairwise z-test was used to compare the proportions across four groups. Bonferroni method was used to adjust *P*-value in multiple comparison.

a, b: Each subscript letter denotes a subset of laser ZP manipulation groups whose proportion did not differ significantly from each other at the 0.05 level.

5.3 Discussion

5.3.1 General summary of main findings

In this chapter, for the first time, the effects of different laser ZP manipulations on embryo hatching completion and attachment capability were investigated using a well-established Ishikawa cell *in vitro* implantation model. These preliminary data here suggest that embryos subjected to laser ZP drilling exhibited delayed hatching completion and an increased risk of entrapment. Such entrapment was more commonly seen in the 5μm opening size groups but was less frequent when the size increased to 10 μm, thus suggesting that small openings in the ZP may induce embryo entrapment. Moreover, in terms of embryo implantation, all three of the laser ZP manipulations tested resulted in a similar level of embryo attachment to epithelial cells compared with the control group when transferring E4.5 blastocysts.

In comparison with the normally developed embryo (E4.5 blastocysts), blastulation-delayed embryos (E5.5 blastocysts) showed damaged hatching completion and reduced embryo attachment. Interestingly, both laser ZP drilling and ZP thinning substantially facilitated the hatching completion of blastulation-delayed embryos. Moreover, laser ZP drilling promoted the attachment of these delayed blastocysts.

5.3.2 The establishment and confirmation of *in vitro* embryo implantation

The initial stages of embryo implantation have been classified as apposition, adhesion, and invasion (Weimar et al., 2013). However, apposition and early attachment to the uterine epithelium, owing to their tenuous and transient nature, are complicated

processes to capture *in vivo* in humans and animals (Enders, 2000). Similar to previous studies (Singh et al., 2010, Ruane et al., 2017), in this study, by combining a categorical scale of blastocysts attachment with microscope analysis, I was able to track the progression of embryo implantation, starting from weak reversible attachment (weak and intermediate attachment) to stable irreversible attachment (stable attachment). This evaluation system is more likely to reflect the progressive degree of embryo adhesion to epithelial cells.

A previous study claimed that mouse blastocysts were competent for stable attachment from E5.5; the stable attachment peaked at E6.5, and extending the co-culture to E7.5 did not lead to a further increase in the attachment (Ruane et al., 2017). Similarly, in this present study, stable embryo attachment could be observed from 48h of co-culture. However, I found that the highest proportion of stably attached embryos was presented at E7.5. This inconsistency may be due to the difference in transferred embryos: In the previous study, *in vitro*-matured, chemically hatched mouse E4.5 blastocysts were transferred directly (Ruane et al., 2017). Whereas in the present study, in order to mimic the clinical situation, I transferred *in vitro*-matured E4.5 embryos without removing the ZP. This might delay the stable embryo attachment as the natural hatching process typically occurs during E4.5 to E7.5 *in vitro*. In addition, complete hatching from the ZP is not required for stable attachment, as some trapped embryos could also stably attach, with the hatched part of embryo cells attaching to Ishikawa cells. Similar findings were also confirmed in the human embryo (Ruane et al., 2020).

5.3.3 The effect of laser ZP manipulation on *in vitro* embryo attachment

Blastocyst attachment experiments based on common clinical applications were performed to reveal the effect of different laser-assisted ZP manipulations during the embryo attachment period. In the present study, a trend towards impeded hatching completion was observed in E4.5 ET embryos subjected to laser ZP drilling, manifested by the higher embryo entrapment rate in the *in vitro* implantation model. In **Chapter 4**, the time-lapse experiment indicated that although the spontaneously '8'-shape hatching embryos could breach ZP earlier, they failed to hatch out by the end of observation. In addition, I also observed that around 70% of the transferred embryos in '8'-shape ended up with entrapment in this *in vitro* model. Together with the higher incidence of '8'-shape hatching shown in laser ZP drilling groups shown in **Chapter 4, Section 4.2.2**, this manipulation was implicated with the increased risk of blastocyst entrapment, which is consistent with previous studies (Cohen et al., 1991, Mantoudis et al., 2001, Chailert et al., 2013). One possible explanation was that the hatching process is restrained by the small opening in the ZP created by drilling; however, no consensus has been reached regarding the minimum size of the opening in the ZP. Cohen J et al.(1991) first showed that embryos with narrow incisions in the ZP (<10 μm) rarely hatch out completely, whereas embryos with medium-sized holes created (11-25 μm) could complete hatching as frequently as control embryos (Cohen et al., 1991). However, Montag et al (1999) suggested that a minimum ZP opening size of 12-15 μm, induced by laser ZP drilling, should be applied to mouse embryos (which is approximately double the diameter of the ZP), in order to allow the efficient hatching (Montag et al., 1999). This was contested by Chailert *et al.*'s data, which suggested

an even larger ZP opening (>20 μm) was needed to facilitate the completion of blastocyst hatching *in vitro* (Chailert et al., 2013). Consistently, Schimmel et al. confirmed that laser-assisted ZP drilling, creating a 25 μm ZP opening, could increase the frequency of fully hatched mouse embryos and shorten the hatching process (Schimmel et al., 2014).

The opening size of the ZP is of significant concern when performing the pre-hatching for TE biopsy (Aoyama et al., 2020). It is not surprising that a large opening size may facilitate the completion of embryo hatching; however, the small ZP opening can be beneficial for biopsy purposes, which advances embryo hatching and causes TE herniation on Day 5. This advanced TE herniation helps embryologists to arrange a working routine; it facilitates the biopsy procedure by thinning the TE area of the cut plane, which producing less constriction of hatching site for micro-cutting (Davidson et al., 2019, Aoyama et al., 2020). As mentioned in **Chapter 3**, drilling a ZP opening smaller than 15 μm on Day 3 and 4 embryos was the most common AHpBP procedure in clinical practice; many clinics even drilled smaller than 10 μm opening in the ZP. Thus, in this study, I compared different opening sizes of mouse ZP ranging from 5 to 10 μm (equivalent to 10 to 20 μm in the human ZP). Results showed that a 5 μm opening further impeded hatching completion, but embryos with a 10 μm opening were less affected. However, the sample size is too small to detect the statical significance. Notably, embryo entrapment has rarely been reported in clinics since the embryos are left in culture for a shorter amount of time if not transferred immediately, meaning that embryologists would not be able to observe embryo entrapment (Rubino et al., 2020). Therefore, these results indicated the importance of refining the ZP drilling protocol for AHpBP. Further studies are warranted to define the optimal size of opening in the ZP using human embryos, especially in the case of biopsy.

Although laser ZP drilling affects the completion of embryo hatching, it seems that ZP drilling did not impact or improve the *in-vitro* attachment capability of embryos. However, considering that only fully hatched embryos could ultimately implant into the uterus, the final implantation/pregnancy rate was predicted to be lower after treated ZP drilling, especially with a small ZP opening. This may partially explain the clinical finding that laser drilling in Day 3 embryos caused poor outcomes when used for assisted hatching or pre-hatching prior to biopsy (Mantoudis et al., 2001, Primi et al., 2004, Rubino et al., 2020). In addition, as Hiraola et al revealed, the size of the ZP opening may have an impact on the clinical pregnancy outcomes; and the author found that drilling 50% of ZP opening showed better pregnancy results when compared with the 40 μm ZP opening and the control group (Hiraoka et al., 2008). Therefore, laser ZP drilling may have an adverse impact on pregnancy outcomes if creating a small opening; it is thus important to refine the ZP drilling protocol to avoid damaging the embryo's implantation competency.

Laser ZP thinning, with an extended ablation area, is performed to mimic the natural hatching process (Mantoudis et al., 2001). However, ZP partial drilling is a more conservative method that involves ZP thinning in one area. Previous studies found that laser ZP thinning is more effective than ZP drilling regarding the hatching completion (Blake et al., 2001, Mantoudis et al., 2001, Park et al., 2014). In contrast, in some other studies, ZP thinning resulted in a prolonged hatching period and disrupted the hatching process compared with ZP drilling (Chailert et al., 2013, Schimmel et al., 2014). However, in the present study, neither laser ZP thinning nor partial drilling caused any adverse impact or improvement on the hatching completion compared with the control group. Still, they did enable higher hatching completion rates compared to laser ZP drilling. This inconsistency between studies is mainly due

to variations in the extent of ZP thinning. The present data indicated that an extended (around a quarter of ZP circumference) or small area (7.5 μm) of ZP thinning did not affect hatching completion. However, no significant improvement was shown in terms of embryo attachment capability after ZP thinning or partial drilling compared to the control group, which corroborates with clinical findings that ZP thinning had no improvement on CPR, IR, or LBR (Baruffi et al., 2000, Çıray et al., 2005, Petersen et al., 2005, Frydman et al., 2006, Balakier et al., 2009, Lu et al., 2015).

5.3.4 Laser ZP manipulations and embryos with delayed blastulation

Although current extended culture practices improve blastocyst survival *in vitro*, clinical data suggested that both fresh and cryopreserved embryos which do not blastulate until Day 6 have lower pregnancy potential (Barrenetxea et al., 2005, Levens et al., 2008, Desai et al., 2016). However, it is unclear whether this is due to asynchrony between the embryo and endometrium, or due to impaired embryo quality, which diminishes the implantation competency (Richter et al., 2006b, Shapiro et al., 2008, Desai et al., 2016). This thesis showed that delayed blastulation embryos are implicated with reduced hatching completion and subsequent reductions in attachment capability. Therefore, the damaged embryo implantation competency may be responsible for the reduced pregnancy potential.

However, this difficulty in hatching might be rescued by laser-assisted hatching (either by drilling or thinning, but not by partial drilling); this was supported by the observation that ZP drilling is efficient at facilitating embryo hatching and attachment in the developmentally delayed E5.5 embryos. Previous clinical data support the notion that assisted hatching improves clinical outcomes when applied to Day 6 blastocysts

(Tucker, 1999, Wan et al., 2014) and even Day 7 blastocysts (Sagoskin et al., 2002). However, the ZP manipulations in my study were all performed at E2.5 (equivalent to Day 3 in the human embryo), which may not fully represent the clinical practice. In addition, the sample size for blastulation delayed embryos were very limited. Therefore, further large-scale investigations performing laser-assisted ZP manipulations on Day 6 blastocyst or developmentally delayed embryos are needed.

5.4 Limitations

The main limitation of this study is that the *in vitro* attachment assay used here may not fully recapitulate the *in vivo* condition since the hatching process and embryo attachment may vary between *in vitro* and *in vivo* conditions (Montag et al., 2000a). In addition, it was not possible to establish implantation and final pregnancy *in vitro*. However, this *in vitro* implantation model is not confounded by any maternal factors involved in blastocyst hatching or implantation. Furthermore, the *in vitro* model enabled the fate of embryos to be tracked after transferred and can be used to study the early stages of implantation, which cannot be achieved once embryos have been transferred to the uterus via in vivo experiments.

The other limitation is the limited sample size. The sample number in some experiments was not large enough. This was due to the unexpected COVID-19 pandemic, which caused a complete lockdown of the laboratory between March and September 2020, thus preventing further laboratory work.

5.5 Concluding remarks

In summary, the results presented in this chapter demonstrate that laser ZP manipulations do not affect the attachment capability of normally developed blastocysts. However, laser ZP drilling may pose a potential risk for blastocyst entrapment, which is related to the size of the opening in the ZP created by drilling; thus, affecting the competency of an embryo to undergo implantation. Nevertheless, laser ZP drilling may be beneficial for blastulation-delayed embryos by improving the damaged attachment capability. Taken together, these findings suggest that when performing laser ZP drilling, the size of the opening is an important factor that embryologist should take into consideration if hatching efficiency is to be improved. In addition, blastulation-delayed embryos may be an indication for laser-assisted hatching.

5.6 Key findings

- The Ishikawa cell and mouse blastocyst co-culture system is a good alternative *in vitro* model for studying hatching and the early stages of implantation
- For normally developed embryos, laser ZP drilling may impede hatching completion, which was implicated by the size of the ZP opening created by drilling. However, these laser ZP manipulations did not affect the embryo attachment capability
- For blastulation-delayed embryos, laser ZP drilling might facilitate embryo hatching and improve embryo attachment



Chapter 6

Revealing the mechanisms underlying mouse embryo hatching and the impact of laser ZP drilling on embryo gene expression by RNA sequencing

6.1 Introduction

Blastocyst hatching and implantation events are two sequential, critically linked, and rate-limiting events, for a prospective pregnancy. The failure of the embryo to hatch out from the ZP has been suggested as a possible cause for implantation failure which represents a major challenge in ART (Margalioth et al., 2006). The structure of the ZP is similar in most species (Green, 1997), but the hatching process is a highly intriguing biological phenomenon. Embryo hatching represents the result of a well-orchestrated sequence of increasing mechanical pressure, protease activation, dynamic cellular actin-based remodelling, and migration. In addition, hormones and growth factor secretion may also play a key role, and this physiological process may be controlled via cross-talk between embryos and the maternal uterus (Hill, 2001, Paria et al., 2002, Chen et al., 2005, Seshagiri et al., 2009, Seshagiri et al., 2016, Leonavicius et al., 2018) (**Figure 6-1**).

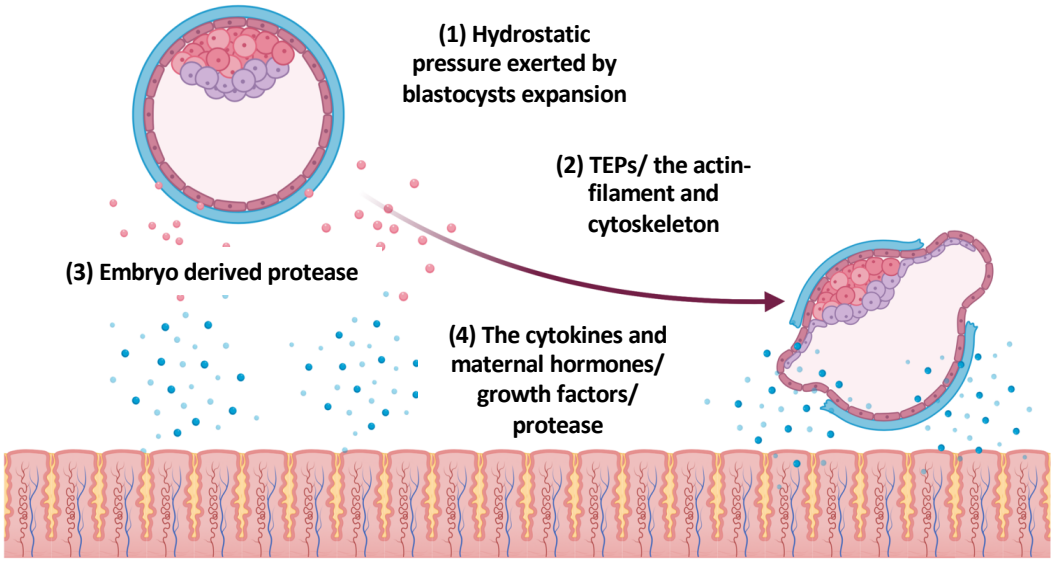


Figure 6-1. A hypothetical schematic for mechanisms underlying embryo hatching

This schematic shows four potential mechanisms underlying embryo hatching. The potential mechanical factors include blastocyst expansion-induced pressure, TEP (trophectodermal projections) formation, and the organisation of the cytoskeleton. The chemical factors could include embryo-derived protease and the regulation by cytokines, hormones, and growth factors.

In most mammals, including rodents, cattle, monkeys, and humans, blastocyst hatching is thought to be subjected to both mechanical and chemical factors (Seshagiri et al., 2009, Shafei et al., 2017). First of all, the ZP can be affected by the hydrostatic pressure exerted by the expanded blastocysts; subsequently, the ZP becomes stretched and thin (Kirkegaard et al., 2012, Leonavicius et al., 2018). Previous studies suggested that the formation of the blastocyst cavity is well regulated by active ion transport, aquaporin water channels (AQPs), and tight junctions, including tight junction proteins (TJPs), occludin, and claudins. The apical localisation of Na^+ channels and the basolateral distribution of Na^+/K^+-ATPases in the outer epithelial cell layer, together with tight junctions, increase the internal Na^+ osmolarity and establish a trans-trophectoderm (TE) osmotic gradient. AQPs are transmembrane channel proteins that function as molecular water channels thus allowing water to flow rapidly across the membrane in the direction of osmotic gradients. These established trans-TE osmotic gradients result in water transport and finally, cavity formation (Edashige et al., 2000, Barcroft et al., 2003, Watson et al., 2004, Moriwaki et al., 2007, Eckert et al., 2008). Trans-TE ionic gradients appear to be energized by the activity of Na^+/K^+-ATPases within the basolateral membrane domains of the TE, as the inhibition of Na^+/K^+-ATPases can block blastocyst formation *in vitro* (Watson et al., 2004). In addition, it has been demonstrated that the reduction of blastocyst cavity pressure, induced by Na^+/K^+-ATPase inhibition could also reduce the probability of hatching (Leonavicius et al., 2018).

The trophectodermal projections (TEPs) are the single, finger-like, F-actin enriched cytoplasmic outgrowths; and the formation of TEPs has been observed during the hatching process in many species (Gonzales et al., 1996, Seshagiri et al., 2009). The kinematics of the TEPs during hatching has been examined in previous studies,

indicating that TEPs participate in the hatching process and the initiation of embryo attachment (Seshagiri et al., 2009, Seshagiri et al., 2016). In addition, the organisation of the cytoskeleton, mostly relating to the actin-based modification (F-actin formation) in trophectoderm cells, was found to potentially take part in shaping the blastocyst to hatch from the ZP (Seshagiri et al., 2009, Lu et al., 2012). However, studies related to TEP biogenesis, embryo cell movement, and cytoskeleton organisation, are sparse. It is not yet clear which active molecules and related biological signaling pathways are involved in this process (Shafei et al., 2017).

Apart from the mechanical force, the enzymatic degradation of the ZP also plays an important role in the hatching process (Thomas et al., 1997). The inhibition of protease could lead to the complete blocking of embryo hatching following the addition of the inhibitor into the embryo culture medium (Seshagiri et al., 2009). However, different classes of protease, including serine proteases, cysteine proteases (cathepsin), and matrix metalloproteinases (MMP), are known to participate in the hatching process in different species (Shafei et al., 2017). For example, ISP (implantation serine protease), expressed in both preimplantation embryos and the endometrium, was reported to play a critical role in hatching and implantation in the mouse (O'Sullivan et al., 2004, Sharma et al., 2006). Meanwhile, the involvement of cathepsin in hatching has been well studied in the hamster, along with the synthesis of cathepsin L and P in blastocysts and localisation in the TEPs region during the hatching process (Sireesha et al., 2008). Apart from the proteases, a large number of cytokines (such as embryo-derived IL-6, GM-GSF, and IL-11), growth factors (HB-EGF and LIF), transcription factors (ERa and NFkB), and hormones (progesterone), have all been found participate in the regulation of hatching (Martin et al., 1998, O'Sullivan et al., 2004, Seshagiri et al., 2009, Shafei et al., 2017). However, the regulatory mechanism of

these maternal derived or embryo derived secretion on embryo hatching is still unknown.

The phenomenon of blastocyst hatching still remains as one of the least studied aspects of early mammalian development, despite the fact that it is of paramount importance in implantation and pregnancy. Therefore, it is necessary to examine hitherto unstudied signaling mechanisms that might regulate embryo hatching. The high-throughput transcriptomic assessment of peri-hatching and hatching embryonic stages blastocysts could provide interesting information regarding gene regulation.

RNA-sequencing (RNA-seq) is a type of next-generation sequencing technology that estimates the gene expression levels in the genome-wide study. With a high degree of accuracy, extension and affordability, RNA-seq has become the standard technology for transcriptomic analyses of genomics and is often used to analyse differential gene expression between samples (Nagalakshmi et al., 2010, Stark et al., 2019). The standard workflow of RNA-seq begins with RNA extraction, cDNA synthesis (or the cDNA can be directly synthesised from cell lysis without RNA extraction (Picelli et al., 2014)), and then the preparation of an adaptor-ligated sequencing library. Finally, the library is sequenced on a high-throughput platform (usually Illumina). After generating the raw data, the computation-based analysis is the final step. This includes aligning the sequenced reads to a transcriptome, quantifying the reads that overlap transcripts, filtering and normalizing between samples, and finally, statistical analysis of significant changes in the expression levels of transcripts between sample groups (Stark et al., 2019). The detailed workflow is shown in **Figure 6-2**.

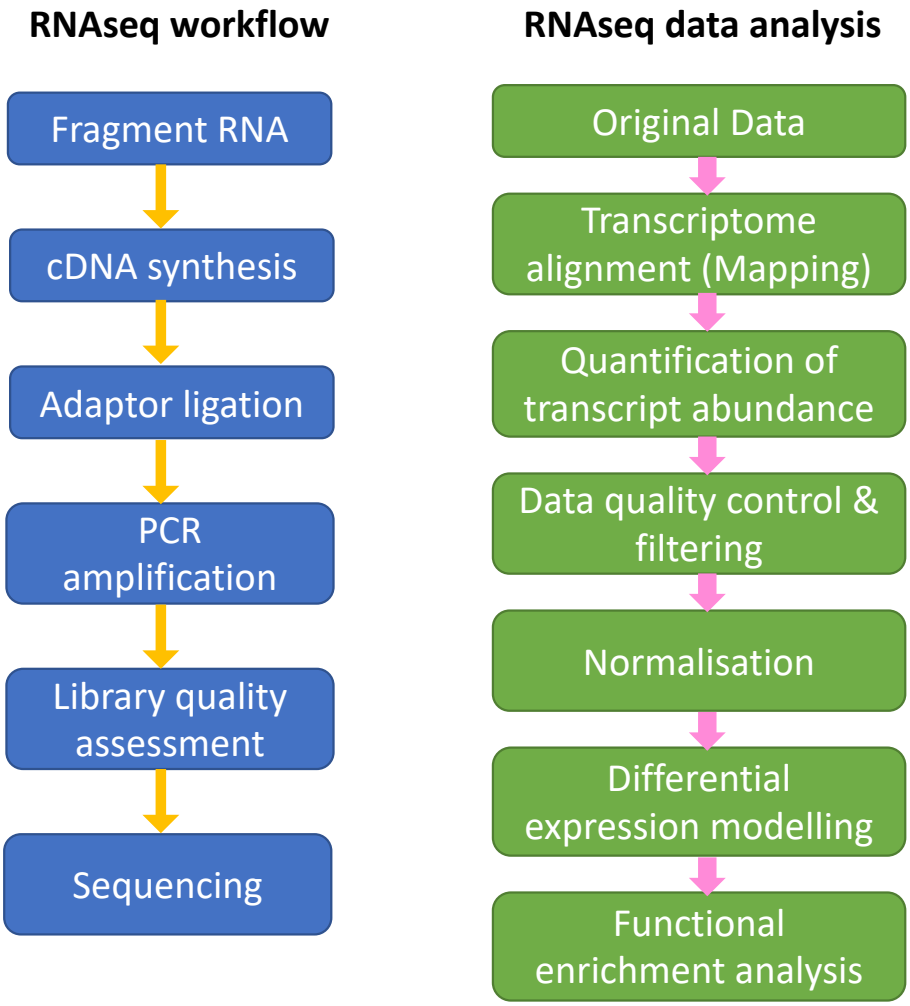


Figure 6-2. The workflow of RNA-sequencing (RNA-seq) and data analysis

The RNA-seq laboratory experiment (left side) begins with the cDNA synthesis from RNA fragmentation, followed by the preparation of an adaptor-ligated sequencing library. Following quality control, the library can be sequenced using different platforms (e.g., Illumina). Once raw RNA-seq reads have been generated, the computational analysis for differential gene expression (DEG) can proceed (right side): the first step is mapping the reads to a reference genome. Then, qualification tools are used for assigning reads to features. The quantified transcript counts are then filtered and normalized to remove low read abundance features and improve the detection of true differential expression. Once the sequence reads have been processed into an expression matrix, the experiment can be modelled to determine DEGs, and functional enrichment analysis can be performed.

With the development of microarray and RNA-seq, many studies have been performed to improve the understanding of the preimplantation embryo transcriptome in mouse (Hamatani et al., 2004, Wang et al., 2004), bovine (Mamo et al., 2006), and human

(Zhang et al., 2009). In addition, the advanced single-cell RNA sequencing technique (scRNA-seq) (Tang et al., 2009) has provided significant insights into transcriptional programs in embryogenesis (Guo et al., 2010, Xue et al., 2013), by revealing cell populations and uncovering regulatory relationships between genes. However, information concerning the genetic regulation involved in embryo hatching remains largely elusive.

Although many animal and human embryological studies have tried to study some of the mechanistic details regarding the embryo hatching, the specific genes and signalling pathways have yet to be determined. Therefore, in this chapter, by using RNA-seq, I aimed to investigate the transcriptional profile and downstream pathways that involved in the process of mouse blastocyst hatching. In addition, I aimed to determine the transcriptome alterations caused by laser-assisted ZP drilling on mouse embryo.

6.2 Method and materials

6.2.1 Sample preparation

Overall, four straws of frozen embryos (4x20 = 80 embryos) were used in the RNA sequencing experiment. After thawing (as described previously in **Chapter 2, Section 2.2.2**), embryos in each straw were randomised into the laser-assisted ZP drilling group (detailed in **Chapter 2. Section 2.3**) or the untreated control group. In total, 35 embryos were treated with laser ZP drilling, while 40 were untreated (control group). After 2 days in culture (detailed in **Chapter 2. Section 2.2.3**), pre-hatching blastocysts (expanded blastocysts) and hatching blastocysts were collected from the KSOM medium and washed three times by transferring embryos into three different drops of 0.01% PVA-PBS buffer. Then, the embryo was transferred individually into lysis buffer (0.8% (vol/vol) Triton X-100 and 2 U/µl of RNase inhibitor (both from Thermo Fisher, UK)).

6.2.2 Library preparation and RNA sequencing

For each sample, one blastocyst was lysed in 2.3 µL of lysis buffer in a 96-well PCR plate (AB0800W, Thermo Fisher, UK), and used for cDNA synthesis in Wellcome Centre for Human Genetics, Oxford. The SmartSeq2 method was used for cDNA synthesis (Picelli et al., 2014), and libraries were prepared using Nextera-XT. ERCC RNA Spike-in mix (4456740, ThermoFisher) was added at a dilution of 1/100,000. Amplified libraries were analysed for size distribution using the Agilent TapeStation High Sensitivity D1000 kit. Libraries were quantified using PicoGreen, and relative volumes were pooled accordingly. Sequencing was performed as 75bp paired-end reads on a HiSeq4000 according to Illumina specifications. These steps

were performed by technicians at the Wellcome Centre for Human Genetics, University of Oxford.

6.2.3 RNA-Seq data processing and quality control

RNA-seq reads were aligned to the mouse reference genome (GRCm38) using HISAT2 (Kim et al., 2015) and duplicate reads were removed using the Picard 'MarkDuplicates' tool [http://broadinstitute.github.io/picard]. Reads that mapped uniquely to Ensembl-annotated genes (~5 million per sample) were summarised using featureCounts (Liao et al., 2014). The raw gene count matrix was imported into the R/BioConductor environment(Gentleman et al., 2004) for further processing and analysis. Further RNA advanced quality control was conducted to test the similarity and distance between the sample library: (1) read assignment by category, (2) count metrics, (3) gene detection curve, (4) read biotype counts, and (5) sample clustering. Further steps included data normalisation and applying a filter to include only genes with a minimum of ten reads in at least 3 of the samples.

6.2.4 Differentially expressed genes (DEGs) analysis

The *edgeR* package (Robinson et al., 2010) was used to test for differentially expressed genes between hatching and pre-hatching blastocysts, and between natural hatching and laser-drilled blastocysts. This package combines the use of the trimmed mean of M-values as the normalisation method for count data, the empirical Bayes approach for estimating tagwise negative binomial dispersion values, and finally, generalized linear models and the quasi-likelihood F-test for detecting DEGs for the main effects of treatment and hatching stage. Embryo batch was included as an additional explanatory variable. Genes that were differentially expressed between

groups were extracted with appropriate contrasts for (i) hatching blastocyst *vs* pre-hatching blastocyst from the control group and (ii) hatching blastocyst from the laser drilling group *vs* hatching blastocyst from the control group. Raw *P*-values were adjusted for multiple testing using the Benjamini-Hochberg (BH) procedure (Benjamini et al., 1995) to control the false discovery rate at 5%. These RNA-seq data processes and bioinformatic analysis, from the annotation pf RNA-seq reads to DEGs analysis, were performed by Mrs Helen Lockstone (Wellcome Centre for Human Genetics, University of Oxford).

6.2.5 Functional enrichment analysis

DEGs were explored using Ingenuity Pathway Analysis (IPA, QIAGEN Inc) software for Core analysis, including Canonical Pathway Analysis and Upstream Regulator Analysis, based on the Ingenuity Pathway Knowledge Base (IPKB). In the results of the IPA analysis, the activation Z-score was computed to infer the activation states ('increased' or 'decreased') of implicated biological functions; the basis for this inference are edges (relationship) in the molecular network that represent experimentally observed relationship between genes and those functions.

In addition, Over Representation Analysis (ORA) is a widely used approach to determine whether known biological functions or processes are over-represented (=enriched) in an experimentally derived gene list (DEGs list) (Boyle et al., 2004). ORA was applied to identify enriched functional profiles among DEGs, including Gene Ontology (GO) analysis (Gene Ontology Consortium, 2004), Reactome pathway (Croft et al., 2010), Kyoto Encyclopedia of Genes and Genomes (KEGG) pathway (Kanehisa et al., 2016), and Wikipathway analysis. These enrichment analyses were performed in the R environment using the *ClusterProfiler* package (Yu et al., 2012). All

enrichment analyses were performed with right-tailed Fisher's Exact testing, and raw *P*-values were adjusted for multiple testing using the BH procedure. The categories and terms with an adjusted *P*-value <0.05 were considered as being significantly enriched. In addition, since GO analysis is organized in a parent-child structure, thus a parent term can be overlap with a large proportion with all its child terms. Thus, the redundant terms were removed by using the *simply* function in Clusterprofiler, and the representative terms were summarized.

6.2.6 Construction and analysis of the protein-protein network

In addition, the protein and protein interactions (PPI) networks corresponding to the DEGs was retrieved from the Search Tool for Retrieval of Interacting Genes (STRING) (*stringAPP*) database; this database provides known and predicted protein-protein association data, including both physical and functional proteins (Szklarczyk et al., 2016). Proteins in the interaction network were represented by nodes, and the interactions between two proteins were represented with edges. The confidence score cut-off value was set as 0.4 (at a confidence of 'medium' or better), so that the PPI networks were constructed when the confidence score was more than 0.4.

In addition, Molecular Complex Detection (MCODE) (Bader et al., 2003) was used to investigate the substructure of the PPI network extracted above and focused on the highly connected node (known as clusters). These clusters can represent proteins that interact with each other to form pathway-like interacting modules. Modules with nodes >4 were considered to further analysis. PPI network analyses were conducted using Cytoscape 3.8.0 software for visualization and editing (Shannon et al., 2003). All software programs, R packages, and related parameters, are listed in **Table 6-1.** The experiments and steps in this chapter are summarized in a flow chat (**Figure 6-**

3); the processes and steps framed in the purple dashed line were conducted by the Wellcome Centre for Human Genetics, University of Oxford.

Table 6-1 Software and parameters for processing RNA seq data

Analysis	Software	Parameter	Remarks
Mapping	HISAT2		Performed by Wellcome Centre for Human Genetics
Quantification	featureCounts		
Differential expression analysis	edgeR package	BH-adjusted P<0.05	
Canonical Pathway Analysis	IPA software	BH-adjusted P<0.05	Z score>2, predicted as activated
Upstream Regulator Analysis	IPA software	BH-adjusted P<0.05	Z score<-2, predicted as inhibited
Gene Ontology (GO) analysis	ClusterProfiler package	BH-adjusted P<0.05	Redundant terms were removed by '*Simply*'
Reactome pathway	ClusterProfiler package	BH-adjusted P<0.05	
KEGG pathway	ClusterProfiler package	BH-adjusted P<0.05	
Protein-protein interaction analysis	Cytoscape: stringAPP	Confidence score: 0.4	Medium confidence for predicting interaction
MCODE cluster	Cytoscape: MCODE plugin	Node density cutoff:0.2 K-score:2	For the pathway-like module

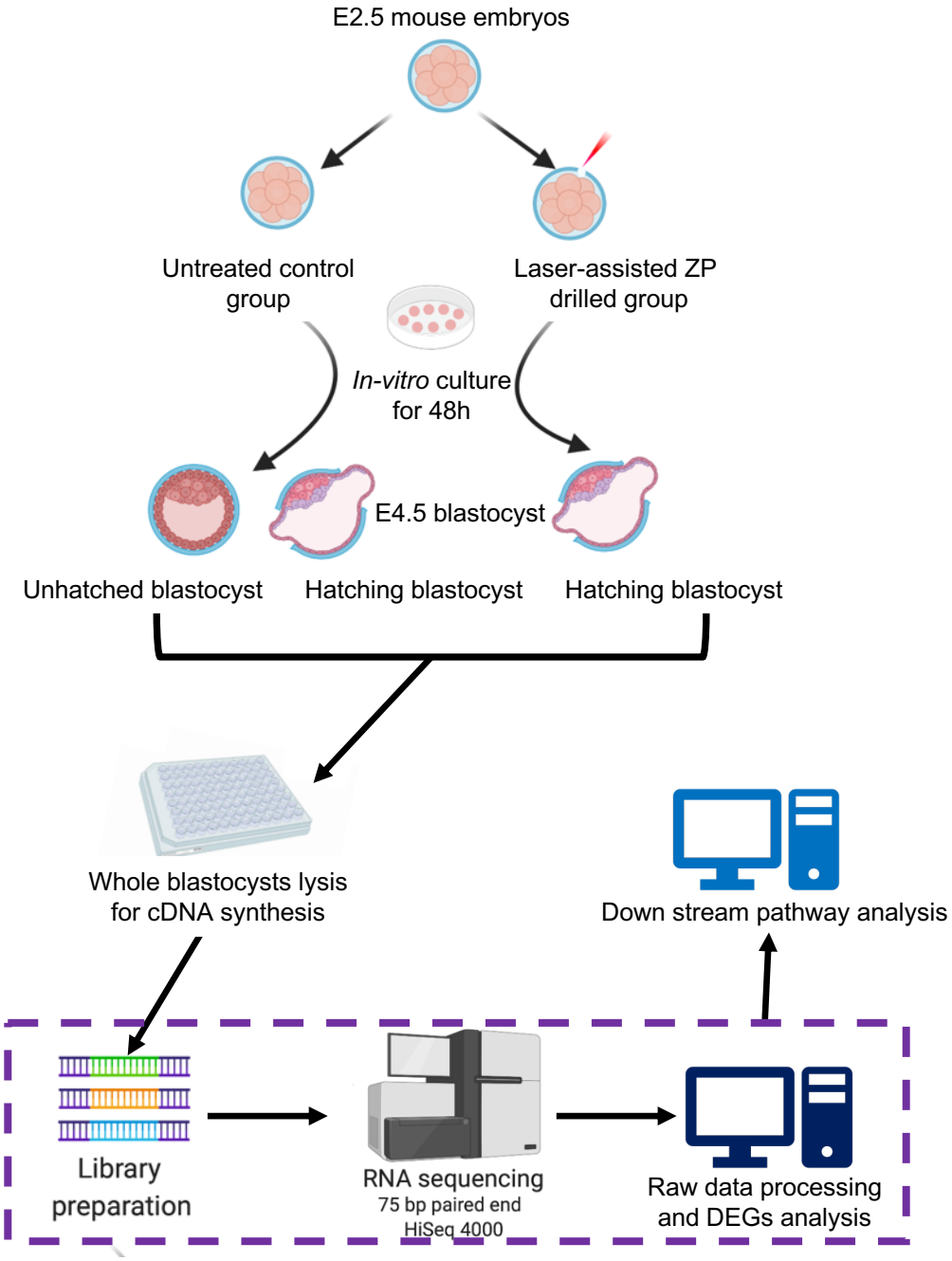


Figure 6-3. A flow-chat showing RNA-seq experiment processing

A flow-chat showing embryo preparation, sample grouping, RNA-seq sample processing, and data analysis. The steps that were processed by the Wellcome Centre for Human Genetics, University of Oxford, are emphasized in the purple dashed frame. Other steps were conducted by the author.

6.3 Results

6.3.1 Embryo sample collection

Overall, 91.4% (32/35) of laser-assisted ZP drilled embryos and 90% (36/40) of untreated embryos survived after 48 hours of *in vitro* culture. In addition, 84.38% (27/32) and 44.4% (16/36) of these surviving embryos were hatching embryos; while 6.35% (2/32) and 25% (9/36) were expanded blastocysts, respectively. Then, 8 blastocysts were randomly collected from each group (control hatching blastocysts, control pre-hatching blastocysts, and laser-drilled hatching blastocysts) (**Figure 6-4**). A total of 24 blastocysts were used for cell lysis and cDNA library preparation.

Table 6-2 Sample preparation for RNA-seq

	Untreated group	Laser-drilled groups	P value
Blastocyst	36 (90%)	32 (91.4%)	>0.9
Hatching blastocyst	16 (44.4%)	27 (84.4%)	0.0009
Expanded blastocysts	9 (25%)	2 (6.35%)	0.049

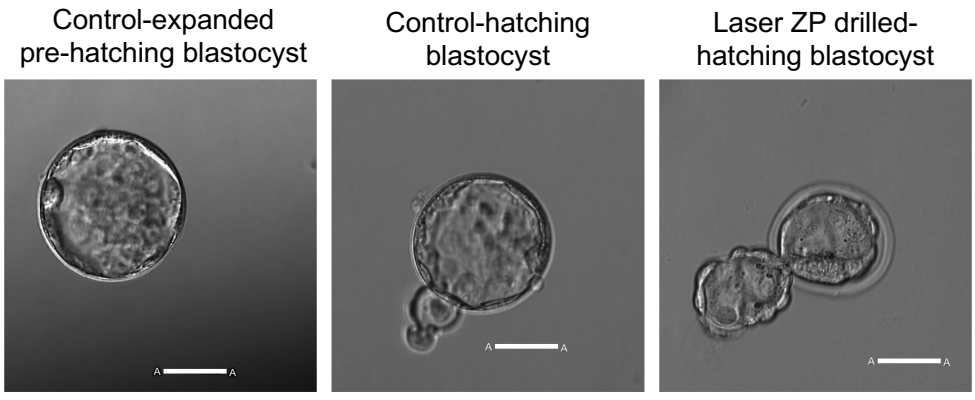


Figure 6-4. Representative images of blastocyst samples for RNA-seq

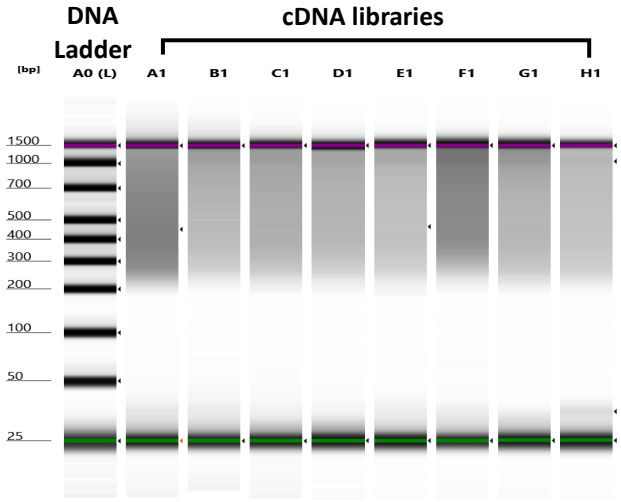
The representative images of the blastocyst samples in three groups used for RNA-seq analysis. Scale bar=50 μm (200× magnification).

6.3.2 cDNA library preparation and quality control

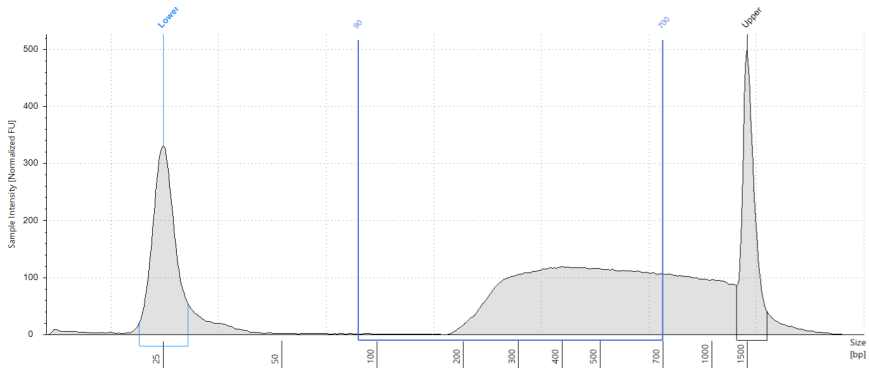
Before sending cell lysis for cDNA library preparation, I have tried to extract the RNA from individual embryos. However, the quantity and quality of the RNA extracted from single blastocysts were too low to perform library preparation (**Appendix 9**). An expert at the Wellcome Centre for Human Genetics suggested starting the Smart-Seq2 library preparation from whole cells rather than extracting the RNA as an alternative. Thus, I lysed a single blastocyst in 2.3 μL of lysis buffer (Picelli et al., 2014); the cell lysis was then processed to allow cDNA synthesis and library preparation (by Welcome Trust for Human Genetic Centre).

Finally, eight generated libraries were randomly picked from 24 experimental samples for QC assessment using an Agilent DNA 1000 bioanalyzer. The results indicated that the average size of the prepared libraries was around 400 bp, and that the concentration of libraries was 1.531 ± 0.56 ng/μL (laser-drilled group), 1.32 ± 0.41 ng/μL (control-hatching group), and 1.545 ± 0.64 ng/μL (control-pre-hatching group). These were then used for subsequent Smart-Seq 2 sequencing (**Figure 6-5**).

A



B



From [bp]	To [bp]	Average Size [bp]	Conc. [pg/µl]	Region Molarity [pmol/l]	% of Total
90	700	442	730	2840	67.71

C

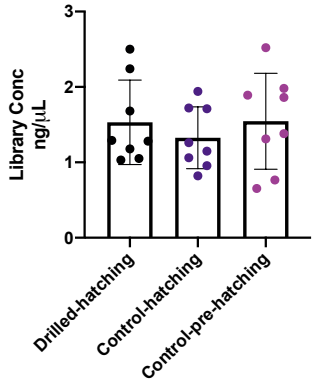


Figure 6-5. Quality control assessment of resulted cDNA library

The amplified cDNA libraries were assessed using the Agilent TapeStation High Sensitivity D1000 kit with high sensitivity RNA Screen Tape. (A) Electropherograms of the eight cDNA libraries. The first lane on the left is an electronic DNA ladder. (B) Agilent Bioanalyzer analysis of column A1, showing that the average size of the fragment was 442 bp. (C) the libraries were quantified by PicoGreen Fluorometry. The concentrations of cDNA are presented as mean ± SD.

6.3.3 RNA sequencing data quality control

Further RNA sequencing data advanced quality control was conducted to test the similarity and distance between library samples from different aspects. The first quality control results with all 24 samples indicated that two samples (Control_pre-hatching_4_4 and control_pre-hatching_2_7) were outliners compared with the rest of the samples. The reads assignment by category of these two outliers showed low reads count assigned to genes; Spearman correlation and PCA (Principal component analysis) results indicated the farthest distance of these two outliers from other samples (**Figure 6-6 A**). Thus, these two samples (Control_pre-hatching_4_4 and control_pre-hatching_2_7) were excluded. Finally, eight control-hatching samples, eight laser drilled-hatching samples, and six control-pre-hatching samples, were processed before another round of QC assessment (**Figure 6-6 B**). A relatively clear segregation of hatching blastocysts and pre-hatching blastocysts was shown by the PCA analysis, reflecting the differential gene expression patterns observed with the hatching statues. Meanwhile, the laser-drilled hatching blastocyst samples did not separate from the control hatching blastocyst samples, thus indicating the low level of gene expression changes; this was highly consistent with the DEGs analysis described in the next section (**Figure 6-6 B-3**).

After normalisation of the data and filtration of the genes with very low expression, a total of 10861 assigned genes passed the filter criteria and were used for differentially expressed gene analysis.

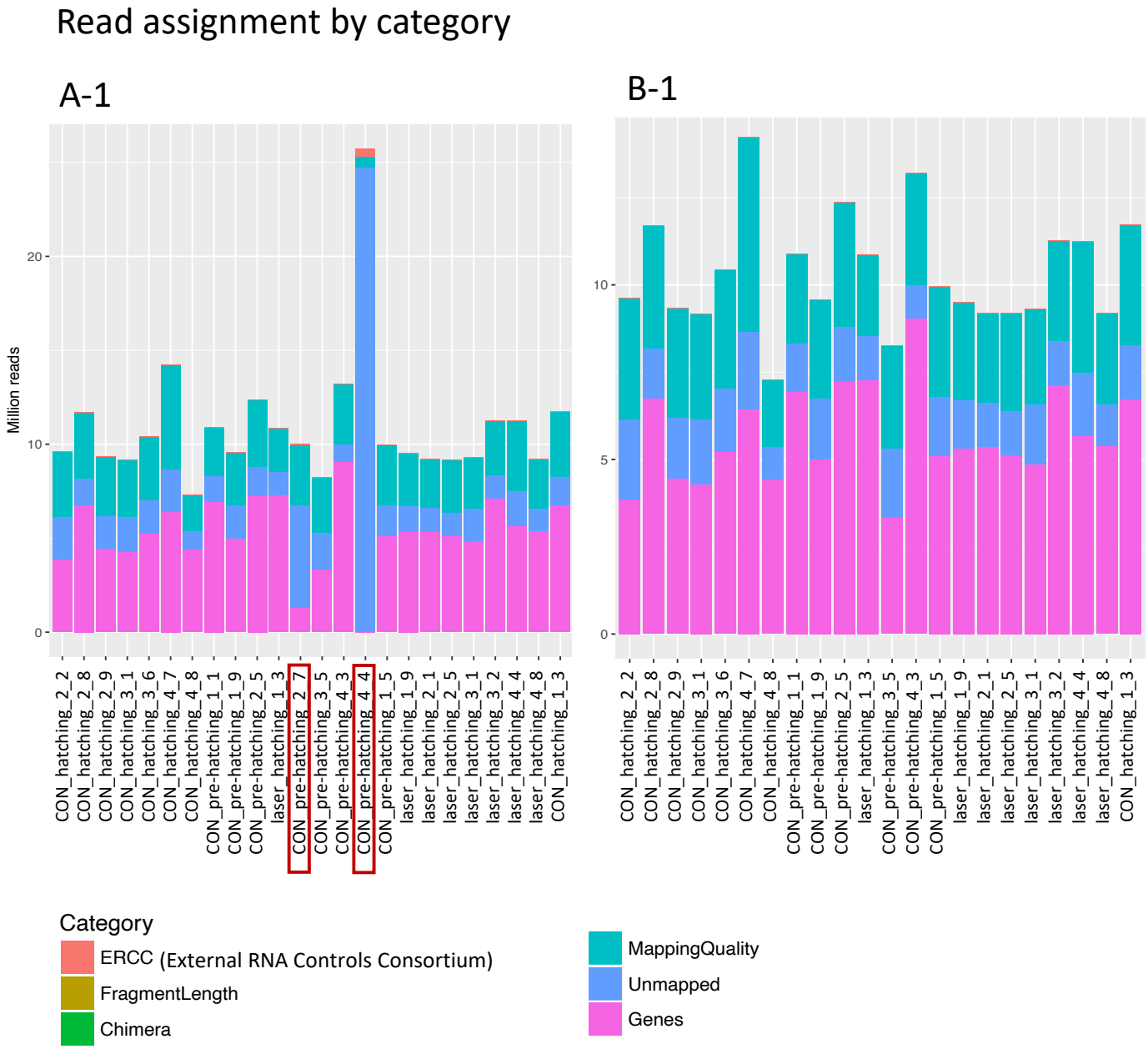


Figure 6-6 (Continued on next page, legend follows)

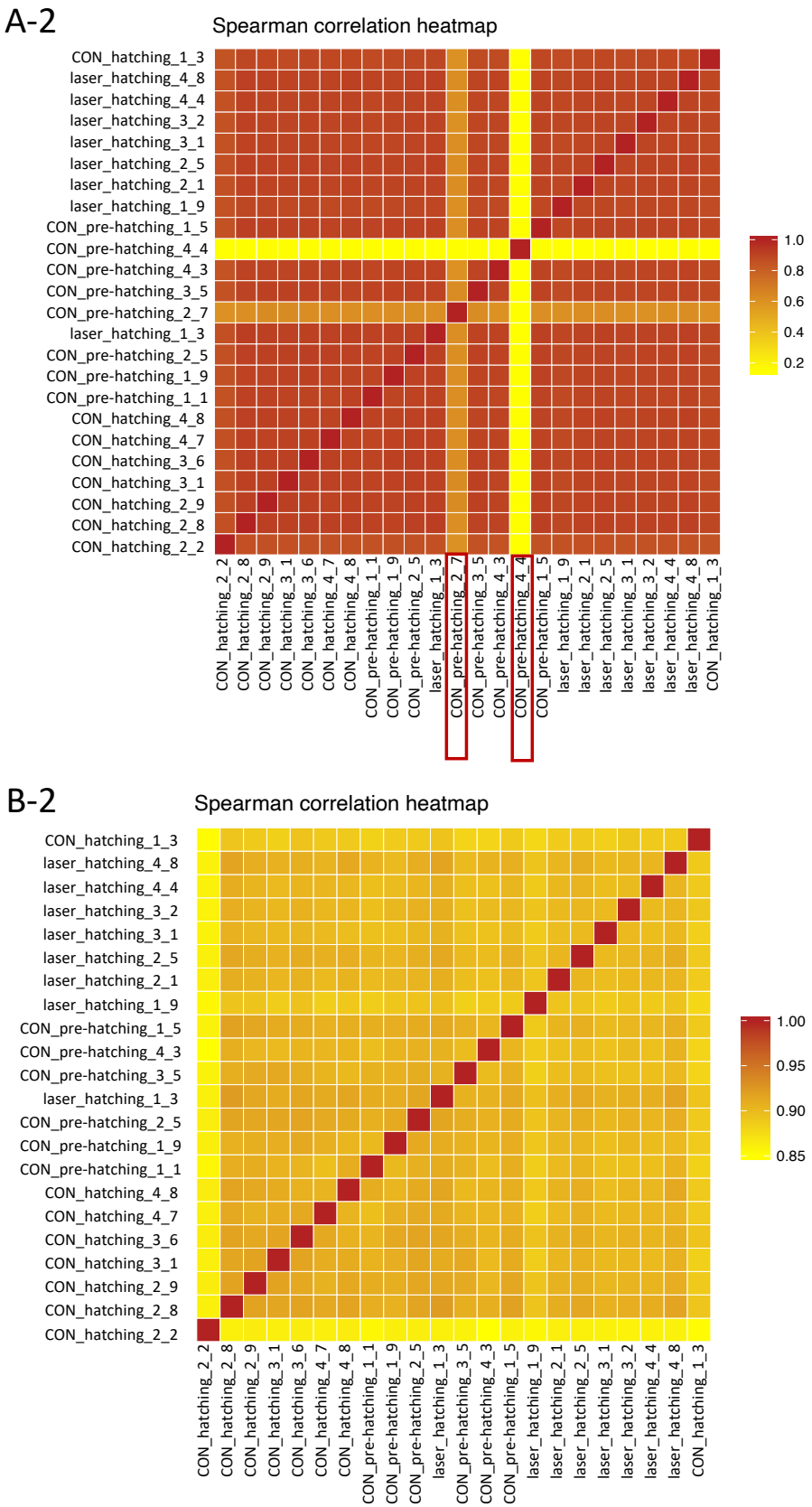
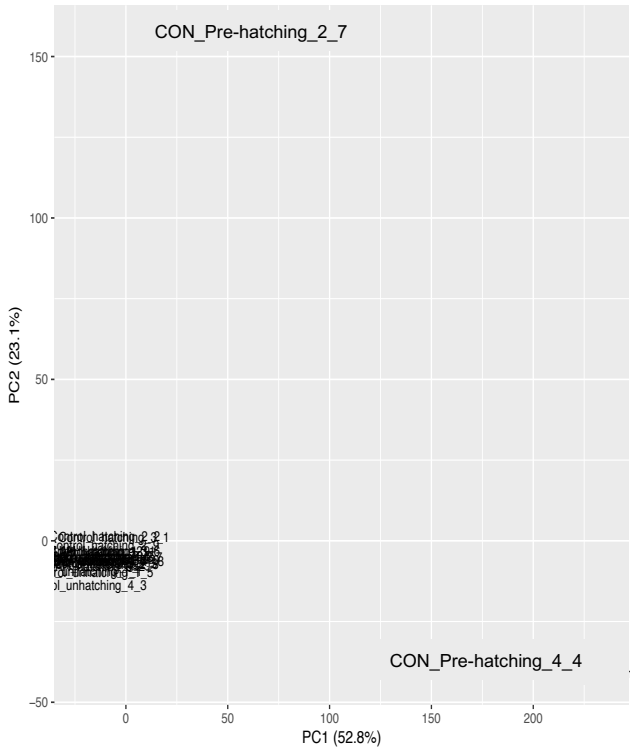


Figure 6-6 (Continued on next page, legend follows)

A-3



B-3

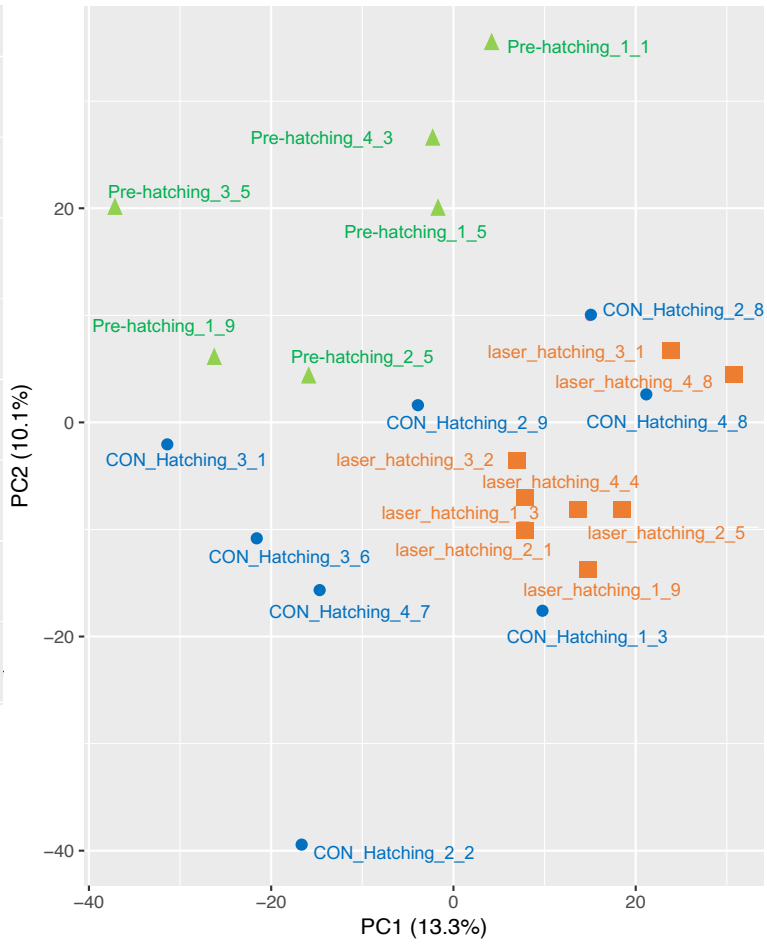


Figure 6-6. Advance quality control results of RNA-seq data from all samples (A) and samples excluding the outliners (B)

The RNA sequencing data was assessed from different perspectives, including (1) the read assignment by category; (2) Spearman's correlation; (3) and PCA (principal component analysis). For the name of each sample: the 'CON_hatching' indicates hatching blastocyst in control group; the 'CON_pre-hatching' indicates expanded pre-hatching blastocyst in control group; and 'laser_hatching' indicates the hatching blastocyst in laser-assisted drilling group. The first and second number represents the straw and embryo number, respectively. Figures generated by Wellcome Centre for Human Genetics.

6.3.4 A comparison of hatching blastocysts and pre-hatching blastocysts from the control group

6.3.4.1 Differential gene expression analysis

Differential expression analysis was used to determine the genes that showed statistically significant differential expression. Alterations in the blastocyst transcriptome at the hatching stage was analysed by comparing hatching blastocysts *vs* pre-hatching blastocysts in control group. Overall, 274 genes were found to be differentially expressed (with BH adjusted $P<0.05$), of which 230 genes were up-regulated, and 44 genes were down-regulated. A volcano plot was used to indicate the overall distribution of differentially expressed genes (DEGs) (**Figure 6-7**). As it shown, the absolute fold changes for these DEGs were relatively small; most of the DEGs were smaller than 2 (logFC <1). **Table 6-3** presents the top 10 genes among the upregulated and downregulated genes, with the largest fold changes.

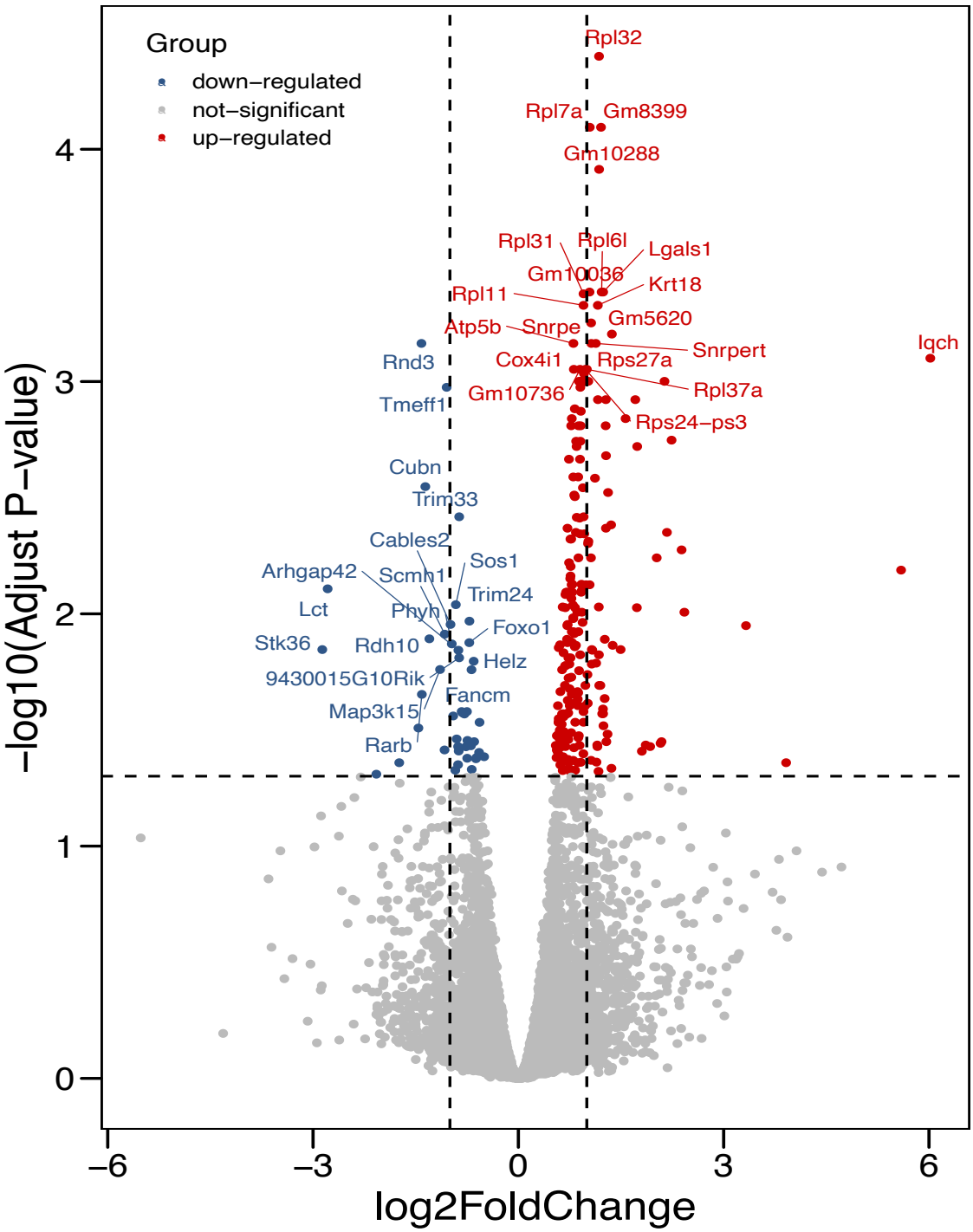


Figure 6-7. Differentially expressed genes (DEGs) between the hatching and pre-hatching blastocysts in the control group

A volcano plot for DEGs: the x-axis shows the fold change in gene expression between samples, and the y-axis shows the statistical significance of the differences. The significantly up- and downregulated genes are highlighted in red and blue, respectively. Top 20 upregulated and downregulated genes by adjusted *P* value are marked by gene name. Gray points represent non-significant DEGs.

Table 6-3 The top 10 upregulated and downregulated DEGs between hatching and pre-hatching blastocysts in the control group

	Gene	logFC	logCPM	adj *P*-value	Description
Upregulated genes	*Iqch*	6.02	0.47	7.9E-04	IQ motif containing H
	Ppef1	5.59	0.13	6.48E-03	protein phosphatase with EF hand calcium-binding domain 1
	Mael	2.17	4.29	4.46E-03	maelstrom spermatogenic transposon silencer
	Sept9	2.14	3.91	9.98E-04	septin 9
	Krt7	1.57	7.63	1.4E-3	keratin 7
	Spry1	1.36	3.64	0.046	sprouty RTK signaling antagonist 1
	Ctsh	1.29	3.25	0.036	cathepsin H
	Hist1h2ag	1.24	4.17	0.03	histone cluster 1, H2ag
	Lgals1	1.24	11.18	4.1E-04	lectin, galactose binding, soluble 1
	Rpl32	1.18	10.40	3.98E-05	ribosomal protein L32
Downregulated genes	*Stk36*	-2.87	1.05	0.014	serine/threonine kinase 36
	Lct	-2.79	2.13	7.8E-5	lactase
	Bend5	-2.07	1.58	0.049	BEN domain containing 5
	Mfap4	-1.74	2.51	0.044	microfibrillar-associated protein 4
	Dusp18	-1.46	3.01	0.031	dual specificity phosphatase 18
	Rnd3	-1.42	5.78	6.8E-4	Rho family GTPase 3
	Rarb	-1.41	3.64	0.022	retinoic acid receptor, beta
	Cubn	-1.36	4.74	2.8E-3	cubilin intrinsic factor-cobalamin receptor
	Rdh10	-1.30	3.76	0.013	retinol dehydrogenase 10
	Map3k15	-1.14	4.16	0.017	mitogen-activated protein kinase 15

6.3.4.2 GO (gene ontology) term enrichment analysis of DEGs

With regards to GO terms, the DEGs between hatching and pre-hatching blastocysts were enriched in 14 cell components terms (GO:CC), 33 biology process terms (GO: BP), and 18 molecular function terms (GO:MF). As shown in **Figure 6-8**, GO: BP terms clustered into three main modules, including ribosome biogenesis and cytoplasmic translation, ATP (adenosine triphosphate) metabolic process and ATP synthesis coupled proton transport, and regulation of cytoskeleton organisation and actin polymerization. The genes enriched in the cytoskeleton regulation include the upregulated *Actb* (Beta-actin), *Myl6* (Myosin, light polypeptide 6), *Gsn* (Gelsolin), *Pfn1* (Profilin 1), *Cfl1* (Cofilin 1), *Arpc2* (Actin related protein 2/3 complex subunit2), *Tmsb10* (Thymosin, beta 10), *Tpi* (Triosephosphate isomerase 1), *Shmt1* (Serine hydroxymethyltransferase 1), *and Ldlrap1* (Low density lipoprotein Receptor Adaptor Protein 1)*;* and the downregulated *Rnd3* (Rho Family GTPase 3: a negative regulator)*, Grb2* (Growth factor receptor-bound protein 2)*,* and *Enah* (Enabled actin regulator).

GO:MF terms enrichment maps suggested that there were 10 functional terms clustered around the proton transmembrane transporter activity; and 13 DEGs were related with this functional term, including 9 ATP synthase coding genes (*Atp5b, Atp5k, Atp5c1, Atp5pb, Atp5a1, Atp5o, Atp5g2, Atp5h,* and *Atp5g1*) and 4 cytochrome C oxidase coding genes (*Cox4i1, Cox8a, Cox7c,* and *Cox7a2*).

Enrichment maps showed that GO:CC terms were clustered around cytosolic ribosome and ATP synthase complex. Interestingly, the term of podosome was significantly enriched in three DEGs (*Actb (Beta-actin), Gsn (Gelsolin),* and *Arpc2 (Actin related protein 2/3 complex subunit2)*). In addition, the term of keratin filament was enriched in *Krt18* (Keratin 18), *Krt7*(Keratin 7), and *Krt8* (Keratin 8) (**Figure 6-8**).

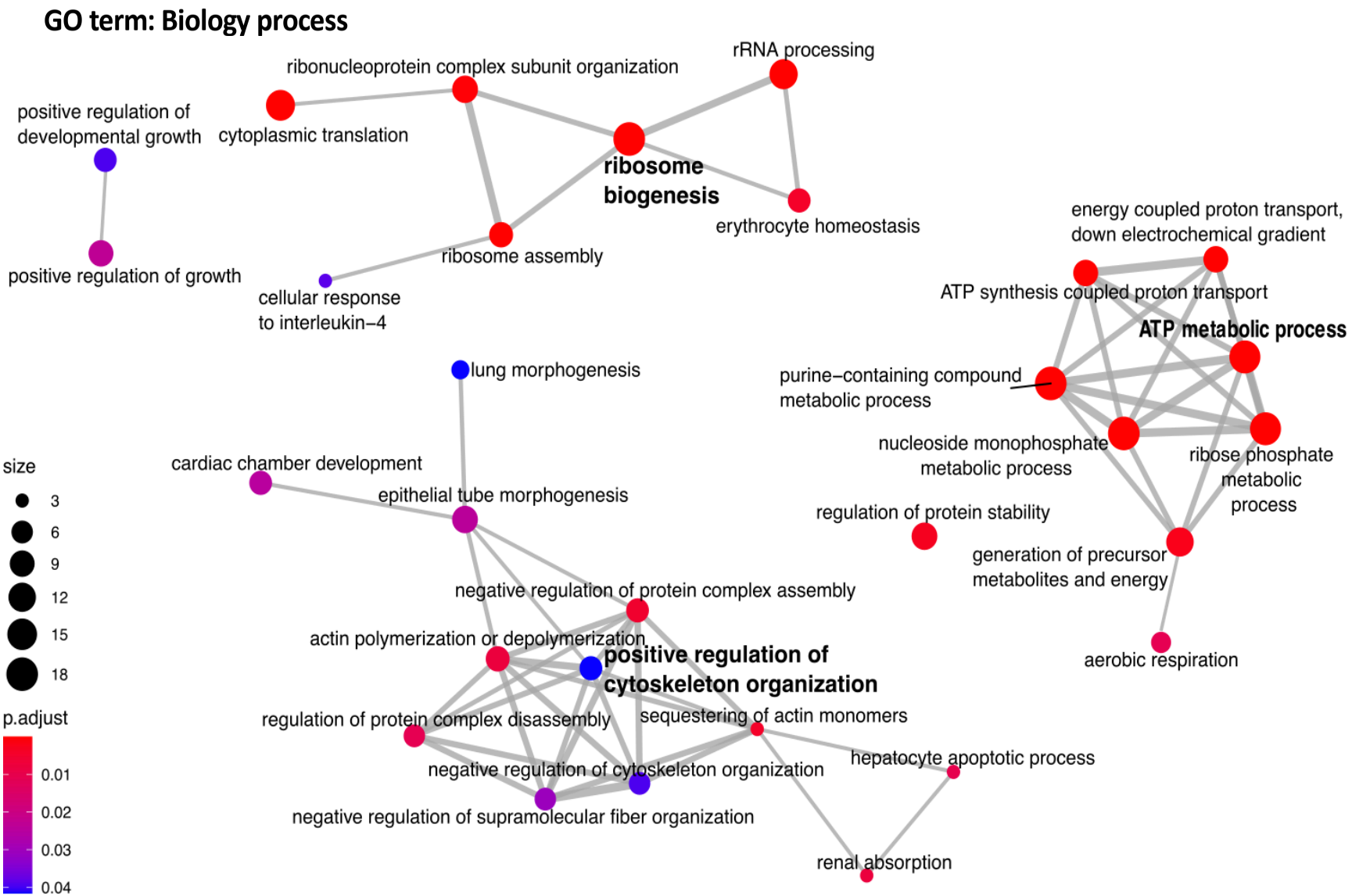


Figure 6-8 (Continued on next page, legend follows)

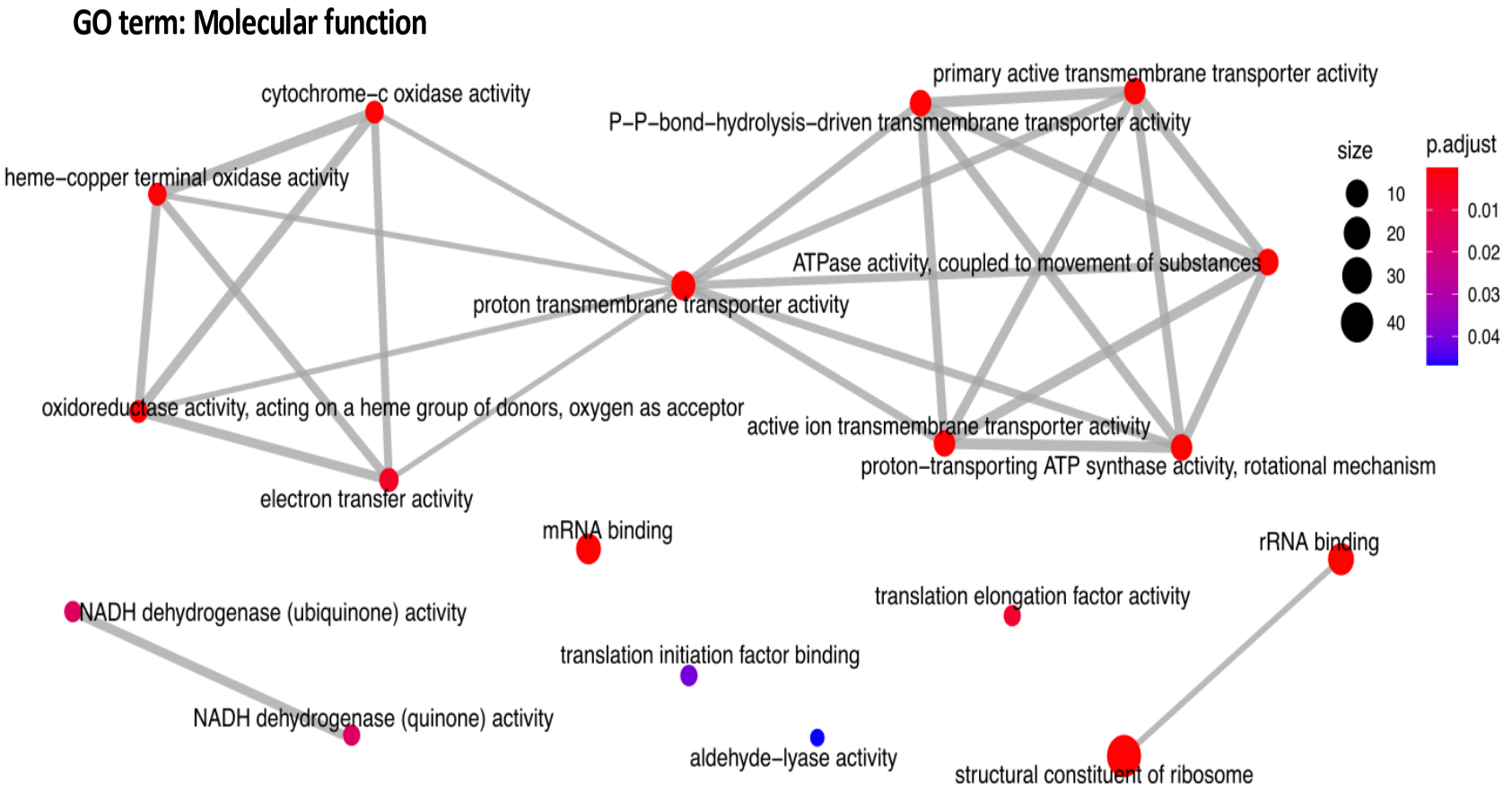


Figure 6-8 (Continued on next page, legend follows)

GO term: Cellular component

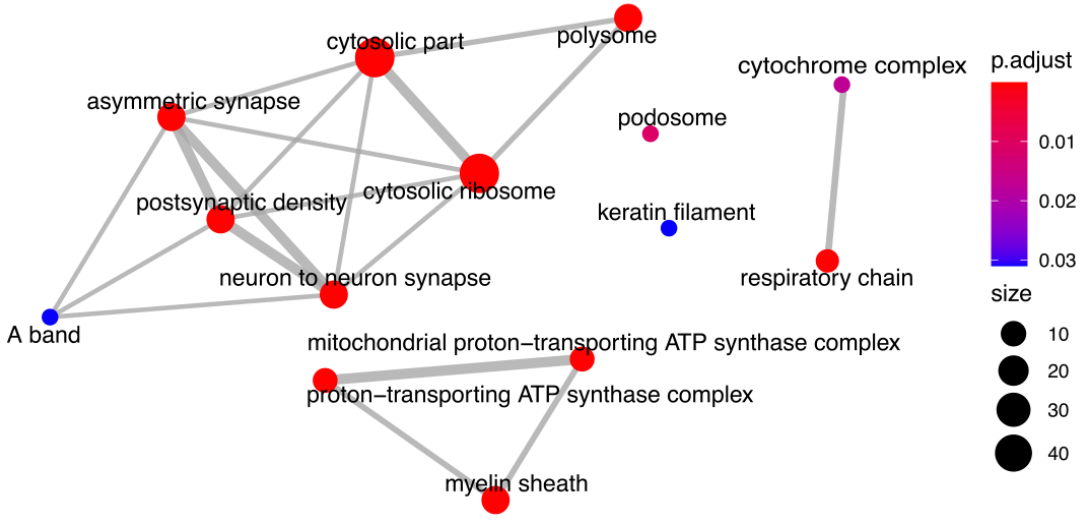


Figure 6-8. The Gene Ontology (GO) analysis of differentially expressed genes (DEGs) between hatching and pre-hatching blastocysts in the control group

The annotation-term network of DEGs includes biological process (BP), molecular function (MF), and cellular component (CC) terms. GO term enrichment analysis was performed using *clusterProfiler*. These enriched terms are represented as separate nodes and organized into a network with edges connecting overlapping gene sets. The node sizes represent the gene numbers, and the term enrichment significance is represented by the colour (adjusted *P* value). Figures were obtained from *emapplot* function in *clusterProfiler* by the author.

GO terms analysis indicated that embryo hatching is an ATP consuming process, which involves active cytoplasmic translations, proton transmembrane transporter activity, and cytoskeleton organisation.

6.3.4.3 Pathway analysis

IPA canonical pathway analysis

When imputing the DEGs into IPA software, there were 63 canonical pathways showing significant enrichment (adjusted $P<0.05$). The top-ranked enriched pathways (-log (p-value)>2) included translation-related signaling pathways (EIF2 (eukaryotic initiation factor 2) signaling and regulation of eIF4 and p70S6K Signaling), metabolic-related signaling pathways (including oxidative phosphorylation, mitochondrial dysfunction, and sirtuin signaling pathway), and actin/cytoskeleton related signaling pathways (mTOR (mammalian target of rapamycin) signaling, regulation of actin-based motility by Rho (Ras homolog), RhoA (Ras Homolog Family Member A) signaling, actin cytoskeleton signaling, and ILK (integrin-linked kinase) signaling. In addition, 7 canonical pathways were predicted to be activated (Z-score>0). Especially, EIF2 signaling (Z-score=4.47), oxidative phosphorylation (Z-score=3.74), and RhoA signaling (Z-score=2.64) were predicted as significantly activated in the hatching blastocysts (Z-score>2). In contrast, the sirtuin signaling pathway (Z-score=-1.134) and the RhoGDI (Rho GDP-dissociation inhibitor) signaling pathway (Z-score=-1) were inhibited, although there was no significance (**Figure 6-9**). All the enriched canonical pathways and their related genes are listed in the **Appendix 10 Table S.2**.

These results suggested that apart from activated translation and metabolism activity, the RhoA signaling (enriched in 7 DEGs, including *Actb, Arpc2, Cfl1, Myl6, Pfn1, Rnd3, and Septin9*) was associated with a dominant role in the mouse embryo hatching process.



Figure 6-9. The canonical pathway analysis of differentially expressed genes (DEGs) between hatching and pre-hatching blastocysts in the control group

The top-ranked enriched canonical pathways were generated by the Ingenuity Pathway Analysis (IPA) of DEGs between hatching and pre-hatching blastocysts. For each significantly enriched pathway, the enrichment significance is plotted by a bar (-log(*P*-value)), and the predicted activity is presented in different colours (activated (orange), inhibited (blue), no predicted activity (gray), and Z-score=0 (white)). The Z-score of each predicted pathway is plotted by a red dot (x-axis above).

Reactome pathway, KEGG pathway, and WIKI pathway enrichment analyses

Pathway enrichment analysis was further conducted based on three different databases: Reactome pathway, KEGG pathway, and Wikipathway. **Figure 6-10** shows 17 Reactome enriched pathways, including six ribosome and translation-related pathways, four ATP metabolism-related pathways, three Rho signaling related pathways [RHO GTPases activate IQGAPs (*Tuba1b, Actb,* and *Calm1*), RHO GTPases effectors (*Arpc2, Pfn1, Taok1, Sos1, Tuba1b, Arhgap42, Actb, Calm1,* and *Myl6*), and Signaling by Rho GTPases (*Arpc2, Pfn1, Taok1, Tuba1b, Actb, Calm1,* and *Myl6*)]. In addition, developmental biology pathway was enriched in 11 DEGs (*Krt7*, *Krt18, Krt8, Actb*, *Tuba1b*, *Arpc2*, *Enah*, *Pfn1* (Profilin 1), *Pkp4* (Plakophilin 4), *Foxo1* (Forkhead box O1), *Sos1* (SOS Ras/Rac guanine nucleotide exchange factor 1)) (**Appendix 10 Table S.3**).

Similarly, the KEGG pathway analysis revealed the DEGs were highly associated with pathways including the ribosome, oxidative phosphorylation, metabolism, and the regulation of the actin cytoskeleton. However, only three Wikipathways (cytoplasmic ribosomal protein, electron transport chain, and oxidative phosphorylation) enriched. The significantly enriched pathways and related genes were presented in **Appendix 10 Table S.4.**

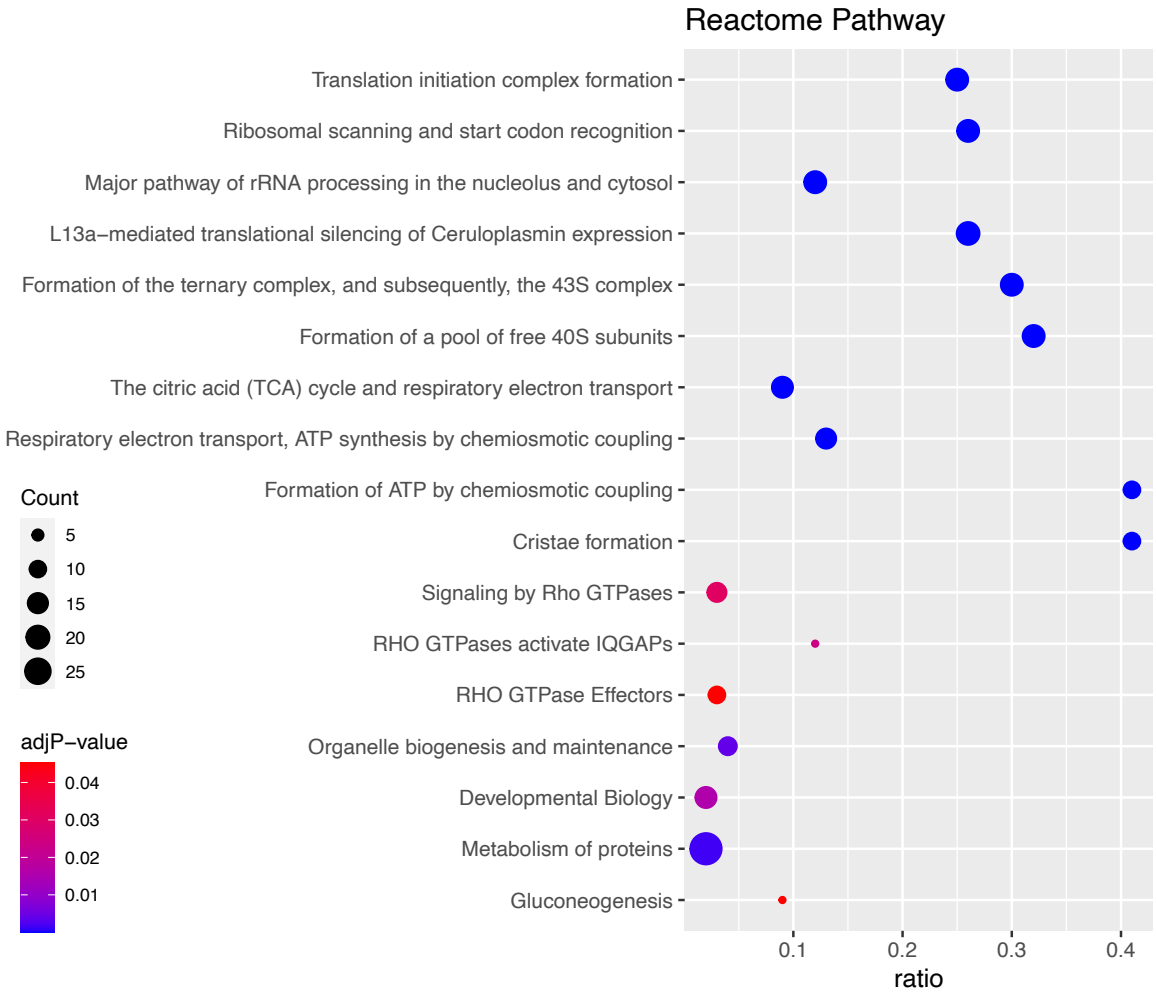


Figure 6-10. The Reactome pathways analysis of differentially expressed genes (DEGs) between hatching and pre-hatching blastocysts

Reactome enrichment analysis was performed using *ClusterProfiler*. For each significantly enriched pathway, the pathway enrichment significance is plotted by the colour according to the adjusted *P*-value, while the gene count in each pathway is represented by the size of the dot.

Together with the all the downstream analysis shown above, embryo hatching is clearly an ATP consuming process with genes enriched in ATP metabolism and oxidative phosphorylation related terms and pathways. In addition, this process is also related to the highly activated translation process. More importantly, actin/cytoskeleton related terms and pathways were significantly associated with this process, especially the RhoA signaling and actin-based motility regulated by RhoA pathway. The interested terms- and pathway-related genes are shown in heatmaps (**Figure 6-11**).

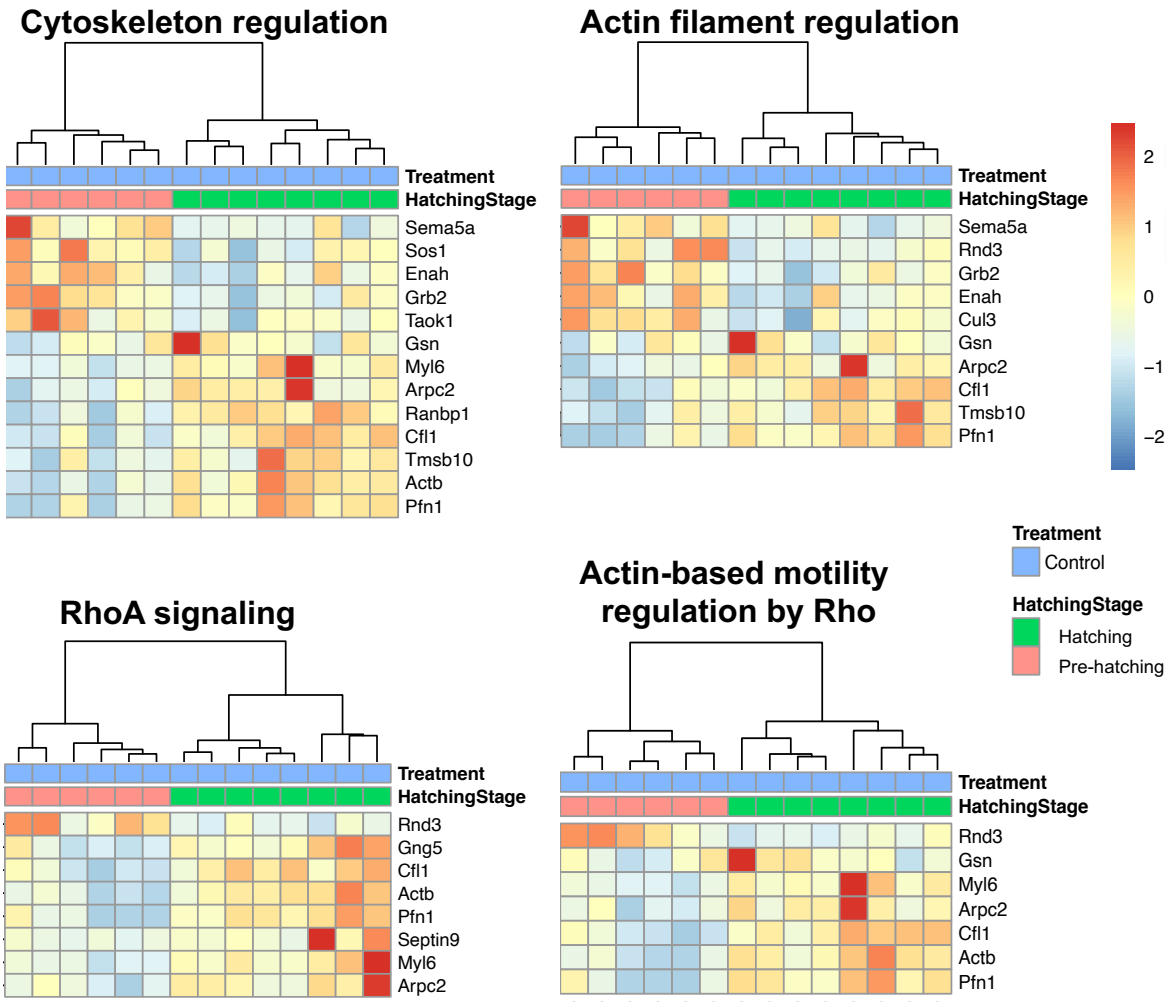


Figure 6-11. Heatmaps of potential terms and pathways and related genes that are involved in the hatching process

The genes implicated in hatching-related terms and pathways were visualised using heatmaps. These include cytoskeleton regulation, actin filament regulation, RhoA signaling pathway, and actin-based motility regulation by Rho. The intensities were normalized for each gene in each row, and samples were clustered according to their similarity in profile using hierarchical cluster analysis. The yellow-red colours represent the elevated levels (red was the highest level), while the blue represents decreased levels. These figures were generated by the *pheatmap* package.

6.3.4.4 Upstream regulators analysis using IPA

The goal of IPA upstream regulator analysis is to identify the cascade of upstream transcriptional regulators that can explain the observed gene expression changes and can help to illuminate the biological activities occurring in blastocysts. Overall, according to these DEGs, 32 predicted upstream regulators were generated by IPA,

after computing *P*-values and activation Z-score; 23 of these were activated upstream regulators (with an activation Z-score>2) and nine were inhibited upstream regulators (with an activation Z-score<-2). Transcription regulator (MYC (MYC proto-oncogene, BHLH transcription factor), TP53 (tumor protein P53), RB1 (RB transcriptional corepressor 1), Esrra (estrogen-related receptor alpha), PPARGC1A (peroxisome proliferator-activated receptor gamma coactivator 1-alpha)), growth factors (AGT (angiotensinogen) and FGF2 (fibroblast growth factor 2)), transmembrane receptor (IGF1R (insulin like growth factor 1 receptor)), the insulin and oestrogen receptor, and the PRL (prolactin) were predicted as activated regulators. In contrast, the inhibited regulators included RICTOR (Rapamycin-insensitive companion of mTOR), KDM5A (Lysine Demethylase 5A), CCND1 (Cyclin D1) and HOXA10 (Homeobox A10)), BDNF (Brain-derived Neurotrophic Factor) **(Figure 6-12).**

Of these upstream regulators, most of the transcription regulators were predicted activated and interacted with cytoplasmic translation, ribosome, and ATP metabolism-related genes. In addition, it was predicted that the activation of growth factor AGT could upregulate *Calm1* (Calmodulin 1), *Cox7c* (Cytochrome C Oxidase Subunit 7C), *Hmgb2* (High Mobility Group Box 2), *Pfn1,* and *Tbx20* (T-Box Transcription Factor 20); while active FGF2 upregulates *Aqp3, Dad1*(Defender Against Cell Death 1), *Foxo1, Spry1* (Sprouty RTK Signaling Antagonist 1), and *Tmsb4x* (Thymosin Beta 4 X-Linked) in hatching blastocysts. Furthermore, the activation of oestrogen receptor was predicted to upregulate developmental-related genes, including *Krt7, Krt18, Krt8*, *Actb*, *Tmeff1* (Transmembrane protein with EGF-like and two follistatin-like domains 1), and *Lgals1* (lectin, galactose binding, soluble 1). The predicted upstream regulators and related genes were listed in **Appendix 11. Table S.5.**

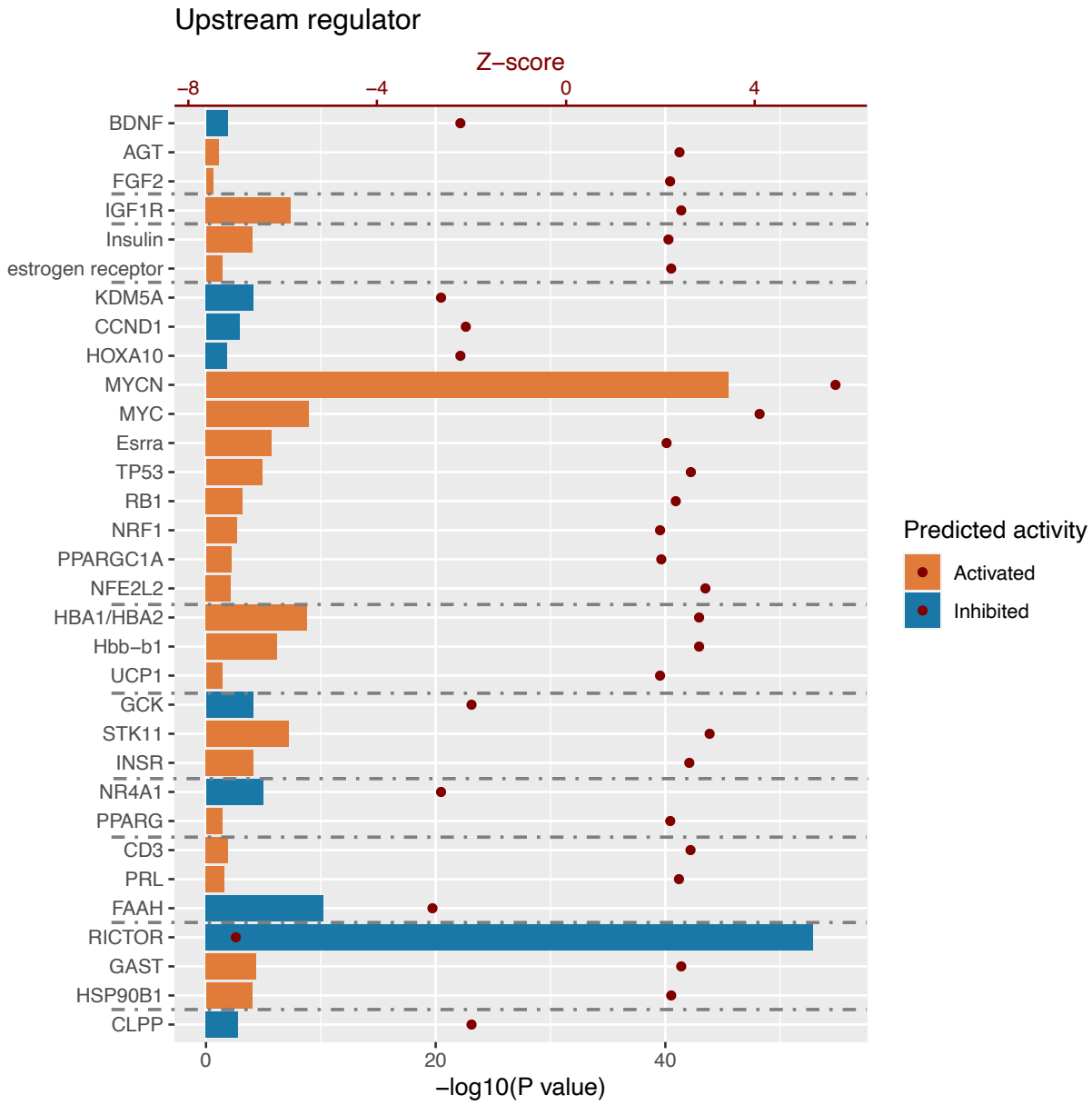


Figure 6-12. Upstream regulator analysis of differentially expressed genes (DEGs) between hatching and pre-hatching blastocysts in the control group

Upstream regulator analysis was conducted in the Ingenuity Pathway Analysis (IPA). Significant upstream regulators are grouped by functional categories. For each enriched pathway, the enrichment significance is plotted by a bar (-log(P-value)), and the predicted activity is presented in different colours (activated (orange), inhibited (blue)). In addition, the Z-score of each predicted pathway is plotted by red dots (x-axis above).

6.3.4.5 The expression of genes that are specific to embryo linage

Unlike single-cell RNA-seq, the bulk RNA-seq used in this study could not distinguish transcriptomes between the ICM and the TE in blastocyst stage embryos. To unravel the lineage specification, I compared the 275 DGEs with previously published lineage-specific single-cell RNA-seq datasets which identified 354 genes enriched in the ICM, and 143 genes enriched in the TE (Deng et al., 2014, Blakeley et al., 2015). As shown in **Figure 6-13**, among the 275 DEGs, 6 genes (*Rnd3, Tmeff1, Rpl13a, Qki, Rps20,* and *Myef2*) were ICM-specific, and 16 genes (*Lgals1, Krt18, Actb, Gpx4, Cldn4, Fabp3, Calm1, Myl6, Psap, Tmsb10, Ctsh, Krt8,* and *Arpc2*) were TE-specific. Interestingly, all these TE-specific genes were up-regulated in hatching blastocysts.

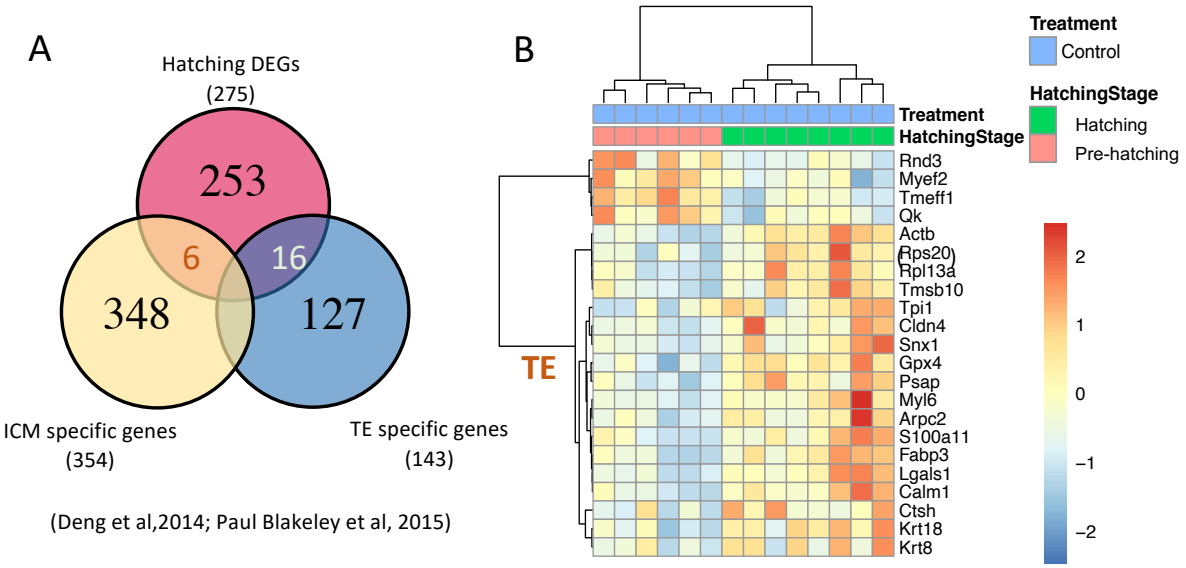


Figure 6-13. The mouse embryo lineage-specific genes and differentially expressed genes between hatching and pre-hatching blastocysts

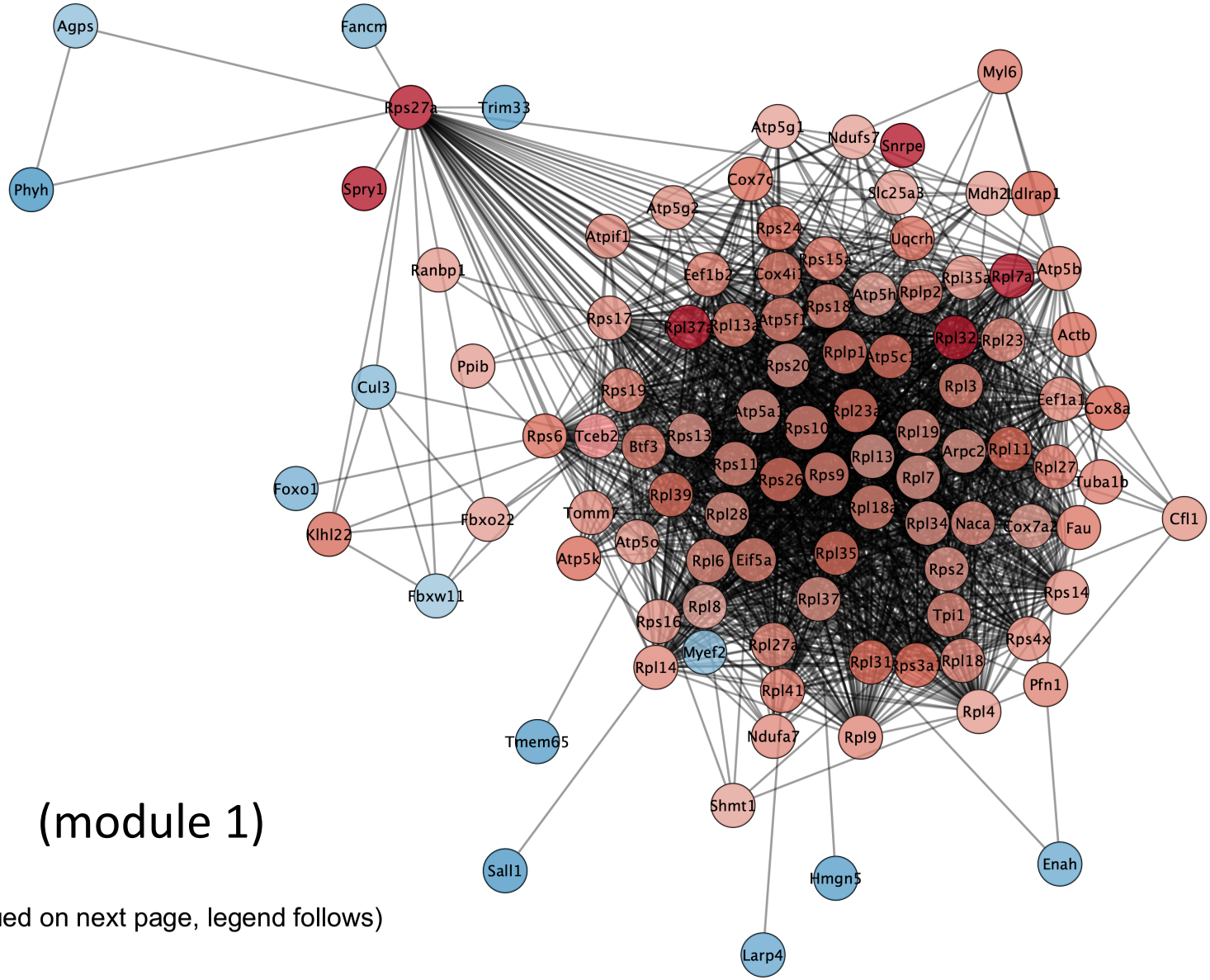
(A) A Venn diagram of DEGs and ICM or TE-specific genes. (B) Heatmap of the expression of embryos lineage-specific gene in hatching and pre-hatching blastocysts. Yellow represents elevated levels (red was the highest level), while blue represents the decreased levels. The intensities were normalized for each gene in each row, and samples and genes were clustered according to their similarity in profile using hierarchical cluster analysis.

6.3.4.6 Protein-protein interaction (PPI) analysis of DEGs

Based on a STRING protein query, a string network of 167 PPI nodes were harvested from these 275 DEGs (**Appendix 12, Figure S.8**). To seek the potential interactions between these nodes, MCODE (Molecular Complex Detection) was used to identify the densely connected networks; four modules were significantly clustered. The first module included 103 genes with 1805 edges (MCODE score:35.4), the second module included 35 nodes with 176 edges (MCODE score 10.4) (**Figure 6-14**). The molecules in these two modules were related with ribosome biogenesis, oxidative phosphorylation, proton-transporting, and actin cytoskeleton organisation related GO terms, KEGG, and Reactome pathways.

In addition, the third module (MCODE score 3.0) included 5 nodes and 6 edges (*Aqp3, Krt18, Krt8, Krt7,* and *Cldn4*). The molecules in this module were related with filament (*Krt8, Krt7,* and *Krt18*), cell-cell junction (*Krt8, Cldn4*, and *Aqp3*), channel activity, and water homeostasis (*Cldn4* and *Aqp3*) (**Figure 6-14**).

The fourth module (MCODE score:2.9) included 12 nodes, 16 edges (*Cfl1, Arpc2, Gsn, Pfn1, Shmt1, Tuba1b, Tmsb10, Tpi1, Ldlrap1, Rnd3, Enab,* and *Grb*); these molecules were related with the regulation of actin cytoskeleton pathway (*Cfl1, Arpc2, Gsn, Pfn1,* and *Enab*) and other GO terms related to actin filament organisation, such as GTPase activity (*Rnd3* and *Tuba1b*) and small GTPase mediated signal transduction (*Rnd3* and *Grb2*) (**Figure 6-14**).



(module 1)

Figure 6-14 (Continued on next page, legend follows)

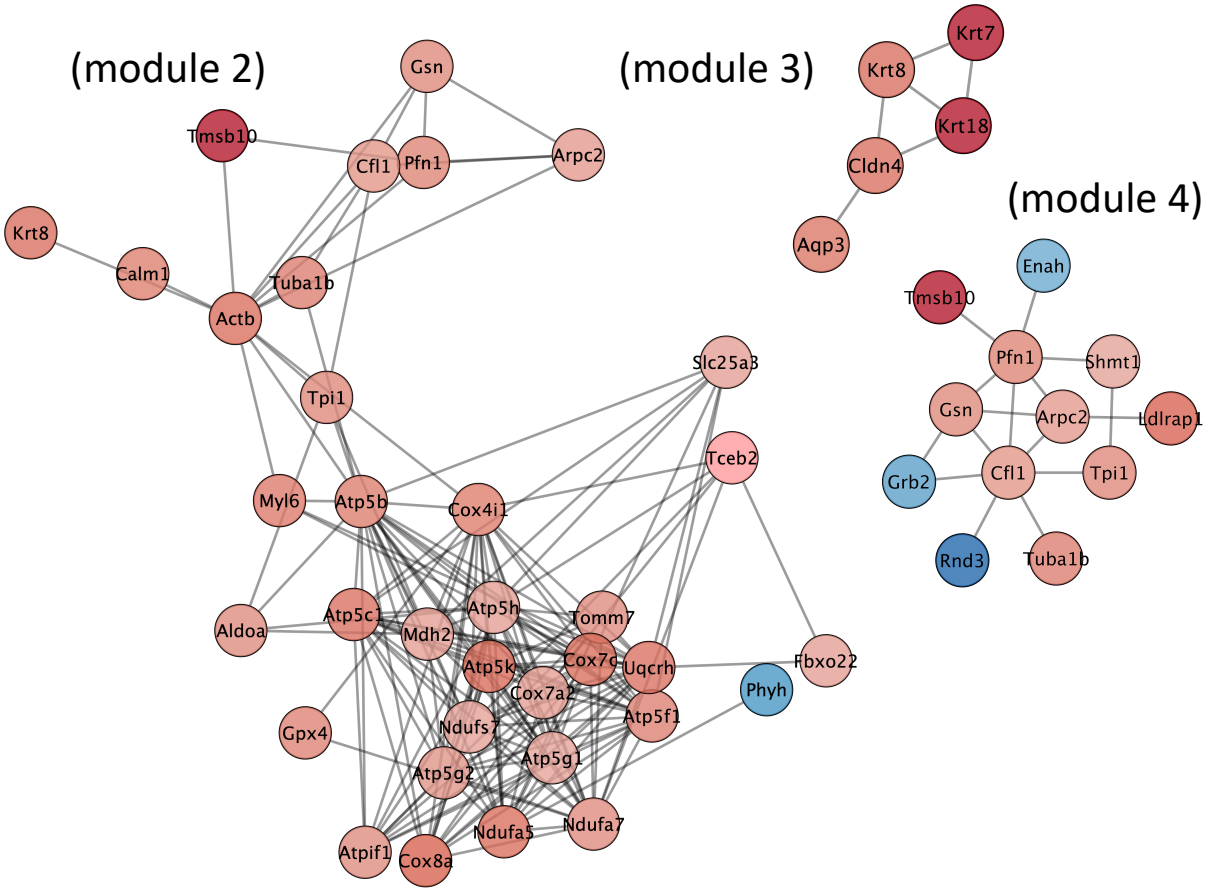


Figure 6-14. The Molecular Complex Detection predicted subnetwork of differentially expressed genes between hatching and pre-hatching blastocysts

The predicted nodes modules generated using Molecular Complex Detection (MCODE). The red nodes represent up-regulated DEGs, the blue nodes represent down-regulated DEGs, and the saturation of nodes indicates the absolute value of logFC (fold change); lines represent the interaction relationship between nodes.

6.3.5 A comparison of laser-drilled hatching blastocysts and control hatching blastocysts

6.3.5.1 Differential gene expression analysis

To understand the transcriptomic changes caused by laser-assisted ZP drilling, differential expression analysis was used to determine the DEGs between laser-drilled hatching blastocysts *vs* natural hatching blastocysts (untreated control). Overall, only 48 genes were found to be differentially expressed (BH adjusted P <0.05), of these 38 genes were up-regulated, and 10 genes were down down-regulated (**Figure 6-15**).

In addition, the fold changes of these DEGs were minimal. There were only 13 DEGs with fold changes larger than 2 (including *Lilra6, Maged2, Cep250, Acbd4, Mvk, Lmna, Acaa1a, Aldh18a1, Mvd*, *Cdk5rap3, Lmln*, and *Gsk3a*), while most of them were smaller than a 2-fold change. The top-ranked genes are listed in **Table 6-4**. This small number and minimal fold change of DEGs between two groups suggested that the laser-assisted drilling could cause subtle transcriptomic changes to E4.5 hatching blastocyst.

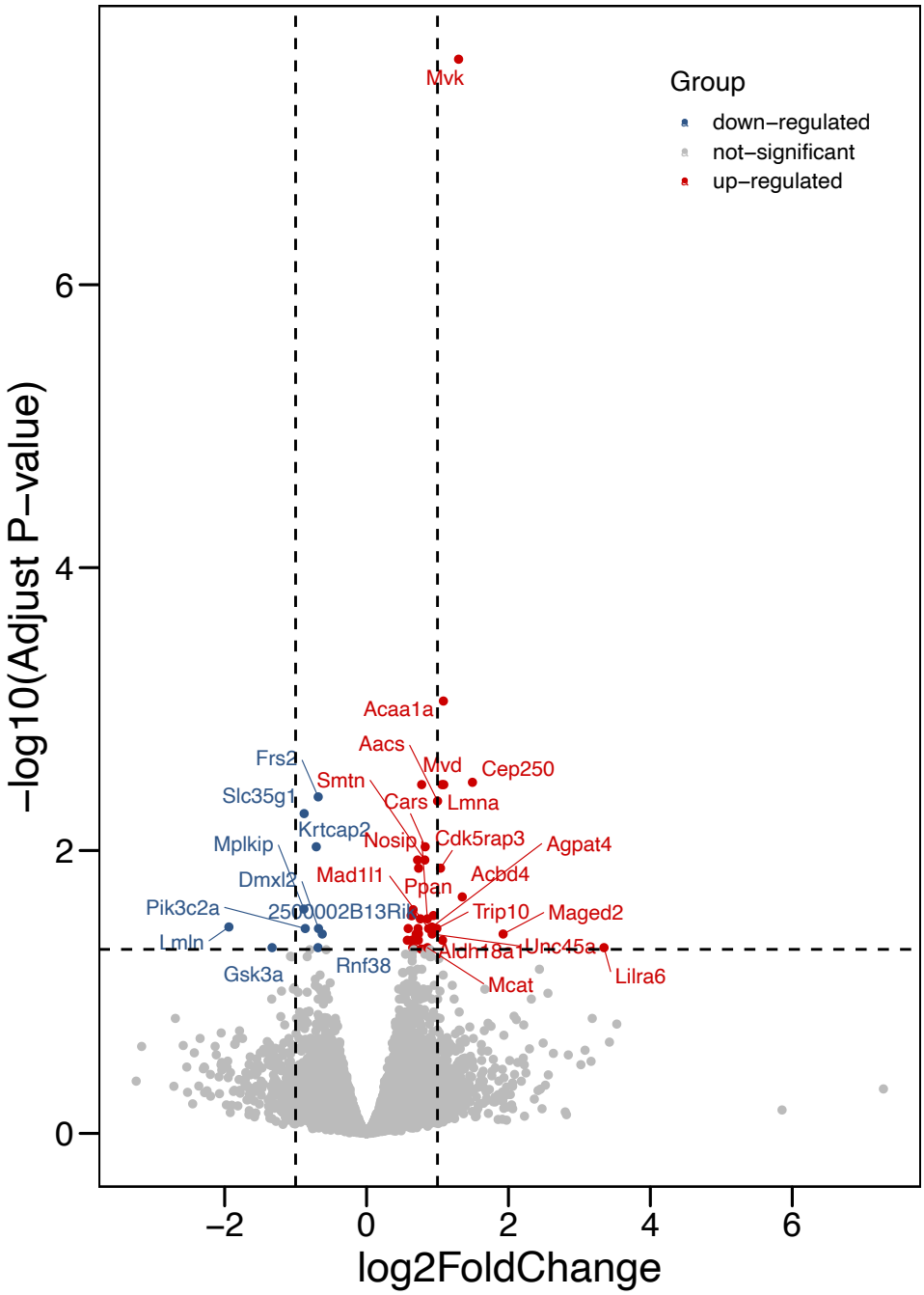


Figure 6-15. Differentially expressed genes (DEGs) between laser-drilled hatching and control hatching blastocysts

(A) A volcano plot for DEGs: the x-axis shows the fold change in gene expression between samples and the y-axis shows the statistical significance of the differences. The significant up and down regulated genes are highlighted in red and blue, respectively. The top 20 up-regulated genes, and the top 10 down-regulated genes, by fold change, are marked with the gene name. The gray points are non-significant DEGs.

Table 6-4 The top-ranked upregulated and downregulated DEGs between laser-drilled hatching and control hatching blastocyst

	Gene	logFC	logCPM	adj *P*-value	Description
Upregulated genes	*Lilra6*	3.35	0.74	0.049	leukocyte immunoglobulin-like receptor, subfamily A (with TM domain), member 6
	Maged2	1.92	2.85	0.039	melanoma antigen, family D, 2
	Cep250	1.49	4.15	0.003	centrosomal protein 250
	Acbd4	1.35	3.57	0.021	acyl-Coenzyme A binding domain containing 4
	Mvk	1.30	7.38	2.54E-08	mevalonate kinase
	Lmna	1.09	8.65	0.003	lamin A
	Acaa1a	1.08	6.68	0.0008	acetyl-Coenzyme A acyltransferase 1A
	Aldh18a1	1.07	5.73	0.043	aldehyde dehydrogenase 18 family, member A1
	Mvd	1.06	7.66	0.003	mevalonate (diphospho) decarboxylase
	Cdk5rap3	1.04	6.18	0.013	CDK5 regulatory subunit associated protein 3
Downregulated genes	*Lmln*	-1.94	1.66	0.035	leishmanolysin-like (metallopeptidase M8 family)
	Gsk3a	-1.33	3.03	0.049	glycogen synthase kinase 3 alpha
	Mplkip	-0.88	5.01	0.026	M-phase specific PLK1 interacting protein
	Slc35g1	-0.88	6.30	0.005	solute carrier family 35, member G1
	Pik3c2a	-0.86	5.54	0.036	phosphatidylinositol-4-phosphate 3-kinase catalytic subunit type 2 alpha

6.3.5.2 GO term analysis

As **Figure 6-16** shows, 19 GO terms were found to be enriched in these 48 DEGs. Of these, the small molecule metabolism process was enriched, with 12 related DEGs upregulated (*Mvd, Cars* (cysteinyl-tRNA synthetase 2), *Tars* (threonyl-tRNA synthetase), *Agpat4* (1-acylglycerol-3-phosphate O-acyltransferase 4)*, Aldh18a1*, *Aacs* (Acetoacetyl-CoA synthetase)*, Aars* (alanyl-tRNA synthetase)*, Amdhd2* (amidohydrolase domain containing 2)*, Mvk, Acaa1a*, *Mcat* (malonyl CoA:ACP acyltransferase), and *Nfe2l1* (Nuclear factor, erythroid derived 2,-like 1). Specifically, 2 lipid metabolism-related biological processes were enriched, including isopentenyl diphosphate biosynthetic process and cellular response to cholesterol. The related DEGs include *Mvd*, *Mvk, Aacs,* and *Nfe2l1*.

For the molecular function, the protein binding, especially the heat shock protein binding was enriched, with 4 related DEGs shown in the dataset (*Mvd, Stub1* (STIP1 Homology And U-Box Containing Protein 1)*, Unc45a* (Unc-45 Myosin Chaperone A)*, Cdc37* (Cell Division Cycle 37).

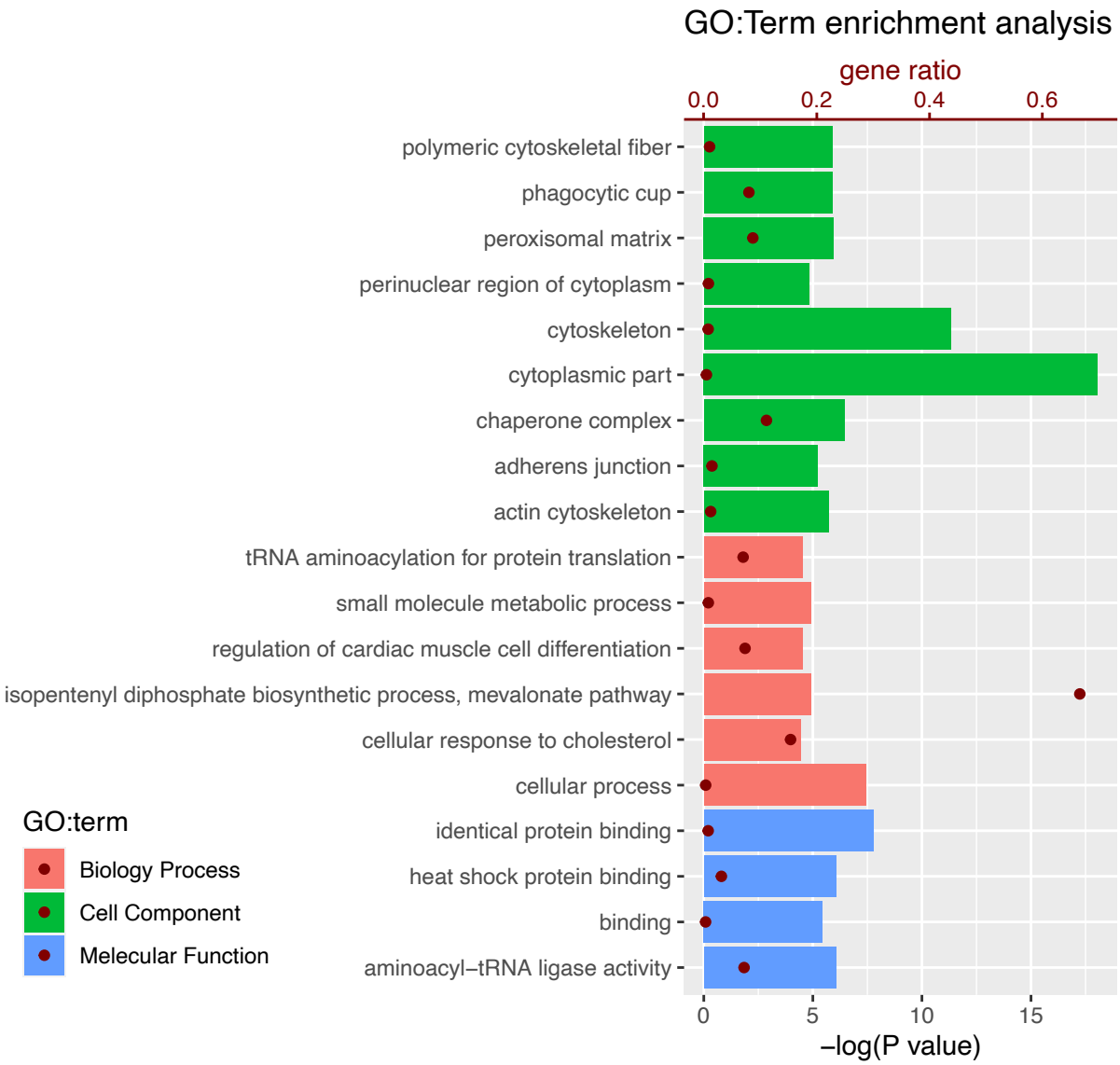


Figure 6-16. Gene Ontology (GO) terms analysis of differentially expressed genes (DEGs) between laser-drilled hatching and control hatching blastocysts

The enriched GO terms of DEGs including the cellular component (green), biological process (red), and molecular function (blue). GO term enrichment analysis was performed using *clusterProfiler*. The significance of term enrichment is represented as the bar (-log (P-value)) (x-axis below), and the gene ratios are presented as red dots (x-axis above).

6.3.5.3 Pathway enrichment analysis

Downstream pathway analysis was performed using different methods, including IPA, KEGG, Reactome, and Wiki. These were 16 canonical pathways, 2 KEGG pathways, and 1 Reactome pathway shown enriched according to 48 DEGs, but no Wiki pathway

was enriched. As shown in **Figure 6-17**, many metabolism-related pathways were enriched, especially lipid metabolism. For example, metabolism of lipids pathways (*Slc25a1* (solute carrier family 25), *Mvd, Acbd4* (acyl-Coenzyme A binding domain containing 4)*, Agpat4* (1-acylglycerol-3-phosphate O-acyltransferase 4), *Aacs, Mvk, Acaa1a, and Mcat*), Mevalonate pathway I (*Mvd* and *Mvk*), L-carnitine Biosynthesis (*Aldh9a1 (*aldehyde dehydrogenase 9, subfamily A1)), and Docosahexaenoic Acid (DHA) Signaling pathway (*Gsk3a (*glycogen synthase kinase 3 alpha), *Pik3c2a* (phosphatidylinositol-4-phosphate 3-kinase catalytic subunit type 2 alpha)) were significantly enriched in the related DEGs.

In addition, xenobiotic metabolism signaling was enriched in four related genes (*Aldh18a1 (*aldehyde dehydrogenase 18 family, member A1*), Aldh9a1(*aldehyde dehydrogenase 9, subfamily A1)*, Keap1 (*Kelch-like ECH-associated protein 1*),* and *Pik3c2a.* Furthermore, other metabolism pathways, such as valine, leucine, and isoleucine degradation pathway (*Aldh9a1, Aacs, Acaa1a*), insulin receptor signaling pathway (*Gsk3a, Pik3c2a, Trip10 (*thyroid hormone receptor interactor 10*)*), and eNOS signaling pathway (*Nosip* (nitric oxide synthase interacting protein), *Pik3c2a, Stub1 (*STIP1 homology and U-Box containing protein 1)) were also significantly enriched (**Figure 6-17**).

Since the number of DEGs was too small, no activation or inhibition of the enriched pathways could be predicted using IPA software. All enriched pathways and related genes were presented in **Appendix 13 Table S.6**. In addition, no predicted upstream pathway could be generated because of the small number of DEGs.

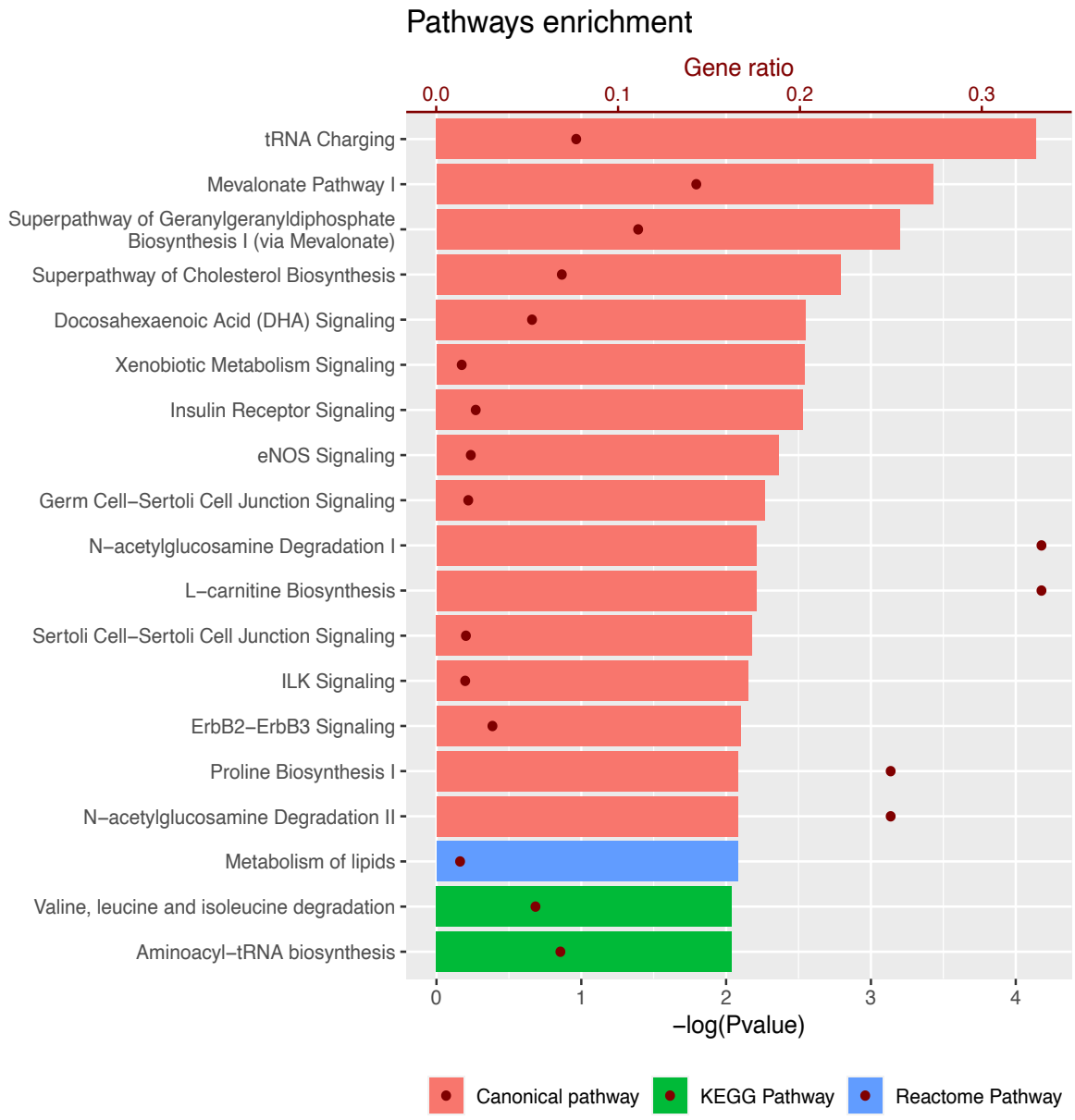


Figure 6-17. Pathway enrichment analysis of differentially expressed genes (DEGs) between laser-drilled hatching and control hatching blastocysts

The significantly enriched pathways include IPA Canonical pathways (red), Reactome pathways (blue), and KEGG pathways (green) for DEGs between laser-drilled hatching and control hatching blastocysts. Enrichment analysis was performed using IPA and *ClusterProfiler*. For each enriched pathway, the significance of pathway enrichment is plotted by the bar (-log(P-value)), while the gene ratios are presented as red dots (x-axis above).

6.3.6 Validation of RNA sequencing results by quantitative real-time PCR

6.3.6.1 Validation of housekeeping genes

Housekeeping gene candidates were selected from a panel of 5 commonly used housekeeping genes, including *B2m (*Beta-2-Microglobulin*), Canx (*Calnexin*), 18S, Gapdh,* and *Ywhaz (*Tyrosine 3/Tryptophan 5 -Monooxygenase Activation Protein, Zeta); these genes are also expressed stably in RNA-seq data. The housekeeping validation was performed using the ∆Ct (Cycle Threshold) approach, by comparing the relative expression of 'pairs of genes' within each sample. On this basis, stability of the candidate housekeeping genes was ranked according to repeatability of the gene expression differences among all samples (Silver et al., 2006).

Housekeeping genes in the comparison of hatching and pre-hatching blastocysts in the control group

The expression profiling of 5 housekeeping genes was determined in all untreated blastocysts (both hatching and pre-hatching blastocysts in control group); the Ct values were all lower than 30. In addition, when comparing *Gapdh* and the other four genes (*Ywhaz, B2m, Canx*, and *18S*), the standard deviations for ∆Ct were relatively larger. These results suggested that *Gapdh* may be variable between samples. However, the standard deviations of ∆Ct were lowest when comparing *Canx* and *Ywhaz;* this means either both genes were stably expressed among samples, or co-regulated. Thus, I used *Canx* and *Ywhaz* as housekeeping genes for the comparison of gene expression between hatching and pre-hatching blastocysts; the average Ct values of these two genes were used as internal controls (**Figure 6-18**).

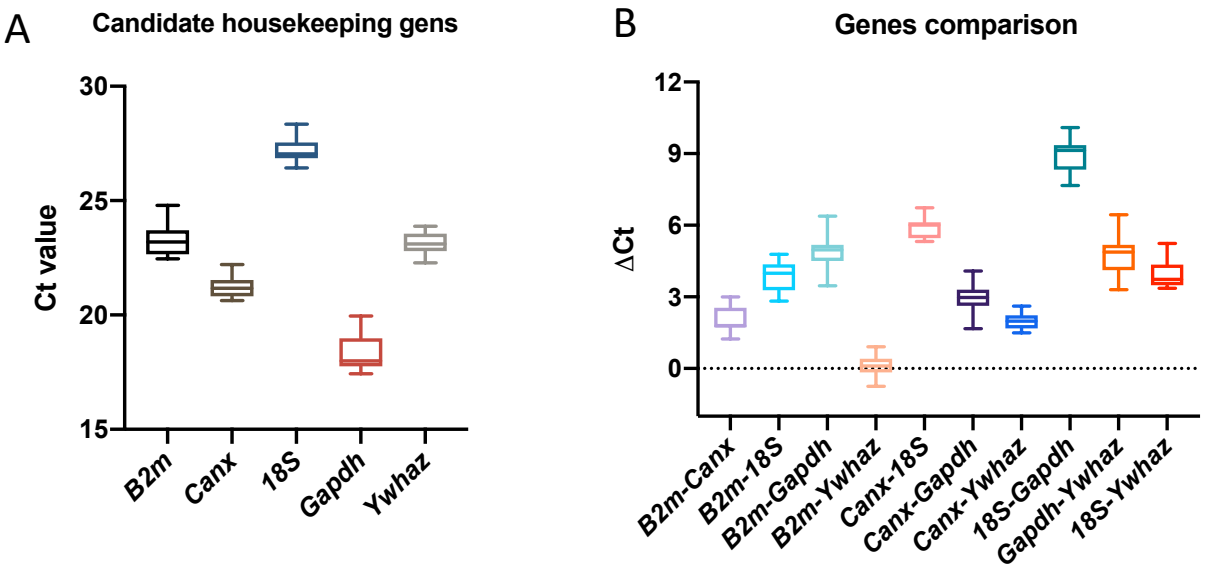


Figure 6-18. Validation of housekeeping genes in the comparison of hatching and pre-hatching blastocysts

(A) The qRT-PCR cycle threshold (Ct) value for five candidate housekeeping gens among all untreated blastocysts samples. (B) The ΔCt (between two candidate housekeeping gene pairs) approach for selecting housekeeping genes. The Ct value of candidate housekeeping genes and the ΔCt variability in candidate housekeeping genes comparisons are shown as medians (line), 25th percentile to the 75th percentile (boxes), and ranges (whiskers).

Housekeeping genes in the comparison of laser-drilled hatching and natural hatching blastocysts

Similarly, the Ct values of all five housekeeping gene candidates were lower than 30 among samples in all hatching blastocysts (laser-drilled group and control group). However, when comparing each two candidate genes, the standard deviations of ΔCt were all small, with the comparison of *B2m* and *Ywhaz* showing the smallest standard deviation of ΔCt. Thus, *B2m* and *Ywhaz* were used as housekeeping genes for comparing the gene expression of laser-drilled hatching and control hatching blastocysts (**Figure 6-19**).

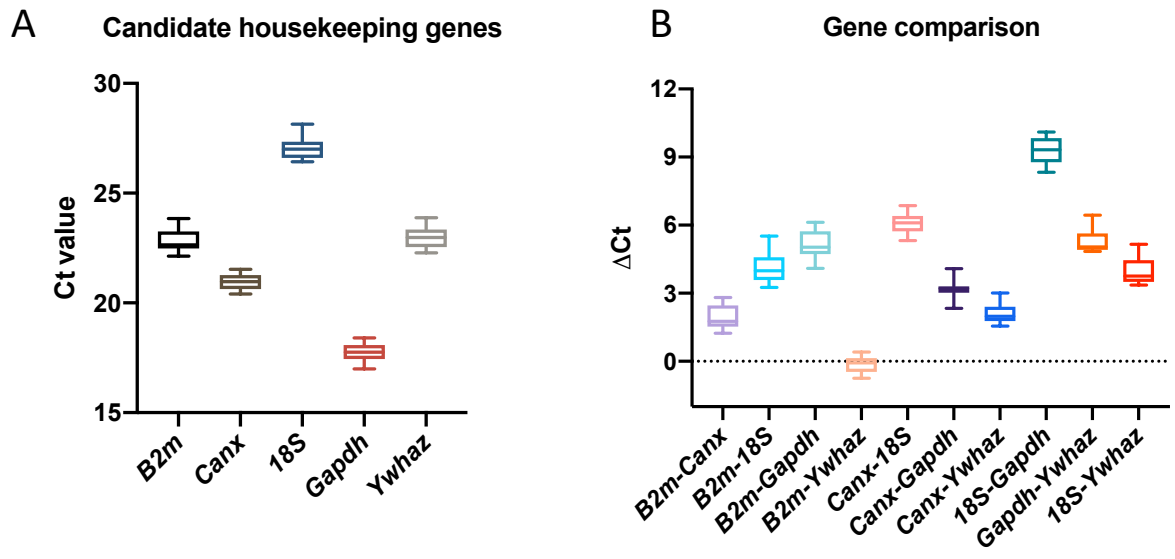


Figure 6-19. Validation of housekeeping genes in the comparison of laser-drilled hatching and control hatching blastocysts

(A) The qRT-PCR cycle threshold (Ct) value for five candidate housekeeping genes among all hatching blastocysts samples. (B) ΔCt approach for selecting housekeeping genes. The Ct value of candidate housekeeping genes and the ΔCt variability in candidate housekeeping genes comparisons are shown as medians (line), 25th percentile to the 75th percentile (boxes), and ranges (whiskers).

6.3.6.2 qRT-PCR validation of selected DEGs

To validate the RNA-seq results, eleven DEGs and one stable expressed gene (*Cdx2*) between hatching and pre-hatching blastocysts were selected. These genes presented with different implicated pathways, including actin-based cytoskeleton (*Actb, Myl6,* and *Rnd3*), oxidative phosphorylation and ATP metabolism [*Atp5b* (ATP synthase, H+ transporting mitochondrial F1 complex, beta subunit), *Cox8a* (Cytochrome c oxidase subunit 8A), *Ndufa7* (NADH: ubiquinone oxidoreductase subunit A7)], ribosome biogenesis [*Rpl13a* (Ribosomal protein L13A)], water channel (*Aqp3*) and embryo-linage specific genes [TE specific genes: *Krt18*, *Ctsh* (Cathepsin H), and *Lgals1* (Lectin, galactose binding, soluble 1)]. The qRT-PCR results showed

all these genes followed the same trend in the expression pattern as with the RNA-seq results. Significant differences were validated for the expression levels of *Actb, Rnd3, Atp5b, Krt18, Ctsh, Lgals1*, *Rpl13a,* and *Aqp3* (P<0.05). In contrast, the expression of *Cdx2* was stable in two groups (**Figure 6-20).**

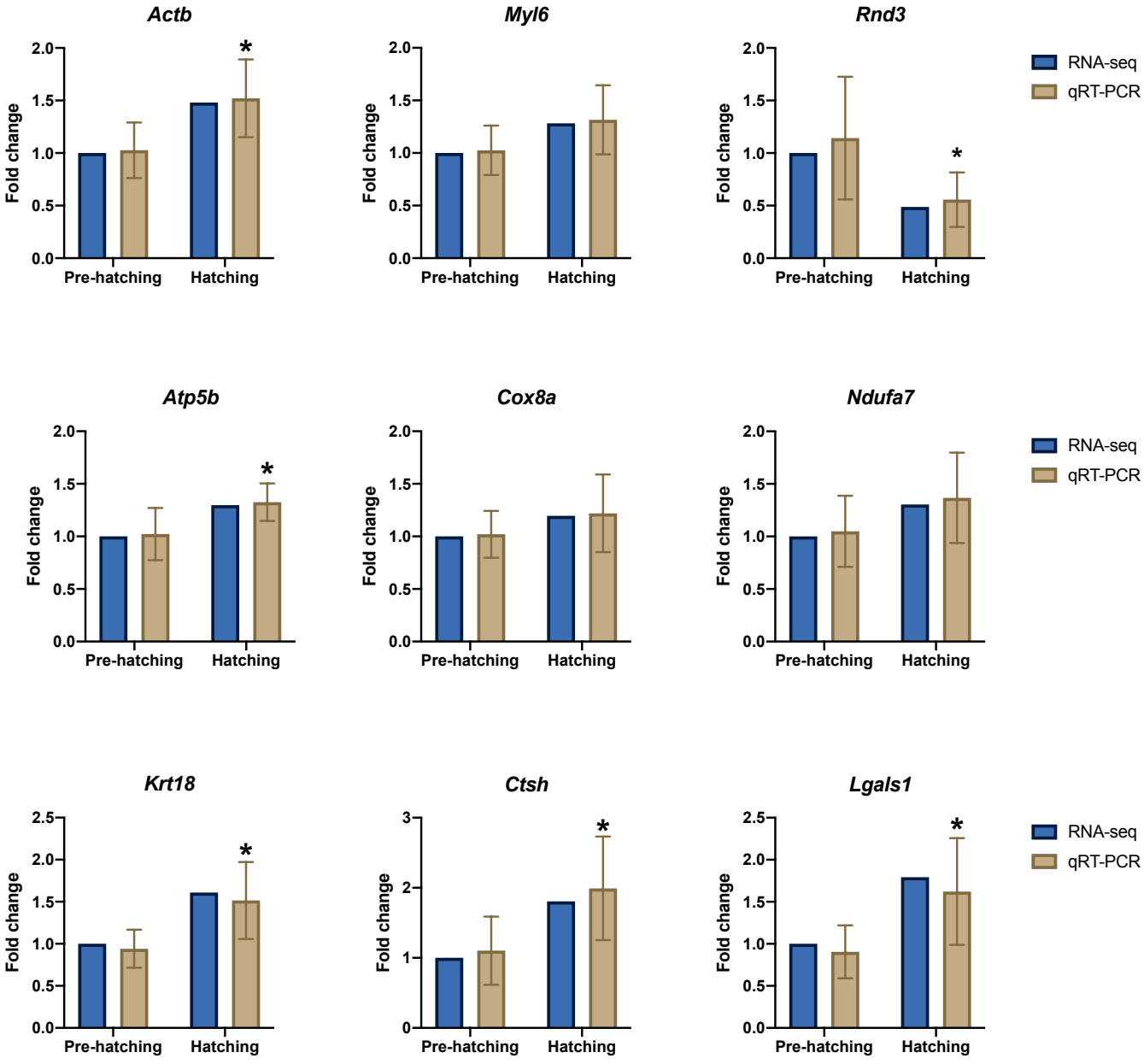


Figure 6-20 (Continued on next page, legend follows)

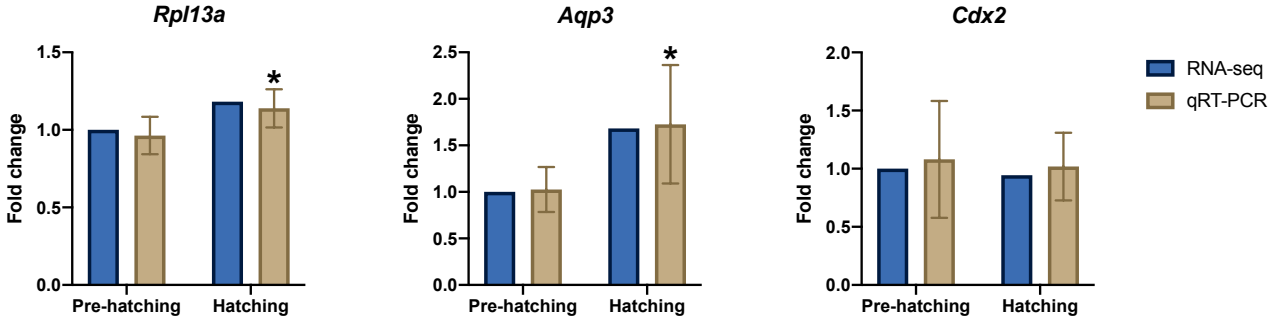


Figure 6-20. Validation of DEGs between hatching and pre-hatching blastocysts using qRT-PCR

The mRNA expression of 12 genes was detected using qRT-PCR and demonstrated differences between hatching and pre-hatching blastocysts. The amount of mRNA was quantified by measuring the cycle threshold (Ct) value. Relative expression of each transcript was normalized to the mean Ct value of *Canx* and *Ywhaz* (ΔCt) and the ΔCt values of each sample was normalized to the mean ΔCt values of all pre-hatching samples (ΔΔCt). Data presented as mean ± SD. Statistical analysis was carried out using the unpaired t-test (**P*<0.05) (n=6-8 biological repeats).

In addition, five genes were selected for the validation of RNA-seq result between laser-drilled hatching and control hatching blastocysts, including four DEGs [*Mvk*, *Mvd,* *Lmna* (Lamin A), and *Dnmt3l* (DNA (cytosine-5)-methyltransferase 3-like)] and *Cdx2*. These five genes all showed the same change in pattern as shown in the RNA-seq results. Furthermore, the differences in *Mvk, Mvd,* and *Lmna* were significant (**Figure 6-21**). In addition, the expression levels of *Cdx2* were similar between two groups.

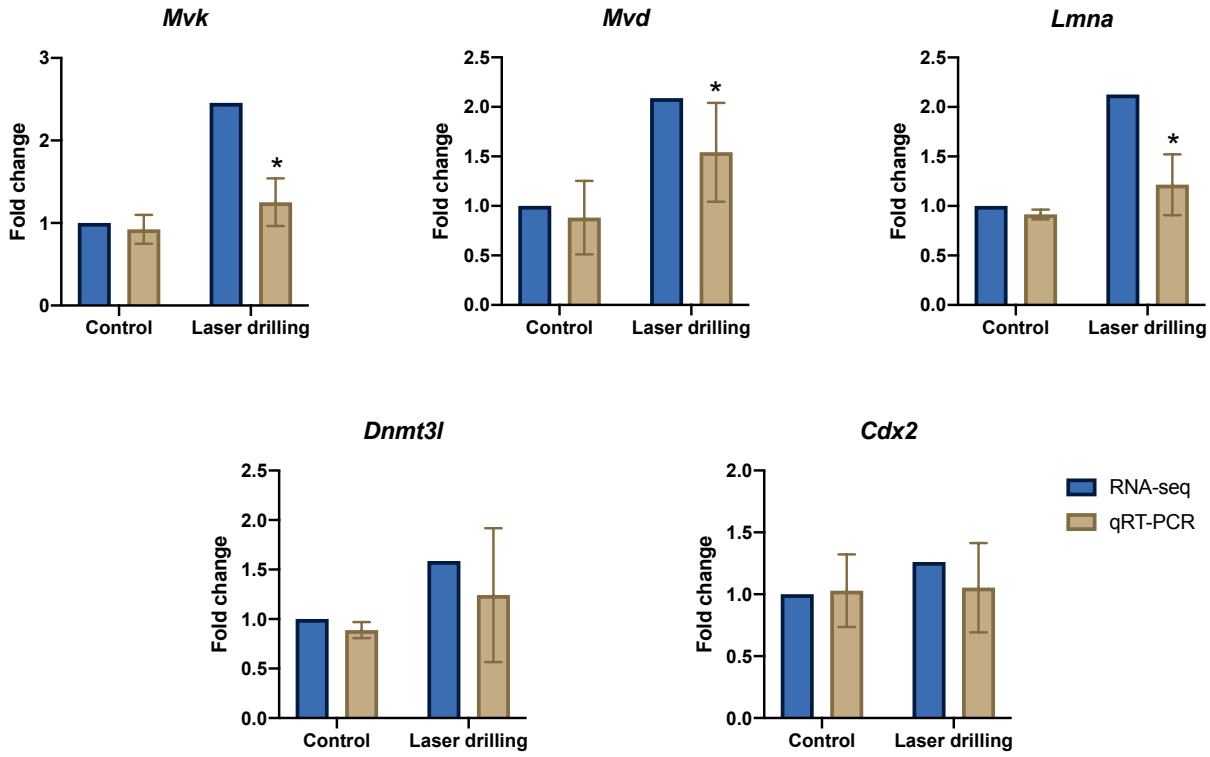


Figure 6-21. Validation of DEGs between laser-drilled hatching and control hatching blastocysts using qRT-PCR

The mRNA expression of five genes was detected using qRT-PCR and demonstrated differences between laser-drilled hatching and control hatching blastocysts. The amount of mRNA was quantified by measuring the cycle threshold (Ct) value. Relative expression of each transcript was normalized to the mean Ct value of *B2m* and *Ywhaz* (ΔCt) and the ΔCt values of each sample was normalized to the mean value of the control hatching group (ΔΔCt). Data presented as mean ± SD. Statistical analysis was carried out using the unpaired t-test (**P*<0.05) (n=6-8 biological repeats).

These validation results of the 11 DEGs between pre-hatching and hatching blastocyst, as well as the four DEGs between laser-drilled hatching and control hatching blastocyst using qRT-PCT were in the agreement with RNA-seq data, indicating that the RNA-seq data is reliable and reproducible.

6.4 Discussion

The embryo hatching is a process that is regulated by multiple factors. Previous studies revealed the potential mechanisms of hatching include embryo-derived proteases, the hydrostatic pressure caused by blastocyst expansion, regulatory molecules, and cell movement caused by cytoskeleton organisation (Shafei et al., 2017). However, the exact molecular network and mechanisms regulating hatching are still unclear.

A research group previously tried to investigate the transcriptome of hatching embryo by profiling the gene expression of pre-hatched and hatched *in vitro* cultured mouse blastocysts with the cDNA array. However, embryos in these two groups were collected at different development timepoint (E4.0 and E4.5) (Chen et al., 2005); this could be a confounding factor since the mouse embryo undergoes a dynamic genetic change from E3.5 to E4.5 (Sozen et al., 2014). Furthermore, that study revealed some cell adhesion and migration-related genes, such as E-cadherin and NCAM, are highly expressed in E4.5 hatched blastocysts (Chen et al., 2005). However, these molecules were found to play a key role in blastocyst development and linage segregation in a later study (Sozen et al., 2014). Thus, it is important to control the embryo development stage when investigating this transitory period of embryo hatching.

In this chapter, in order to avoid the confounding factor of different embryo stages, I used the blastocysts at the same culture timepoint (E4.5), but different hatching statues; RNA-seq was used to provide insight into the landscape of the mouse embryo transcriptome undergoing hatching. The results in this chapter highlighted transcriptomic changes in ATP metabolism, protein synthesis, and cytoskeleton

organisation. In addition, results determined the transcriptomic alteration following laser-drilling ZP manipulation and the potential impact on embryo metabolism.

6.4.1 Genes and pathways related to the mouse blastocyst hatching process *in vitro*

The actin cytoskeleton system was first related to hatching in a pioneering study, showing that the expression of actin filaments rises significantly in TE cells at the site of hatching; in addition, the inhibition of actin polymerisation (cytochalasin B) could completely inhibit the mouse embryo hatching (Cheon et al., 1999). Furthermore, a novel function of the actin network was revealed in TE cells, since TE cells possessed a motile phenotype as they passed through the ZP (Cheon et al., 1999, Gallicano, 2001). Since then, two other molecules were found important in hatching: SK3 (small-conductance calcium-activated K+ channels 3) and amotL2 (angiomotin like 2) (Lu et al., 2012, Hildebrand et al., 2017). SK3 was demonstrated to regulate blastocyst hatching by controlling F-actin formation (Lu et al., 2012). Furthermore, the genetic inactivation of amotL2 was found to block blastocyst hatching due to the loss of contractile actin filaments. In addition, treating embryos with the myosin II inhibitor (blebbistatin) could also block hatching process (Hildebrand et al., 2017). Collectively, these previous results suggested that TE cells can briefly modify their actin network to produce actomyosin contractility, thus forcing themselves into shape during blastocysts hatching process. However, the involved molecules and underlying mechanism has yet to be fully understood. In this chapter, by using RNA-seq, I found that the network of genes, including *Actb, Myl6, Cfl1, Gsn, Pfn1, Arpc2, Rnd3, Grb2, Tuba1b, Tpi1, Shmt1, Ldlrap1,* and *Tmsb10,* by participating the organisation of the

cytoskeleton, especially the actin polymerisation, play a vital role in the hatching process.

Furthermore, the IPA analysis results suggested that the active regulation of actin-based motility by Rho, especially the RhoA signaling pathway, might be the primarily signaling mechanism, responsible during the hatching process. It is known that RhoA pathway plays a crucial role in actomyosin contractility, which could regulate cell motility, change cell shape, and movement (Wheeler et al., 2004, Hanna et al., 2013, Murrell et al., 2015). RhoA was previously suggested to regulate the expression of p-Cofilin and ARP2 in embryos, and the inhibition of RhoA was shown to affect early cleavage of porcine embryos (Zhang et al., 2014). For the first time, I have shown that a network of *Actb, Arpc2, Cfl1, Gng5, Myl6, Pfn1, Setp9,* and *Rnd3* might regulate the actomyosin contractility through RhoA signaling pathway, thus participating in mouse blastocyst hatching process. This is the first time these molecules have been highlighted, thus providing useful information for further study.

Furthermore, as discovered previously, TEPs are actin-based extensive membranous extensions of TE; and it is shown that TEPs enrich hatching-associated ZP lysing molecules such as cathepsin-L/-B/-P in hamster (Gonzales et al., 1996, Sireesha et al., 2008, Seshagiri et al., 2009). Consistently, the existence of cytoplasmic extensions in other species, such as bovine, mouse, and human blastocysts, are also observed (Seshagiri et al., 2009, Shafei et al., 2017). However, the regulatory mechanism of TEP biogenesis remains unknown. The GO analysis results suggested podosomes (*Actb, Gsn,* and *Arpc2*) were enriched in the hatching embryos. Podosomes are the dynamic actin-rich cellular protrusions that degrade the extracellular matrix through local proteolysis; and it consist of a dense core of F-actin and a ring structure of actin-

associated proteins (Linder et al., 2005). Considering the F-actin enriched structure in hatching blastocysts and the ability of matrix degradation (Salas-Vidal et al., 2004), podosomes may be implicated in TEPs biogenesis during the hatching process. However, further study, including immunoassays and functional assays, are needed to confirm these findings.

In this study, ATP metabolism and oxidative phosphorylation related genes were found upregulated in hatching blastocysts (*Cox8a*, *Ndufa5, Cox7c, Uqcrh*, and many ATP synthase coding genes), suggesting that ATP metabolism is activated in hatching embryos. It is known that the ATP production, which is predominantly derived by oxidative phosphorylation, rise dramatically at the blastocyst stage (Houghton et al., 2004). The increased ATP production observed at the blastocyst stage is due to the activity of Na^+/K^+ ATPase, together with the increased requirement for macromolecular synthesis, such as DNA, RNA, protein, and lipid (Houghton et al., 2004). In this study, genes related to ribosome biogenesis and translation-related pathways were also upregulated, thus indicating the activation of protein biosynthesis during the hatching process. This activation may partially explain the high demand of ATP production.

Na^+/K^+ ATPase is a critical mediator of blastocyst formation as it establishes a trans-TE ionic gradient that directs fluid movement across the TE epithelium (Watson et al., 2004). My RNA-seq data determined the mRNA expression of Na^+/K^+ ATPase subunits coding genes in mouse embryos, including *Atp1a1, Atp1a3, ATP1b1, ATP1b2,* and *ATP1b3;* this was consistent with previous study (Watson et al., 2004). However, no difference was detected between the hatching blastocyst and expanded pre-hatching blastocyst in respect of the Na^+/K^+ ATPase related genes, thus

suggesting that the abundance of Na^+/K^+ ATPase (at lease at the mRNA level) might be not crucial for the hatching process. This hypothesis agreed with Houghton's previous findings, that once the blastocyst is fully expanded, Na^+/K^+ ATPase activity decreases to basal levels, and that ATP is no longer required for Na^+/K^+ ATPase (Houghton et al., 2003).

Interestingly, in the present study, the network of *Aqp3*, *Cldn4*, *Krt18, Krt8,* and *Krt7*, by participating in the cell-cell junction, water channel activity, and water homeostasis, might be heavily involved in the blastocyst hatching process. It is known that aquaporins (AQP3/7) mediate water movement across TE; the expression of *Aqp3* is influenced by osmatic changes in mammal's cells (Sugiyama et al., 2001, Bell et al., 2009). Furthermore, previous studies demonstrated that the establishment of cell sealing by tight junction [TJP1/2 (Tight junction protein 1/2)] and CLDN4/6 (claudin4/6) could block the leakage of water during blastocyst formation (Watson et al., 2004, Sheth et al., 2008, Xiong et al., 2013). In addition, it has been found recently that all TE cells are covered with a dense of keratin filament network at blastocyst stage(Lim et al., 2020). Previous study has demonstrated that mechanical pressure of the expanded blastocysts is critical for embryo hatching, and the inhibition of Na^+/K^+ ATPase could reduce the hatching probability (Leonavicius et al., 2018). Together with the data revealed in this present study, it is supposed that the elevated osmotic pressure of an expanded blastocyst (mainly by regulated by Na^+/K^+ ATPase activity) increases the expression of *Aqp3*, thus further facilitating water flow to the cavity. Combining with the reinforced cell-cell junction by *Cldn4* as well as a dense keratin filament network (*Krt18, Krt8,* and *Krt7*), the further increase in hydrostatic pressure of expanded blastocysts will then induce the hatching process. However, functional

studies are now needed to assess the importance of AQP3, CLDN4, and keratin filament in the blastocyst hatching process.

In this chapter, I showed that 16 TE-specific genes (e.g., *Ctsh* (cathepsin H), and *Lgals1* (lectin, galactose binding, soluble 1)) were upregulated in hatching blastocysts; thus, suggesting TE cells may play an important role in hatching blastocysts. This result was consistent with previous findings in that the enhanced development of the TE lead to advanced embryo hatching, a higher percentage of attached blastocysts, and enhanced trophoblast outgrowth *in vitro* (Xu et al., 2001). Previously, the role of cathepsin P and L have been extensively studied in gold Syrian hamster (Sireesha et al., 2008). However, cathepsin has not been studied in hatching process of mouse embryo. On the other hand, it was demonstrated that advanced TE development improves the *in vitro* blastocyst attachment and trophoblast outgrowth; this may be related with the embryo secreted cathepsin (*Ctsb* and *Ctsl*) and galectin (*Lgals1*), which was demonstrated in both mouse (Afonso et al., 1997, 1999, You et al., 2018) and human (Barrientos et al., 2014). In this study, I found that *Ctsh* (cathepsin H) and *Lgals1* (lectin, galactose binding, soluble 1) were significantly increased in hatching blastocyst, but the coding genes for cathepsin B and L (*Ctsb* and *Ctsl*) did not pop up in the RNA-seq dataset. These results provide a clue that cathepsin H and Galectin-1 may contribute to the hatching process or preparation for early implantation in mice.

6.4.2 Potential upstream regulators during mouse blastocyst hatching

The autocrine and paracrine growth factors have been shown involved in the hamster blastocyst hatching, such as HB-EGF (heparin binding-EGF), TGF-β (transforming growth factor-β), and LIF (leukemia inhibitory factor) (Seshagiri et al., 2009). By the

first time, this present study revealed several novel upstream regulators in the mouse embryo hatching process. The growth factors/receptors, such as IGF1R (Insulin-like growth factor receptor), AGT(Angiotensin), and FGF2 (beta fibroblast growth factor), were found to positively regulate the hatching process. A previous study showed that IGF1R signaling is indispensable for blastocyst formation (Bedzhov et al., 2012). Interestingly, I showed in this study that IGF1R could regulate the hatching process, by increasing the expression of ATP synthase complex and ribosome proteins coding-genes. Furthermore, I found that AGT might target and rise the expression of *Calm1, Cox4i1, Cox7a2, Cox7c, Hmgb2, Pfn1, and Tbx20,* thus promoting embryo hatching. This could explain the previous study that the supplementation of angiotensin (Ang II) could improve embryos development and increase the hatching rate (Naderi et al., 2016). FGF2, a uterine factor, was previously found important for blastocyst formation (Fields et al., 2011, Yang et al., 2011). It is reported that FGF2/ FGFR2 may act in an autocrine manner and activate the downstream PKC/p39 pathway, thus increasing the expression of E-cadherin, TJP-1, Na+/K+/ATPase, and AQP3&9 in the TE during the blastocyst formation in mice (Yang et al., 2015). Intriguingly, my results further showed that FGF2 could also positively regulate the hatching process by targeting at *Aqp3, Dad1, Spry1,* and *Tmsb10.*

Apart from growth factors, hormones might also be important for hatching. Previous study showed that the treatment of hamster embryo with ER-α antagonist could induce a profound reversible inhibition of blastocyst hatching, thus scribing a definitive regulatory role of ER-α in the hatching process (Seshagiri et al., 2009). However, the mechanisms underlying the regulation of oestrogen receptor-α signaling has yet to be studied. In this study, I identified that the activation of oestrogen receptor could increase the expression of *Actb, Lgals1*, *Cldn4, Krt18, Krt7,* and *Krt8*, thus positively

regulating the blastocyst hatching. In addition, it has been reported that PRL (Prolactin) plays a role in the blastocyst formation, showing by the higher blastocyst rates when adding of PRL in culture medium (Kiapekou et al., 2009). My RNA-seq result, for the first time, showed that PRL (Prolactin) might also positively regulate the embryo hatching, by targeting at *Actb, Atp5h, Cox4i1, Tmsb10*, and *Tuba1b*.

The RNA-seq and upstream analysis herein indicate the connection between maternal hormones and growth factors and the embryo development and hatching process, which could explain the difference between the *in vitro* and the *in vivo* hatching rates (Mahdavinezhad et al., 2019). Furthermore, these hormones and growth factors might be the promising supplement for the *in vitro* culture medium, in order to enhance the embryo hatching possibility.

6.4.3 Transcriptomic alterations in mouse blastocysts following laser-assisted ZP drilling

Although laser-assisted ZP manipulation is used commonly, no previous studies has investigated the potential impact of this technique on global gene expression in the embryo. In this study, for the first time, the transcriptomic changes in embryos following laser-drilled were detected using RNA-seq. However, the result suggested that laser-assisted drilling at the cleavage stage would not induce overt transcriptome alterations at the blastocyst stage since only 48 DEGs with small fold changes were found.

One hypothesis regarding the improvement of implantation by ZP drilling was that this technique provides a route for transferring nutrients from the culture medium to embryos, thus enhancing embryo development (Hershlag et al., 2005). In contrast, the

early exposure of embryos to the outside environment through the artificial ZP opening has become a concern of ZP drilling, which implying that this may be harmful to embryo (Hammadeh et al., 2011). Downstream enrichment analysis in present study further revealed that the laser-assisted drilling might lead to changes in embryo metabolism, at least at the mRNA level. A previously study tried to investigate the metabolism changes of the human embryo in 24 hours after cleavage-stage laser-assisted hatching; however, the component analysis of metabolites found no significant differences (Uppangala et al., 2016). It is known that embryo metabolism is relatively low before the morula stage; but it becomes highly activated following the formation of the blastocyst until implantation (Leese, 2012). Thus, it is understandable that in that previous study, the changes in metabolism activity following laser-assisted hatching cannot be detected from Day 2 to Day 3 embryos (Uppangala et al., 2016). Nevertheless, potential changes in embryonic metabolism caused by laser-assisted drilling might happen at the blastocyst stage. In this chapter, I cultured the embryos for 48 hours from Day 3 after laser-assisted drilling to Day 5; the DEGs related to lipids and amnio acids metabolism pathways revealed the potential changes in embryo metabolic activity.

Lipids are hydrophobic substances that are essential for cell metabolism and signaling; lipid metabolism is an important source of energy during the early stages of embryo development in several species (Sudano et al., 2016). In laser-assisted drilled embryos, some genes related to lipids metabolism were all upregulated, for example, the genes related to cholesterol biosynthesis pathways (*Mvd* and *Mvk*) and L-carnitine Biosynthesis (*Aldh9a1*). Endogenous cholesterol biosynthesis is required for embryo development at blastocyst stage; the deletion of HMGR (converts HMGCoA to mavelonate) could result in 100% embryonic lethality before implantation (Ohashi et

al., 2003). Furthermore, L-carnitine (LC) is a water-soluble antioxidant that plays a supportive role in embryo development and the supplementation of LC into culture medium could improve the blastocyst formation (Khanmohammadi et al., 2016). Therefore, the upregulated genes suggested that lipid metabolism is activated in the blastocysts subjected to laser-assisted drilling, which maybe the benefit of laser-assisted ZP drilling. Apart from lipid metabolism, I also found that the genes associated with the degradation of valine, leucine, and isoleucine (*Aldh9a1, Aacs,* and *Acaa1a*) were also upregulated. Essential amino acids (AAs) could promote cell division and blastocysts development in mouse embryos. In addition, these essential AAs have been proven to be important for embryo hatching, attachment, and trophoblastic outgrowth (Lane et al., 1997, Van Winkle, 2001). Collectively, the upregulation of these genes related to lipid and amnio acid metabolism indicates that laser-assisted drilling might activate embryo metabolism; this result provides a clue that laser-assisted drilling might be beneficial for embryo development, by creating a route for transferring nutrients from the culture medium to embryos (Hershlag et al., 2005).

Nevertheless, xenobiotic metabolism signaling was also enriched (*Aldh18a1, Aldh9a1, Keap1*, and *Pik3c2a*). A xenobiotic is referred to as the synthetic compounds or the higher-than-normal concentrated substance within an organism. Xenobiotic metabolism aims to remove xenobiotics by deactivation and excretion (Mansuy, 2013). This result raises a concern that the direct exposure of mouse embryos to the culture medium by ZP drilling might lead to the presence of xenobiotics in embryos. However, further studies are now needed to understand the metabolic changes caused by embryo ZP-manipulation.

The transcriptomic variations described in this chapter might be the result of the enhanced transferring of nutrients/chemicals from culture medium through the opening in the ZP or the stress caused by laser-assisted ZP drilling. However, further studies, particularly with regards to metabolomics analysis, are needed to investigate the embryonic metabolic response to ZP manipulation. In addition, it would be interesting to compare the different impacts between ZP-drilling and ZP-thinning on embryo transcriptome. Furthermore, it is crucial to understand whether the changes in embryonic metabolism at the blastocyst stage will have lasting influences on the health of the offspring. Longer periods of follow-up involving the offspring arising from ZP drilling in mice will be crucial in future studies and should focus particularly on metabolic activity.

6.5 Concluding remarks

This is the first study to characterise the mouse blastocyst transcriptome during the *in vitro* hatching process with the application of RNA-seq. Results indicated that mouse embryo hatching *in vitro* is ATP dependent, and a process that protein biosynthesis is highly activated. The findings described herein reveal the novel genes and pathways involved in the dynamic process of hatching, particularly with regards to cytoskeleton organisation; the RhoA signaling pathway may play an important role during hatching process. Upstream regulators, including growth factors (AGT and FGF2), oestrogen receptor, and PRL, are ideal candidates for future investigation as they have the potential to alter the expression of important downstream genes for the hatching process. In addition, this study pointed towards the key genes and pathways impacted by laser-assisted ZP drilling, which have never been directly associated with the

influence of ZP manipulation on embryos previously. Overall, this work serves as the basis for more extensive research to investigate the candidate genes and pathways that involved in embryo hatching and combat the potential impact of laser-assisted ZP manipulation with the ultimate goal of improving embryo developmental competence.

6.6 Key findings

- The *in vitro* hatching of mouse blastocysts is an ATP-dependent process, and protein biosynthesis is highly activated
- Cytoskeleton organisation, enriched in the network genes of *Arpc2, Cfl1, Gsn, Pfn1, Shmt1, Tpi1, Tuba1b, Grb2, Tmsb10, Enah, Ldlrap1, and Rnd3*, plays a key role in the hatching of mouse blastocysts. In addition, the RhoA signaling could be a vital regulatory pathway that participated in the hatching process
- The clustered genes: *Krt8, Krt7, Krt18, Cldn4*, and *Aqp3*, involved in cell-cell junction and water homeostasis, are implicated in the hatching process
- Upstream regulators, such as growth factors (AGT and FGF2) and hormones (oestrogen receptor and PRL), are predicted to regulate the hatching process
- Laser-assisted ZP drilling could induce the subtle transcriptome alteration in the embryo, and may potentially change the blastocysts metabolic activity



Chapter 7

General discussion and future work

7.1 General summary of main findings

ART has undergone tremendous advancements over the past few decades and is widely applied to help with various infertility problems (Adamson et al., 2018); however, the success rate of ART cycles remains low, and implantation failure is a significant challenge (HFEA, 2019). As a powerful technique in ART, IR diode laser technology is highly efficient, reproducible, and easy to use; and it has been widely used in the various oocyte, sperm, and embryo manipulations (Davidson et al., 2019).

Although the mechanism underlying embryo hatching is unclear, ZP manipulations have been proven to assist the hatching process. Nevertheless, the efficiency of ZP manipulation remains contradictory, and there is a paucity of literature pertaining to the safety of such laser ZP manipulations, particularly at the molecular level. Therefore, this thesis attempted to characterize the current clinical practice of ZP manipulations, investigate the potential deleterious effect of laser-assisted ZP manipulations on mouse embryos, and reveal the potential mechanisms underlying blastocyst hatching.

7.1.1 The disparity of assisted hatching (AH) practice

AH has been used to improve implantation (AHpET) as well as facilitate the subsequent embryo biopsy (AHpBP); however, there is no consensus on the overall efficiency or the optimal protocol (Hammadeh et al., 2011, Alteri et al., 2018). Furthermore, there is a notable absence of literature relating to the current clinical practice of AH.

Therefore, **Chapter 3** investigated the application of AHpBP and AHpET and characterised the patterns of clinical practice for both applications. According to the results of 181 online questionnaires, I found that AH is widely used in clinics, and 89.2%

of respondents claimed AHpBP is routinely used. Intriguingly, AHpET is also commonly used in clinics, especially in the area outside the UK (76.4%). But these respondents claimed that AHpET is applied with clear clinical indicators, including patients with a poor prognosis, embryos with a thick ZP, or thaw/warm embryos. Although most clinics use non-contact laser for AH, there is a wide disparity in AH protocols, such as embryo stage, the time interval between AH and biopsy/ET, and the ZP manipulation. In addition, I found that ZP drilling is the primary method used for AHpBP (78.4%); while both the ZP thinning and ZP drilling methods are commonly used for AHpET in clinics (46.4% and 37.1%). The importance of the opening size in the ZP for hatching completion has been demonstrated in previous studies (Montag et al., 2000a, Chailert et al., 2013); however, in this survey, I showed that majority of responders perform laser ZP drilling to create the small size of the opening (<15 μm) for both AHpBP (71.1%) and AHpET (72.1%). In addition, ZP thinning was more frequently used in AHpET with the ablation area less than (33.3%) or equal to (37.8%) ¼ of the ZP circumference. On the other hand, despite ongoing controversy relating to the efficacy of AH, most responders believed that AH is a safe technique and could be beneficial to embryo implantation. However, concerns regarding the potential damage caused by laser treatment on embryos were raised.

Collectively, although more extensive investigations are required, this present data provided an overview of the clinical AH application and revealed the commonalities and disparities in the current clinical practice. These results might partially explain the inconsistency of clinical efficacy, thus highlighting the importance of the standardisation and refinement of AH in the future study.

7.1.2 The safety of laser-assisted ZP manipulations on preimplantation embryos

Concerns about thermal damage have been raised with respect to the application of lasers to embryos. Previous studies regarding the effect of laser-assisted ZP manipulations on embryos from both humans and animals have been predominantly focused on the whole organism level; however, there is a notable absence of evidence evaluating the impact at the molecular level. Therefore, the second aim of this thesis sought to evaluate any deleterious effect(s) of the commonly used laser-assisted ZP manipulations. To mimic the clinical practice of ZP drilling, I set the opening size for ZP drilling as 7.5 μm (equivalent to 15 μm in human embryos). In addition, ZP- partial drilling and quarter ZP thinning were also used to mimic the different extensions of ZP thinning in the clinic.

In **Chapter 4**, I investigated the effect of laser-assisted ZP manipulations on preimplantation mouse embryos from a variety of different aspects, but with particular focus on blastocyst formation, hatching pattern, embryonic cell number and differentiation, cell stress and apoptosis, and transcriptomic alternations. I found that neither laser-assisted ZP-drilling, ZP-partial drilling, nor ZP thinning interfered with the formation of blastocysts. Furthermore, these ZP manipulations did not affect blastocyst cell proliferation or cell differentiation, as determined by the unchanged cell numbers (total cells, the TE and the ICM cells) and the mRNA expression levels of embryo segregation markers (*Pou5f1, Cdx2,* and *Nanog*). In addition, the data obtained suggested that the laser-assisted ZP manipulations would not induce embryonic cell apoptosis, as indicated by DNA fragmentation, caspase-3/7 activation, and the mRNA expression levels of apoptosis-related genes (*Bax* and *Bcl2l2*) and

oxidative stress-related genes (*Gpx7* and *Sod1*). Furthermore, no increase in the protein expression of HSP70 was detected in the resulting blastocysts following ZP manipulations; thus, suggesting that these tested ZP manipulations do not induce further cell stress in preimplantation embryos.

In line with previous studies, I found that ZP drilling significantly advanced the initiation of embryo hatching. In addition, the reduced number of cells in hatching embryos from the ZP drilling group also supported the fact that the laser-drilled ZP opening allows embryos to begin hatching without reaching a certain embryonic cell number. Furthermore, the ZP drilling led to the '8-shape' hatching pattern referred to as 'herniation' (Blake et al., 2001). This induced 'herniation' was believed to facilitate the TE separation during the blastocyst biopsy; thus, laser-assisted ZP drilling is more suitable for the pre-hatching of blastocyst biopsy (Capalbo et al., 2016, Rubino et al., 2020). This was consistent with the findings shown in **Chapter 3**. In contrast, the ZP thinning led to a greater proportion of 'U-shape' hatching embryos; this pattern is more frequently seen in the in vivo developed embryos (Yan et al., 2015). In addition, ZP thinning was shown to suppress the expression of HSP70 in the blastocyst. These results suggested that ZP thinning might decrease the blastocyst cell stress by changing the integrity of the ZP. The difference in hatching patterns induced by ZP drilling and ZP thinning suggest that these two methods may have different impacts on embryos. It would be interesting to use time-lapse to investigate how these induced hatching patterns are related to pregnancy outcomes.

Thus far, previous investigations have not detected any changes in the expression levels of genes related to apoptosis, oxidative stress, or epigenetic modification following laser-assisted ZP manipulations (Honguntikar et al., 2017, Huang et al.,

2019). Nevertheless, no research to date has investigated the effect of laser manipulation on the embryonic transcriptome. Thus, in **Chapter 6**, for the first time, I used RNA-seq to investigate the potential transcriptional alterations induced by cleavage-stage laser-ZP drilling by comparing the transcriptome between the laser-assisted ZP drilled blastocysts and untreated blastocysts. However, only 48 DEGs were detected with low fold changes, thus suggesting that laser-assisted ZP drilling does not induce overt alterations at the transcriptional level. However, the downstream analysis suggested that ZP drilling at the cleavage stage potentially affects blastocyst metabolism; because the lipid, amino acid, and Xenobiotic metabolism-related pathways were significantly enriched in the DEGs. To the best of my knowledge, it is the first time that transcriptomic changes induced by laser-assisted ZP drilling were detected, thus implicating the impact of the ZP manipulations on embryos at the molecular level. Further investigation of the alteration at protein levels, and the potential changes in metabolic activity, will be crucial.

7.1.3 The effect of laser-assisted ZP manipulations on the competency of embryo implantation

The precise efficiency of laser ZP manipulations on clinical outcomes remains controversial; this may be due to the variety of protocols and patient groups described in the IVF centre. Therefore, the aim of **Chapter 5** was to investigate the effect of commonly applied laser ZP manipulations on the embryonic competence for implantation. I utilised the Ishikawa cell-based *in vitro* implantation model so that no maternal factors would affect embryo hatching or embryo attachment.

Although laser ZP drilling could advance hatching initiation and induce the TE herniation for the benefit of blastocyst biopsy, the implantation model in **Chapter 5**

suggested that laser ZP drilling may cause embryo entrapment, which may be related to the size of the perforation in the ZP. These findings indicated the potential risk of embryo entrapment when applying ZP drilling in clinics practice since most clinics drill the ZP to create the small opening for AHpBP. Nevertheless, such embryo entrapment is rarely observed in clinics because of the short period of *in vitro* culture (Rubino et al., 2020). Therefore, results here highlight the importance of optimising the laser-assisted drilling protocol in the clinic, especially the ZP opening size, in order to avoid the risk of embryo entrapment and to maintain embryo hatching efficiency. Interestingly, embryo attachment assays suggested that laser ZP manipulations do not impact the attachment capability of embryos. However, the entrapment caused by ZP drilling may affect the embryo implantation since only fully hatched embryos could implant into the uterus ultimately. Therefore, further *in vivo* observations are required to understand how these ZP manipulations affect embryo implantations and live birth.

Furthermore, in **Chapter 5**, I also investigated the effect of laser-assisted ZP manipulation on blastulation-delayed embryos. The reason for the poor pregnancy outcomes of transferring this type of embryos remains unclear (Desai et al., 2016). In this study, blastulation-delayed embryos (E5.5 blastocysts) showed the reduced possibility of hatching completion and attachment capability, which may explain the poor clinical outcomes. Interestingly, I found that laser-assisted ZP manipulations, especially ZP drilling, could improve the hatching completion and attachment capability of E5.5 blastocysts. Although preliminary and in need of more extensive validation studies, the present data indicates the therapeutic potential of ZP manipulation for blastulation-delayed embryos.

7.1.4 Potential genes and mechanisms involved in blastocyst hatching

Blastocyst hatching remains one of the least studied aspects of early mammalian development; most previous studies investigated the hatching mechanism by using different inhibitors and activators to target specific molecules and then observing the hatching results. In **Chapter 6**, I used the RNA-seq to characterise the transcriptomic profile of the hatching blastocyst for the first time. I aimed to identify potential genes and pathways involved in the hatching process of the mouse embryo.

Analysis of DEGs between hatching and pre-hatching blastocysts suggested that hatching *in vitro* is an ATP-dependent process; protein biosynthesis and cytoskeleton organisation are highly activated. Downstream analysis indicated that RhoA signaling, by regulating the actin-based cell motility, might be a critical signaling pathway in the hatching process. In addition, the network of genes, including *Actb, Myl6, Cfl1, Gsn, Pfn1, Arpc2, Rnd3, Grb2, Tuba1b, Tpi1, Shmt1, Ldlrap1,* and *Tmsb10,* may be involved in the hatching process by participating in the organisation of the cytoskeleton. In addition, the RNA-seq result indicated that the clustered genes (*Krt8, Krt7, Krt18, Cldn4*, and *Aqp3*), by participating in the cell-cell junction and water homeostasis, are important for the hatching process. Furthermore, upstream regulator analysis revealed that growth factors and hormones, such as AGT, FGF2, oestrogen receptor, and PRL, are predicted to actively regulating the hatching process.

For the first time, this present study provides further insight, at the transcriptome level, into the molecular mechanisms underlying embryo hatching. This data revealed potential genes and molecular regulatory pathways involved in the blastocyst hatching

process in mice, which broadens the knowledge of embryo development and provides valuable information to explore the mechanism underlying embryo hatching.

7.2 Limitations of this thesis

Apart from the restrictions related to experimental design and technique described in each chapter, one of the main limitations of this thesis is species-specific differences. The difference in embryonic physiology and metabolism should be considered when interpreting data derived from mice and extrapolating to human conditions. For example, the size of the ZP opening used in this study should not be extrapolated to human embryos since the human ZP is thicker and the volume of the embryo is larger than those of the mouse embryos. The mean diameter of a human cleavage embryo is round two times compared with mouse embryos; thus, any hole created in human embryos should be two times larger than that used for mouse embryos. Furthermore, the potential metabolic response to laser ZP drilling in mouse embryos revealed by RNA-seq may not reflect those in human embryos due to differences in embryonic metabolism between these two species (Lane et al., 1997). Although mouse embryos remain the powerful and informative models to monitor and test the ART manipulations; however, the research on donated human embryos is obviously essential to study human embryo development and confirm the safety of ART techniques.

In addition, the potential mechanisms revealed by RNA-seq might only reflect the embryo hatching process *in vitro* due to differences between *in vitro* and *in vivo* hatching patterns. Ideally, RNA-seq study should also be carried out using *in vivo* hatching and pre-hatching mouse embryos in the same experiment; this would provide information about differences in the embryonic transcriptome between *in vitro* and *in*

vivo culture conditions. This information may be useful in the future optimisation of the *in vitro* culture system.

7.3 Future directions

7.3.1 Further investigation of the embryo metabolism following laser-assisted ZP drilling

Transcriptomic changes and potential impact on embryonic metabolism were, for the first time, found to be induced by laser-assisted ZP drilling; however, further substantial evidence is required. Firstly, gene expression alternation should also be assessed at the protein level, and the changes in the related pathways need to be validated. Secondly, the metabolomic profile of the embryo culture medium can aid to understand the embryo metabolic activity changes over various time-courses after ZP drilling. Furthermore, it is crucial to understand whether the embryonic metabolism changes at the blastocyst stage will have lasting influences on the health of offspring. Thus, the longer-term follow-up of the treated mouse offspring, primarily focusing on the metabolic syndrome, will provide valuable information.

7.3.2 Investigating the embryo implantation following laser-assisted ZP manipulation using *in vivo* model

In this study, the *in vitro* implantation model investigated the attachment capability following different laser ZP manipulations but failed to yield the data related to implantation and live birth results. Therefore, it is urgent to gain further understanding the effect of these ZP manipulations on final pregnancy outcomes. However, using an

appropriate *in vivo* model is critical. In the mice model, treated and untreated embryos could be exposed to the same microenvironment when transferred bilaterally into each uterine horns; thus, avoiding the confounding maternal factor for assessing implantation and pregnancy outcomes. Therefore, in the future study, embryos subjected to different ZP manipulations can be transferred into surrogate mice, and the numbers of offspring and the health of resulting foetuses and new-borns can be observed.

7.3.3 The future clinical studies

First of all, considering the species-specific differences, all safety assessments need to be checked in the donated human embryos, particularly with regards to transcriptomic changes following laser-assisted ZP manipulations. In addition, it would be interesting to study the effect of clinical ZP manipulation on the embryo hatching patterns in human embryos using time-lapse since the alteration of hatching patterns was demonstrated in this study. Thus, the clinical retrospective study could provide useful information on how these different ZP manipulations (e.g., AHpET, AHpBP, and ICSI) affect the hatching process and the pregnancy outcomes. Furthermore, only a few follow-up studies have focused on the children born following LAH so far; thus, large-scare long-term follow-up studies are now needed in order to confirm the safety of different ZP manipulations on the health of offspring.

The apparent disparities in clinical AH application were revealed by the survey, emphasising the importance of refinement and standardisation for these clinical AH procedures. In addition, it also provided information about research priorities for further clinical studies. Thus, more comprehensive clinical studies are needed to investigate the actual value of different AHpET strategies, focusing on the embryo stages, ZP

manipulation methods, and time for ET after AH. Furthermore, considering the high application rate of AHpBP, it is vital that we understand how these different pre-hatching strategies, for example, the size of drilling induced ZP opening and the time to perform ZP drilling, could affect the TE biopsy procedure and the subsequent pregnancy outcomes. Therefore, in order to improve clinical embryo implantation and live birth outcomes, well-designed prospective studies or RCTs, especially multi-centre studies, are crucial in the future to refine and optimise clinical AH protocols.

7.3.4 Investigating the mechanism underlying embryo hatching

RNA-seq data in the present study revealed potential molecular mechanisms underlying hatching in mice, but further studies are critical for deep understanding. Firstly, the expression of DEGs needs to be assessed at the protein level, both quantitively and locationally. Secondly, to investigate the function of target genes and pathways in the blastocyst hatching process, the RNA interference (RNAi)-mediated knockdown method could be applied to embryos. Precisely, small interfering RNA (siRNA) expression vector will be microinjected into the nucleus of mouse zygotes, followed by culturing embryos to the blastocyst stage. Then, the expression of related genes and the embryo hatching ability could be observed.

On the other hand, the results here indicated that blastulation-delayed embryo is related to the risk of hatching and attachment problem. Therefore, detecting the expression level of those hatching-related genes can help to understand the reason for the poor pregnancy outcomes in blastulation delayed embryos; these results could potentially help to develop diagnosis targets in this clinical scenario.

Furthermore, this present study revealed the novel upstream regulators that could regulate the hatching process. Future experiments could be performed by adding specific growth factors or hormones of interest into the embryo culture medium in order to explore the roles of these regulators in the hatching process. In addition, the pregnancy outcomes can be observed after transferring the resulting embryos. The supplementation of growth factors or hormones to the *in vitro* culture medium could potentially achieve the maximal embryo hatching probability. Therefore, these data could facilitate the optimisation of the culture medium in ART treatment.

7.4 General conclusion

Collectively, the present study characterises the clear disparity in the clinical application of assisted hatching and describes the potential impact of laser-assisted ZP manipulations on mouse embryos, especially at the molecular level; thus, emphasising the importance of clinical ZP manipulations optimisation. Furthermore, this study broadens the knowledge of embryo development. For the first time, data in this research provides novel transcriptional information on the mouse embryo hatching, which serves as the basis for further investigation of the hatching mechanism. Future studies, such as applying *in vivo* models and large-scale clinical studies to optimise the laser-assisted ZP manipulation protocols, and functional studies of interesting hatching-related molecules, could improve ART treatment and strengthen understanding of mammalian embryo development.



References

Abdelmassih, S., Cardoso, J., Abdelmassih, V., Dias, J., Abdelmassih, R., Nagy, Z., 2002. Laser-assisted icsi: A novel approach to obtain higher oocyte survival and embryo quality rates. Human Reproduction. 17, 2694-2699

Achache, H., Revel, A., 2006. Endometrial receptivity markers, the journey to successful embryo implantation. Hum. Reprod. Update. 12, 731-746

Adamson, G.D., De Mouzon, J., Chambers, G.M., Zegers-Hochschild, F., Mansour, R., Ishihara, O., et al., 2018. International committee for monitoring assisted reproductive technology: World report on assisted reproductive technology, 2011. Fertil. Steril. 110, 1067-1080

Afonso, S., Romagnano, L., Babiarz, B., 1997. The expression and function of cystatin c and cathepsin b and cathepsin l during mouse embryo implantation and placentation. Development. 124, 3415-3425

Afonso, S., Romagnano, L., Babiarz, B., 1999. Expression of cathepsin proteinases by mouse trophoblast in vivo and in vitro. Dev. Dyn. 216, 374-384

Aghajanova, L., Hoffman, J., Mok-Lin, E., Herndon, C.N., 2017. Obstetrics and gynecology residency and fertility needs: National survey results. Reprod. Sci. 24, 428-434

Alteri, A., Viganò, P., Maizar, A.A., Jovine, L., Giacomini, E., Rubino, P., 2018. Revisiting embryo assisted hatching approaches: A systematic review of the current protocols. J. Assist. Reprod. Genet. 1-25

Aoyama, N., Kato, K., 2020. Trophectoderm biopsy for preimplantation genetic test and technical tips: A review. Reprod. Med. Biol. 19, 222-231

Aplin, J.D., 2000. The cell biological basis of human implantation. Best Practice & Research Clinical Obstetrics & Gynaecology. 14, 757-764

Aplin, J.D., Ruane, P.T., 2017. Embryo–epithelium interactions during implantation at a glance. J. Cell Sci. 130, 15-22

Avella, M.A., Milne, K.A., Dawood, S., Dawood, A., Tucker, M.J., 2019. Assisted hatching of human embryos for successful implantation. In vitro fertilization. Springer, pp. 567-579.

Bader, G.D., Hogue, C.W., 2003. An automated method for finding molecular complexes in large protein interaction networks. BMC Bioinformatics. 4, 2

Balaban, B., Urman, B., Alatas, C., Mercan, R., Mumcu, A., Isiklar, A., 2002. A comparison of four different techniques of assisted hatching. Human Reproduction. 17, 1239-1243

Balakier, H., Mandel, R., Sojecki, A., Motamedi, G., Zaver, S., Librach, C., 2009. Laser zona thinning in women aged⩽ 37 years: A randomized study. Fertil. Steril. 91, 1479-1482

Balakier, H., Sojecki, A., Motamedi, G., Bashar, S., Mandel, R., Librach, C., 2012. Is the zona pellucida thickness of human embryos influenced by women's age and hormonal levels? Fertil. Steril. 98, 77-83

Baltaci, V., Satiroglu, H., Kabukçu, C., Ünsal, E., Aydinuraz, B., Üner, Ö., et al., 2006. Relationship between embryo quality and aneuploidies. Reprod. Biomed. Online. 12, 77-82

Bar-El, L., Kalma, Y., Malcov, M., Schwartz, T., Raviv, S., Cohen, T., et al., 2016. Blastomere biopsy for pgd delays embryo compaction and blastulation: A time-lapse microscopic analysis. J. Assist. Reprod. Genet. 33, 1449-1457

Barcroft, L.C., Offenberg, H., Thomsen, P., Watson, A.J., 2003. Aquaporin proteins in murine trophectoderm mediate transepithelial water movements during cavitation. Dev. Biol. 256, 342-354

Barrenetxea, G., De Larruzea, A.L., Ganzabal, T., Jiménez, R., Carbonero, K., Mandiola, M., 2005. Blastocyst culture after repeated failure of cleavage-stage embryo transfers: A comparison of day 5 and day 6 transfers. Fertil. Steril. 83, 49-53

Barrientos, G., Freitag, N., Tirado-Gonzalez, I., Unverdorben, L., Jeschke, U., Thijssen, V.L., et al., 2014. Involvement of galectin-1 in reproduction: Past, present and future. Hum. Reprod. Update. 20, 175-193

Baruffi, R.L., Mauri, A.L., Petersen, C.G., Ferreira, R.C., Coelho, J., Franco, J.G., 2000. Zona thinning with noncontact diode laser in patients aged⩽ 37 years with no previous failure of implantation: A prospective randomized study. J. Assist. Reprod. Genet. 17, 557-560

Bashiri, A., Halper, K.I., Orvieto, R., 2018. Recurrent implantation failure-update overview on etiology, diagnosis, treatment and future directions. Reprod. Biol. Endocrinol. 16, 121

Bedzhov, I., Liszewska, E., Kanzler, B., Stemmler, M.P., 2012. Igf1r signaling is indispensable for preimplantation development and is activated via a novel function of e-cadherin. PLoS Genet. 8, e1002609

Beere, H.M., Green, D.R., 2001. Stress management–heat shock protein-70 and the regulation of apoptosis. Trends Cell Biol. 11, 6-10

Behr, B., Milki, A.A., 2003. Visualization of atypical hatching of a human blastocyst in vitro forming two identical embryos. Fertil. Steril. 80, 1502-1503

Bell, C.E., Larivière, N.M., Watson, P.H., Watson, A.J., 2009. Mitogen-activated protein kinase (mapk) pathways mediate embryonic responses to culture medium osmolarity by regulating aquaporin 3 and 9 expression and localization, as well as embryonic apoptosis. Hum. Reprod. 24, 1373-1386

Benjamini, Y., Hochberg, Y., 1995. Controlling the false discovery rate: A practical and powerful approach to multiple testing. Journal of the Royal statistical society: series B (Methodological). 57, 289-300

Benkhalifa, M., Kasakyan, S., Clement, P., Baldi, M., Tachdjian, G., Demirol, A., et al., 2005. Array comparative genomic hybridization profiling of first‐trimester spontaneous abortions that fail to grow in vitro. Prenatal Diagnosis: Published in Affiliation With the International Society for Prenatal Diagnosis. 25, 894-900

Bergh, P.A., Navot, D., 1992. The impact of embryonic development and endometrial maturity on the timing of implantation. Fertil. Steril. 58, 537-542

Betts, D., King, W., 2001. Genetic regulation of embryo death and senescence. Theriogenology. 55, 171-191

Betts, D., Madan, P., 2008. Permanent embryo arrest: Molecular and cellular concepts. MHR: Basic science of reproductive medicine. 14, 445-453

Blake, D., Forsberg, A., Johansson, B., Wikland, M., 2001. Laser zona pellucida thinning—an alternative approach to assisted hatching. Hum. Reprod. 16, 1959-1964

Blakeley, P., Fogarty, N.M., Del Valle, I., Wamaitha, S.E., Hu, T.X., Elder, K., et al., 2015. Defining the three cell lineages of the human blastocyst by single-cell rna-seq. Development. 142, 3151-3165

Bleil, J.D., Wassarman, P.M., 1980. Structure and function of the zona pellucida: Identification and characterization of the proteins of the mouse oocyte's zona pellucida. Dev. Biol. 76, 185-202

Boada, M., Carrera, M., De La Iglesia, C., Sandalinas, M., Barri, P., Veiga, A., 1998. Successful use of a laser for human embryo biopsy in preimplantation genetic diagnosis: Report of two cases. J. Assist. Reprod. Genet. 15, 302-307

Boyle, E.I., Weng, S., Gollub, J., Jin, H., Botstein, D., Cherry, J.M., et al., 2004. Go:: Termfinder—open source software for accessing gene ontology information and finding significantly enriched gene ontology terms associated with a list of genes. Bioinformatics. 20, 3710-3715

Braude, P., Bolton, V., Moore, S., 1988. Human gene expression first occurs between the four-and eight-cell stages of preimplantation development. Nature. 332, 459-461

British Fertility Society Policy Practice Sub-Committee, 2001. Survey of laboratory practice—assisted hatching. Hum. Fertil. 4, 219-220

Cao, S., Zhao, C., Zhang, J., Wu, X., Guo, X., Ling, X., 2014. Retrospective clinical analysis of two artificial shrinkage methods applied prior to blastocyst vitrification on the outcome of frozen embryo transfer. J. Assist. Reprod. Genet. 31, 577-581

Capalbo, A., Romanelli, V., Cimadomo, D., Girardi, L., Stoppa, M., Dovere, L., et al., 2016. Implementing pgd/pgd-a in ivf clinics: Considerations for the best laboratory approach and management. J. Assist. Reprod. Genet. 33, 1279-1286

Carbone, L., Chavez, S.L., 2015. Mammalian pre-implantation chromosomal instability: Species comparison, evolutionary considerations, and pathological correlations. Syst. Biol. Reprod. Med. 61, 321-335

Carney, S.K., Das, S., Blake, D., Farquhar, C., Seif, M.M., Nelson, L., 2012. Assisted hatching on assisted conception (in vitro fertilisation (ivf) and intracytoplasmic sperm injection (icsi)). The Cochrane Library.

Carter, A.M., 2007. Animal models of human placentation–a review. Placenta. 28, S41-S47

Chailert, C., Sanmee, U., Piromlertamorn, W., Samchimchom, S., Vutyavanich, T., 2013. Effects of partial or complete laser-assisted hatching on the hatching of mouse blastocysts and their cell numbers. Reprod. Biol. Endocrinol. 11, 21

Chatzimeletiou, K., Morrison, E.E., Panagiotidis, Y., Prapas, N., Prapas, Y., Rutherford, A.J., et al., 2005. Comparison of effects of zona drilling by non-contact infrared laser or acid tyrode's on the development of human biopsied embryos as revealed by blastomere viability, cytoskeletal analysis and molecular cytogenetics. Reprod. Biomed. Online. 11, 697-710

Chatzimeletiou, K., Picton, H.M., Handyside, A.H., 2001. Use of a non-contact, infrared laser for zona drilling of mouse embryos: Assessment of immediate effects on blastomere viability. Reprod. Biomed. Online. 2, 178-187

Chavez, S.L., Loewke, K.E., Han, J., Moussavi, F., Colls, P., Munne, S., et al., 2012. Dynamic blastomere behaviour reflects human embryo ploidy by the four-cell stage. Nature communications. 3, 1-12

Chen, H.-W., Chen, J.J., Yu, S.-L., Li, H.-N., Yang, P.-C., Su, C.-M., et al., 2005. Transcriptome analysis in blastocyst hatching by cdna microarray. Hum. Reprod. 20, 2492-2501

Cheon, Y.P., Gye, M.C., Kim, C.-H., Kang, B.M., Chang, Y.S., Kim, S.R., et al., 1999. Role of actin filaments in the hatching process of mouse blastocyst. Zygote. 7, 123-129

Chiang, T., Schultz, R.M., Lampson, M.A., 2012. Meiotic origins of maternal age-related aneuploidy. Biol. Reprod. 86, 3, 1-7

Choi, K.H., Lee, J.H., Yang, Y.H., Yoon, T.K., Lee, D.R., Lee, W.S., 2011. Efficiency of laser-assisted intracytoplasmic sperm injection in a human assisted reproductive techniques program. Clinical and experimental reproductive medicine. 38, 148-152

Christianson, M.S., Stern, J.E., Sun, F., Zhang, H., Styer, A.K., Vitek, W., et al., 2020. Embryo cryopreservation and utilization in the united states from 2004–2013. F&S Reports. 1, 71-77

Çıray, H.N., Bener, F., Karagenç, L., Ulug, U., Bahçeci, M., 2005. Impact of assisted hatching on art outcome in women with endometriosis. Hum. Reprod. 20, 2546-2549

Cockburn, K., Rossant, J., 2010. Making the blastocyst: Lessons from the mouse. The Journal of clinical investigation. 120, 995-1003

Cohen, J., 2002. Sorting out chromosome errors. American Association for the Advancement of Science.

Cohen, J., Elsner, C., Kort, H., Malter, H., Massey, J., Mayer, M.P., et al., 1990. Impairment of the hatching process following ivf in the human and improvement of implantation by assisting hatching using micromanipulation. Hum. Reprod. 5, 7-13

Cohen, J., Feldberg, D., 1991. Effects of the size and number of zona pellucida openings on hatching and trophoblast outgrowth in the mouse embryo. Mol. Reprod. Dev. 30, 70-78

Comins-Boo, A., Garcia-Segovia, A., Nunez, P., 2016. Evidence-based update: Immunological evaluation of recurrent implantation failure. Reprod Immunol Open Acc. 1, 1-8

Coonen, E., Van Montfoort, A., Carvalho, F., Kokkali, G., Moutou, C., Rubio, C., et al., 2020. Eshre pgt consortium data collection xvi-xviii: Cycles from 2013 to 2015. Hum Reprod Open. 2020, hoaa043

Croft, D., O'kelly, G., Wu, G., Haw, R., Gillespie, M., Matthews, L., et al., 2010. Reactome: A database of reactions, pathways and biological processes. Nucleic Acids Res. 39, D691-D697

Cutting, R., Morroll, D., Roberts, S.A., Pickering, S., Rutherford, A., 2008. Elective single embryo transfer: Guidelines for practice british fertility society and association of clinical embryologists. Hum. Fertil. 11, 131-146

Danfour, M.A., Elmahaishi, M.S., 2010. Human oocyte oolemma characteristic is positively related to embryo developmental competence after icsi procedure. Middle East Fertility Society Journal. 15, 269-273

Das, M., Holzer, H.E., 2012. Recurrent implantation failure: Gamete and embryo factors. Fertil. Steril. 97, 1021-1027

Davidson, L.M., Coward, K., 2016. Molecular mechanisms of membrane interaction at implantation. Birth Defects Research Part C: Embryo Today: Reviews. 108, 19-32

Davidson, L.M., Liu, Y., Griffiths, T., Jones, C., Coward, K., 2019. Laser technology in the art laboratory: A narrative review. Reprod. Biomed. Online. 38, 725-739

De Vos, A., Van Steirteghem, A., 2000. Zona hardening, zona drilling and assisted hatching: New achievements in assisted reproduction. Cells Tissues Organs. 166, 220-227

Debrock, S., Peeraer, K., Spiessens, C., Willemen, D., De Loecker, P., D'hooghe, T., 2011. The effect of modified quarter laser-assisted zona thinning on the implantation rate per embryo in frozen/vitrified-thawed/warmed embryo transfer cycles: A prospective randomized controlled trial. Hum. Reprod. 26, 1997-2007

Deng, Q., Ramsköld, D., Reinius, B., Sandberg, R., 2014. Single-cell rna-seq reveals dynamic, random monoallelic gene expression in mammalian cells. Science. 343, 193-196

Desai, N., Ploskonka, S., Goodman, L., Attaran, M., Goldberg, J.M., Austin, C., et al., 2016. Delayed blastulation, multinucleation, and expansion grade are independently associated with live-birth rates in frozen blastocyst transfer cycles. Fertil. Steril. 106, 1370-1378

Desai, N., Szeptycki, J., Scott, M., Abdelhafez, F.F., Goldfarb, J., 2008. Artificial collapse of blastocysts before vitrification: Mechanical vs. Laser technique and effect on survival, cell number, and cell death in early and expanded blastocysts. Cell Preservation Technology. 6, 181-190

Dey, S., Lim, H., Das, S.K., Reese, J., Paria, B., Daikoku, T., et al., 2004. Molecular cues to implantation. Endocr. Rev. 25, 341-373

Douglas-Hamilton, D.H., Conia, J., 2001. Thermal effects in laser-assisted pre-embryo zona drilling. J. Biomed. Opt. 6, 205-214

Ebner, T., Moser, M., Tews, G., 2005. Possible applications of a non-contact 1.48 µm wavelength diode laser in assisted reproduction technologies. Hum. Reprod. Update. 11, 425-435

Eckert, J.J., Fleming, T.P., 2008. Tight junction biogenesis during early development. Biochimica et Biophysica Acta (BBA)-Biomembranes. 1778, 717-728

Edashige, K., Sakamoto, M., Kasai, M., 2000. Expression of mrnas of the aquaporin family in mouse oocytes and embryos. Cryobiology. 40, 171-175

Edirisinghe, W.R., Ahnonkitpanit, V., Promviengchai, S., Suwajanakorn, S., Pruksananonda, K., Chinpilas, V., et al., 1999. A study failing to determine significant benefits from assisted hatching: Patients selected for advanced age, zonal thickness of embryos, and previous failed attempts. J. Assist. Reprod. Genet. 16, 294-301

Edwards, J., Ealy, A., Hansen, P., 1995. Regulation of heat shock protein 70 synthesis by heat shock in the preimplantation murine embryo. Theriogenology. 44, 329-337

Edwards, R.G., 2005. An astonishing journey into reproductive genetics since the 1950's. Reproduction Nutrition Development. 45, 299-306

Egashira, M., Hirota, Y., 2013. Uterine receptivity and embryo–uterine interactions in embryo implantation: Lessons from mice. Reprod. Med. Biol. 12, 127-132

El Mouatassim, S., Hazout, A., Bellec, V., Menezo, Y., 1999. Glucose metabolism during the final stage of human oocyte maturation: Genetic expression of hexokinase, glucose phosphate isomerase and phosphofructokinase. Zygote. 7, 45-50

El-Toukhy, T., Khalaf, Y., Al-Darazi, K., Andritsos, V., Taylor, A., Braude, P., 2003. Effect of blastomere loss on the outcome of frozen embryo replacement cycles. Fertil. Steril. 79, 1106-1111

Elhussieny, A., El Mandouh, M., Hanafi, S., Mansour, G.M., El-Kotb, A., 2013. Effect of laser assisted hatching on outcome of assisted reproductive technology. Open Journal of Obstetrics and Gynecology. 3, 18

Elnahas, A., Elnahas, T., Azmy, O., Elnoury, A., Abdelhalim, A., Aboelghar, M., et al., 2018. The use of laser assisted hatching of frozen/thawed embryos versus laser assisted hatching of fresh embryos in human intracytoplasmic sperm injection. J. Obstet. Gynaecol. 38, 729-729

Enders, A.C., 2000. Trophoblast-uterine interactions in the first days of implantation: Models for the study of implantation events in the human. Semin. Reprod. Med. Copyright© 2000 by Thieme Medical Publishers, Inc., 333 Seventh Avenue, New …, pp. 255-264.

Eshre Pgt Consortium, Group, S.-E.B.W., Kokkali, G., Coticchio, G., Bronet, F., Celebi, C., et al., 2020. Eshre pgt consortium and sig embryology good practice recommendations for polar body and embryo biopsy for pgt. Human Reproduction Open. 2020, hoaa020

Eshre Special Interest Group of Embryology and Alpha Scientists in Reproductive Medicine, 2017. The vienna consensus: Report of an expert meeting on the development of art laboratory performance indicators. Reprod. Biomed. Online. 35, 494-510

European Societry of Human Reproduction and Embryology, 2016. Art fact sheet.

Farquhar, C., Marjoribanks, J., 2018. Assisted reproductive technology: An overview of cochrane reviews. Cochrane Database Syst. Rev.

Fawzy, M., Emad, M., Mahran, A., Abdelrahman, M.Y., Fetih, A.N., Abdelghafar, H., et al., 2020. A randomized controlled trial of laser-assisted icsi. Hum. Reprod. 35, 2692-2700

Feichtinger, W., Strohmer, H., Fuhrberg, P., Radivojevic, K., Antinori, S., Pepe, G., et al., 1992. Photoablation of oocyte zona pellucida by erbium-yag laser for in-vitro fertilisation in severe male infertility. The Lancet. 339, 811

Feng, H.L., Hershlag, A., Scholl, G.M., Cohen, M.A., 2009. A retroprospective study comparing three different assisted hatching techniques. Fertil. Steril. 91, 1323-1325

Fernández-Gonzalez, R., Moreira, P., Bilbao, A., Jiménez, A., Pérez-Crespo, M., Ramírez, M.A., et al., 2004. Long-term effect of in vitro culture of mouse embryos with serum on mrna expression of imprinting genes, development, and behavior. Proceedings of the National Academy of Sciences. 101, 5880-5885

Festing, M.F., 2004. The choice of animal model and reduction. Alternatives to Laboratory Animals. 32, 59-64

Fields, E., Chard, J., James, D., Treasure, T., 2013. Fertility (update): Summary of nice guidance. BMJ. 346,

Fields, S.D., Hansen, P.J., Ealy, A.D., 2011. Fibroblast growth factor requirements for in vitro development of bovine embryos. Theriogenology. 75, 1466-75

Frydman, N., Madoux, S., Hesters, L., Duvernoy, C., Feyereisen, E., Le Du, A., et al., 2006. A randomized double-blind controlled study on the efficacy of laser zona pellucida thinning on live birth rates in cases of advanced female age. Hum. Reprod. 21, 2131-2135

Fujifilm Irvine Scientific, I., 2020. Collapsing protocol for human blastocyst. .

Gallicano, G.I., 2001. Composition, regulation, and function of the cytoskeleton in mammalian eggs and embryos. Front. Biosci. 6, D1089-1108

Gardner, D.K., Reed, L., Linck, D., Sheehan, C., Lane, M., 2005. Quality control in human in vitro fertilization. Semin. Reprod. Med. Copyright© 2005 by Thieme Medical Publishers, Inc., 333 Seventh Avenue, New …, pp. 319-324.

Geber, S., Bossi, R., Lisboa, C.B., Valle, M., Sampaio, M., 2011. Laser confers less embryo exposure than acid tyrode for embryo biopsy in preimplantation genetic diagnosis cycles: A randomized study. Reprod. Biol. Endocrinol. 9, 58

Gene Ontology Consortium, 2004. The gene ontology (go) database and informatics resource. Nucleic Acids Res. 32, D258-D261

Gentleman, R.C., Carey, V.J., Bates, D.M., Bolstad, B., Dettling, M., Dudoit, S., et al., 2004. Bioconductor: Open software development for computational biology and bioinformatics. Genome Biol. 5, R80

Germond, M., Nocera, D., Senn, A., Rink, K., Delacrétaz, G., Fakan, S., 1995a. Microdissection of mouse and human zona pellucida using a 1.48 µm diode laser beam: Efficacy and safety of the procedure. Fertil. Steril. 64, 604-611

Germond, M., Primi, M.-P., Senn, A., Rink, K., Descloux, L., Delacrétaz, G., 2000. Diode laser for assisted hatching. Photomedicine in gynecology and reproduction. Karger, Basel. 352-365

Germond, M., Senn, A., Rink, K., Delacrétas, G., De Grandi, P., 1995b. Is assisted hatching of frozen-thawed embryos enhancing pregnancy outcome in patients who had several previous indation failures. J Reprod Fertil. 3, 41-42

Gonzales, D.S., Boatman, D.E., Bavister, B.D., 1996. Kinematics of trophectoderm projections and locomotion in the peri‐implantation hamster blastocyst. Developmental dynamics: an official publication of the American Association of Anatomists. 205, 435-444

Graham, M.C., Hoeger, K.M., Phipps, W.R., 2000. Initial ivf-et experience with assisted hatching performed 3 days after retrieval followed by day 5 embryo transfer. Fertil. Steril. 74, 668-671

Green, C.J., Fraser, S.T., Day, M.L., 2015. Insulin-like growth factor 1 increases apical fibronectin in blastocysts to increase blastocyst attachment to endometrial epithelial cells in vitro. Hum. Reprod. 30, 284-298

Green, D.P., 1997. Three-dimensional structure of the zona pellucida. Rev. Reprod. 2, 147-156

Gu, Y.-F., Zhou, Q.-W., Zhang, S.-P., Lu, C.-F., Gong, F., Tan, Y.-Q., et al., 2018. Inner cell mass incarceration in 8-shaped blastocysts does not increase monozygotic twinning in preimplantation genetic diagnosis and screening patients. PLoS One. 13, e0190776

Guerif, F., Bidault, R., Cadoret, V., Couet, M.-L., Lansac, J., Royere, D., 2002. Parameters guiding selection of best embryos for transfer after cryopreservation: A reappraisal. Hum. Reprod. 17, 1321-1326

Guo, G., Huss, M., Tong, G.Q., Wang, C., Sun, L.L., Clarke, N.D., et al., 2010. Resolution of cell fate decisions revealed by single-cell gene expression analysis from zygote to blastocyst. Dev. Cell. 18, 675-685

Hagemann, A.R., Lanzendorf, S.E., Jungheim, E.S., Chang, A.S., Ratts, V.S., Odem, R.R., 2010. A prospective, randomized, double-blinded study of assisted hatching in women younger than 38 years undergoing in vitro fertilization. Fertil. Steril. 93, 586-591

Hamatani, T., Daikoku, T., Wang, H., Matsumoto, H., Carter, M.G., Ko, M.S., et al., 2004. Global gene expression analysis identifies molecular pathways distinguishing blastocyst dormancy and activation. Proceedings of the National Academy of Sciences. 101, 10326-10331

Hammadeh, M.E., Fischer-Hammadeh, C., Ali, K.R., 2011. Assisted hatching in assisted reproduction: A state of the art. J. Assist. Reprod. Genet. 28, 119-128

Hammoud, I., Molina-Gomes, D., Albert, M., Bergere, M., Bailly, M., Wainer, R., et al., 2010. Are zona pellucida laser drilling and polar body biopsy safe for in vitro matured oocytes? J. Assist. Reprod. Genet. 27, 423-427

Hanna, S., El-Sibai, M., 2013. Signaling networks of rho gtpases in cell motility. Cell. Signal. 25, 1955-1961

Hannan, N.J., Paiva, P., Dimitriadis, E., Salamonsen, L.A., 2010. Models for study of human embryo implantation: Choice of cell lines? Biol. Reprod. 82, 235-245

Hardy, K., 1999. Apoptosis in the human embryo. Rev. Reprod. 4, 125-134

Harton, G., Magli, M., Lundin, K., Montag, M., Lemmen, J., Harper, J., 2011. Eshre pgd consortium/embryology special interest group—best practice guidelines for polar body and embryo biopsy for preimplantation genetic diagnosis/screening (pgd/pgs). Hum. Reprod. 26, 41-46

Hartshorn, C., Anshelevich, A., Jia, Y., Wangh, L.J., 2007. Early onset of heat-shock response in mouse embryos revealed by quantification of stress-inducible hsp70i rna. Gene Regul. Syst. Bio. 1, 117762500700100024

Hartshorn, C., Anshelevich, A., Wangh, L.J., 2005. Laser zona drilling does not induce hsp70i transcription in blastomeres of eight-cell mouse embryos. Fertil. Steril. 84, 1547-1550

Herrero, G.L., Cascales Romero, L., Ortiz Salcedo, J.A., Aparicio Gonzalez, M., Ten Morro, J., Bernabeu Perez, R., 2019. Does the trophectoderm biopsy technique affect the result of the genetic analysis in pgt-a cycles? HUMAN REPRODUCTION 34, 111

Hershlag, A., Feng, H.L., 2005. Effect of prefreeze assisted hatching on postthaw survival of mouse embryos. Fertil. Steril. 84, 1752-1754

Hildebrand, S., Hultin, S., Subramani, A., Petropoulos, S., Zhang, Y., Cao, X., et al., 2017. The e-cadherin/amotl2 complex organizes actin filaments required for epithelial hexagonal packing and blastocyst hatching. Sci. Rep. 7, 1-17

Hill, J.A., 2001. Maternal-embryonic cross-talk. Ann. N. Y. Acad. Sci. 943, 17-25

Hiraoka, K., Fuchiwaki, M., Hiraoka, K., Horiuchi, T., Murakami, T., Kinutani, M., et al., 2008. Effect of the size of zona pellucida opening by laser assisted hatching on clinical outcome of frozen cleaved embryos that were cultured to blastocyst after thawing in women with multiple implantation failures of embryo transfer: A retrospective study. J. Assist. Reprod. Genet. 25, 129-135

Hiraoka, K., Hiraoka, K., Horiuchi, T., Kusuda, T., Okano, S., Kinutani, M., et al., 2009. Impact of the size of zona pellucida thinning area on vitrified-warmed cleavage-stage embryo transfers: A prospective, randomized study. J. Assist. Reprod. Genet. 26, 515-521

Honguntikar, S.D., Salian, S.R., D'souza, F., Uppangala, S., Kalthur, G., Adiga, S.K., 2017. Epigenetic changes in preimplantation embryos subjected to laser manipulation. Lasers Med. Sci. 1-7

Honguntikar, S.D., Uppangala, S., Salian, S.R., Kalthur, G., Kumar, P., Adiga, S.K., 2015. Laser-assisted hatching of cleavage-stage embryos impairs developmental potential and increases DNA damage in blastocysts. Lasers Med. Sci. 30, 95-101

Houghton, F.D., Hawkhead, J.A., Humpherson, P.G., Hogg, J.E., Balen, A.H., Rutherford, A.J., et al., 2002. Non-invasive amino acid turnover predicts human embryo developmental capacity. Hum. Reprod. 17, 999-1005

Houghton, F.D., Humpherson, P.G., Hawkhead, J.A., Hall, C.J., Leese, H.J., 2003. Na+, k+, atpase activity in the human and bovine preimplantation embryo. Dev. Biol. 263, 360-366

Houghton, F.D., Leese, H.J., 2004. Metabolism and developmental competence of the preimplantation embryo. European Journal of Obstetrics & Gynecology and Reproductive Biology. 115, S92-S96

Hsieh, Y.-Y., Huang, C.-C., Cheng, T.-C., Chang, C.-C., Tsai, H.-D., Lee, M.-S., 2002. Laser-assisted hatching of embryos is better than the chemical method for enhancing the pregnancy rate in women with advanced age. Fertil. Steril. 78, 179-182

Huang, L., Mivechi, N.F., Moskophidis, D., 2001. Insights into regulation and function of the major stress-induced hsp70 molecular chaperone in vivo: Analysis of mice with targeted gene disruption of the hsp70. 1 orhsp70. 3 gene. Mol. Cell. Biol. 21, 8575-8591

Huang, Z., Liu, J., Gao, L., Zhuan, Q., Luo, Y., Zhu, S., et al., 2019. The impacts of laser zona thinning on hatching and implantation of vitrified-warmed mouse embryos. Lasers Med. Sci. 34, 939-945

Human Fertilisation and Embryology Authority, 2019. Fertility treatment 2017: Trends and figures.

Human Fertilisation and Embryology Authority, 2020. Fertility treatment 2018: Trends and figures.

Hur, Y.S., Park, J.H., Ryu, E.K., Yoon, H.J., Yoon, S.H., Hur, C.Y., et al., 2011. Effect of artificial shrinkage on clinical outcome in fresh blastocyst transfer cycles. Clinical and experimental reproductive medicine. 38, 87-92

Hurst, B.S., Tucker, K.E., Awoniyi, C.A., Schlaff, W.D., 1998. Assisted hatching does not enhance ivf success in good-prognosis patients. J. Assist. Reprod. Genet. 15, 62-64

Ikemoto, Y., Kuroda, K., Ochiai, A., Yamashita, S., Ikuma, S., Nojiri, S., et al., 2018. Prevalence and risk factors of zygotic splitting after 937 848 single embryo transfer cycles. Hum. Reprod. 33, 1984-1991

Illera, M.J., Cullinan, E., Gui, Y., Yuan, L., Beyler, S.A., Lessey, B.A., 2000. Blockade of the αvβ3 integrin adversely affects implantation in the mouse. Biol. Reprod. 62, 1285-1290

Irvine, D.S., 1998. Epidemiology and aetiology of male infertility. Hum. Reprod. 13, 33-44

Jacob, S., Moley, K.H., 2005. Gametes and embryo epigenetic reprogramming affect developmental outcome: Implication for assisted reproductive technologies. Pediatr. Res. 58, 437-446

Jamieson, S., 2004. Likert scales: How to (ab) use them. Med. Educ. 38, 1217-1218

Jing, Z., Zhang, N.-Y., Xu, Z.-P., Chen, L.-J., Xia, Z., Zeng, H.-M., et al., 2015. Effects of abnormal zona pellucida on fertilization and pregnancy in ivf/icsi-et. Journal of Reproduction and Contraception. 26, 73-80

Jones, A.E., Wright, G., Kort, H.I., Straub, R.J., Nagy, Z.P., 2006. Comparison of laser-assisted hatching and acidified tyrode's hatching by evaluation of blastocyst development rates in sibling embryos: A prospective randomized trial. Fertil. Steril. 85, 487-491

Joris, H., De Vos, A., Janssens, R., Devroey, P., Liebaers, I., Van Steirteghem, A., 2003. Comparison of the results of human embryo biopsy and outcome of pgd after zona drilling using acid tyrode medium or a laser. Hum. Reprod. 18, 1896-1902

Joshi, A., Kale, S., Chandel, S., Pal, D.K., 2015. Likert scale: Explored and explained. British Journal of Applied Science & Technology. 7, 396

Kanehisa, M., Sato, Y., Kawashima, M., Furumichi, M., Tanabe, M., 2016. Kegg as a reference resource for gene and protein annotation. Nucleic Acids Res. 44, D457-D462

Kang, Y.-J., Forbes, K., Carver, J., Aplin, J.D., 2014. The role of the osteopontin–integrin αvβ3 interaction at implantation: Functional analysis using three different in vitro models. Hum. Reprod. 29, 739-749

Kannan, K., Jain, S.K., 2000. Oxidative stress and apoptosis. Pathophysiology. 7, 153-163

Kanyo, K., Konc, J., 2003. A follow-up study of children born after diode laser assisted hatching. European Journal of Obstetrics & Gynecology and Reproductive Biology. 110, 176-180

Keefe, D., Tran, P., Pellegrini, C., Oldenbourg, R., 1997. Polarized light microscopy and digital image processing identify a multilaminar structure of the hamster zona pellucida. Human reproduction (Oxford, England). 12, 1250-1252

Kelk, D., Sawarkar, S., Liu, Y., Dufton, M., Ribustello, L., Munne, S., 2017. Does laser assisted biopsy introduce mosaic or chaotic changes to biopsied cells? Fertil. Steril. 108, e88

Khalili, M.A., Nottola, S.A., Shahedi, A., Macchiarelli, G., 2013. Contribution of human oocyte architecture to success of in vitro maturation technology. Iranian journal of reproductive medicine. 11, 1

Khanmohammadi, N., Movahedin, M., Safari, M., Sameni, H.R., Yousefi, B., Jafari, B., et al., 2016. Effect of l-carnitine on in vitro developmental rate, the zona

pellucida and hatching of blastocysts and their cell numbers in mouse embryos. International Journal of Reproductive BioMedicine. 14, 649

Kiapekou, E., Loutradis, D., Mastorakos, G., Bletsa, R., Beretsos, P., Zapanti, E., et al., 2009. Effect of prl on in vitro follicle growth, in vitro oocyte maturation, fertilization and early embryonic development in mice. Cloning Stem Cells. 11, 293-300

Kim, D., Langmead, B., Salzberg, S.L., 2015. Hisat: A fast spliced aligner with low memory requirements. Nature methods. 12, 357-360

Kim, D., Sul, H., Jung, Y.-G., Roh, S., 2017. Holding of bovine blastocysts at suprazero temperatures using small molecules. Scientific reports. 7, 9490

Kimura, Y., Yanagimachi, R., 1995. Intracytoplasmic sperm injection in the mouse. Biol. Reprod. 52, 709-720

Kiraz, Y., Adan, A., Yandim, M.K., Baran, Y., 2016. Major apoptotic mechanisms and genes involved in apoptosis. Tumour Biol. 37, 8471-8486

Kirillova, A., Lysenkov, S., Farmakovskaya, M., Kiseleva, Y., Martazanova, B., Mishieva, N., et al., 2020. Should we transfer poor quality embryos? Fertility research and practice. 6, 1-7

Kirkegaard, K., Juhl Hindkjaer, J., Ingerslev, H.J., 2012. Human embryonic development after blastomere removal: A time-lapse analysis. Hum. Reprod. 27, 97-105

Kissin, D.M., Kawwass, J.F., Monsour, M., Boulet, S.L., Session, D.R., Jamieson, D.J., 2014. Assisted hatching: Trends and pregnancy outcomes, united states, 2000–2010. Fertil. Steril. 102, 795-801

Knopman, J.M., Krey, L.C., Oh, C., Lee, J., Mccaffrey, C., Noyes, N., 2014. What makes them split? Identifying risk factors that lead to monozygotic twins after in vitro fertilization. Fertil. Steril. 102, 82-89

Knudtson, J.F., Failor, C.M., Gelfond, J.A., Goros, M.W., Chang, T.A., Schenken, R.S., et al., 2017. Assisted hatching and live births in first-cycle frozen embryo transfers. Fertil. Steril. 108, 628-634

Kochevar, I.E., 1989. Cytotoxicity and mutagenicity of excimer laser radiation. Lasers in surgery and medicine. 9, 440-445

Kokkali, G., Traeger-Synodinos, J., Vrettou, C., Stavrou, D., Jones, G., Cram, D., et al., 2007. Blastocyst biopsy versus cleavage stage biopsy and blastocyst transfer for preimplantation genetic diagnosis of β-thalassaemia: A pilot study. Hum. Reprod. 22, 1443-1449

Kung, F.-T., Lin, Y.-C., Tseng, Y.-J., Huang, F.-J., Tsai, M.-Y., Chang, S.-Y., 2003. Transfer of frozen–thawed blastocysts that underwent quarter laser-assisted hatching at the day 3 cleaving stage before freezing. Fertil. Steril. 79, 893-899

Kutlu, P., Atvar, O., Vanlioglu, O.F., 2010. Laser assisted zona thinning technique has no beneficial effect on the art outcomes of two different maternal age groups. J. Assist. Reprod. Genet. 27, 457-461

Lane, M., Gardner, D., 1997. Differential regulation of mouse embryo development and viability by amino acids. Reproduction. 109, 153-164

Lanzendorf, S.E., Nehchiri, F., Mayer, J.F., Oehninger, S., Muasher, S.J., 1998. A prospective, randomized9 double-blind study for the evaluation of assisted hatching in patients with advanced nlaternal age. Hum. Reprod. 13, 409-413

Lanzendorf, S.E., Ratts, V.S., Moley, K.H., Goldstein, J.S., Dahan, M.H., Odem, R.R., 2007. A randomized, prospective study comparing laser-assisted hatching and assisted hatching using acidified medium. Fertility and sterility. 87, 1450-1457

Leese, H.J., 2012. Metabolism of the preimplantation embryo: 40 years on. Reproduction. 143, 417-27

Leonavicius, K., Royer, C., Preece, C., Davies, B., Biggins, J.S., Srinivas, S., 2018. Mechanics of mouse blastocyst hatching revealed by a hydrogel-based microdeformation assay. Proceedings of the National Academy of Sciences. 115, 10375-10380

Lessey, B.A., Yeh, I.-T., Castelbaum, A.J., Fritz, M.A., Ilesanmi, A.O., Korzeniowski, P., et al., 1996. Endometrial progesterone receptors and markers of uterine receptivity in the window of implantation. Fertil. Steril. 65, 477-483

Levens, E.D., Whitcomb, B.W., Hennessy, S., James, A.N., Yauger, B.J., Larsen, F.W., 2008. Blastocyst development rate impacts outcome in cryopreserved blastocyst transfer cycles. Fertil. Steril. 90, 2138-2143

Li, D., Yang, D.-L., An, J., Jiao, J., Zhou, Y.-M., Wu, Q.-J., et al., 2016. Effect of assisted hatching on pregnancy outcomes: A systematic review and meta-analysis of randomized controlled trials. Sci. Rep. 6, 31228

Liao, Y., Smyth, G.K., Shi, W., 2014. Featurecounts: An efficient general purpose program for assigning sequence reads to genomic features. Bioinformatics. 30, 923-930

Liebermann, J., Nawroth, F., Isachenko, V., Isachenko, E., Rahimi, G., Tucker, M.J., 2002. Potential importance of vitrification in reproductive medicine. Biol. Reprod. 67, 1671-1680

Lightfoot, D.A., Kouznetsova, A., Mahdy, E., Wilbertz, J., Höög, C., 2006. The fate of mosaic aneuploid embryos during mouse development. Dev. Biol. 289, 384-394

Lim, H.Y.G., Alvarez, Y.D., Gasnier, M., Wang, Y., Tetlak, P., Bissiere, S., et al., 2020. Keratins are asymmetrically inherited fate determinants in the mammalian embryo. Nature. 585, 404-409

Lim, J., Thiery, J.P., 2012. Epithelial-mesenchymal transitions: Insights from development. Development. 139, 3471-3486

Linder, S., Kopp, P., 2005. Podosomes at a glance. J. Cell Sci. 118, 2079-2082

Liu, C., Su, K., Shang, W., Ji, H., Yuan, C., Cao, M., et al., 2020. Higher implantation and live birth rates with laser zona pellucida breaching than thinning in single frozen-thawed blastocyst transfer. Lasers Med. Sci. 1-7

Liu, W.-X., Zheng, Y., Luo, M.-J., Huang, P., Yue, L.-M., Wang, L., et al., 2005. Effects of removal of necrotic blastomeres from mouse cryopreserved embryos on blastocyst formation and hatching. Theriogenology. 64, 1114-1120

Livak, K.J., Schmittgen, T.D., 2001. Analysis of relative gene expression data using real-time quantitative pcr and the 2− δδct method. Methods. 25, 402-408

Lu, H.-F., Peng, F.-S., Chen, S.-U., Chiu, B.-C., Yeh, S.-H., Hsiao, S.-M., 2015. The outcomes of intracytoplasmic sperm injection and laser assisted hatching in women undergoing in vitro fertilization are affected by the cause of infertility. International journal of fertility & sterility. 9, 33

Lu, Y.-C., Ding, G.-L., Yang, J., Zhang, Y.-L., Shi, S., Zhang, R.-J., et al., 2012. Small-conductance calcium-activated k+ channels 3 (sk3) regulate blastocyst hatching by control of intracellular calcium concentration. Hum. Reprod. 27, 1421-1430

Luft, J.C., Dix, D.J., 1999. Hsp70 expression and function during embryogenesis. Cell Stress Chaperones. 4, 162

Lyu, Q., Yan, Z., 2015. Small openings in the zona pellucida increase the risk of inner cell mass splitting in hatching blastocysts during in vitro culture. Fertil. Steril. 104, e314

Macklon, N., Ahuja, K., Fauser, B., 2019. Building an evidence base for ivf 'add-ons'. Reprod Biomed Online. 38, 853-856

Madissoon, E., Töhönen, V., Vesterlund, L., Katayama, S., Unneberg, P., Inzunza, J., et al., 2014. Differences in gene expression between mouse and human for dynamically regulated genes in early embryo. PLoS One. 9,

Mahdavinezhad, F., Kazemi, P., Fathalizadeh, P., Sarmadi, F., Sotoodeh, L., Hashemi, E., et al., 2019. In vitro versus in vivo: Development-, apoptosis-, and implantation- related gene expression in mouse blastocyst. Iran J Biotechnol. 17, e2157

Malter, H.E., Cohen, J., 1989. Blastocyst formation and hatching in vitro following zona drilling of mouse and human embryos. Mol. Reprod. Dev. 24, 67-80

Mamo, S., Sargent, C., Affara, N., Tesfaye, D., El‐Halawany, N., Wimmers, K., et al., 2006. Transcript profiles of some developmentally important genes detected in

bovine oocytes and in vitro-produced blastocysts using rna amplification and cdna microarrays. Reproduction in domestic animals. 41, 527-534

Mansuy, D., 2013. [metabolism of xenobiotics: Beneficial and adverse effects]. Biol. Aujourdhui. 207, 33-7

Mantoudis, E., Podsiadly, B., Gorgy, A., Venkat, G., Craft, I., 2001. A comparison between quarter, partial and total laser assisted hatching in selected infertility patients. Hum. Reprod. 16, 2182-2186

Margalioth, E., Ben-Chetrit, A., Gal, M., Eldar-Geva, T., 2006. Investigation and treatment of repeated implantation failure following ivf-et. Hum. Reprod. 21, 3036-3043

Marina, N., Do, T.P., Namireddy, P., Sharma, N., Cherry, C.R., Parent, T., et al., 2019. The use of liquid and tissue biopsy genomic testing in lung cancer: A single-institution experience. J. Clin. Oncol. 37, e20692-e20692

Martin, K., Barlow, D., Sargent, I., 1998. Heparin-binding epidermal growth factor significantly improves human blastocyst development and hatching in serum-free medium. Human Reproduction (Oxford, England). 13, 1645-1652

Martins, W.P., Rocha, I.A., Ferriani, R.A., Nastri, C.O., 2011. Assisted hatching of human embryos: A systematic review and meta-analysis of randomized controlled trials. Hum. Reprod. Update. 17, 438-453

Matsuura, K., Hayashi, N., Takiue, C., Hirata, R., Habara, T., Naruse, K., 2010. Blastocyst quality scoring based on morphologic grading correlates with cell number. Fertil. Steril. 94, 1135-1137

Mclaren, A., 1970. The fate of the zona pellucida in mice. Development. 23, 1-19

Mclaughlin, J.E., Choi, B.Y., Liu, Q., Gelfond, J.A., Robinson, R.D., Chang, T.A., et al., 2019. Does assisted hatching affect live birth in fresh, first cycle in vitro fertilization in good and poor prognosis patients? J. Assist. Reprod. Genet. 36, 2425-2433

Ménézo, Y.J., Hérubel, F., 2002. Mouse and bovine models for human ivf. Reprod. Biomed. Online. 4, 170-175

Miyata, H., Matsubayashi, H., Fukutomi, N., Matsuba, J., Koizumi, A., Tomiyama, T., 2010. Relevance of the site of assisted hatching in thawed human blastocysts: A preliminary report. Fertil. Steril. 94, 2444-2447

Mo, B., Vendrov, A.E., Palomino, W.A., Dupont, B.R., Apparao, K., Lessey, B.A., 2006. Ecc-1 cells: A well-differentiated steroid-responsive endometrial cell line with characteristics of luminal epithelium. Biol. Reprod. 75, 387-394

Montag, M., Koll, B., Holmes, P., Ven, H.V.D., 2000a. Significance of the number of embryonic cells and the state of the zona pellucida for hatching of mouse blastocysts in vitro versus in vivo. Biol. Reprod. 62, 1738-1744

Montag, M., Rink, K., Delacrétaz, G., Van Der Ven, H., 2000b. Laser-induced immobilization and plasma membrane permeabilization in human spermatozoa. Hum. Reprod. 15, 846-852

Montag, M., Van Der Ven, H., 1999. Laser-assisted hatching in assisted reproduction

. Croat. Med. J. 40, 398-403

Montag, M., Van Der Ven, K., Delacrétaz, G., Rink, K., Van Der Ven, H., 1998. Laser-assisted microdissection of the zona pellucida facilitates polar body biopsy. Fertil. Steril. 69, 539-542

Montag, M.H., Klose, R., Köster, M., Rösing, B., Van Der Ven, K., Rink, K., et al., 2009. Application of non-contact laser technology in assisted reproduction. Medical Laser Application. 24, 57-64

Moriwaki, K., Tsukita, S., Furuse, M., 2007. Tight junctions containing claudin 4 and 6 are essential for blastocyst formation in preimplantation mouse embryos. Dev. Biol. 312, 509-522

Mosser, D.D., Caron, A.W., Bourget, L., Denis-Larose, C., Massie, B., 1997. Role of the human heat shock protein hsp70 in protection against stress-induced apoptosis. Mol. Cell. Biol. 17, 5317-5327

Mukaida, T., Oka, C., Goto, T., Takahashi, K., 2006. Artificial shrinkage of blastocoeles using either a micro-needle or a laser pulse prior to the cooling steps of vitrification improves survival rate and pregnancy outcome of vitrified human blastocysts. Hum. Reprod. 21, 3246-3252

Murrell, M., Oakes, P.W., Lenz, M., Gardel, M.L., 2015. Forcing cells into shape: The mechanics of actomyosin contractility. Nature reviews Molecular cell biology. 16, 486-498

Naderi, M.M., Borjian Boroujeni, S., Sarvari, A., Heidari, B., Akhondi, M.M., Zarnani, A.H., et al., 2016. The effect of angiotensin on the quality of in vitro produced (ivp) sheep embryos and expression of na(+)/k(+)/atpase. Avicenna J Med Biotechnol. 8, 9-15

Nagalakshmi, U., Waern, K., Snyder, M., 2010. Rna ‐ seq: A method for comprehensive transcriptome analysis. Curr. Protoc. Mol. Biol. 89, 4.11. 1-4.11. 13

Nagy, Z.P., Taylor, T., Elliott, T., Massey, J.B., Kort, H.I., Shapiro, D.B., 2005. Removal of lysed blastomeres from frozen–thawed embryos improves implantation and pregnancy rates in frozen embryo transfer cycles. Fertil. Steril. 84, 1606-1612

National Center for Chronic Disease Prevention and Health Promotion, 2016. 2016 assisted reproductive technology fertility clinic success rates report.

National Institute for Health and Care Excellence, 2017. Fertility problems: Assessment and treatment [nice guideline156].

Nicholls, P.K., Sun, Z., Heng, S., Li, Y., Wang, J., Nie, G., 2011. Embryo implantation is closely associated with dynamic expression of proprotein convertase 5/6 in the rabbit uterus. Reprod. Biol. Endocrinol. 9, 1-10

Nichols, J., Zevnik, B., Anastassiadis, K., Niwa, H., Klewe-Nebenius, D., Chambers, I., et al., 1998. Formation of pluripotent stem cells in the mammalian embryo depends on the pou transcription factor oct4. Cell. 95, 379-391

Niimura, S., 2003. Time-lapse videomicrographic analyses of contractions in mouse blastocysts. Journal of Reproduction and Development. 49, 413-423

Nimbkar-Joshi, S., Rosario, G., Katkam, R., Manjramkar, D., Metkari, S., Puri, C.P., et al., 2009. Embryo-induced alterations in the molecular phenotype of primate endometrium. J. Reprod. Immunol. 83, 65-71

Niwa, H., Toyooka, Y., Shimosato, D., Strumpf, D., Takahashi, K., Yagi, R., et al., 2005. Interaction between oct3/4 and cdx2 determines trophectoderm differentiation. Cell. 123, 917-929

Norwitz, E.R., Schust, D.J., Fisher, S.J., 2001. Implantation and the survival of early pregnancy. N. Engl. J. Med. 345, 1400-8

O'sullivan, C.M., Ungarian, J.L., Singh, K., Liu, S., Hance, J., Rancourt, D.E., 2004. Uterine secretion of isp1 & 2 tryptases is regulated by progesterone and estrogen during pregnancy and the endometrial cycle. Molecular Reproduction and Development: Incorporating Gamete Research. 69, 252-259

O'neill, C., 1997. Evidence for the requirement of autocrine growth factors for development of mouse preimplantation embryos in vitro. Biol. Reprod. 56, 229-237

Obruca, A., Strohmer, H., Sakkas, D., Menezo, Y., Kogosowski, A., Barak, Y., et al., 1994. Fertilization and early embryology: Use of lasers in assisted fertilization and hatching. Human Reproduction. 9, 1723-1726

Ohashi, K., Osuga, J.-I., Tozawa, R., Kitamine, T., Yagyu, H., Sekiya, M., et al., 2003. Early embryonic lethality caused by targeted disruption of the 3-hydroxy-3-methylglutaryl-coa reductase gene. J. Biol. Chem. 278, 42936-42941

Onodera, Y., Takahashi, K., Goto, M., Anzai, M., Ono, N., Shirasawa, H., et al., 2017. The location of "8"-shaped hatching influences inner cell mass formation in mouse blastocysts. PLoS One. 12, e0175150

Osorno, R., Chambers, I., 2011. Transcription factor heterogeneity and epiblast pluripotency. Philosophical Transactions of the Royal Society B: Biological Sciences. 366, 2230-2237

Owusu-Akyaw, A., Krishnamoorthy, K., Goldsmith, L.T., Morelli, S.S., 2019. The role of mesenchymal–epithelial transition in endometrial function. Hum. Reprod. Update. 25, 114-133

Palermo, G., Joris, H., Devroey, P., Van Steirteghem, A.C., 1992. Pregnancies after intracytoplasmic injection of single spermatozoon into an oocyte. The Lancet. 340, 17-18

Paria, B., Dey, S., 1990. Preimplantation embryo development in vitro: Cooperative interactions among embryos and role of growth factors. Proceedings of the National Academy of Sciences. 87, 4756-4760

Paria, B., Reese, J., Das, S.K., Dey, S.K., 2002. Deciphering the cross-talk of implantation: Advances and challenges. Science. 296, 2185-2188

Parikh, F.R., Athalye, A.S., Naik, N.J., Naik, D.J., Sanap, R.R., Madon, P.F., 2018. Preimplantation genetic testing: Its evolution, where are we today? J. Hum. Reprod. Sci. 11, 306

Park, K.R., Inoue, T., Ueda, M., Hirano, T., Higuchi, T., Maeda, M., et al., 2000. Cd9 is expressed on human endometrial epithelial cells in association with integrins α6, α3 and β1. Mol. Hum. Reprod. 6, 252-257

Park, S.B., Kim, H.J., Choi, Y.B., Ahn, K.H., Lee, K.H., Yang, J.B., et al., 2014. The effect of various assisted hatching techniques on the mouse early embryo development. Clinical and Experimental Reproductive Medicine. 41, 68

Park, S.Y., Kim, E.Y., Cui, X.S., Tae, J.C., Lee, W.D., Kim, N.H., et al., 2006. Increase in DNA fragmentation and apoptosis-related gene expression in frozen-thawed bovine blastocysts. Zygote. 14, 125

Penaloza, C., Lin, L., Lockshin, R.A., Zakeri, Z., 2006. Cell death in development: Shaping the embryo. Histochem. Cell Biol. 126, 149

Petersen, C.G., Mauri, A., Baruffi, R., Oliveira, J., Massaro, F., Elder, K., et al., 2005. Implantation failures: Success of assisted hatching with quarter-laser zona thinning. Reprod. Biomed. Online. 10, 224-229

Petersen, C.G., Mauri, A.L., Baruffi, R.L.R., Oliveira, J.B.A., Felipe, V., Massaro, F.C., et al., 2006. Laser-assisted hatching of cryopreserved—thawed embryos by thinning one quarter of the zona. Reprod. Biomed. Online. 13, 668-675

Picelli, S., Faridani, O.R., Björklund, Å.K., Winberg, G., Sagasser, S., Sandberg, R., 2014. Full-length rna-seq from single cells using smart-seq2. Nat. Protoc. 9, 171

Practice Committee of the American Society for Reproductive Medicine, 2013. Definitions of infertility and recurrent pregnancy loss: A committee opinion. Fertil. Steril. 99, 63

Practice Committee of the American Society for Reproductive Medicine, 2017. Guidance on the limits to the number of embryos to transfer: A committee opinion. Fertil. Steril. 107, 901

Practice Committee of the American Society for Reproductive Medicine, Technology, P.C.O.T.S.F.a.R., 2014. Role of assisted hatching in in vitro fertilization: A guideline. Fertil. Steril. 102, 348-351

Practice Committee of the American Society for Reproductive Medicine and Practice Committee of the Society for Assisted Reproductive Technology, 2014. Role of assisted hatching in in vitro fertilization: A guideline. Fertil. Steril. 102, 348-351

Practice Committee of the Society for Assisted Reproductive Technology and Practice Committee of the American Society for Reproductive Medicine, 2008. The role of assisted hatching in in vitro fertilization: A review of the literature. A committee opinion. Fertil. Steril. 90, S196-S198

Primi, M.-P., Senn, A., Montag, M., Van Der Ven, H., Mandelbaum, J., Veiga, A., et al., 2004. A european multicentre prospective randomized study to assess the use of assisted hatching with a diode laser and the benefit of an immunosuppressive/antibiotic treatment in different patient populations. Hum. Reprod. 19, 2325-2333

Quenby, S., Brosens, J.J., 2013. Human implantation: A tale of mutual maternal and fetal attraction. Biol. Reprod. 88, 81, 1-2

Quinn, P., Horstman, F.C., 1998. Is the mouse a good model for the human with respect to the development of the preimplantation embryo in vitro? Hum. Reprod. 13, 173-183

Quinn, P., Kerin, J., 1986. Experience with the cryopreservation of human embryos using the mouse as a model to establish successful techniques. J. In Vitro Fert. Embryo Transf. 3, 40-45

Ray, A., Shah, A., Gudi, A., Homburg, R., 2012. Unexplained infertility: An update and review of practice. Reprod. Biomed. Online. 24, 591-602

Ren, X., Liu, Q., Chen, W., Zhu, G., Zhang, H., 2013. Effect of the site of assisted hatching on vitrified-warmed blastocyst transfer cycles: A prospective randomized study. J. Assist. Reprod. Genet. 30, 691-697

Richter, K.S., Davis, A., Carter, J., Greenhouse, S.J., Mottla, G.L., Tucker, M.J., 2006a. No advantage of laser-assisted over conventional intracytoplasmic sperm injection: A randomized controlled trial [nct00114725]. J. Exp. Clin. Assist. Reprod. 3, 5

Richter, K.S., Shipley, S.K., Mcvearry, I., Tucker, M.J., Widra, E.A., 2006b. Cryopreserved embryo transfers suggest that endometrial receptivity may contribute to reduced success rates of later developing embryos. Fertil. Steril. 86, 862-866

Rienzi, L., Gracia, C., Maggiulli, R., Labarbera, A.R., Kaser, D.J., Ubaldi, F.M., et al., 2017. Oocyte, embryo and blastocyst cryopreservation in art: Systematic review and meta-analysis comparing slow-freezing versus vitrification to produce evidence for the development of global guidance. Hum. Reprod. Update. 23, 139-155

Rienzi, L., Nagy, Z.P., Ubaldi, F., Iacobelli, M., Anniballo, R., Tesarik, J., et al., 2002. Laser-assisted removal of necrotic blastomeres from cryopreserved embryos that were partially damaged. Fertil. Steril. 77, 1196-1201

Rienzi, L., Ubaldi, F., Iacobelli, M., Minasi, M.G., Romano, S., Ferrero, S., et al., 2005. Developmental potential of fully intact and partially damaged cryopreserved embryos after laser-assisted removal of necrotic blastomeres and post-thaw culture selection. Fertil. Steril. 84, 888-894

Rienzi, L., Ubaldi, F., Martinez, F., Minasi, M., Iacobelli, M., Ferrero, S., et al., 2004. Clinical application of laser-assisted icsi: A pilot study. European Journal of Obstetrics & Gynecology and Reproductive Biology. 115, S77-S79

Rink, K., Delacrétaz, G., Salathé, R.P., Senn, A., Nocera, D., Germond, M., et al., 1996a. Non-contact microdrilling of mouse zona pellucida with an objective-delivered 1.48-μm diode laser. Lasers Surg. Med. 18, 52-62

Rink, K., Delacretaz, G.P., Salathe, R.-P., Senn, A., Nocera, D., Germond, M., et al., 1994. 1.48-um diode laser microdissection of the zona pellucida of mouse zygotes. Society of Photo-Optical Instrumentation Engineers (SPIE) Conference Series. pp. 412-422.

Rink, K., Descloux, L., Delacretaz, G.P., Senn, A., Nocera, D., Germond, M., 1996b. Zona pellucida drilling by a 1.48-um laser: Influence on the biomechanics of the hatching process. International Society for Optics and Photonics. 2624, 27-32

Robinson, M.D., Mccarthy, D.J., Smyth, G.K., 2010. Edger: A bioconductor package for differential expression analysis of digital gene expression data. Bioinformatics. 26, 139-140

Ruane, P.T., Berneau, S.C., Koeck, R., Watts, J., Kimber, S.J., Brison, D.R., et al., 2017. Apposition to endometrial epithelial cells activates mouse blastocysts for implantation. MHR: Basic science of reproductive medicine. 23, 617-627

Ruane, P.T., Buck, C.J., Babbington, P.A., Aboussahoud, W., Berneau, S.C., Westwood, M., et al., 2020. The effects of hyaluronate-containing medium on human embryo attachment to endometrial epithelial cells in vitro. Human reproduction open. 2020, hoz033

Rubino, P., Tapia, L., De Assin Alonso, R.R., Mazmanian, K., Guan, L., Dearden, L., et al., 2020. Trophectoderm biopsy protocols can affect clinical outcomes: Time to focus on the blastocyst biopsy technique. Fertil. Steril.

Sagoskin, A.W., Han, T., Graham, J.R., Levy, M.J., Stillman, R.J., Tucker, M.J., 2002. Healthy twin delivery after day 7 blastocyst transfer coupled with assisted hatching. Fertil. Steril. 77, 615-617

Sagoskin, A.W., Levy, M.J., Tucker, M.J., Richter, K.S., Widra, E.A., 2007. Laser assisted hatching in good prognosis patients undergoing in vitro fertilization-embryo transfer: A randomized controlled trial. Fertil. Steril. 87, 283-287

Salamonsen, L.A., Edgell, T., Rombauts, L.J., Stephens, A.N., Robertson, D.M., Rainczuk, A., et al., 2013. Proteomics of the human endometrium and uterine fluid: A pathway to biomarker discovery. Fertil. Steril. 99, 1086-1092

Salas-Vidal, E., Lomeli, H., 2004. Imaging filopodia dynamics in the mouse blastocyst. Dev. Biol. 265, 75-89

Sallam, H.N., Sadek, S.S., Agameya, A.F., 2003. Assisted hatching—a meta-analysis of randomized controlled trials. J. Assist. Reprod. Genet. 20, 332-342

Sampino, S., Zacchini, F., Swiergiel, A.H., Modlinski, A.J., Loi, P., Ptak, G.E., 2014. Effects of blastomere biopsy on post-natal growth and behavior in mice. Hum. Reprod. 29, 1875-83

Sathananthan, H., Gunasheela, S., Menezes, J., 2003. Mechanics of human blastocyst hatching in vitro. Reprod. Biomed. Online. 7, 228-234

Scarica, C., Montalvo, V., Novo, S., Castelló, C., & López-Teijón, M, 2018. Mosaicism in human blastocysts and technical factors of laser trophectoderm biopsy. Culture. 6, 23-2

Schenk, M., Groselj-Strele, A., Eberhard, K., Feldmeier, E., Kastelic, D., Cerk, S., et al., 2018. Impact of polar body biopsy on embryo morphokinetics-back to the roots in preimplantation genetic testing? J. Assist. Reprod. Genet. 35, 1521-1528

Schieve, L.A., Meikle, S.F., Peterson, H.B., Jeng, G., Burnett, N.M., Wilcox, L.S., 2000. Does assisted hatching pose a risk for monozygotic twinning in pregnancies conceived through in vitro fertilization? Fertil. Steril. 74, 288-294

Schimmel, T., Cohen, J., Saunders, H., Alikani, M., 2014. Laser-assisted zona pellucida thinning does not facilitate hatching and may disrupt the in vitro hatching process: A morphokinetic study in the mouse. Hum. Reprod. 29, 2670-2679

Scott, R.T., Jr., Upham, K.M., Forman, E.J., Hong, K.H., Scott, K.L., Taylor, D., et al., 2013a. Blastocyst biopsy with comprehensive chromosome screening and fresh embryo transfer significantly increases in vitro fertilization implantation and delivery rates: A randomized controlled trial. Fertil. Steril. 100, 697-703

Scott, R.T., Upham, K.M., Forman, E.J., Zhao, T., Treff, N.R., 2013b. Cleavage-stage biopsy significantly impairs human embryonic implantation potential while blastocyst biopsy does not: A randomized and paired clinical trial. Fertil. Steril. 100, 624-630

Serdarogullari, M., Findikli, N., Goktas, C., Sahin, O., Ulug, U., Yagmur, E., et al., 2014. Comparison of gender-specific human embryo development characteristics by time-lapse technology. Reprod. Biomed. Online. 29, 193-199

Seshagiri, P.B., Roy, S.S., Sireesha, G., Rao, R.P., 2009. Cellular and molecular regulation of mammalian blastocyst hatching. J. Reprod. Immunol. 83, 79-84

Seshagiri, P.B., Vani, V., Madhulika, P., 2016. Cytokines and blastocyst hatching. Am. J. Reprod. Immunol. 75, 208-217

Shafei, R., Syrkasheva, A., Romanov, A.Y., Makarova, N., Dolgushina, N., Semenova, M., 2017. Blastocyst hatching in humans. Russ. J. Dev. Biol. 48, 5-15

Shannon, P., Markiel, A., Ozier, O., Baliga, N.S., Wang, J.T., Ramage, D., et al., 2003. Cytoscape: A software environment for integrated models of biomolecular interaction networks. Genome Res. 13, 2498-2504

Shapiro, B.S., Daneshmand, S.T., Garner, F.C., Aguirre, M., Ross, R., 2008. Contrasting patterns in in vitro fertilization pregnancy rates among fresh autologous, fresh oocyte donor, and cryopreserved cycles with the use of day 5 or day 6 blastocysts may reflect differences in embryo-endometrium synchrony. Fertil. Steril. 89, 20-26

Sharma, N., Liu, S., Tang, L., Irwin, J., Meng, G., Rancourt, D.E., 2006. Implantation serine proteinases heterodimerize and are critical in hatching and implantation. BMC Dev. Biol. 6, 1-11

Sheth, B., Nowak, R.L., Anderson, R., Kwong, W.Y., Papenbrock, T., Fleming, T.P., 2008. Tight junction protein zo-2 expression and relative function of zo-1 and zo-2 during mouse blastocyst formation. Exp. Cell Res. 314, 3356-3368

Silver, N., Best, S., Jiang, J., Thein, S.L., 2006. Selection of housekeeping genes for gene expression studies in human reticulocytes using real-time pcr. BMC Mol. Biol. 7, 1-9

Simon, A., Laufer, N., 2012. Assessment and treatment of repeated implantation failure (rif). J. Assist. Reprod. Genet. 29, 1227-1239

Singh, H., Aplin, J.D., 2009. Adhesion molecules in endometrial epithelium: Tissue integrity and embryo implantation. J. Anat. 215, 3-13

Singh, H., Nardo, L., Kimber, S., Aplin, J., 2010. Early stages of implantation as revealed by an in vitro model. Reproduction. 139, 905

Sireesha, G., Mason, R.W., Hassanein, M., Tonack, S., Navarrete Santos, A., Fischer, B., et al., 2008. Role of cathepsins in blastocyst hatching in the golden hamster. MHR: Basic science of reproductive medicine. 14, 337-346

Smith, S., Pfeifer, S.M., Collins, J.A., 2003. Diagnosis and management of female infertility. JAMA. 290, 1767-1770

Sozen, B., Can, A., Demir, N., 2014. Cell fate regulation during preimplantation development: A view of adhesion-linked molecular interactions. Dev. Biol. 395, 73-83

Stachecki, J., Anderson, R., Schiewe, M., 2014. Sodium hyaluronate supports high survival and clinical pregnancy rates of blastocysts using a microsecure, dmso-free vitrification system. Fertility and Sterility. 101, e19

Stachecki, J.J., Garrisi, J., Sabino, S., Caetano, J.P., Wiemer, K.E., Cohen, J., 2008. A new safe, simple and successful vitrification method for bovine and human blastocysts. Reprod. Biomed. Online. 17, 360-367

Stark, R., Grzelak, M., Hadfield, J., 2019. Rna sequencing: The teenage years. Nature Reviews Genetics. 20, 631-656

Stein, A., Rufas, O., Amit, S., Avrech, O., Pinkas, H., Ovadia, J., et al., 1995. Assisted hatching by partial zona dissection of human pre-embryos in patients with recurrent implantation failure after in vitro fertilization. Fertil. Steril. 63, 838-841

Stones, R., Coates, A., Matteri, R., Hesla, J., 2004. Assisted hatching of embryos at the cleavage stage (d3) followed by embryo transfer at the blastocyst stage (d5). Fertil. Steril. 82, S268-S269

Strumpf, D., Mao, C.-A., Yamanaka, Y., Ralston, A., Chawengsaksophak, K., Beck, F., et al., 2005. Cdx2 is required for correct cell fate specification and differentiation of trophectoderm in the mouse blastocyst. Development. 132, 2093-2102

Sudano, M.J., Rascado, T.D., Tata, A., Belaz, K.R., Santos, V.G., Valente, R.S., et al., 2016. Lipidome signatures in early bovine embryo development. Theriogenology. 86, 472-484.e1

Sugiyama, Y., Ota, Y., Hara, M., Inoue, S., 2001. Osmotic stress up-regulates aquaporin-3 gene expression in cultured human keratinocytes. Biochimica et Biophysica Acta (BBA)-Gene Structure and Expression. 1522, 82-88

Summers, M.C., Biggers, J.D., 2003. Chemically defined media and the culture of mammalian preimplantation embryos: Historical perspective and current issues. Hum. Reprod. Update. 9, 557-582

Sutherland, K., Leitch, J., Lyall, H., Woodward, B., 2018. Time-lapse imaging of inner cell mass splitting with monochorionic triamniotic triplets after eset: A case report. Reprod. Biomed. Online.

Szklarczyk, D., Morris, J.H., Cook, H., Kuhn, M., Wyder, S., Simonovic, M., et al., 2016. The string database in 2017: Quality-controlled protein–protein association networks, made broadly accessible. Nucleic Acids Res. gkw937

Tadir, Y., Douglas-Hamilton, D.H., 2007. Laser effects in the manipulation of human eggs and embryos for in vitro fertilization. Methods Cell Biol. 82, 409-431

Tadir, Y., Wright, W., Vafa, O., Liaw, L., Asch, R., Berns, M., 1991. Micromanipulation of gametes using laser microbeams. Hum. Reprod. 6, 1011-1016

Tadir, Y., Wright, W.H., Vafa, O., Ord, T., Asch, R.H., Berns, M.W., 1990. Force generated by human sperm correlated to velocity and determined using a laser generated optical trap. Fertil. Steril. 53, 944-947

Tadir, Y., Wright, W.H., Vafa, O., Ord, T., Asch, R.H., Berns, M.W., 1989. Micromanipulation of sperm by a laser generated optical trap. Fertil. Steril. 52, 870-873

Taft, R.A., 2008. Virtues and limitations of the preimplantation mouse embryo as a model system. Theriogenology. 69, 10-16

Tang, F., Barbacioru, C., Wang, Y., Nordman, E., Lee, C., Xu, N., et al., 2009. Mrna-seq whole-transcriptome analysis of a single cell. Nature methods. 6, 377-382

Tarín, J.J., Handyside, A.H., 1993. Embryo biopsy strategies for preimplantation diagnosis. Fertil. Steril. 59, 943-952

Taylor, T.H., Gilchrist, J.W., Hallowell, S.V., Hanshew, K.K., Orris, J.J., Glassner, M.J., et al., 2010. The effects of different laser pulse lengths on the embryo biopsy procedure and embryo development to the blastocyst stage. J. Assist. Reprod. Genet. 27, 663-667

Tharakan, F.A., Jayaprakasan, K.M., 2018. Assisted reproduction treatments. Donald School Textbook of Human Reproductive & Gynecological Endocrinology. 163

Thomas, M., Jain, S., Kumar, G., Laloraya, M., 1997. A programmed oxyradical burst causes hatching of mouse blastocysts. J. Cell Sci. 110, 1597-1602

Tucker, M., 1999. Relevance of assisted hatching with blastocyst stage transfer. Proceedings of the 1st World Congress on Controversies in Obstetrics/Gynecology and Infertility. Prague, Bologna, Italy: Monduzzi Editore. pp. 49-52.

Ueno, S., Ezoe, K., Yabuuchi, A., Uchiyama, K., Okimura, T., Okuno, T., et al., 2016. Complete zona pellucida removal from vitrified-warmed human blastocysts facilitates earlier in-vitro attachment and outgrowth. Reprod. Biomed. Online. 33, 140-148

Uppangala, S., D'souza, F., Pudakalakatti, S., Atreya, H.S., Raval, K., Kalthur, G., et al., 2016. Laser assisted zona hatching does not lead to immediate impairment in human embryo quality and metabolism. Syst. Biol. Reprod. Med. 62, 396-403

Valojerdi, M.R., Eftekhari-Yazdi, P., Karimian, L., Hassani, F., Movaghar, B., 2010. Effect of laser zona thinning on vitrified–warmed embryo transfer at the cleavage stage: A prospective, randomized study. Reprod. Biomed. Online. 20, 234-242

Van Langendonckt, A., Wyns, C., Godin, P.A., Toussaint-Demylle, D., Donnez, J., 2000. Atypical hatching of a human blastocyst leading to monozygotic twinning: A case report. Fertil. Steril. 74, 1047-1050

Van Soom, A., Mateusen, B., Leroy, J., De Kruif, A., 2003. Assessment of mammalian embryo quality: What can we learn from embryo morphology? Reprod. Biomed. Online. 7, 664-670

Van Winkle, L.J., 2001. Amino acid transport regulation and early embryo development. Biol. Reprod. 64, 1-12

Vanderzwalmen, P., Bertin, G., Debauche, C., Standaert, V., Bollen, N., Roosendaal, E.V., et al., 2003. Vitrification of human blastocysts with the hemi-straw carrier: Application of assisted hatching after thawing. Hum. Reprod. 18, 1504-1511

Vanderzwalmen, P., Bertin, G., Debauche, C., Standaert, V., Van Roosendaal, E., Vandervorst, M., et al., 2002. Births after vitrification at morula and blastocyst stages: Effect of artificial reduction of the blastocoelic cavity before vitrification. Hum. Reprod. 17, 744-751

Vanneste, E., Voet, T., Le Caignec, C., Ampe, M., Konings, P., Melotte, C., et al., 2009. Chromosome instability is common in human cleavage-stage embryos. Nat. Med. 15, 577-583

Verza, S., Schneider, D., Siqueira, S., Esteves, S., 2013. Laser-assisted intracytoplasmic sperm injection (la-icsi) is safe and less traumatic than conventional icsi. Fertil. Steril. 100, S236

Walters, E.A., Brown, J.L., Krisher, R., Voelkel, S., Swain, J.E., 2020. Impact of a controlled culture temperature gradient on mouse embryo development and morphokinetics. Reprod. Biomed. Online. 40, 494-499

Wan, C.-Y., Song, C., Diao, L.-H., Li, G.-G., Bao, Z.-J., Hu, X.-D., et al., 2014. Laser-assisted hatching improves clinical outcomes of vitrified–warmed blastocysts developed from low-grade cleavage-stage embryos: A prospective randomized study. Reprod. Biomed. Online. 28, 582-589

Wang, H., Dey, S.K., 2006. Roadmap to embryo implantation: Clues from mouse models. Nature Reviews Genetics. 7, 185

Wang, Q.T., Piotrowska, K., Ciemerych, M.A., Milenkovic, L., Scott, M.P., Davis, R.W., et al., 2004. A genome-wide study of gene activity reveals developmental signaling pathways in the preimplantation mouse embryo. Dev. Cell. 6, 133-144

Wassarman, P.M., 2008. Zona pellucida glycoproteins. J. Biol. Chem. 283, 24285-24289

Wassarman, P.M., 1988. Zona pellucida glycoproteins. Annu. Rev. Biochem. 57, 415-442

Waterston, R.H., Pachter, L., 2002. Initial sequencing and comparative analysis of the mouse genome. Nature. 420, 520-562

Watson, A., Natale, D., Barcroft, L., 2004. Molecular regulation of blastocyst formation. Anim. Reprod. Sci. 82, 583-592

Watson, A.J., Barcroft, L.C., 2001. Regulation of blastocyst formation. Frontiers in bioscience: a journal and virtual library. 6, 708

Weimar, C.H., Uiterweer, E.D.P., Teklenburg, G., Heijnen, C.J., Macklon, N.S., 2013. In-vitro model systems for the study of human embryo–endometrium interactions. Reprod. Biomed. Online. 27, 461-476

Wheeler, A.P., Ridley, A.J., 2004. Why three rho proteins? Rhoa, rhob, rhoc, and cell motility. Exp. Cell Res. 301, 43-49

Wong, B.C., Boyd, C.A., Lanzendorf, S.E., 2003. Randomized controlled study of human zona pellucida dissection using the zona infrared laser optical system: Evaluation of blastomere damage, embryo development, and subsequent hatching. Fertil. Steril. 80, 1249-1254

Xiong, Y., Tan, Y.-J., Xiong, Y.-M., Huang, Y.-T., Hu, X.-L., Lu, Y.-C., et al., 2013. Expression of aquaporins in human embryos and potential role of aqp3 and aqp7 in preimplantation mouse embryo development. Cell. Physiol. Biochem. 31, 649-658

Xu, J.-S., Cheung, T.-M., Ting-Hon Chan, S., Ho, P.-C., Shu-Biu Yeung, W., 2001. Temporal effect of human oviductal cell and its derived embryotrophic factors on mouse embryo development. Biol. Reprod. 65, 1481-1488

Xue, Z., Huang, K., Cai, C., Cai, L., Jiang, C.-Y., Feng, Y., et al., 2013. Genetic programs in human and mouse early embryos revealed by single-cell rna sequencing. Nature. 500, 593-597

Yamanaka, Y., Lanner, F., Rossant, J., 2010. Fgf signal-dependent segregation of primitive endoderm and epiblast in the mouse blastocyst. Development. 137, 715-724

Yamashita, S., Ikemoto, Y., Ochiai, A., Yamada, S., Kato, K., Ohno, M., et al., 2019. Analysis of 122 triplet and 1 quadruplet pregnancies after single embryo transfer in japan. Reprod Biomed Online.

Yan, Z., Liang, H., Deng, L., Long, H., Chen, H., Chai, W., et al., 2015. Eight-shaped hatching increases the risk of inner cell mass splitting in extended mouse embryo culture. PLoS One. 10, e0145172

Yang, J., Zhang, D., Yu, Y., Zhang, R.J., Hu, X.L., Huang, H.F., et al., 2015. Binding of fgf2 to fgfr2 in an autocrine mode in trophectoderm cells is indispensable for mouse blastocyst formation through pkc-p38 pathway. Cell Cycle. 14, 3318-30

Yang, Q.E., Fields, S.D., Zhang, K., Ozawa, M., Johnson, S.E., Ealy, A.D., 2011. Fibroblast growth factor 2 promotes primitive endoderm development in bovine blastocyst outgrowths. Biol. Reprod. 85, 946-53

Yano, K., Kubo, T., Ôhashi, I., Yano, C., 2006. Assisted hatching using a 1.48-μm diode laser: Evaluation of zona opening and zona thinning techniques in human embryos. Reprod. Med. Biol. 5, 221-226

Yano, K., Yano, C., Kubo, T., Ôhashi, I., Maeda, N., Fukaya, T., 2007. Chemical zona pellucida thinning with acidified tyrode's solution: Comparison between partial and circumferential techniques. J. Assist. Reprod. Genet. 24, 471-475

Yoshinaga, K., 2013. A sequence of events in the uterus prior to implantation in the mouse. J. Assist. Reprod. Genet. 30, 1017-1022

You, J.-L., Wang, W., Tang, M.-Y., Ye, Y.-H., Liu, A.-X., Zhu, Y.-M., 2018. A potential role of galectin-1 in promoting mouse trophoblast stem cell differentiation. Mol. Cell. Endocrinol. 470, 228-239

Yu, G., Wang, L.G., Han, Y., He, Q.Y., 2012. Clusterprofiler: An r package for comparing biological themes among gene clusters. OMICS. 16, 284-7

Zacchini, F., Arena, R., Abramik, A., Ptak, G.E., 2017. Embryo biopsy and development: The known and the unknown. Reproduction. 154, R143-R148

Zeng, M., Su, S., Li, L., 2017. The effect of laser-assisted hatching on pregnancy outcomes of cryopreserved-thawed embryo transfer: A meta-analysis of randomized controlled trials. Lasers Med. Sci. 1-12

Zhan, S., Cao, S., Du, H., Sun, Y., Li, L., Ding, C., et al., 2018. Parental genetic material and oxygen concentration affect hatch dynamics of mouse embryo in vitro. Reprod. Biol. Endocrinol. 16, 1-12

Zhang, P., Zucchelli, M., Bruce, S., Hambiliki, F., Stavreus-Evers, A., Levkov, L., et al., 2009. Transcriptome profiling of human pre-implantation development. PLoS One. 4,

Zhang, Y., Duan, X., Cao, R., Liu, H.-L., Cui, X.-S., Kim, N.-H., et al., 2014. Small gtpase rhoa regulates cytoskeleton dynamics during porcine oocyte maturation and early embryo development. Cell cycle. 13, 3390-3403

Zhao, H., Tao, W., Li, M., Liu, H., Wu, K., Ma, S., 2019. Comparison of two protocols of blastocyst biopsy submitted to preimplantation genetic testing for aneuploidies: A randomized controlled trial. Arch. Gynecol. Obstet. 299, 1487-1493

Zheng, X., Liu, P., Chen, G., Qiao, J., Wu, Y., Fan, M., 2008. Viability of frozen-thawed human embryos with one–two blastomeres lysis. J. Assist. Reprod. Genet. 25, 281-285

Zhou, H., Zao, W., Zhang, W., Shi, J., Shi, W., 2014. No adverse effects were identified on the perinatal outcomes after laser-assisted hatching treatment. Reprod Biomed Online. 29, 692-698

Zinaman, M.J., Clegg, E.D., Brown, C.C., O'connor, J., Selevan, S.G., 1996. Estimates of human fertility and pregnancy loss. Fertil. Steril. 65, 503-509



Supplementary Appendices

Supplementary appendix 1

The application of assisted hatching in IVF centres

I would like to invite you to take this anonymous survey which is conducted by a research group at the University of Oxford. The survey should only take a few minutes to complete. Although assisted hatching has been widely used for more than 20 years, the efficacy and safety of this application remain controversial. Your answers will help us to better understand how assisted hatching is currently being used in clinical scenarios.

1. What is your job title?
   - o Clinician
   - o Embryologist
   - o Nurse
   - o Other, _____

2. What type of clinic are you working at?
   - o Publically funded, eg. NHS
   - o Private clinic, providing privately funded cycles only
   - o Private clinic – providing privately and publicly funded cycle
   - o Research
   - o Other, ____

3. What is the name of your clinic? (optional)

4. Where is your clinic (country)?
   - o UK
   - o Other EU countries (specifically),_____
   - o Outside EU (specifically), _____

5. Which treatments can your clinic provide? (Please tick any that apply) multiple choice
   - o Basic fertility treatment, e.g. IUI
   - o IVF
   - o ICSI
   - o Embryo cryopreservation
   - o PGT

6. Does your clinic perform assisted hatching routinely before biopsy?
   - o Yes
   - o No
   - o Not available for biopsy.

7. If no, what is the reason? Please tick all that apply
   - o No equipment
   - o No evidence for efficacy
   - o Unsure about the safety

- No needs

8. Does your clinic use assisted hatching without performing biopsy?
   - Yes
   - No

9. If yes, in which cases do you use assisted hatching? (Please tick any that apply) multiple choice
   - All embryos.
   - Embryos from patients with poor prognosis, such as recurrent implantation failure and advanced age.
   - The embryos with a thick zona pellucida.
   - Frozen-thaw embryos.
   - Other, _____

10. If no, is there a specific reason? (Please tick any that apply) multiple choice
    - No equipment.
    - No embryo biopsy needs.
    - Unsure of efficiency
    - Unsure of safety
    - Add a comment:_____

11. Which stage of embryos are treated with assisted hatching? (Please tick any that apply) multiple choice
    - 2-cells stage (Day 2)
    - 8-cell stage (Day 3)
    - Morula stage (Day 4)
    - Blastocyst stage

12. Do you continue embryo culture following assisted hatching?
    - No, embryo(s) will be transferred very soon (within few hours).
    - Yes, the embryo(s) will be cultured to blastocyst stage.
    - Both, depends on embryo development or biopsy needs.

13. Do you treat fresh or frozen-thawed embryos with assisted hatching? (Please tick any that apply)
    - Fresh embryos
    - Frozen-thawed embryos
    - Both

14. Do you only apply assisted hatching to frozen-thawed embryos, what is the reseason? (Please tick any that apply)
    - No, assisted hatching was applied to both frozen-thawed and fresh embryos.
    - Yes, because embryo cryopreservation cuase zona pellucida hardening.
    - Yes, because virtrification may impair hatching of embryos.
    - Other,_____

15. What technique do you use for assisted hatching?
    - Laser method
    - Chemical method
    - Mechanical method

16. How do you process the assisted hatching?
    - Zona pellucida drilling/Opening
    - Zona pellucida thinning
    - Both
    - Other, _____

17. If drilling, what is the size of the opening?
    - Less than 10µM
    - 10-15 µM
    - 15-25µM
    - More than 25µM
    - Other, _____

18. If thinning, what is the extension of ZP ablation?
    - Less than a quarter of the circumference
    - A quarter of the circumference
    - A quarter to a half of the circumference
    - Half of the circumference
    - More than half of the circumference
    - Other, ____

19. How helpful do you think assisted hatching is to your routine work?

Extremely helpful	Very helpful	Somewhat helpful	Not so helpful	Not at all helpful

20. Based on your experience, do you think assisted hatching is safe?

Very unlikely	Unlikely	Neither likely nor unlikely	Likely	Very likely

20. Based on your experience, do you think assisted hatching may impact upon embryo development?

Very unlikely	Unlikely	Neither likely nor unlikely	Likely	Very likely

21. Based on your experience/knowledge, do you think assisted hatching leads to an improvement in implantation rate?

Very unlikely	Unlikely	Neither likely nor unlikely	Likely	Very likely

22. Based on your experience/knowledge, do you think assisted hatching leads to an improvement in live birth rate?

Very unlikely	Unlikely	Neither likely nor unlikely	Likely	Very likely

24. Based on your experience, is there any side-effect of children born as results of assisted hatching procedure? If yes, please specify?

- Yes, specify:
- No

25. Is the assisted offering as a research setting?

- Yes, specify:
- No, it is a clinical practice

26. Do you charge extra for assisted hatching procedure and if so which scenario would you charge?

- No
- Yes, for biopsy only
- Yes, for improved outcome
- Yes, for all AH procedures

27. How much do you charge?

- No extra charge
- specific_____

Supplementary appendix 2

Cell counting

The coverslip was moistened and affixed to the cleaned hemocytometer. The presence of Newton's refraction rings under the coverslip indicated the proper adhesion. Following resuspension of the cell pellets with 1 mL of media, cells were diluted in Trypan Blue dye exclusion medium (1 in 10 dilutions). 20 µL of diluted cells were transferred to a haemocytometer chamber underneath the coverslip, allowing the cell suspension to be drawn out by capillary action. Cells on the counting plane of four large corner squares were counted under a microscope with 10X objective. The dead cells appeared blue, while live cells were unstained. Using a hand tally counter, the live cells in the 16 squares (1 mm) in the four corners were counted. Finally, to calculate the number of viable cells (cells/mL): (1) take the average cell count from each of the sets of 4 corner squares; (2) multiply by 10,000 (10^4); (3) Multiply by 10 to correct for the 1:10 dilution from the trypan blue addition.

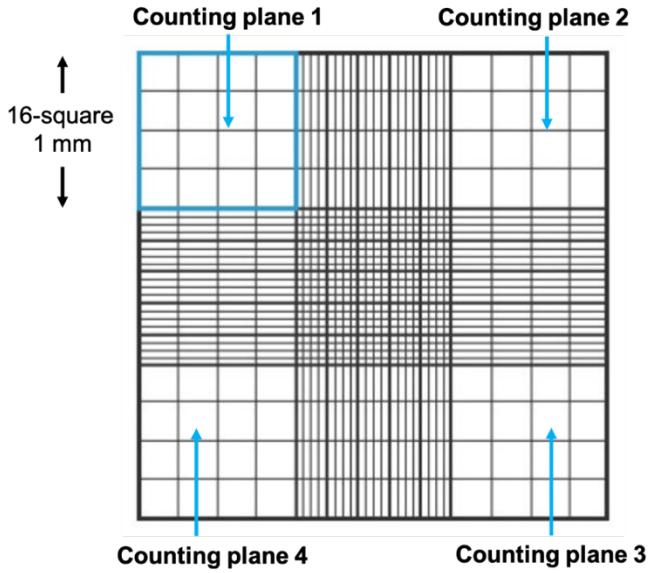


Figure S. 1 Haemocytometer gridlines

Haemocytometer diagram indicating one of the sets of 16 squares that should be used for counting.

Freezing and thawing Ishikawa cells

After trypsinisation and cell counting, approximately 1-2 x 10^6 cells were resuspended in 1 ml of freezing medium consisting of 90% (v/v) FBS and 10% (v/v) Dimethyl Sulfoxide (DMSO) (Sigma-Aldrich, UK), and transferred into a cryovial (Nunc, UK), before storage in a freezing container (Thermo Fisher, UK) overnight at -80°C. For long term storage, the cryovial was transferred into a liquid nitrogen container the following day.

For thawing Ishikawa cells, cryovials from liquid nitrogen were transferred immediately into a water bath and incubated at 37°C until the frozen medium had transitioned to a liquid state. The thawed cells were then immediately and carefully transferred into a 15 ml Falcon tube, followed by the slow addition of 10 ml of pre-warmed conditioned media. The cell suspension was then centrifuged at 150 g for 5 minutes, and the supernatant was discarded to remove DMSO. The resultant cell pellet was resuspended in 8-10 ml of conditioned media and transferred into a 75 cm^2 flask for cell culture.

Supplementary appendix 3

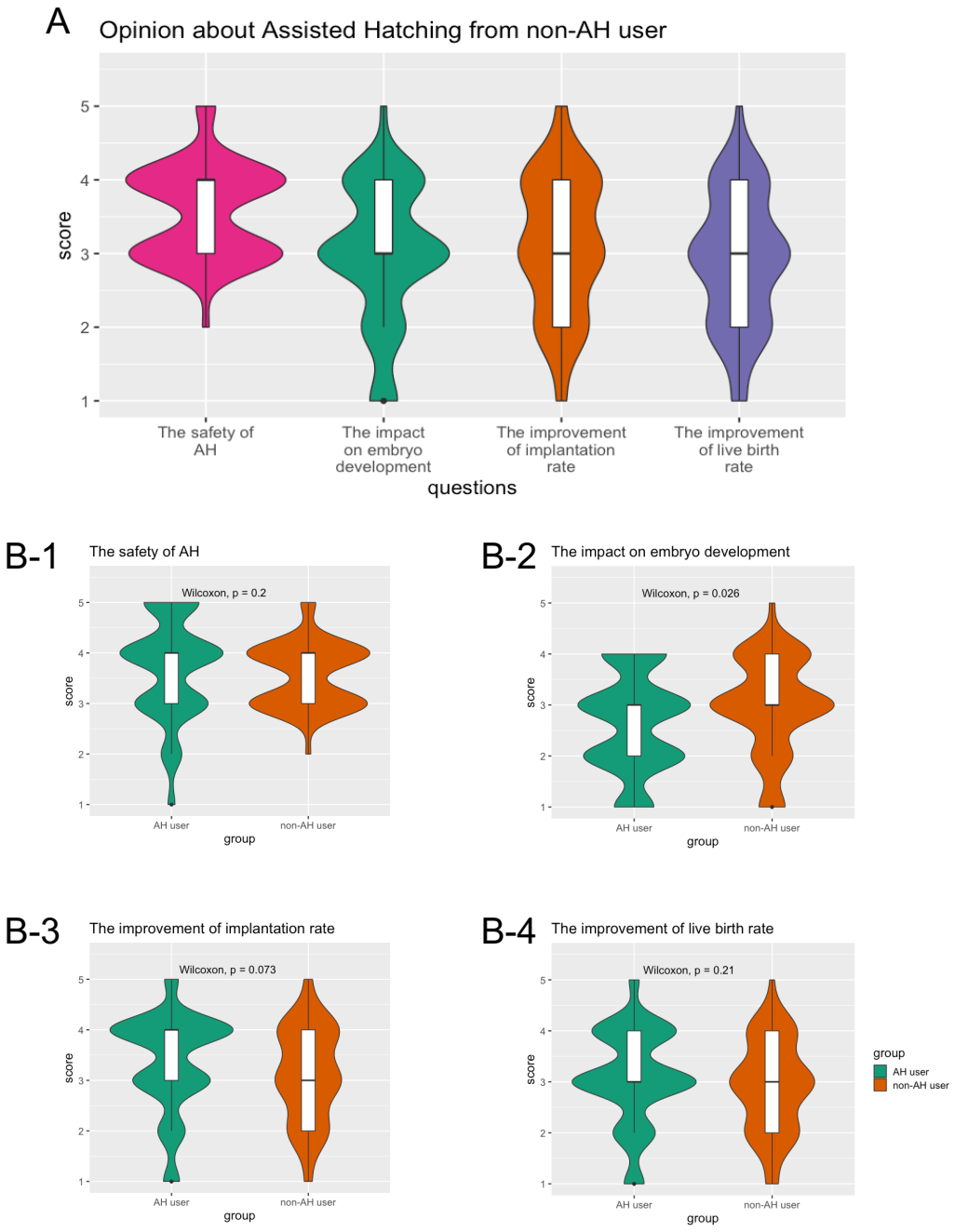


Figure S. 2 Opinion relating to AH among the non-AH users

The violin plots show the Likert scale resulting for the opinions relating to AH from all non-AH users (A); The comparison of the scores between AH user and non-AH user: (B-1) the safety of AH, (B-2) the impact on embryo development, (B-3) the improvement of implantation, and (B-4) the improvement of live birth. Boxplots present the median and range of the first quantile to the third quantile. The Wilcoxon rank-sum test was used to compare scores between two groups.

Supplementary appendix 4

The validation of CDX2 and OCT4 antibodies were conducted; the dilution of 1:50 and 1:100 for CDX2 antibody and 1:100 and 1:200 for OCT4 antibody were compared; the slightly lower background signals in the higher dilution groups. Therefore, I used the dilution of 1:100 for CDX2 antibody and 1:200 for OCT4 antibody for subsequent experiments.

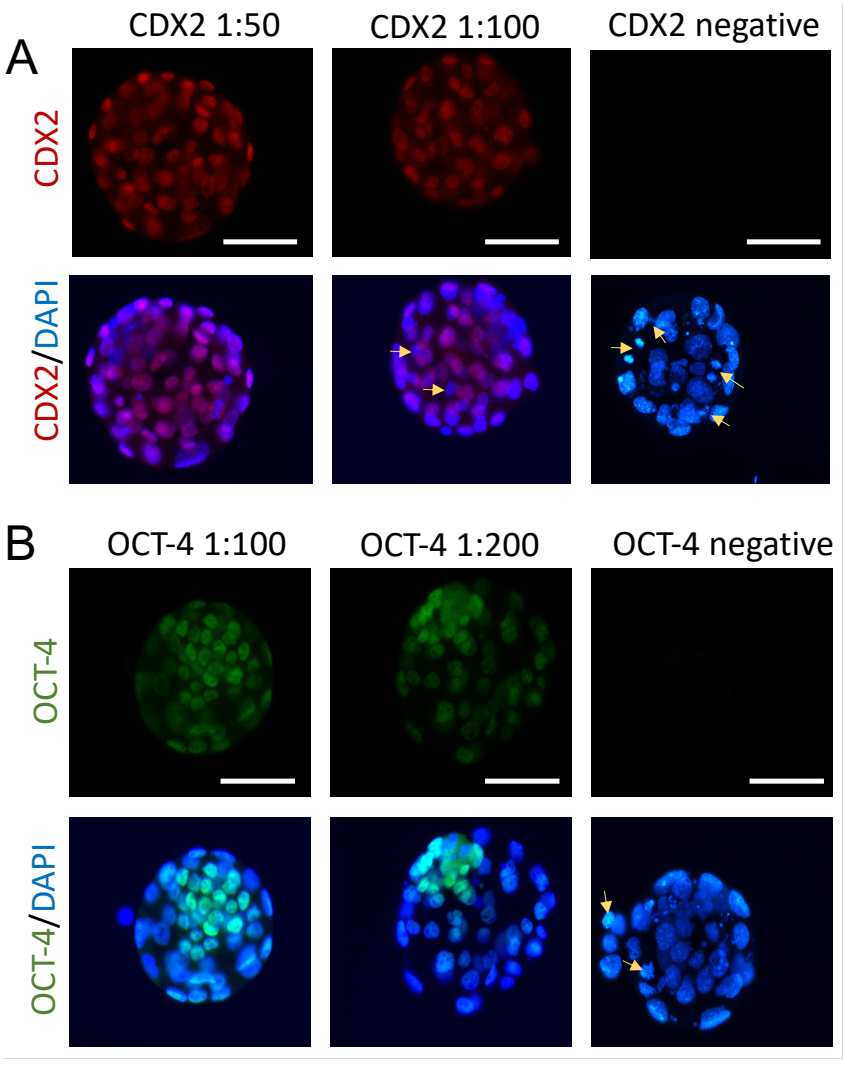


Figure S. 3 Representative images of the validation of CDX2 and OCT4 staining

The antibody titration experiment was conducted by diluting CDX2 antibody to 1:50 and 1:100 (A), and diluting OCT antibody to 1:100 and 1:200 (B). The negative controls were performed by incubating embryos with 3% BSA buffer instead of primary antibody. The yellow arrows indicate cells in mitosis phase. Scale bar=50 μm. (400× magnification).

Supplementary appendix 5

The ratio of TE/ICM was also compared; **Figure S.4** shows that there were no significant differences detected across the four groups. Notably, the TE/ICM ratio of hatching blastocyst was substantially higher in the LA-ZP thinning group (5.97±1.03) when compared to the other three groups, although there was no statistical significance (*P*>0.05).

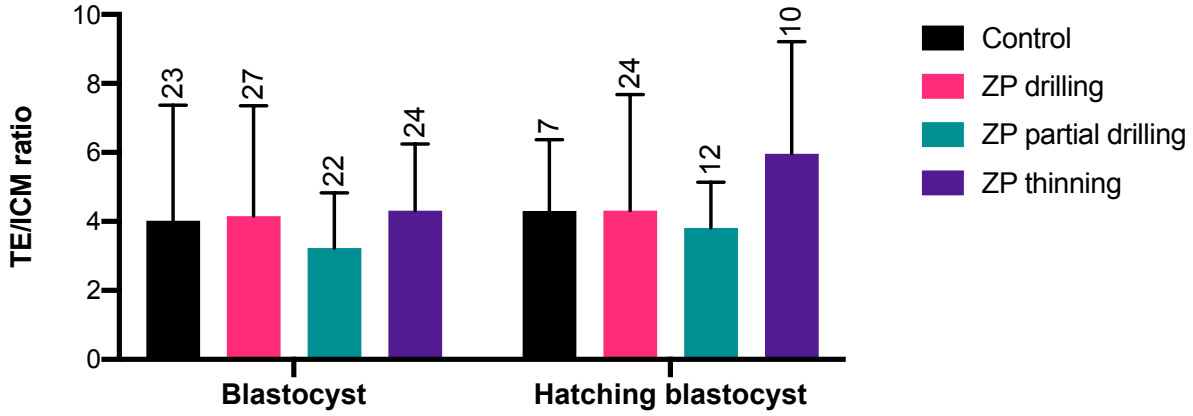


Figure S. 4 A comparison of the ratio of TE/ICM across different laser ZP manipulation

The ratio of TE/ICM of all blastocysts and hatching embryos were compared across the four LAH groups. Values are presented as mean ± SD. Statistical analysis was carried out using one-way ANOVA with Dunnett's multiple comparisons test to identify differences between each treatment group and the control group. The number of embryos tested was shown above each bar.

Supplementary appendix 6

HSP70 staining validation

To validate the HSP70 staining, an antibody titration was conducted. As shown in **Figure S.5**, three types of signals were found in the images generated using different HSP70 antibody dilutions: dot-like signals outside embryos (yellow arrow), un-even signals inside embryos (blue arrow), and evenly distributed signals in embryos (red arrow) (**Figure S.5 A**). Since embryos are spherical, Z-stacked scanning confocal microscopy was used to determine the location of these signals (**Figure S.5 B**). The evenly distributed signals were evident around the embryos and were even found in the no-primary antibody negative controls; this is presumed to represent non-specific binding between the anti-mouse secondary antibody and the endogenous IgG antigen on embryo zona pellucida. The un-even signal shown in the cytoplasm inside embryos was consistent with a previous report (Kim et al., 2017). Meanwhile, the dot-like signals were shown outside of the embryos; this is considered to be caused by the high concentration of the antibody. To eliminate the non-specific binding, M.O.M (mouse on mouse) blocking buffer (VECTOR laboratories, UK) was used to optimise the blocking such that the non-specific signal was substantially diminished (**Figure S.5 C**). Therefore, the subsequent experiment, he HSP70 antibody was diluted to 1:150, the secondary antibody diluted to 1:500, and the M.O.M blocking buffer was used.

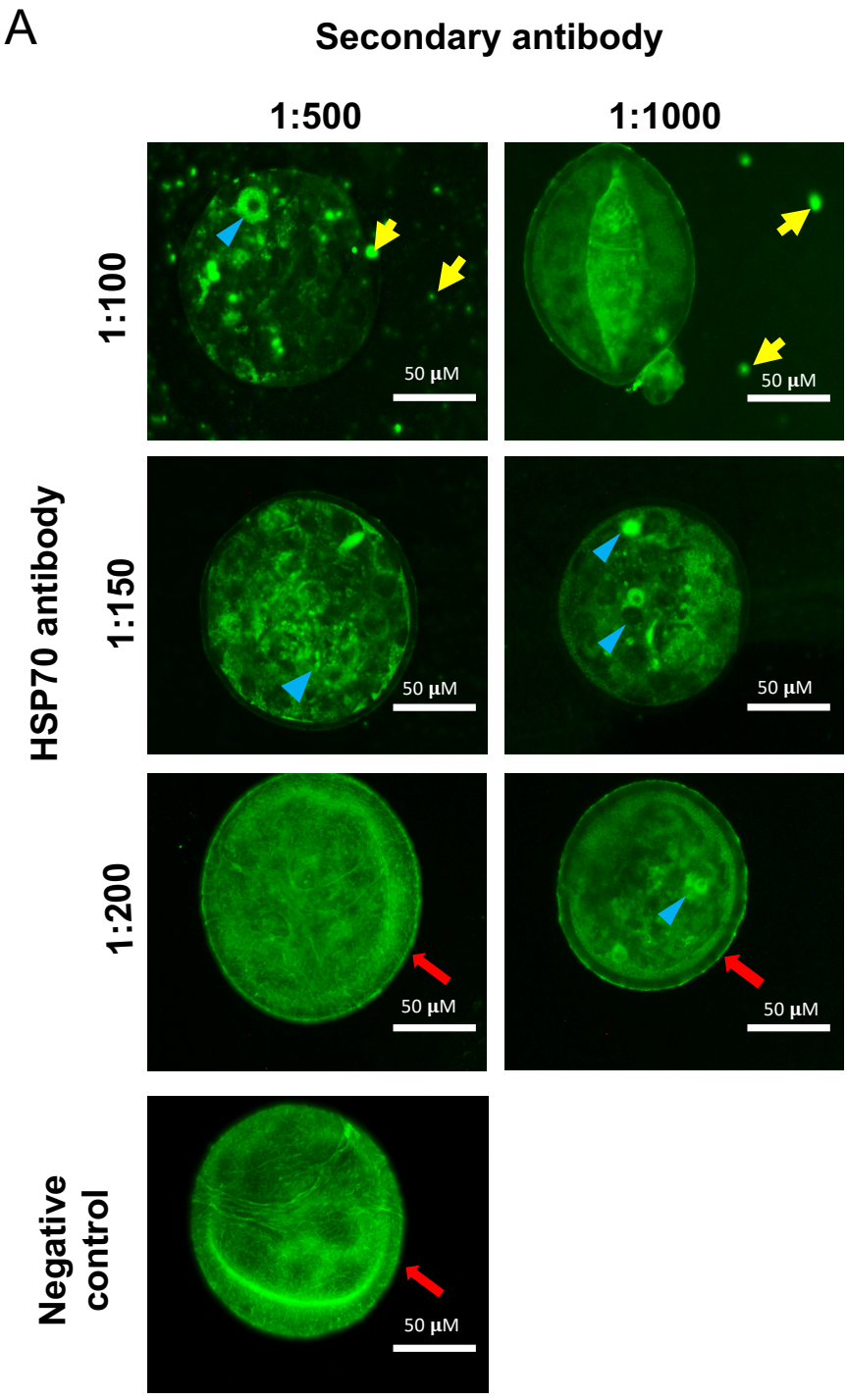


Figure S.5 (Continued on next page, legend follows)

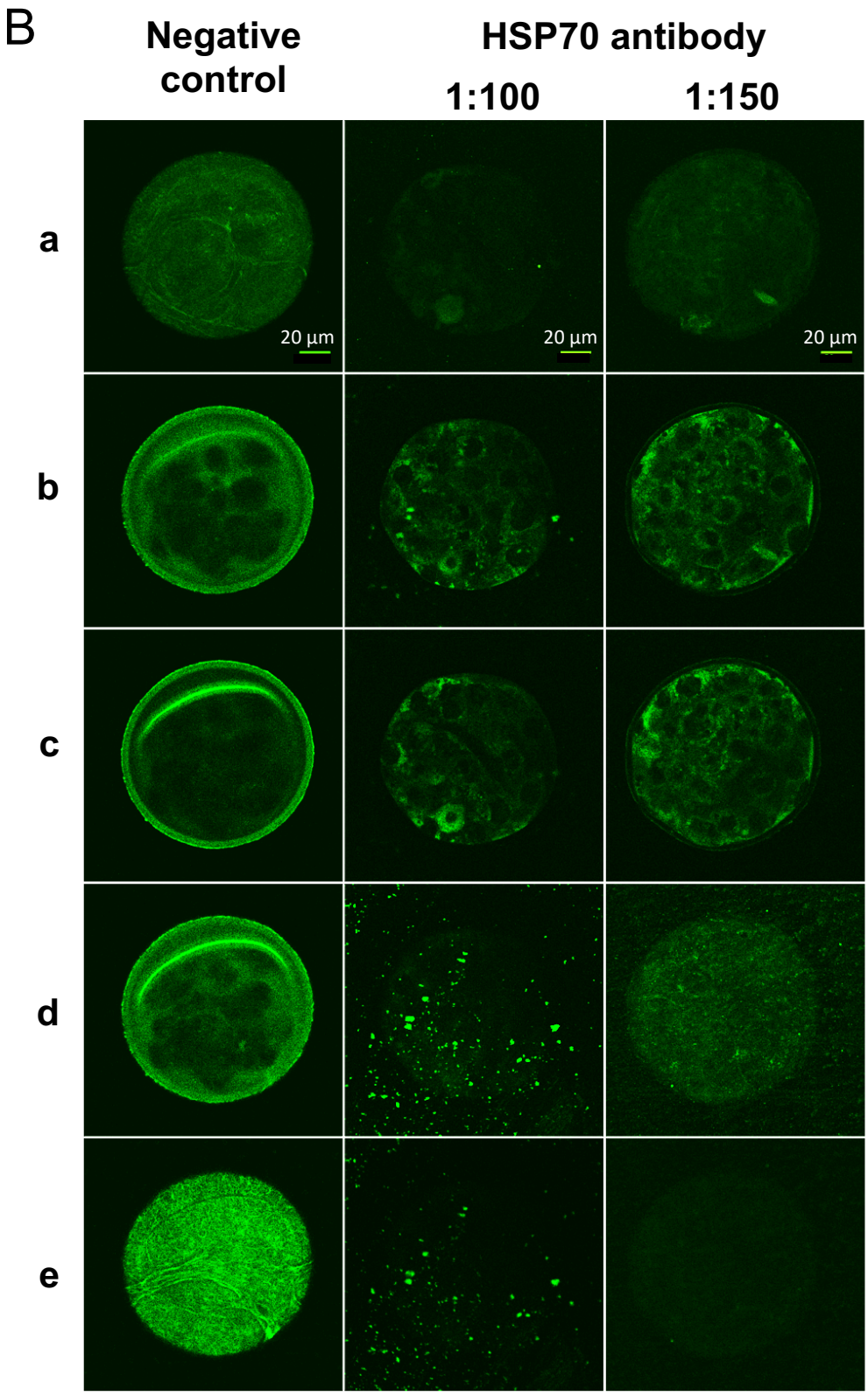


Figure S.5 (Continued on next page, legend follows)

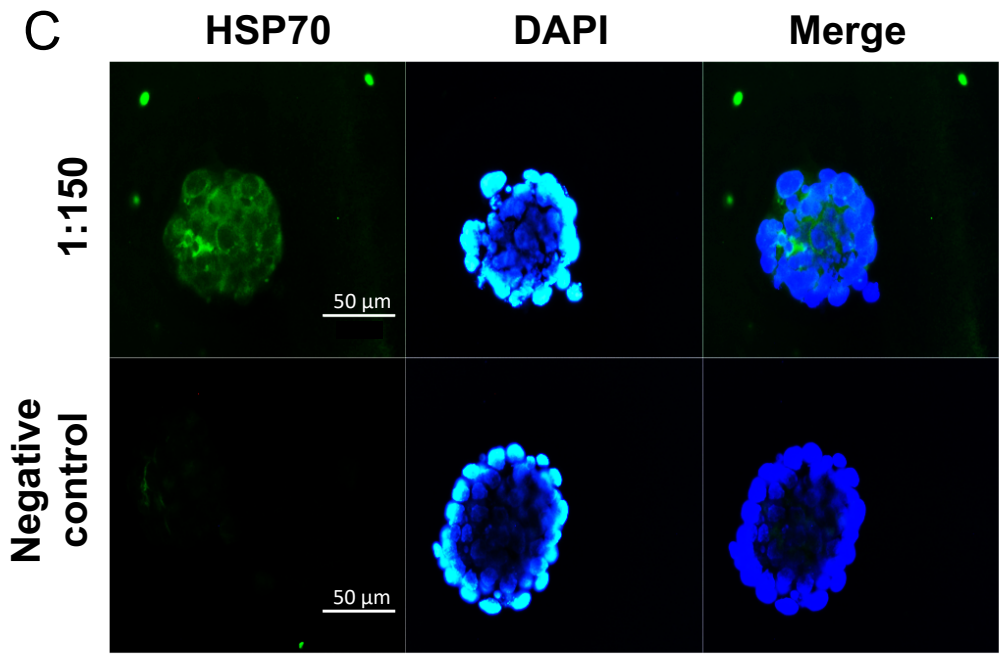


Figure S. 5 Representative images of HSP70 staining validation

(A): A antibody titration experiments: dilutions of 1:100, 1:150, and 1:200 of anti-HSP70 antibody; and dilutions of 1:500 and 1:1000 of the secondary antibody were used to determine the optimal antibody concentration. The signals shown outside the embryos (yellow arrow), inside the embryos (blue triangle), and evenly distributed through the embryos (red arrow) are shown in the images (Scale bar=50 µM). (B): The Z-stack confocal images were obtained from the upper (a) to lower layer (e) of the embryo (Scale bar=20 µM). (C): Blocking method validation: the blocking buffer was modified by replacing 5% BSA buffer (A, B) with M.O.M blocking buffer (Scale bar=50 µM).

Supplementary appendix 7

For the starting materials of embryo RT-qPCR experiment, I tried to use single, three, five and ten blastocysts for cDNA synthesis. I found that all genes showed amplification in qPCR when using more than three blastocysts for cDNA synthesis directly, with the pre-amplified cDNA diluted 1 in 5. However, most of the genes did not amplify with the cDNA generated from single blastocyst.

Table S. 1 Blastocyst number and qRT-PCR amplification signal

Number of blastocyst	**1**		**3**	**5**	**10**
Dilution of cDNA	1:5	1:2	1:5	1:5	1:5
Gapdh	✓	✓	✓	✓	✓
Sod1	✓	✓	✓	✓	✓
Nanog	✓	✗	✓	✓	✓
Bax	✗	✗	✓	✓	✓
Bcl2l2	✗	✗	✓	✓	✓
Dnmt3a	✗	✗	✓	✓	✓
Gpx7	✗	✗	✓	✓	✓
Pou5f1	✓	✓	✓	✓	✓

✓: qPCR showing amplification ✗: No amplification in qPCR

Supplementary appendix 8

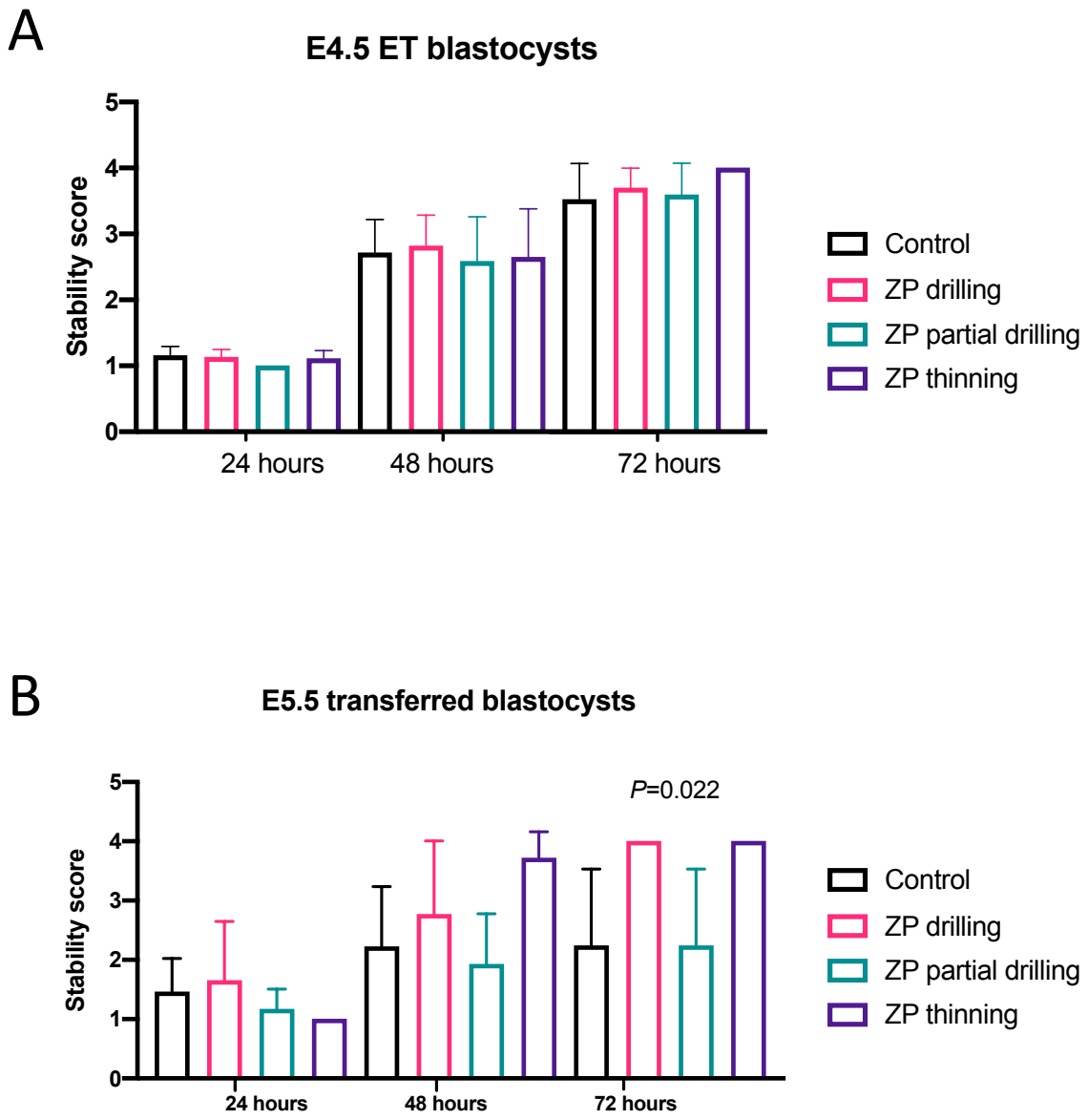
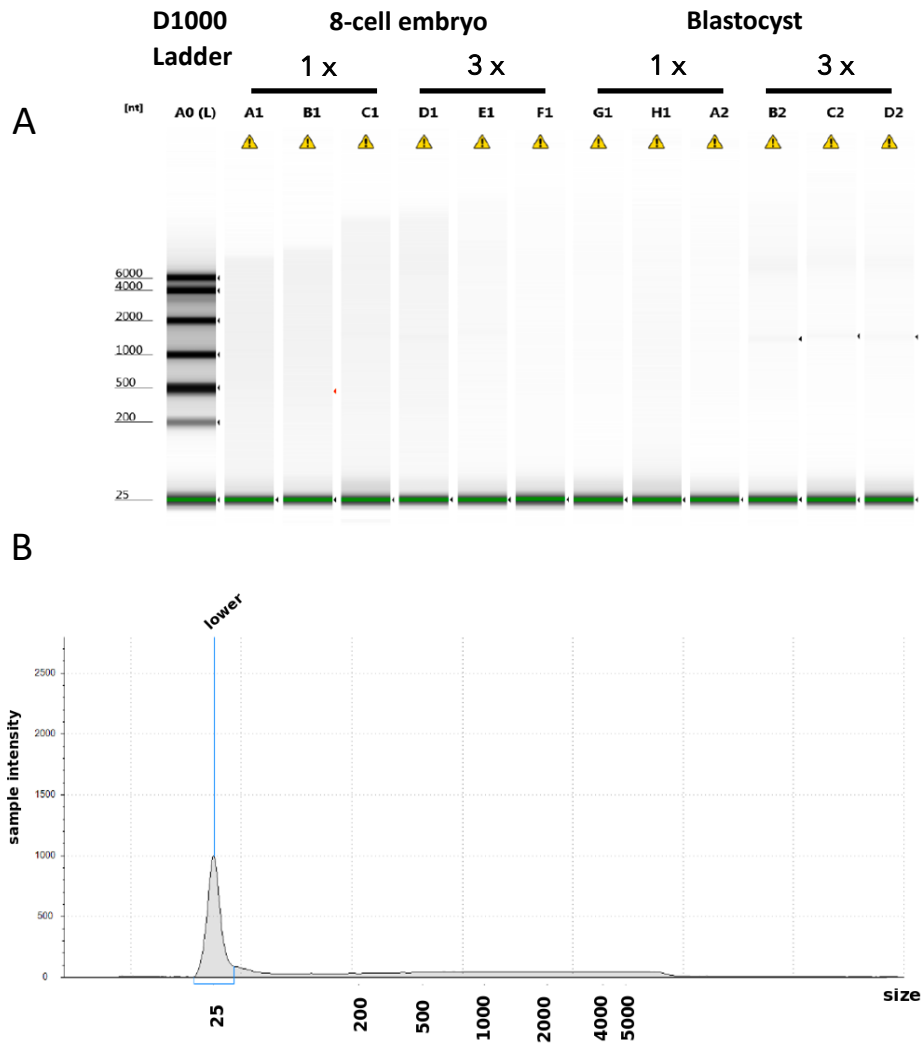


Figure S. 6 A comparison of the attachment stability score across different laser ZP manipulations groups

The attachment stability of each live embryo was scored every 24 hours. (A) The implantation model of transferring E4.5 blastocysts. (B) The implantation model of transferring E5.5 blastocysts. Values are presented as geometric mean with 95% CI. Statistical analysis was carried out using one-way ANOVA with Dunnett's multiple comparisons test to identify differences between each treatment group and the control group.

Supplementary appendix 9

A column method (Column-based PicoPure RNA isolation kit (Applied Biosystems, UK)) with DNase treatment was tried to extract RNA from single/three 8-cell embryos and blastocysts for cDNA library preparation. The extracted RNA samples were sent to the Wellcome Centre for Human Genetics for RNA quantification and quality control (QC) testing, using a high-sensitivity RNA chip with High Sensitivity RNA Screen Tape (Agilent Bioanalyzer 2100). However, the quantification results indicated that the mRNA concentration of these samples were all <0.5 ng/μL, and that the mRNA quality was lower than the recommendation for SMARTer preparation with a RINe (RNA integrity number equivalent) value lower than 3. RINe is a representative index (from 1 to 10) to assess RNA quality, where 10 represents the highest quality (**Figure S.7**).



Well	RINe	28s/18s	Conc (pg/µl)	Observation
A1	2.5	--	291	RNA concentration outside recommended range of RNIe

Size	Calibrated Conc (pg/µl)	Peak Molarity (pmol/l)	% Integrated Area	Observation
25	700	82400	-	Lower marker

Figure S. 7 Quality control of extracted RNA from embryos

Extracted RNA from one or three 8-cell embryos and blastocysts, were assessed on AN Agilent2100 Bioanalyzer system with high sensitivity RNA Screen Tape. (A) electropherograms of extracted RNA. The first lane on the left is an electronic DNA ladder. Embryo types are labelled above. (B) Agilent Bioanalyzer 2100 analysis of column A1, showing only one peak at the 25bp marker. The quality of RNA was very low with an RINe (RNA integrity number equivalent) value lower than 3.0.

Supplementary appendix 10

Table S. 2 IPA canonical pathway and related DEGs between hatching and pre-hatching blastocysts

Ingenuity Canonical Pathways	-log(*P*-value)	Ratio	z-score	Molecules
EIF2 Signaling	56.30	0.21	4.747	*Actb, Fau, Grb2, Rpl11 ,Rpl13, Rpl13a ,Rpl14, Rpl17, Rpl18, Rpl18a, Rpl19, Rpl23, Rpl27, Rpl27a, Rpl28, Rpl3, Rpl31, Rpl35, Rpl35a, Rpl37, Rpl37a, Rpl39, Rpl4, Rpl41, Rpl6, Rpl7, Rpl7a, Rpl8, Rpl9, Rplp2, Rps10, Rps11, Rps13, Rps14, Rps15a, Rps16,r Ps17, Rps18, Rps19, Rps2, Rps20, Rps24, Rps26, Rps27a, Rps4y1, Rps6, Rps9, Sos1*
Regulation of eIF4 and p70S6K Signaling	18.40	0.13	NaN	*FAu, Grb2, Rps10, Rps11, Rps13, Rps14, Rps15a, Rps16, Rps17, Rps18, Rps19, Rps2, Rps20, Rps24, Rps26, Rps27a, Rps4y1, Rps6, Rps9, Sos1*
mTOR Signaling	14.70	0.09	NaN	*Fau, Rnd3, Rps10, Rps11, Rps13, Rps14, Rps15a, Rps16, Rps17, Rps18, Rps19, Rps2, Rps20, Rps24, Rps26, Rps27a, Rps4y1, Rps6, Rps9*
Oxidative Phosphorylation	13.10	0.13	3.742	*Atp5f1a, Atp5f1b, Atp5f1c, Atp5mc1, Atp5mc2, Atp5pb, Atp5pd, Atp5po, Cox4i1, Cox7a2, Cox8a, Ndufa5, Ndufa7, Ndufs7*
Mitochondrial Dysfunction	11.50	0.09	NaN	*Atp5f1a, Atp5f1b, Atp5f1c, Atp5mc1, Atp5mc2, Atp5pb, Atp5pd, Atp5po, Cox4i1, Cox7a2, Cox8a, Gpx4, Ndufa5, Ndufa7, Ndufs7*
Sirtuin Signaling Pathway	5.68	0.04	-1.134	*Atp5f1a, Atp5f1b, Atp5f1c, Atp5mc1, Atp5pb, Foxo1, Ndufa5, Ndufa7, Ndufs7, Rarb, Tomm7, Tuba1b*
Regulation of Actin-based Motility by Rho	5.16	0.07	1.342	*Actb, Arpc2, Cfl1, Gsn, Myl6, Pfn1, Rnd3*
RhoA Signaling	4.40	0.06	2.646	*Actb, Arpc2, Cfl1, Myl6, Pfn1, Rnd3, Septin9*
Huntington's Disease Signaling	4.11	0.04	0	*Atp5f1a, Atp5f1b, Atp5f1c, Atp5mc1, Atp5pb, Gng5, Grb2, Rps27a, Sos1*
Actin Cytoskeleton Signaling	3.61	0.04	0	*Actb, Arpc2, Cfl1, Grb2, Gsn, Myl6, Pfn1, Sos1*
Cardiac Hypertrophy Signaling	3.33	0.03	-0.378	*Calm1 (Includes Others), Gng5, Grb2, Hand1, Map3k15, Myl6, Rnd3, Sos1*
Lactose Degradation III	3.09	0.33	NaN	*Lct, Psap*
Integrin Signaling	2.94	0.03	0	*Actb, Arpc2, Grb2, Gsn, Pfn1, Rnd3, Sos1*
Germ Cell-Sertoli Cell Junction Signaling	2.74	0.04	NaN	*Actb, Cfl1, Gsn, Map3k15, Rnd3, Tuba1b*
Sucrose Degradation V (Mammalian)	2.71	0.22	NaN	*Aldoa, Tpi1*
Actin Nucleation by ARP-WASP Complex	2.68	0.06	NaN	*Arpc2, Grb2, Rnd3, Sos1*
RhoGDI Signaling	2.62	0.03	-0.447	*Actb, Arpc2, Cfl1, Gng5, Myl6, Rnd3*
Signaling by Rho Family GTPases	2.61	0.03	1.342	*Actb, Arpc2, Cfl1, Gng5, Myl6, Rnd3, Septin9*

Table S. 2 (continued)

Ingenuity Canonical Pathways	-log(*P*-value)	Ratio	z-score	Molecules
B Cell Receptor Signaling	2.56	0.03	0	*Calm1* (Includes Others), *Cfl1, Foxo1, Grb2, Map3k15, Sos1*
ILK Signaling	2.51	0.03	1.633	*Actb, Cfl1, Krt18, Myl6, Naca, Rnd3*
Clathrin-mediated Endocytosis Signaling	2.47	0.03	NaN	*Actb, Ap1s1, Arpc2, Grb2, Ldlrap1, Rps27a*
Axonal Guidance Signaling	2.44	0.02	NaN	*Arpc2, Cfl1, Gng5, Grb2, Myl6, Pfn1, Sema5a, Sos1, Stk36, Tuba1b*
PAK Signaling	2.21	0.04	NaN	*Cfl1, Grb2, Myl6, Sos1*
VEGF Signaling	2.18	0.04	NaN	*Actb, Foxo1, Grb2, Sos1*
GNRH Signaling	2.01	0.03	-1	*Calm1 (Includes Others), Gng5, Grb2, Map3k15, Sos1*
Ephrin Receptor Signaling	1.94	0.03	0.447	*Arpc2, Cfl1, Gng5, Grb2,s Os1*
ErbB2-ErbB3 Signaling	1.89	0.05	NaN	*Foxo1, Grb2, Sos1*
Phospholipase C Signaling	1.89	0.02	0	*Calm1 (Includes Others), Gng5, Grb2, Myl6, Rnd3, Sos1*
Remodeling of Epithelial Adherens Junctions	1.84	0.04	NaN	*Actb, Arpc2, Tuba1b*
Glycine Biosynthesis I	1.83	0.50	NaN	*Shmt1*
RAR Activation	1.82	0.03	NaN	*Actb, Rarb, Rdh10, Rpl7a, Trim24*
Glycolysis I	1.79	0.08	NaN	*Aldoa, Tpi1*
Gluconeogenesis I	1.79	0.08	NaN	*Aldoa, Mdh2*
Gap Junction Signaling	1.78	0.03	NaN	*Actb, Grb2,s Os1, Sox15, Tuba1b*
Non-Small Cell Lung Cancer Signaling	1.76	0.04	NaN	*Grb2, Rarb, Sos1*
Breast Cancer Regulation by Stathmin1	1.76	0.03	NaN	*Calm1 (Includes Others), Gng5, Grb2, Sos1, Tuba1b*
Angiopoietin Signaling	1.73	0.04	NaN	*Foxo1, Grb2, Sos1*
Neurotrophin/TRK Signaling	1.71	0.04	NaN	*Grb2, Sos1, Spry1*
Thrombin Signaling	1.69	0.02	NaN	*Gng5, Grb2, Myl6, Rnd3, Sos1*
IL-7 Signaling Pathway	1.68	0.04	NaN	*Foxo1, Grb2, Sos1*
IL-3 Signaling	1.67	0.04	NaN	*Foxo1, Grb2, Sos1*
Renal Cell Carcinoma Signaling	1.65	0.04	NaN	*Grb2, Rps27a, Sos1*

Table S. 2 (continued)

Ingenuity Canonical Pathways	-log(*P*-value)	Ratio	z-score	Molecules
D-glucuronate Degradation I	1.65	0.33	NaN	*Akr1a1*
Hypusine Biosynthesis	1.65	0.33	NaN	*Eif5a*
Role of NFAT in Cardiac Hypertrophy	1.65	0.02	NaN	*Calm1 (Includes Others), Gng5, Grb2, Hand1, Sos1*
HER-2 Signaling in Breast Cancer	1.60	0.04	NaN	*Foxo1, Grb2, Sos1*
Epithelial Adherens Junction Signaling	1.56	0.03	NaN	*Actb, Arpc2, Myl6, Tuba1b*
RANK Signaling in Osteoclasts	1.55	0.03	NaN	*Calm1 (Includes Others), Gsn, Map3k15*
Regulation of IL-2 Expression in Activated and Anergic T Lymphocytes	1.53	0.03	NaN	*Calm1 (Includes Others), Grb2, Sos1*
Prostate Cancer Signaling	1.51	0.03	NaN	*Foxo1, Grb2, Sos1*
ErbB Signaling	1.47	0.03	NaN	*Foxo1, Grb2, Sos1*
FAK Signaling	1.46	0.03	NaN	*Actb, Grb2, Sos1*
Neuregulin Signaling	1.45	0.03	NaN	*Grb2, Rps6, Sos1*
Glioblastoma Multiforme Signaling	1.45	0.02	-1	*Foxo1, Grb2, Rnd3, Sos1*
dTMP De Novo Biosynthesis	1.43	0.20	NaN	*Shmt1*
Folate Polyglutamylation	1.43	0.20	NaN	*Shmt1*
Glucocorticoid Receptor Signaling	1.39	0.02	NaN	*Actb, Grb2, Krt18, Krt7, Krt8, Sos1*
Oncostatin M Signaling	1.39	0.05	NaN	*Grb2, Sos1*
SAPK/JNK Signaling	1.39	0.03	NaN	*Gng5, Grb2, Sos1*
IGF-1 Signaling	1.36	0.03	NaN	*Foxo1, Grb2, Sos1*
T Cell Receptor Signaling	1.35	0.03	NaN	*Calm1 (Includes Others), Grb2, Sos1*
Role of NFAT in Regulation of the Immune Response	1.33	0.02	NaN	*Calm1 (Includes Others), Gng5, Grb2, Sos1*
Paxillin Signaling	1.32	0.03	NaN	*Actb, Grb2, Sos1*
Glioma Signaling	1.30	0.03	NaN	*Calm1 (Includes Others), Grb2, Sos1*
Sertoli Cell-Sertoli Cell Junction Signaling	1.30	0.02	NaN	*Actb, Cldn4, Map3k15, Tuba1b*

Table S. 3 The enriched Reactome pathways and related DEGs between hatching and pre-hatching blastocysts

Description	-log(*P*-value)	Genes	Background genes
L13a-mediated translational silencing of Ceruloplasmin expression	12.30	*Rps11, Rps9, Rps18, Rps14, Rps3a1, Rps4x, Rps2, Rps16, Rps10, Rpl13a, Rps15a, Rps20, Rps13*	50
Formation of a pool of free 40S subunits	12.30	*Rps11, Rps9, Rps18, Rps14, Rps3a1, Rps4x, Rps2, Rps16, Rps10, Rps15a, Rps20, Rps13*	37
Formation of the ternary complex, and subsequently, the 43S complex	12.30	*Rps11, Rps9, Rps18, Rps14, Rps3a1, Rps4x, Rps2, Rps16, Rps10, Rps15a, Rps20, Rps13*	40
Ribosomal scanning and start codon recognition	11.90	*Rps11, Rps9, Rps18, Rps14, Rps3a1, Rps4x, Rps2, Rps16, Rps10, Rps15a, Rps20, Rps13*	46
Translation initiation complex formation	11.79	*Rps11, Rps9, Rps18, Rps14, Rps3a1, Rps4x, Rps2, Rps16, Rps10, Rps15a, Rps20, Rps13*	48
Major pathway of rRNA processing in the nucleolus and cytosol	8.52	*Rps11, Rps9, Rps18, Rps14, Rps3a1, Rps4x, Rps2, Rps16, Rps10, Rps15a, Rps20, Rps13*	102
Formation of ATP by chemiosmotic coupling	7.90	*Atp5b, Atp5a1, Atp5k, Atp5h, Atp5c1, Atp5f1, Atp5g2*	17
Cristae formation	7.90	*Atp5b, Atp5a1, Atp5k, Atp5h, Atp5c1, Atp5f1, Atp5g2*	17
Respiratory electron transport, ATP synthesis by chemiosmotic coupling, and heat production by uncoupling proteins.	7.46	*Ndufa5, Atp5b, Atp5a1, Ndufa7, Atp5k, Ndufs7, Atp5h, Atp5c1, Atp5f1, Atp5g2*	78
The citric acid (TCA) cycle and respiratory electron transport	6.63	*Mdh2, Ndufa5, Atp5b, Atp5a1, Ndufa7, Atp5k, Ndufs7, Atp5h, Atp5c1, Atp5f1, Atp5g2*	129
Metabolism of proteins	2.77	*Rps11, Rps9, Rps18, Rps14, Rps3a1, Rps4x, Fbxo22, Ctsh, Eif5a, Tceb2, Fbxw11, Tuba1b, Lgals1, Gng5, Rps2, Actb, Scmh1, Rps16, Calm1, Rps10, Klhl22, Rpl13a, Rps15a, Rps20, Rps13, Cul3*	1497
Organelle biogenesis and maintenance	2.39	*Atp5b, Atp5a1, Atp5k, Tuba1b, Atp5h, Atp5c1, Atp5f1, Atp5g2*	199
Developmental Biology	1.80	*Arpc2, Pfn1, Krt18, Krt8, Foxo1, Sos1, Krt7, Tuba1b, Enah, Actb, Pkp4*	450
RHO GTPases activate IQGAPs	1.63	*Tuba1b, Actb, Calm1*	25
Signaling by Rho GTPases	1.52	*Arpc2, Pfn1, Taok1, Sos1, Tuba1b, Arhgap42, Actb, Calm1, Myl6*	349
Gluconeogenesis	1.34	*Mdh2, Aldoa, Tpi1*	33
RHO GTPase Effectors	1.34	*Arpc2, Pfn1, Taok1, Tuba1b, Actb, Calm1, Myl6*	238

Table S. 4 The enriched KEGG pathways and Wiki pathways and related DEGs between hatching and pre-hatching blastocysts

KEGG ID	Description	Gene Ratio	-log(*P*-value)	Genes
mmu03010	Ribosome	49/119	50.88	*Rpl32, Rpl7a, Rpl31, Rpl11, Rps27a, Rpl37a, Rps6, Rpl41, Rps24, Rps9, Rpl27, Fau, Rpl9, Rpl35, Rpl23a, Rps15a, Rps26, Rplp1, Rpl18, Rpl3, Rps10, Rps19, Rplp2, Rpl39, Rps14, Rpl27a, Rps17, Rpl6, Rpl13a, Rpl23, Rps11, Rpl37, Rpl14, Rpl19, Rps3a1, Rpl18a, Rpl34, Rpl7, Rps2, Rps13, Rpl4, Rps16, Rpl28, Rpl13, Rpl8, Rps20, Rpl35a, Rps4x, Rps18*
mmu00190	Oxidative phosphorylation	17/119	9.79	*Atp5b, Cox4i1, Atp5k, Cox8a, Uqcrh, Ndufa5, Atp5c1, Atp5f1, Atp5a1, Cox7c, Atp5o, Cox7a2, Ndufa7, Atp5g2, Ndufs7, Atp5h, Atp5g1*
mmu04714	Thermogenesis	21/119	9.76	*Atp5b, Cox4i1, Rps6, Atp5k, Cox8a, Uqcrh, Ndufa5, Atp5c1, Actb, Atp5f1, Sos1, Atp5a1, Cox7c, Atp5o, Cox7a2, Ndufa7, Atp5g2, Grb2, Ndufs7, Atp5h, Atp5g1*
mmu05012	Parkinson disease	16/119	8.57	*Atp5b, Cox4i1, Cox8a, Uqcrh, Ndufa5, Atp5c1, Atp5f1, Atp5a1, Cox7c, Atp5o, Cox7a2, Ndufa7, Atp5g2, Ndufs7, Atp5h, Atp5g1*
mmu05010	Alzheimer disease	17/119	8.33	*Atp5b, Cox4i1, Cox8a, Uqcrh, Ndufa5, Atp5c1, Atp5f1, Calm1, Atp5a1, Cox7c, Atp5o, Cox7a2, Ndufa7, Atp5g2, Ndufs7, Atp5h, Atp5g1*
mmu05016	Huntington disease	17/119	5.69	*Atp5b, Cox4i1, Cox8a, Uqcrh, Ndufa5, Atp5c1, Tuba1b, Atp5f1, Atp5a1, Cox7c, Atp5o, Cox7a2, Ndufa7, Atp5g2, Ndufs7, Atp5h, Atp5g1*
mmu04932	Non-alcoholic fatty liver disease (NAFLD)	8/119	1.64	*Cox4i1, Cox8a, Uqcrh, Ndufa5, Cox7c, Cox7a2, Ndufa7, Ndufs7*
Wiki ID	**Description**	**Gene Ratio**	**-log(*P*-value)**	**Genes**
WP163	Cytoplasmic Ribosomal Proteins	47/106	51.01	*Rps27a, Rpl18a, Rpl34, Rps13, Rpl41, Rpl4, Rps20, Rpl37, Rpl39, Rplp2, Rps10, Rpl11, Rpl35, Rpl35a, Rplp1, Rps26, Rpl3, Rps11, Rpl7a, Rpl13, Rpl8, Rpl23a, Rps15a, Rpl27a, Rpl13a, Rps6, Rps4x, Rps3a1, Rps24, Rps19, Rps18, Rps17, Rps16, Rps14, Rpl9, Rpl7, Rpl6, Rpl37a, Rpl32, Rpl28, Rpl27, Rpl19, Rpl18, Rps2, Fau, Rpl31*
WP295	Electron Transport Chain	16/106	7.59	*Ndufs7, Atp5h, Ndufa5, Atp5g2, Uqcrh, Ndufa7, Atp5o, Cox8a, Cox7a2, Cox4i1, Atpif1, Atp5k, Atp5f1, Atp5c1, Atp5b, Atp5a1*
WP1248	Oxidative phosphorylation	11/106	5.65	*Ndufs7, Atp5h, Ndufa5, Atp5g2, Ndufa7, Atp5o, Atp5k, Atp5g1, Atp5f1, Atp5b, Atp5a1*

Supplementary appendix 11

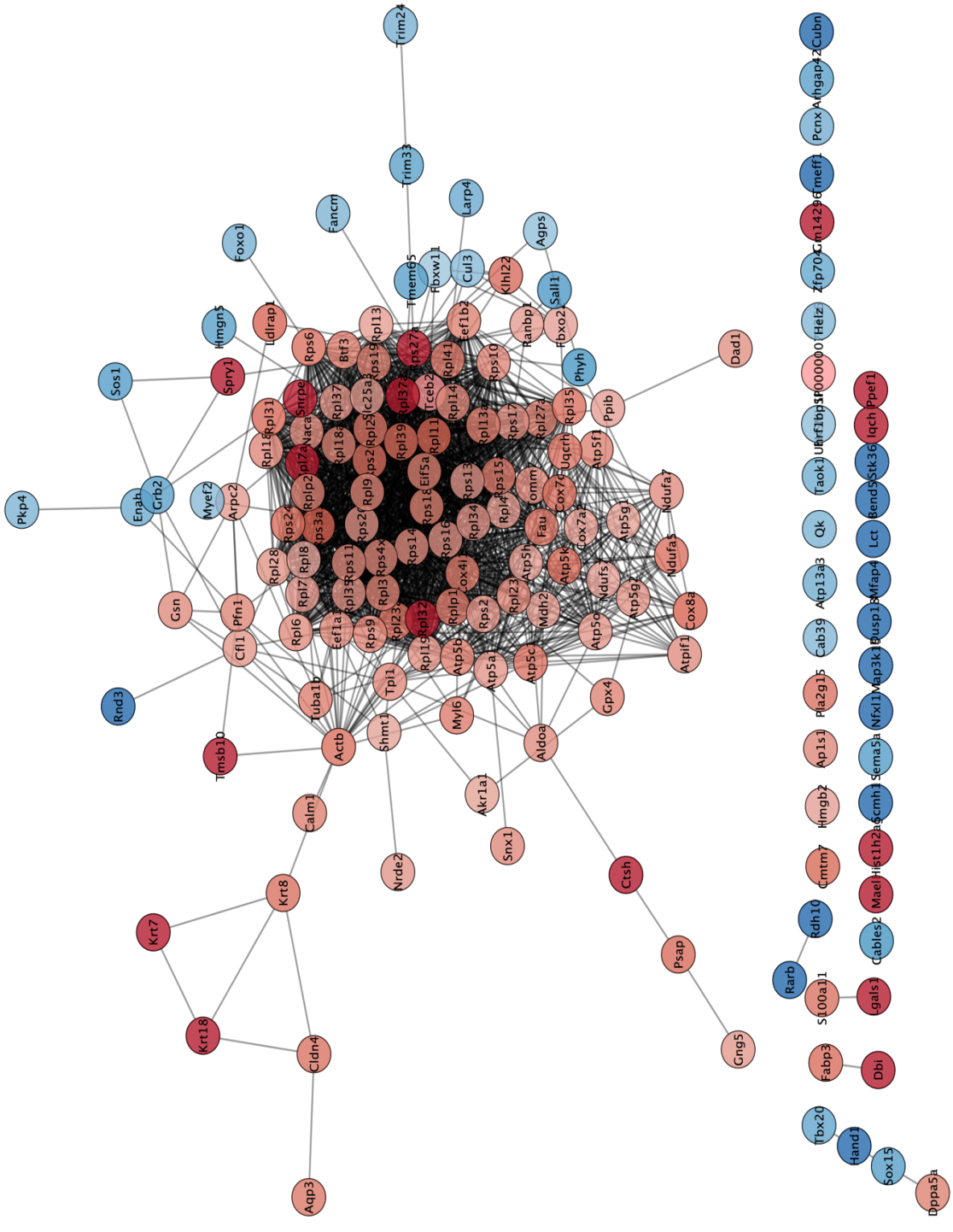
Table S. 5 The predicted upstream regulator and related molecules involved in hatching

Upstream Regulator	Molecule Type	Activation z-score	-log(*P*-value)	Target Molecules in Dataset
PRL	cytokine	2.401	1.62	*Actb, Atp5pd, Cox4i1, Ctsh, Tmsb4x, Tuba1b*
Esrra	transcription regulator	2.138	5.71	*Aldoa, Atp5f1b, Atp5mc1, Atp5pb, Atp5po, Cox7c, Cox8a, Ndufa5*
INSR	kinase	2.621	4.14	*Atp5f1a, Atp5f1b, Atp5mc1, Atp5pd, Atp5po, Calm1, Cfl1, Cox4i1, Lgals1, Mdh2, Rpl7a, Rps16*
HBA1/HBA2	transporter	2.828	8.79	*Atp5f1c, Atp5mc1, Atp5mc2, Atp5po, Cox8a, Ndufa5, Ndufa7, Ndufs7*
Hbb-b1	transporter	2.828	6.17	*Atp5f1c, Atp5mc1, Atp5mc2, Atp5po, Cox8a, Ndufa5, Ndufa7, Ndufs7*
HOXA10	transcription regulator	-2.236	1.86	*Actb, Krt18, Rpl37a, Snrpe, Sos1*
AGT	growth factor	2.412	1.12	*Calm1, Cox4i1, Cox7a2, Cox7c, Hmgb2, Pfn1, Tbx20*
Insulin	group	2.177	4.03	*Actb, Aldoa, Atp5mc1, Atp5mc2, Cox4i1, Cox7c, Dbi, Foxo1, Mdh2, Ppib, Rpl32, Rps16, Rps6*
BDNF	growth factor	-2.236	1.88	*Atp5mc2, Lgals1, Rpl13, Rpl23a, Rpl35a, Rpl37a, Tmsb4x*
RB1	transcription regulator	2.333	3.19	*Actb, Atp5f1a, Atp5k, Cox4i1, Cox7a2, Hmgb2, Krt18, Ndufa5, Ndufs7, Ranbp1, Tomm7*
CD3	complex	2.646	1.93	*Aqp3, Atp5f1c, Dad1, Mdh2, Pfn1, Psap, Rpl35a, Rpl6, Rps14, Sos1, Trim24*
TP53	transcription regulator	2.653	4.87	*Actb, Aldoa, Aqp3, Atp5f1a, Atp5f1c, Atp5k, Atp5mc1, Atp5pb, Cox7a2, Ctsh, Dbi, Eef1a1, Fabp3, Fbxo22, Foxo1, Grb2, Gsn, Hmgb2, Krt18, Krt8, Mdh2, Pfn1, Psap, Rnd3, Rpl34 (Includes Others), Rpl7, Rps16, Rps18, Rps19, Rps20, Rps26, Scmh1, Tmsb4x*
RICTOR	other	-7	52.85	*Atp5f1a, Atp5f1b, Atp5f1c, Atp5mc1, Atp5mc2, Atp5pb, Atp5pd, Atp5po, Cox4i1, Cox7a2, Cox7c, Cox8a, Fau, Ndufa5, Ndufa7, Ndufs7, Rpl11, Rpl13a, Rpl14, Rpl17, Rpl18, Rpl23, Rpl23a, Rpl28, Rpl34 (Includes Others), Rpl35a, Rpl4, Rpl41, Rpl6, Rpl7, Rpl7a, Rpl8, Rpl9, Rplp1 (Includes Others), Rplp2, Rps10, Rps11, Rps13, Rps18, Rps19, Rps2, Rps24, Rps26, Rps27a, Rps3a1, Rps4y1, Rps6, Rps9, Uqcrhl*
MYC	transcription regulator	4.111	8.93	*Actb, Aldoa, Atp5if1, Dbi, Hand1, Krt7, Lgals1, Ranbp1, Rarb, Rpl11, Rpl13, Rpl19, Rpl23, Rpl27, Rpl3, Rpl32, Rpl35, Rpl41, Rpl6, Rpl7, Rpl7a, Rpl9, Rps15a, Rps16, Rps18, Rps19, Rps20, Rps6, Rps9, Shmt1, Tpi1*
MYCN	transcription regulator	5.721	45.46	*Actb, Aldoa, Eef1a1, Eif5a, Fau, Grb2, Lgals1, Naca, Rpl11, Rpl13, Rpl13a, Rpl17, Rpl18, Rpl18a, Rpl19, Rpl23, Rpl27, Rpl27a, Rpl28, Rpl3, Rpl31, Rpl35, Rpl35a, Rpl37, Rpl37a, Rpl39, Rpl4, Rpl41, Rpl6, Rpl7, Rpl8, Rpl9, Rplp2, Rps13, Rps16, Rps17, Rps19, Rps2, Rps20, Rps24, Rps26, Rps6, Rps9, Tpi1, Tuba1b*

Table S.5 (continued)

Upstream Regulator	Molecule Type	Activation z-score	-log(*P*-value)	Target Molecules in Dataset
IGF1R	transmembrane receptor	2.449	7.36	*Aldoa, Atp5f1a, Atp5f1b, Atp5mc1, Atp5pd, Atp5po, Cox4i1, Rpl3, Rpl35a, Rpl37a, Rpl7, Rpl9, Rps24, Rps26*
FAAH	enzyme	-2.828	10.23	*Atp5pd, Mael, Rpl17, Rpl7, Rps18, Rps2, Rps3a1, Rps6*
Estrogen receptor	group	2.236	1.39	*Cldn4, Krt18, Krt7, Krt8, Tmeff1*
FGF2	growth factor	2.213	0.63	*Aqp3, Dad1, Foxo1, Spry1, Tmsb4x (Includes Others)*
GCK	kinase	-2	4.08	*Atp5f1a, Atp5f1c, Atp5mc1, Atp5mc2*
STK11	kinase	3.051	7.17	*Akr1a1, Aldoa, Atp5f1c, Atp5k, Atp5mc1, Atp5mc2, Btf3, Cox7a2, Cox7c, Cox8a, Mdh2, Ndufs7, Rps6, Tpi1*
NR4A1	ligand-dependent nuclear receptor	-2.646	4.95	*Aldoa, Atp5f1a, Atp5f1b, Cox7a2, Krt18, Krt8, Mdh2, Ndufa7, Ndufs7, Rarb, Uqcrhl*
PPARG	ligand-dependent nuclear receptor	2.216	1.40	*Aqp3, Atp5po, Fabp3, Gm12854/S100a11, Krt18, Ndufa5, Rarb, Snx1*
HSP90B1	other	2.236	4.01	*Eif5a, Rpl27a, Rplp2, Rps14, Rps20*
GAST	other	2.449	4.38	*Hmgb2, Mdh2, Naca, Rpl35a, Rpl7, Rps19*
CLPP	peptidase	-2	2.78	*Aldoa, Atp5f1a, Atp5f1b, Mdh2*
KDM5A	transcription regulator	-2.646	4.13	*Atp5f1a, Atp5k, Cox4i1, Cox7a2, Ndufa5, Ndufs7, Tomm7*
CCND1	transcription regulator	-2.121	2.89	*Aqp3, Eef1b2, Pkp4, Qki, Rpl13, Rpl27a, Rps6, Tpi1, Tuba1b*
NRF1	transcription regulator	2	2.68	*Cox4i1, Cox7a2, Cox7c, Cox8a*
PPARGC1A	transcription regulator	2.026	2.21	*Atp5f1a, Atp5f1b, Atp5pd, Atp5po, Cox4i1, Fabp3, Mdh2, Phyh*
NFE2L2	transcription regulator	2.961	2.14	*Akr1a1, Aldoa, Calm1, Cox4i1, Dad1, Ppib, Rpl18, Rps16, Tpi1*
UCP1	transporter	2	1.40	*Btf3, Eef1a1, Gpx4, Shmt1*

Supplementary appendix 12


Trim24
Trim33
Tmem65
Fbxw11
Cul3
Larp4
Agps
Sall1
Fbxo2
Phyh
Ppib
Dad1
Ranbp1
Klhl22
Fancm
Foxo1
Ldlrap1
Hmgn5
Sos1
Spry1
Rps6
Btf3
Rps19
Rpl13
Rpl37a
Rpl41
Eef1b2
Tceb2
Rps10
Rpl13a
Rps17
Rpl27a
Rpl35
Uqcrh
Atp5f1
Rpl39
Rpl11
Rpl37
Rps27a
Snrpe
Naca
Rpl37
Rpl18a
Rpl23
Rpl31
Rpl18
Rpl7a
Rpl9
Rps2
Rpl10a
Rpsa
Rps3a
Rpl2
Rps24
Rps2
Rps4x
Rps11
Rpl3
Rpl3
Rpl28
Rpl8
Rpl7
Rpl6
Cfl1
Pfn1
Gsn
Rnd3
Tmsb10
Actb
Tuba1b
Calm1
Krt8
Krt7
Krt18
Cldn4
Aqp3
Nrde2
Tpi1
Shmt1
Myl6
Akr1a1
Snx1
Rps14
Rps18
Eif5a
Rps16
Rpl34
Rps13
Rpl4
Rps15
Omm
Fau
Cox7c
Cox7a2
Atp5g1
Ndufa7
Ndufa4
Cox8a
Atpif1
Gpx4
Ctsh
Psap
Gng5
Rpl10
Rpl32
Rpl23
Rps9
Rpl3
Eef1a1
Rpl6
Rpl7
Rpl8
Rpl28
Rps11
Rps4x
Rpl3
Rpl23
Rpl10
Rpsa
Rpl32
Rpl10a
Rpl2
Rps2
Rpl23
Rpl1p1
Cox4i
Rps13
Rpl34
Rps15
Rpl4
Rps16
Rps18
Rps14
Rpl11
Rpl39
Rpl37a
Rpl41
Rpl14
Tceb2
Rpl37
Rpl18a
Rpl23
Rpl31
Rpl18
Rpl7a
Rpl9
Rps2
Rpl10a

Supplementary appendix 13

Table S. 3 The pathways and related differentially expressed genes between laser-drilled hatching and control hatching blastocysts

Pathways	Category	-log(*P*-value)	Ratio	Molecules
tRNA Charging	Canonical pathway	4.14	0.0769	*Aars1, Cars1, Tars1*
Mevalonate Pathway I		3.43	0.143	*Mvd, Mvk*
Superpathway of Geranylgeranyldiphosphate Biosynthesis I (via Mevalonate)		3.2	0.111	*Mvd, Mvk*
Superpathway of Cholesterol Biosynthesis		2.79	0.069	*Mvd, Mvk*
Docosahexaenoic Acid (DHA) Signaling		2.55	0.0526	*Gsk3a, Pik3c2a*
Xenobiotic Metabolism Signaling		2.54	0.0139	*Aldh18a1, Aldh9a1, Keap1, Pik3c2a*
Insulin Receptor Signaling		2.53	0.0216	*Gsk3a, Pik3c2a, Trip10*
eNOS Signaling		2.36	0.0189	*Nosip, Pik3c2a, Stub1*
Germ Cell-Sertoli Cell Junction Signaling		2.27	0.0175	*Actn4, Keap1, Pik3c2a*
L-carnitine Biosynthesis		2.21	0.333	*Aldh9a1*
N-acetylglucosamine Degradation I		2.21	0.333	*Amdhd2*
Sertoli Cell-Sertoli Cell Junction Signaling		2.18	0.0162	*Actn4, Gsk3a, Keap1*
ILK Signaling		2.15	0.0158	*Actn4, Gsk3a, Pik3c2a*
ErbB2-ErbB3 Signaling		2.1	0.0308	*Gsk3a, Pik3c2a*
Proline Biosynthesis I		2.08	0.25	*Aldh18a1*
N-acetylglucosamine Degradation II		2.08	0.25	*Amdhd2*
Metabolism of lipids	Reactome Pathway	2.08	0.013	*Slc25a1, Mvd, Acbd4, Agpat4, Aacs, Mvk, Acaa1a, Mcat*
Valine, leucine and isoleucine degradation	KEGG Pathway	2.04	0.0545	*Aldh9a1, Aacs, Acaa1a*
Aminoacyl-tRNA biosynthesis	KEGG Pathway	2.04	0.0682	*Cars, Tars, Aars*

Research output

International peer-reviewed papers

1. Davidson LM[1], **Liu Y**[1], Griffiths T, Jones C, Coward K. Laser technology in the assisted reproductive technology laboratory: a narrative review. Reproductive Biomedicine Online. 2019 May;38(5):725-739.[1]Joint First Author

2. **Liu Y**, Jones C, Coward K. The effect of laser zona pellucida drilling on preimplantation mouse embryo competency and global gene expression. F&S Science (2021) (In press)

3. **Liu Y**, Jones C, Coward K. The mechanism of mouse embryo hatching: an RNA sequencing study. (In preparation)

Presentation at international and university conferences

1. **Liu Y**, Jones C, Coward K. The mechanism of mouse embryo hatching and the impact of laser drilling the zona pellucida: an RNA sequencing study. ESHRE virtual 37th Annual Meeting (2021). (Poster presentation)

2. **Liu Y**, Jones C, Coward K. Effects of different infra-red laser-assisted hatching (LAH) protocols on preimplantation mouse embryos and embryo attachment. Fertility 2020, Edinburgh, UK (2020). (Oral presentation)

3. **Liu Y**, Jones C, Coward K. The effect of laser-assisted hatching in embryo implantation capability and global gene expression. Fertility 2019, Birmingham, UK (2019). (Poster presentation)

4. **Liu Y**, Jones C, Coward K. Annual Oxford Developmental Biology Meeting. University of Oxford, UK (2019). (Poster presentation)

5. **Liu Y**, Jones C, Coward K. Medical Sciences Division DPhil Day, University of Oxford, UK (2018). (Poster presentation)

6. **Liu Y**, Jones C, Coward K. Graduate student symposium, University of Oxford, UK (2017). (Oral Presentation)

Prizes and awards

2019 Henry and Lester Trust Grant
Awarded £1500 grant to support the research project

2018 Chinese Scholarship Council PhD student scholarship
A fully funded scholarship to cover tuition, college fees and living expenses for the duration of the PhD degree.

2018 Primerdesign Company excellent postgraduate student award
£3000 worth of consumable funding awarded to research

2020-2019 Society for Reproductive and Fertility Bursary
Financial endorsement from the Society for Reproductive and Fertility to attend the Fertility conferences in Birmingham (2019) and Edinburgh (2020)

2018 Society for Reproductive and Fertility Travel Grant
Financial endorsement from the Society for Reproductive and Fertility to attend IVF 40 conference in Manchester (2018)

2018 Travel and research fund from St. Cross College, University of Oxford
Financial endorsement from St. Cross college to attend the ESHRE conference in Barcelona (2018)